

UCSF

UC San Francisco Electronic Theses and Dissertations

Title

Spliceosomal RNA rearrangements

Permalink

<https://escholarship.org/uc/item/51k8s1xh>

Author

Madhani, Hiten D.

Publication Date

1993

Peer reviewed|Thesis/dissertation

**SPLICEOSOMAL RNA REARRANGEMENTS: IMPLICATIONS FOR THE MECHANISM
OF RNA SPLICING
by**

HITEN D. MADHANI

DISSERTATION

Submitted in partial satisfaction of the requirements for the degree of

DOCTOR OF PHILOSOPHY

in

GENETICS

in the

GRADUATE DIVISION

of the

UNIVERSITY OF CALIFORNIA

San Francisco



ACKNOWLEDGEMENTS

I wish to express gratitude to my graduate advisor Christine Guthrie for her encouragement and support over the past several years. I continue to be impressed by her outstanding talents as an advisor, teacher, and writer. I would also like to thank the other members of my thesis committee, Ira Herskowitz and Andrew Murray, for their interest in my work and for their critical reading of this thesis. Harold Varmus helped me get my start in science at UCSF and has continued to be a supporter and mentor. Thanks also go to Peter Walter, Cynthia Kenyon, and David Agard in whose laboratories I was a rotation student during my first year of graduate school. Suzanne Noble, who has contributed to every aspect of the work presented here, has been a strong influence both scientifically and otherwise. I wish also to thank the other members of the laboratory, both past and present, for lively discussions, advice, and criticism. Special thanks go to Jim Umen, Pratima Raghunathan, Sean Burgess, Shelly Jones, and Yan Wang for reading part or all of this dissertation. Of course, none of this would have been possible without the support of my parents, Dhanvant and Minakshi Madhani.

SPLICEOSOMAL RNA REARRANGEMENTS: IMPLICATIONS FOR THE MECHANISM OF RNA SPLICING

Hiten D. Madhani

ABSTRACT

Since the discovery of RNA catalysis, it has been widely speculated that the splicing of nuclear mRNA precursors is mediated by the snRNA components of the eukaryotic spliceosome. This view has been galvanized by fundamental similarities between the chemical pathway of nuclear pre-mRNA splicing and Group II self-splicing. This thesis describes an analysis in yeast of the function of the highly conserved U6 spliceosomal snRNA. This RNA is associated with U4 snRNA through an extensive base-pairing interaction that is disrupted prior to the chemical steps of splicing. We identified two mutationally-sensitive domains of this molecule. One occurs in a region of U6 that interacts with U4 snRNA. Genetic and biochemical analysis of this region revealed it to have a function independent of base-pairing with U4. The nature of this additional interaction was made clear by our genetic demonstration of a novel base-pairing interaction, termed U2-U6 helix I, between this region of U6 and a sequence in U2 snRNA that is immediately upstream of the intron branchpoint recognition region of U2. As a result, highly conserved and functionally important residues in U6 can be juxtaposed with the intron substrate. These properties led to an explicit model for the active site of the spliceosome in which U2-U6 helix I might participate directly in catalysis. Because this helix is mutually exclusive with the U4-U6 interaction, its formation offers a mechanistic rationale for the disruption of the U4-U6 interaction prior to the chemical steps of splicing. Further experiments revealed evidence for a higher order interaction in which the terminal residue of the conserved ACAGAG hexanucleotide that lies upstream of helix I interacts

with the helix I bulge. This tertiary interaction, the first to be described for the spliceosomal snRNAs, can juxtapose the two clusters of residues in the U2-U6 helix I region that are specifically required for the second chemical step of splicing. Finally, our finding of spliceosomal rearrangements, which involve the swapping of mutually exclusive base-pairing partners, suggests that the many helicase-like proteins involved in pre-mRNA splicing might function to catalyze and regulate these RNA conformational isomerizations. Using a genetic screen, we obtained evidence for functional interaction between the helicase-like splicing factor, Prp16, and the U2 and U6 spliceosomal snRNAs. Several aspects of the data are consistent with the intriguing possibility that the U2-U6 complex is the RNA ligand for Prp16. Taken together, our data suggests that spliceosomal RNA rearrangements are critical for the assembly, regulation, and catalytic function of the eukaryotic splicing apparatus.

Christine Guthrie

TABLE OF CONTENTS

Prologue	Split Genes and Small RNAs: The Ribozyme Hypothesis	1
Chapter 1	Multiple Roles for U6 snRNA in the Splicing Pathway	11
Chapter 2	A Novel Base-Pairing Interaction Between U2 and U6 snRNAs Suggests a Mechanism for the Catalytic Activation of the Spliceosome	54
Chapter 3	Randomization-Selection Analysis of snRNAs: Evidence for a Tertiary Interaction in the Spliceosome	109
Chapter 4	Genetic Interactions Between the RNA Helicase Homolog Prp16 and Spliceosomal snRNAs Identify Candidate Ligands for the Prp16 RNA-dependent ATPase	170

Epilogue	Dynamic RNA-RNA Interactions in the Pre-mRNA Splicing Mechanism: A Principle of Spliceosomal Design	213
Appendix 1	Randomization-Selection Analysis of Residues in the U2-U6 Helix I Region Required Prior to the First Chemical Step of Splicing	249
Appendix 2	Factors Required for the Synthesis and Function of U6 snRNA Identified Through a Genetic Screen for Synthetic Lethal Mutants	260
References		270

LIST OF TABLES

Chapter 1

Table 1	U6 Mutants	51
Table 2	Phenotypes of Mutations in Stem I of U4 and U6	53

Chapter 2

Table 1	Summary of Genetic Suppression Experiments	104
Table 2	Comparison of Phenotypes of U2 and U6 Mutants that Disrupt Helix I	106
Table 3	Splicing Defects Exhibited by U2 Mutants: Quantitation of Pre-mRNA and Lariat-Intermediate	108

Chapter 3

Table 1	Base Appositions Seen Between U6 nt 58 and U2 nt 26 in Functional Variants Shown in Figure 3	159
Table 2	Phenotypes of Base Appositions Between U6 nt 58 and U2 nt 26	161
Table 3	Base Appositions Seen Between U6 nt 59 and U2 nt 23 in Functional Variants Shown in Figure 3	163
Table 4	Phenotypes of Base Appositions Between U6 nt 59 and U2 nt 23	165
Table 5	Phenotypes of Mutants in the Bulge Regions of U2-U6 Helix I	167
Table 6	Specificity of Suppression of G52A and G52C by Bulge-Region Variants	169

Chapter 4

Table 1	Growth of YS78 Derivatives Containing Alleles of <i>PRP16</i>	202
Table 2	Growth of YHM187 Derivatives Containing Site-Directed Mutants in U6 or U2 snRNAs as the Sole Copy of the Respective Gene	204
Table 3	Comparison of Dominant Versus Recessive Suppression of <i>prp16-302</i> by U6 Suppressor Alleles	206
Table 4	Allele-Specificity of Suppression	208
Table 5	Overexpression of cs <i>PRP16</i> Alleles Antagonizes Suppression by U6 Mutants	210
Table 6	<i>Saccharomyces cerevisiae</i> Strains Used in This Study	212

Appendix 1

Table 1	Evidence for Base-Pairing Between U6-C61 and U2-G21	257
Table 2	Base Appositions Found in U2 Stem I in Functional Variants Shown in Figure 1	259

Appendix 2

Table 1	Allele-Specificity of Synthetic Lethality	269
---------	-------------------------------------------	-----

LIST OF FIGURES

Prologue

Figure 1	Two-Step Chemical Pathway of Nuclear Pre-mRNA Splicing	8
Figure 2	Simplified View of Spliceosome Assembly	10

Chapter 1

Figure 1	<i>S. cerevisiae</i> U4-U6 Structure and Location of Mutants	38
Figure 2	Scheme for Isolation of U6 Mutants	40-1
Figure 3	Phenotypes of Mutations in the Invariant ACAGAGA Motif	43
Figure 4	Northern Analysis of U6 Mutants	45
Figure 5	Velocity Sedimentation Analysis of U6 Mutants	47
Figure 6	Splicing Activity of Mutant U6 Extracts	49

Chapter 3

Figure 1	<i>S. cerevisiae</i> U4 and U6 snRNAs	82
Figure 2	U2-U6 Base-Pairing Model	84
Figure 3	Plasmid Shuffle Assay for Mutants	86
Figure 4	Specific Suppression of U6 Mutants at Positions 56-57 by Compensatory U2 Mutants	88
Figure 5	Specific Suppression of U6 Mutants at Position 58 by Compensatory U2 Mutants	90
Figure 6	Specific Suppression of U6 Mutants at Position 59 by Compensatory U2 Mutants	92

Figure 7	Mutants in U2 Inhibit Both Steps of Splicing In Vivo	95-8
Figure 8	Structural Similarity Between the Spliceosome and Group II Introns	100
Figure 9	Conformational Isomers and Phylogenetic Conservation of U2, U4, and U6 snRNAs	102
 Chapter 3		
Figure 1	RNA-RNA Interactions Between the Intron, U2 and U6 snRNAs	138
Figure 2	Strategy for In Vivo Selection of Functional Covariants of Two Interacting Molecules	140
Figure 3	Selected Variant Pairs	142
Figure 4	Recovered Nucleotides of Variant Pairs	144
Figure 5	Analysis of the U5-C58/ U2-G26 Base-Pair	146-7
Figure 6	Analysis of G52A-Containing Variants	149
Figure 7	Analysis of G52C-Containing Variants	151
Figure 8	Specificity of Suppression	153
Figure 9	Model for Suppression	155
Figure 10	Network of RNA-RNA Interactions Involving the 3' Splice Site	157
 Chapter 4		
Figure 1	RNA-RNA Interactions Between U2 snRNA, U6 snRNA, and the pre-mRNA	192
Figure 2	Suppressor of <i>prp16-302</i>	194

Figure 3	Sequence of the U6 Coding Sequence for the Suppressor Alleles Shown in Figure 2	196
Figure 4	Growth of YHM187 Derivatives Containing the Indicated Alterations in U2-U6 Helix Ia	198
Figure 5	Model for Suppression	200
Epilogue		
Figure 1	U1 and U2 snRNAs Interact with the Pre-mRNA via Watson-Crick Base-Pairing	236
Figure 2	U4 and U6 snRNAs Base-Pair with Each Other	238
Figure 3	U2-U6 Helix I	240
Figure 4	Conformational Isomers and Phylogenetic Conservation of U2, U4, and U6 snRNAs	242
Figure 5	U6-5' Splice Site Interaction	244
Figure 6	U5-Exon Interactions	246
Figure 7	Structural Similarities Between the Spliceosome and Group II Introns	248
Appendix 1		
Figure 1	Sequences of Selected Variants	253
Figure 2	Consensus Sequences for Variants	255
Appendix 2		
Figure 1	<i>sud5-1</i> Exhibits the Accumulation of Unspliced Pre-mRNA at the Nonpermissive Temperature	267



SCHOOL OF MEDICINE
DEPARTMENT OF BIOCHEMISTRY AND BIOPHYSICS
SAN FRANCISCO, CALIFORNIA 94143-0448
(415) 476-4324 FAX # (415) 476-0961

November 17, 1993

Genes and Development
Cold Spring Harbor Laboratory Press
Box 100
1 Bungtown Road
Cold Spring Harbor, New York 1172-2205

To whom it may concern,

I would like the permission of Genes and Development to reprint, for my Ph.D. thesis the article "Multiple Roles for U6 snRNA in the Splicing Pathway" by myself, Rémy Bordonné, and Christine Guthrie (Genes and Development, 4: 2264-2277). The dissertation will be placed on microfilm by University Microfilms who request permission to supply single copies on demand. Please respond by fax to (415)476-0943

Thank you for your consideration.

Sincerely,

Hiten D. Madhani

Permission granted by the copyright owner, contingent upon the consent of the original author, provided complete credit is given to the original source and copyright date.

BY DATE 12/6/93

Cold Spring Harbor Laboratory, PO Box 100, Cold Spring Harbor, NY: 11724



SCHOOL OF MEDICINE
DEPARTMENT OF BIOCHEMISTRY AND BIOPHYSICS
SAN FRANCISCO, CALIFORNIA 94143-0448
(415) 476-4324 FAX # (415) 476-0961

November 17, 1993

Cell Press
50 Church Street
Cambridge, MA 02138

To whom it may concern,

I would like the permission of Cell to reprint, for my Ph.D. thesis, the article "A Novel Base-Pairing Interaction Between U2 and U6 snRNAs Suggests a Mechanism for the Catalytic Activation of the Spliceosome" by myself and Christine Guthrie (Cell, 71, 803-817). The dissertation will be placed on microfilm by University Microfilms who request permission to supply single copies on demand. Please respond by fax to (415) 476-0943

Thank you for your consideration.

Sincerely,

A handwritten signature in cursive script that reads "Hiten D. Madhani".

Hiten D. Madhani

Permission granted subject to citation
of the original manuscript, and notation
that copyright is held by Cell Press.
(Our permission is contingent on
permission of the author.)

A handwritten signature in cursive script that reads "Albert H. Yuan".

12.1.93

PROLOGUE

Split Genes and Small RNAs: The Ribozyme Hypothesis

Genes in eukaryotes are often interrupted by intervening sequences or introns that must be removed during gene expression. This is accomplished by an RNA splicing process in which the functional segments of pre-mRNAs (exons) are joined. Splicing occurs in a large and dynamic ribonucleoprotein complex, the spliceosome. Five small nuclear RNAs (U1, U2, U4, U5, and U6 snRNAs) constitute key components of this enzyme. Packaged by proteins into ribonucleoproteins (snRNPs), these RNA molecules assemble onto the pre-mRNA substrate in an ordered ATP-dependent pathway. The discovery of RNA catalysis led to the proposal that nuclear pre-mRNA splicing might be a fundamentally RNA catalyzed process mediated by the spliceosomal snRNAs (Sharp, 1985; Cech, 1986). This hypothesis has been galvanized by the discovery that Group II self-splicing introns are removed by a two-step chemical pathway that is highly similar if not identical to that which accomplishes nuclear pre-mRNA splicing (Ruskin et al., 1984; Konarska et al., 1985; Peebles et al., 1986; van der Veen et al., 1986; Figure 1). In the first cleavage/ligation step of this reaction, the 2' hydroxyl of an internal adenosine residue attacks the phosphate at the 5' splice site, releasing the 5' exon and resulting in formation of a branched molecule, the lariat intermediate, that contains an unusual 5'-2' phosphodiester bond between the 5' end of the intron and the internal adenosine (the branchpoint adenosine). During the second cleavage/ligation step, the 3' hydroxyl of the 5' exon attacks the phosphate at the 3' splice site. This results in the ligation of the two exons and the release of the intron lariat. Both of the chemical steps of the spliceosomal reaction result in the inversion of stereochemical configuration at the reacting phosphorous atoms, consistent with an in-line "S_N2" displacement mechanism for the both transesterifications (Moore and Sharp, 1993).

As an enzyme, the spliceosome must accomplish two tasks: substrate recognition and catalysis. Because splicing occurs via two chemical steps that involve distinct reaction partners, these tasks must themselves be accomplished twice. Since the products of the

first chemical step are the reactants for the second, the two steps must be coupled and coordinated. Substrate recognition in both steps is made challenging by the relative dearth of information present in introns, yet splicing must occur with single-nucleotide precision. Virtually nothing is known regarding the mechanism of catalysis. Answering these questions requires a detailed understanding of the splicing apparatus itself.

The spliceosome forms through a highly ordered ATP-dependent pathway, which has been well-characterized in yeast and human *in vitro* splicing systems. Among the more prominent events of this assembly mechanism (Figure 2) are 1) the initial binding of U1 and U2 snRNPs to the pre-mRNA, 2) the binding of the tripartite U4-U6.U5 snRNP, and 3) the release of the U4 snRNP prior to the two chemical steps of splicing (Figure 2). Because the structure of this pathway has been conserved from yeast to mammals, it is likely to hold answers to the fundamental questions of substrate recognition and catalysis, yet these relationships are not immediately apparent from our current understanding of the assembly process. Once fully assembled, the machine somehow accomplishes the two chemical steps of splicing. The ribonucleoprotein nature of the spliceosome has long been suggested to reflect a central role for snRNAs in splicing; however, evidence for this notion was weak at best.

The work described in this thesis was motivated by the hypothesis that snRNAs are key catalytic components of the spliceosomal splicing apparatus. A strong emphasis is placed on the U6 spliceosomal snRNA, which is among the most conserved RNAs in eukaryotic phylogeny. U6 snRNA is associated with U4 snRNA through an extensive base-pairing interaction (Hashimoto and Stetiz, 1984; Bringmann et al., 1984; Brow and Guthrie, 1988), which is disrupted in the assembled spliceosome prior to the first cleavage-ligation event (Pikielny et al., 1986; Konarska and Sharp, 1987; Cheng and Abelson, 1987; Lamond et al., 1988). This temporal correlation together with the high conservation of U6 led to speculation that it might be a catalytic component of the spliceosome and that U4 might function to negatively regulate its activity (Guthrie and Patterson, 1988). This

view was fueled by the finding of rare mRNA-type introns in the U6 genes of unrelated fungi (Tani and Ohshima, 1989; 1991). Following the discovery of the first of these introns, it was suggested that it might have originated in a rare reverse splicing accident in which an excised intron integrated into a component of the spliceosomal active site, namely U6 snRNA (Brow and Guthrie, 1989). However, in the absence any information regarding the specific intermolecular interactions of U6 snRNA (besides the U4-U6 interaction), these notions remained highly speculative.

Chapter 1 is reprinted from a published article that appeared in Genes and Development. It describes the first step towards analyzing the function of U6 snRNA in pre-mRNA splicing: the identification of the functionally important nucleotides of this molecule. This was accomplished through degenerate chemical synthesis of the U6 gene followed by a genetic screen in yeast for deleterious mutants. This screen identified two main clusters of mutationally sensitive residues. One cluster occurred in the phylogenetically invariant ACAGAG hexanucleotide. Further mutants in this region were created by site-directed mutagenesis and analyzed in detail by Rémy Bordonné, who was then a postdoctoral fellow in the laboratory. The other of the two mutationally-sensitive stretches is in a region involved in base-pairing with U4 snRNA. Interestingly, my biochemical and genetic experiments revealed that these residues in U6 that base-pair with U4 must have an additional, unknown role.

Chapter 2 is reprinted from an article published in Cell and answers this conundrum. Starting with the premise that U6 is involved in catalysis and that U4 snRNA regulates this function, I searched for potential base-pairing interactions between U6 and other snRNAs that might juxtapose U6 with the intron substrate. This led me to discover a novel base-pairing interaction between U6 and a region of U2 snRNA immediately upstream of the sequence in U2 snRNA that interacts with the intron branchpoint region. I was able to prove the existence of this interaction, which is termed U2-U6 helix I, by showing that mutations in U6 snRNA that I predicted would disrupt base-pairing could be

suppressed by compensatory mutations in U2 snRNA that restore base-pairing (Chapter 2). Biochemical experiments demonstrate that residues in U2 snRNA that participate in this structure are important for both chemical steps of splicing. Finally, because the U2-U6 helix is mutually exclusive with the U4-U6 interaction, it offers a pleasing mechanistic explanation for the previously enigmatic unwinding of the U4-U6 interaction prior to catalysis. The residues that participate in U2-U6 helix I are among the most conserved in the spliceosomal snRNAs. These observations led to a proposal for the active site of the spliceosome in which U2-U6 helix I is poised to participate directly in the chemical steps of splicing. This notion is reinforced by my observation that the U2-U6 structure exhibits a striking resemblance to the most conserved domain of Group II self-splicing introns, domain 5.

In Chapter 3, I describe the application of a novel *in vivo* bimolecular randomization-selection method to search for tertiary interactions in the U2-U6 helix I region. An analysis of 60 variant pairs revealed evidence for a tertiary interaction between the region of the two-nucleotide bulge of U2-U6 helix I and the terminal guanosine of the adjacent ACAGAG hexanucleotide. This higher order interaction, the first to be described for spliceosomal snRNAs, can bring together the two clusters of residues in the U2-U6 complex that are specifically involved in the second step of splicing. Taking into consideration other recent results (see Epilogue), I suggest that this tertiary interaction participates in a network of RNA-RNA interactions that juxtaposes residues in U2 and U6 involved in the second step of splicing with the 3' splice site.

The work described above suggests spliceosomal snRNA rearrangements as a general and novel paradigm for spliceosome assembly. This observation immediately leads to a hypothesis for the roles of the many RNA helicase-like proteins required for splicing: the mediation and regulation of these RNA conformational isomerizations. A major stumbling block in the analysis of the function of these factors is that their RNA ligands are unknown. This gap in understanding motivated me to search for interactions between

snRNAs and this class of splicing factors. Chapter 4 describes genetic evidence for a functional interaction between one member of this protein family, Prp16, and the U2 and U6 spliceosomal snRNAs. Specifically, I found that cold-sensitive mutants of *PRP16* can be suppressed by specific point mutations in U2 and U6 snRNAs. Properties of the suppressors suggest that they act by disrupting an interaction between the snRNAs and another factor, which becomes trapped in the cold-sensitive *prp16* alleles. An intriguing possibility, which is supported by the effects of overexpression of mutant forms of Prp16, is that this other factor might be Prp16 itself. This study identifies U2 and U6 as excellent candidate ligands for Prp16 and points the way for future studies of this important class of ATP-consuming proteins.

In the Epilogue, I review my findings in the context of other results that have appeared in the past several years. I describe additional evidence favoring a direct role for snRNAs in splicing which has been inferred from genetic and biochemical experiments in several different experimental systems. This has led to an increasingly detailed picture of active site architecture in the spliceosome in which the reaction partners for the two transesterification reactions are brought together through a network of RNA-RNA interactions. Finally, I discuss evidence for potential analogs of several of the spliceosomal structures in Group II introns. These similarities complement the established chemical relationships between the two mechanisms, but they also raise interesting questions regarding the origins of introns and the spliceosome.

Figure 1

Two-Step Chemical Pathway of Nuclear Pre-mRNA Splicing.

Exons are represented by the black rectangles. Intron sequences that are virtually phylogenetically invariant are shown in large bold letters. Smaller letters show somewhat less conserved sequences. The consensus for *Saccharomyces cerevisiae* introns is shown. An apparently identical pathway is utilized by Group II self-splicing introns.

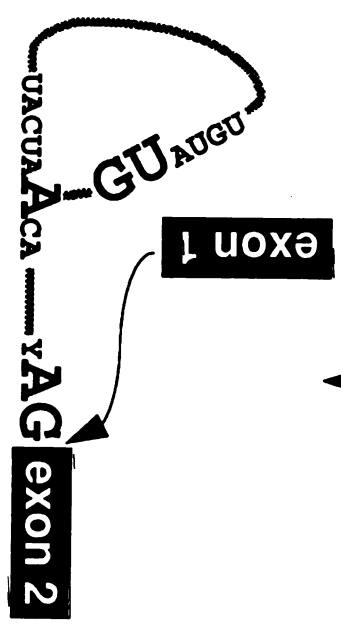
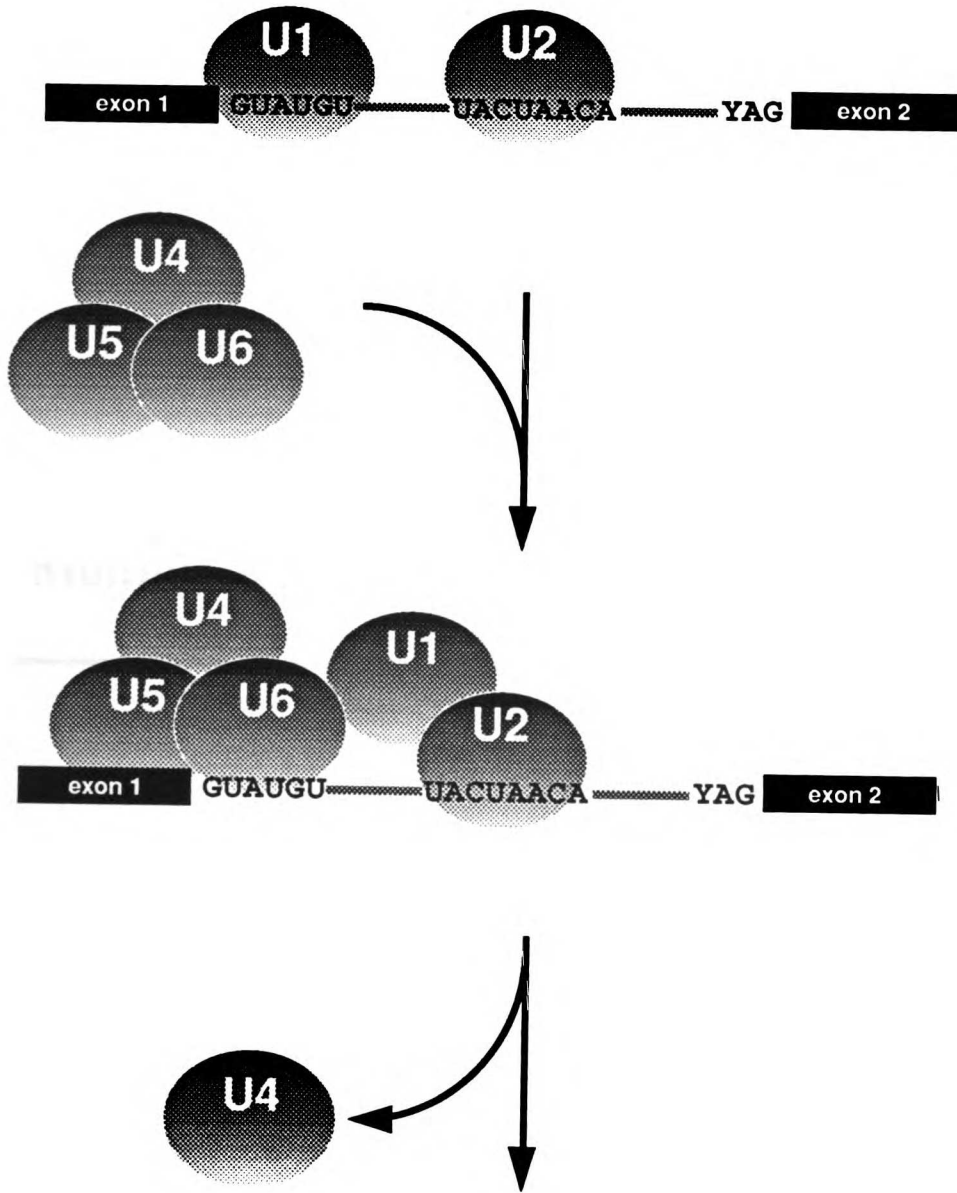


Figure 2.

Simplified View of Spliceosome Assembly

Following binding of U1 and U2 snRNPs to the pre-mRNA, a U4-U6.U5 triple snRNP binds to the complex. U4 snRNP is released prior to the first cleavage-ligation event.



CHEMICAL STEPS

CHAPTER 1

Multiple Roles for U6 snRNA in the Splicing Pathway

Summary

U6 is the most highly conserved of the five spliceosomal RNAs. It is associated with U4 by an extensive base-pairing interaction, which is disrupted immediately prior to the first nucleolytic step of splicing. It has been proposed that this event activates catalysis by unmasking U6. Using a combination of doped synthesis and site-directed mutagenesis to generate point mutations in U6, we have now identified 12 positions, in three domains, at which single nucleotide substitutions or deletions result in lethal or temperature-sensitive phenotypes. Biochemical analysis demonstrates that most of these mutants retain the ability to assemble into U4/U6 and U4/U5/U6 snRNPs. Notably, in three cases tested, mutations in U4 opposite to lethal mutations in U6 are fully viable in the context of wild-type U6. Furthermore, compensatory mutations in U4 that restore base-pairing fail to suppress the phenotypes of the U6 mutations. This demonstrates a function for U6 independent of its role in base-pairing. Remarkably, two of the three essential regions in U6 identified genetically correspond to intron insertion points in two yeast species. A temperature-sensitive mutation at one of these sites is defective in the second step of splicing *in vitro*.

Introduction

The removal of introns from messenger RNA precursors is an essential and often regulated step in the expression of eukaryotic genes. Splicing proceeds via a characteristic two-step transesterification reaction. In the first step, the 2' hydroxyl of an adenosine residue embedded in the intron attacks the phosphodiester bond that demarcates the 5' splice site, releasing the 5' exon and forming the so-called lariat intermediate. Attack of the phosphodiester bond that defines the 3' splice site by the 3' hydroxyl of the 5' exon results in the production of ligated exons and release of the intron as a lariat. Since this chemistry is apparently shared by Group II introns, some of which are capable of autocatalytic self-splicing, it has been proposed that the enzymatic functions of the nuclear mRNA splicing machinery are also mediated by RNA (Sharp, 1985; Cech, 1986).

Indeed, five evolutionarily conserved small nuclear RNAs (U1, U2, U4, U5, U6 snRNAs) packaged in ribonucleoprotein particles (snRNPs) are essential components of the eukaryotic splicing machinery (reviewed in Sharp, 1987; Maniatis and Reed, 1987; Steitz et al., 1988). Comparisons between the yeast and metazoan spliceosomal RNAs have revealed unexpected variation in size and sequence (reviewed in Guthrie and Patterson, 1988). For instance, the yeast U1, U2 and U5 snRNAs are from two to six times larger than their mammalian homologs; interestingly, these differences in size can be accounted for by nonessential yeast-specific domains that separate regions of conservation (Igel and Ares, 1988; Shuster and Guthrie, 1988, 1990; Kretzner et al., 1990; D. Frank and C.G., unpublished results). In contrast, yeast U4 and U6 are conserved in size (Siliciano et al., 1987; Brow and Guthrie, 1988), and, like their mammalian counterparts, are found base-paired to each other in a single snRNP (Siliciano et al., 1987; Brow and Guthrie, 1988; Hashimoto and Steitz, 1984; Bringmann et al., 1984).

Unlike U4, U6 is highly conserved at the primary sequence level, being 80 percent identical to metazoan U6 over half its length (Brow and Guthrie, 1988). This extraordinary conservation argues for a key role for U6 in the splicing reaction. U6 is unusual in several

other aspects: it lacks the 2,2,7-trimethylguanosine cap and binding site for the core (Sm) proteins found in the other spliceosomal RNAs (reviewed in Lührmann, 1988), and it is transcribed by RNA polymerase III rather than RNA polymerase II (Kunkel et al., 1986; Reddy et al., 1987; Krol et al., 1987; Brow and Guthrie, 1990). Based on phylogenetic comparisons, it was proposed that the base-pairing interaction between U4 and U6 snRNAs consists of two intermolecular helices termed stem I and stem II (see Figure 1; Brow and Guthrie, 1988). The stem I interaction was previously identified directly by psoralen cross-linking studies (Rinke et al., 1985). Recent data from mammalian *in vitro* assembly experiments as well as studies in yeast provide strong support for this model and indicate that both stems are required for the formation of the U4/U6 snRNP (Hamm and Mattaj, 1989; Bindereif et al., 1990; K. Shannon and C.G., in prep.).

The assembly of the spliceosome is a highly ordered process that requires ATP hydrolysis. In both yeast and mammals, the U1 and U2 snRNPs are involved in substrate recognition by binding sequences located at the 5' end and lariat branch point regions of the intron, respectively; these interactions are mediated in part by Watson-Crick base-pairing (Mount et al., 1983; Black et al., 1985; Parker et al., 1987; Zhuang and Weiner, 1986; 1989; Séraphin et al., 1988; Siliciano and Guthrie, 1988; Wu and Manley, 1989). Following binding of U1 and U2 snRNPs, the U5 and U4/U6 snRNPs assemble onto the pre-mRNA, possibly as a tripartite complex (Pikielny et al., 1986; Cheng and Abelson, 1987; Konarska and Sharp, 1987, 1988; Bindereif and Green, 1987). Subsequently, U4 appears to be destabilized from the spliceosome or at least is subjected to a large conformational change; this event is accompanied by the appearance of splicing intermediates and products (Pikielny et al., 1986; Cheng and Abelson, 1987; Lamond et al., 1988; Blencowe et al., 1989). Given that the native U4/U6 snRNP has a T_m of 53 °C (Brow and Guthrie, 1988), the destabilization of U4 is presumed to require an active process.

The temporal correlation between the apparent disruption of U4/U6 base-pairing and the nucleolytic steps of the splicing reaction has led to the hypothesis that the unwinding of the two RNAs allows U6 to be activated for participation in catalysis (Brow and Guthrie, 1989). Such a model would also account for the observation that the sequence of U6 within the base-paired interaction domain shows higher conservation than the corresponding region of U4 (18 vs. 11 nucleotides, respectively) by proposing that the nucleotides in U6 are under dual functional constraints (Guthrie and Patterson, 1988). According to this view, U4 might act primarily as a negative regulator, sequestering U6 in a catalytically inert conformation. A final motivation to the hypothesis was provided by the discovery of an mRNA-type intron in stem I of the *S. pombe* U6 gene (Tani and Ohshima, 1989): this intron may have arisen via an aberrant reverse splicing reaction, placing the region of intron insertion near potential catalytic residues (Brow and Guthrie, 1989).

Here we present the first detailed genetic analysis of the *S. cerevisiae* U6 gene as a first step in testing the model that U6 plays a role in addition to base-pairing with U4, conceivably in the chemical steps of splicing. Our strategy involved a combination of doped synthesis and site-directed mutagenesis to generate point mutations in U6; using a simple genetic screen, we then identified mutants with lethal or conditionally lethal phenotypes. Mutants of further interest are those which 1) produce stable U6 RNA, 2) assemble into U4/U6 and U4/U5/U6 snRNPs, and 3) ideally, enter the spliceosome and progress beyond the event of U4 destabilization. We report here the identification of 12 positions at which single nucleotide substitutions or deletions result in lethal or temperature-sensitive phenotypes. The location as well as the genetic and biochemical behavior of these mutants suggest that highly conserved nucleotides within U6 are required for multiple steps in the splicing pathway; among these may be plausible candidates for residues that may be directly involved in the splicing reaction.

Results

Mutant Isolation

We sought to identify point mutations in the yeast U6 snRNA that confer lethal and conditional lethal phenotypes. Towards this end, we synthesized the coding sequence of the *S. cerevisiae* U6 gene (SNR6) from degenerate oligonucleotides as described in Figure 2A. A large library of mutant U6 genes was created by using this pool of mutagenized oligonucleotides to replace the wild type U6 sequence present on a yeast-*E. coli* shuttle vector (Figure 2A and Experimental Procedures). In order to assess the content of the mutant library we have sequenced a limited number of randomly-selected clones from the library; the frequency of single nucleotide substitutions observed agreed with that expected from the initial level of oligonucleotide degeneracy (see Experimental Procedures).

SNR6 is a single-copy essential gene (Brow and Guthrie, 1988). This allowed us to use a simple genetic screen based on the plasmid shuffle method (Boeke et al., 1987) to identify lethal and conditional lethal mutants in the U6 snRNA (Figure 2B). DNA prepared from the mutant library described above was introduced by transformation into the yeast strain YHM1, which contains a precise deletion of the yeast U6 gene (snr6::LEU2) complemented by a wild type copy of U6 carried by a CEN, URA3 plasmid.

Approximately 5000 such yeast transformants, initially plated at 30°C, were replica-plated to plates containing 5-fluoroorotic acid (FOA), which selects for cells that have lost the URA3-marked plasmid. Cells that fail to grow on FOA therefore contain an SNR6 gene with a lethal mutation. Replica-plating onto FOA plates which are incubated at 18°C or 37°C allows the isolation of conditional mutants. To identify the mutation, DNA was isolated from the mutant strains and used to transform *E. coli*. The sequence of the U6 coding region was then determined for each mutant. In addition, we assessed the phenotype of the randomly-selected mutants described above; all of these were viable.

In our genetic screen, we expected to isolate a substantial fraction, but by no means all, of the possible lethal and conditional nucleotide substitutions in the yeast U6 snRNA;

this expectation is borne out by observation that mutants that map to a conserved hexanucleotide comprise 4/12 of the possible lethal point mutations in this region as determined by saturation site-directed mutagenesis (see below). Thus, because our screen is subsaturating (covering roughly one-third of possible point mutations), the absence of a particular mutant cannot be taken as evidence for its viability.

The yeast U6 snRNA can be described by five phylogenetically-defined structural domains: the 5' stem-loop, a single-stranded central domain, stem I and stem II of the U4/U6 interaction domain, and the 3' terminal domain (Brow and Guthrie, 1988; Guthrie and Patterson, 1988; and Figure 1). The U6 mutants found using the mutagenesis strategy described above are shown in Table 1. For lethal mutants, only single nucleotide substitutions and deletions are listed, although we did obtain a number of multiple mutants as well. In the case of the conditional mutants, three larger deletions are also shown as these proved to be informative (see below). For viable mutants, both single and multiple substitutions as well as deletions and insertions are listed, as these identify nucleotides that can be altered with no phenotypic consequences even in combination with other changes (although the possibility of intragenic suppression cannot be ruled out). Of the 15 mutations identified as lethal or conditional lethal single nucleotide substitutions or deletions (Table I), all affect invariant residues (11 in total). Conversely, we obtained viable changes affecting a total of 21 nucleotides, 11 of which are invariant residues. The location and phenotypes of the point mutants listed in Table 1 are summarized in Figure 1 in the context of the structural model proposed by Brow and Guthrie (1988). Below, we describe these mutants in terms of this structure.

5' stem-loop

Most of the size variation observed in U6 snRNAs across evolution can be accounted for by differences in the 5' stem-loop (Roiha et al., 1989; Guthrie and Patterson, 1988). As shown in Figure 1, few nucleotides in this domain are phylogenetically invariant: the G-C pair at the base of the stem, a C-G pair within the stem and the

conserved C at position 14 in the loop. Our analysis indicates that changes in some of these conserved elements are viable (see Figure 1). Deletion of the G at position 1 does, however, result in a cold-sensitive phenotype, as do several other mutations containing changes at or near the transcription start site (Table 1 and data not shown). This phenotype may result from a transcriptional defect, consistent with the finding of Mattaj et al. (1988) that nucleotides around the start site of a *Xenopus* U6 gene are determinants of transcriptional efficiency. Interestingly, the mutation Δ U3-G7 introduces a large disruption of the 5' part of the stem loop and results in cold-sensitivity, whereas a mutation which deletes the 3' half of the stem-loop, Δ U21-C25, exhibits a more severe phenotype, growing very poorly and only at 30°C (Table I). A potential explanation for this discrepancy is suggested by recent analysis of the promoter of the yeast U6 gene, which implicates an intragenic A block promoter element (spanning nucleotides 21-31) in the transcription of SNR6 by RNA Polymerase III (Brow and Guthrie, 1990). Thus, the phenotype of Δ U21-C25 may be due to a defect in transcription.

Central Domain

With the exception of mutations lying in the A block consensus sequence, we have not recovered mutations affecting U6 function in the 5' three-quarters of this region. In fact, numerous mutations that alter invariant nucleotides in this area have no phenotype (see Figure 1). In contrast, a concentration of lethal and temperature sensitive point mutations are found in the 3' end of the central domain, in the sequence ACAGAGA (positions 47-53) which is invariant in all species examined (Guthrie and Patterson, 1988).

Stem I

We also recovered several lethal and temperature sensitive nucleotide substitutions and deletions in the conserved stem I region (Figure 1 and Table 1), in the trinucleotide AGC (positions 59-61). Interestingly, this cluster of lethal mutations is in a region that base-pairs with U4 snRNA.

Stem II

This helix, like stem I, is highly conserved in primary sequence (11 invariant residues out of 17). In contrast to the central domain and stem I, we recovered only one lethal single-nucleotide substitution in this domain, U80G (recovered twice). However, given the subsaturating extent of our mutagenesis, there may well be other lethal single nucleotide substitutions in this domain. Two other single nucleotide deletions in this region are lethal ($\Delta A75$ and $\Delta G77$). Notably, deletions in stem II per se do not always result in lethality: deletion of positions 69 or 72 (in A34U G39A $\Delta C72$) and substitution of position 68 (A34C G68G C92U) are viable.

3' terminal domain

This region is poorly conserved in sequence but is between 29 and 32 nucleotides in all species. This strict size conservation may reflect structural constraints. Consistent with this notion, we recovered no lethal point mutations in this domain. However, alterations in the length of the 3' terminal domain, such as deletion of nucleotides 90-98 (Table 1) and insertion of 4 nucleotides after position 86 in a complex mutant (data not shown) each result in a leaky cold-sensitive phenotype.

In summary, our genetic screen allowed us to recover 15 point mutations (single-nucleotide substitutions or deletions) identifying 11 positions of the U6 snRNA that confer lethal or conditional phenotypes. These nucleotides map to five regions of the molecule: position 1, the ACAGAGA box in the central domain, the trinucleotide AGC in stem I of the U4/U6 interaction domain and the 3' terminal nucleotide of stem II. Our interest in the ACAGAGA and AGC motifs was further spurred by the finding that they are interrupted by unusual mRNA-type introns in the yeast species *R. dacyroidum* (ACAGA/G; "/" indicates intron position) and *S. pombe* (/AGC) (Tani and Ohshima, 1989; personal communication). These observations led us to investigate these two regions in more detail.

Saturation Mutagenesis of the ACAGAGA Box

We constructed all possible single nucleotide substitutions in the ACAGAGA box (positions 47-53 in Figure 1) by oligonucleotide-directed mutagenesis. The U6 point

mutants were subcloned into the vector pSE358 (CEN, TRP1), transformed into YHM1 and their phenotypes assessed by the plasmid shuffle method. The results are summarized in Figure 3. Notably, despite the small size (7 nts) of the mutagenized region, we obtained a complex array of mutant phenotypes. Any change in positions 48, 49, and 51 results in lethality. Substitution of G52 by an A or a C is also lethal; a U, however, results in leaky temperature-sensitivity. The phenotype of mutants at position 47 also depends on the substituted nucleotide: a C is lethal, a U is viable and a G results in a leaky temperature-sensitive phenotype. Curiously, a deletion of nucleotide 47 which brings the nucleotide at position 46, a U, into position 47 (creating the sequence UCAGAGA) is not fully viable but exhibits leaky temperature-sensitive growth (Table I). This may reflect spacing constraints in this region. A spectrum of phenotypes is also seen at position 50: substitution of this G with a C is viable at all temperatures, a U is temperature-sensitive and an A allows the cells to grow very poorly at 18°C or 23°C, and not at all at higher temperatures. Changing the nucleotide A53 to a G or a C has no effect on growth.

Asymmetric Phenotypes in the U4/U6 Interaction Domain

Since the invariant nucleotides AGC in stem I are part of a phylogenetically conserved intermolecular helix (Figure 1), a straightforward explanation for the lethal phenotypes of stem I mutants is that they are defective in base-pairing with U4 snRNA. This hypothesis makes two predictions: first, analogous mutations in U4 that disrupt stem I should have a deleterious phenotype; second, compensatory mutations in U4 that restore base-pairing in stem I should suppress the lethal or temperature-sensitive phenotype of the U6 stem I mutants as has been shown for mutants in stem II (K. Shannon and C. G., unpublished).

In order to test this hypothesis, we constructed eight mutations in the yeast U4 gene (which is encoded by the SNR14 gene; Siliciano et al., 1987) in stem I at positions that base-pair with the conserved AGC trinucleotide in U6 described above (positions 58, 59, 60 in SNR14). The U4 mutant genes were subcloned into the pSE362 vector

(CEN,HIS3) and transformed into a strain containing a disruption of the chromosomal U4 gene (snr14::TRP1). Their phenotypes were tested using the plasmid shuffle method and are shown in Table II. Surprisingly, all U4 mutant strains were viable at every temperature tested and exhibited no detectable growth defects (Table II, column 1). To test whether or not compensatory mutations in U4 could suppress the phenotype of U6 mutants in stem I, U4 mutants at position 59, which base-pairs with position 60 in U6, were introduced in strains containing a deletion of the chromosomal U6 gene and either of the two lethal U6 mutant RNAs at position 60 (G60U or G60C; G60C was constructed by site-directed mutagenesis). In addition, they also contained a rescuing U6 wild type gene on a URA3-marked plasmid. The resultant strains failed to grow on FOA, indicating an inability to lose the wild type U6 URA3-marked plasmid, regardless of the U4 mutant introduced (Table II). Moreover, transformation of a strain harboring the temperature-sensitive mutation C61G with the U4 genes mutated at position 58, results in no suppression: such strains are viable at 18-34°C but fail to grow at 37°C regardless of the U4 allele present (Table II). We cannot rule out the possibility that the U4 compensatory mutants exhibit a recessive defect that prevent them from competing with the wild type U4 for association with U6. This seems unlikely, however, since strains harboring only the mutant U4 genes have no obvious growth defects. Taken together, these results indicate that the lethality of the U6 stem I mutations cannot be attributed (solely) to defects in base pairing with the U4 snRNA.

RNA Accumulation of Lethal U6 Mutants

It is important to determine whether the phenotype of lethal U6 mutants might be due to defects in their expression and/or stability, as opposed to functional defects per se. We thus assessed RNA levels in vivo by Northern hybridization. Since these mutants are inviable in the absence of a wild type U6 gene, this analysis had to be performed on heterozygous strains containing both mutant and wild type U6 RNAs. Due to similarities in sizes, however, these two RNAs could not be resolved by gel electrophoresis. To

circumvent this problem, we constructed a "pseudowildtype" U6 gene (U6-5'Sp) in which the 25 nt *S. cerevisiae* 5' stem-loop is replaced by the 12 nt 5' stem-loop of *S. pombe* (nts 1-12; Tani and Ohshima, 1989); the remainder of this hybrid encodes wild type *S. cerevisiae* U6 sequences. The U6-5'Sp chimeric RNA was cloned into the vector pSE360 (CEN, URA3) and a strain derived from YHM1 was constructed in which this gene was the sole copy of U6. The growth rate of this strain is identical to the wild type parent (data not shown). Various U6 mutants cloned into pSE358 (CEN, TRP1) were transformed into this strain to generate heterozygotes, as diagrammed in Figure 4A. Since the chimeric RNA is only 99 nucleotides in length, compared to 112 nucleotides in the case of point substitutions, the two U6 species can be easily separated by electrophoresis through denaturing polyacrylamide gels.

Northern analyses were performed as described in the Experimental Procedures. The results are shown in Figure 4B. In a control heterozygous strain containing a copy of both the pseudowildtype (U6-5'Sp) and wild type U6 genes, the pseudowildtype RNA is found at approximately three-fold lower steady-state levels (as determined by densitometric scanning) compared to the wild type U6 snRNA (Figure 4B, lane 23). This is likely to be due to differences in transcriptional efficiency since the replacement of the *S. cerevisiae* 5' stem loop with that of *S. pombe* alters the A block consensus sequence found at positions 21-31 (Brow and Guthrie, 1990). As expected, a deletion in the A block in the mutant Δ U21-C25 results in barely-detectable amounts of RNA compared to the pseudowildtype internal control (Figure 4B, lane 24). Interestingly, this deletion mutant actually grows at 30°C, albeit slowly, demonstrating that a drastic reduction in U6 RNA levels can be tolerated without preventing growth. This is consistent with the fact that in yeast U6 is present in 5-10 fold excess over U4 (Siliciano et al., 1987; D. Brow and C.G., unpublished).

As shown in Figure 4B, point mutations in the ACAGAGA box at positions 47 (lanes 3 to 5) and 52 (lanes 18 to 20) as well as substitutions at position 50 (lanes 12 to 14)

result in RNA levels comparable to the pseudowildtype RNA. Similarly, Northern analysis of the 6 lethal mutants in stem I and stem II of the interaction domain demonstrates that they are stable in heterozygous strains (Figure 4B, lanes 25 to 30). In contrast, mutants at positions 48 and 49 (lanes 6 to 11) and to a lesser extent position 51 (lanes 15 to 17) contain 3-5 fold less steady-state levels of RNA. This is unlikely to be due to a transcriptional defect since genes with multiple changes in the ACAGAGA box are transcribed as well as the wild type gene (data not shown) in a *in vitro* yeast transcription system (Brow and Guthrie, 1990).

The decreased steady-state levels of mutants at positions 48, 49 and 51 may be a consequence of defects in snRNP formation and/or stability. In this regard, it is interesting to note that the amount of the U6-5'Sp RNA in all the heterozygous strains carrying a mutant U6 gene is 3 fold higher than in a heterozygous strain carrying the wild type U6 gene (Figure 4, compare all lanes with lane 23). One possible explanation for this is that the mutant RNAs compete less well than the wild type U6 snRNA for factors involved in snRNP formation and/or stability. However, the same effect is observed in heterozygous strains carrying fully viable alleles (for example, A47U and mutations at position 53). This and the observation that large reductions in the steady-state level of U6 can be tolerated (see above) indicate that the lethality of mutants in the ACAGAG hexanucleotide cannot solely be explained by defects in snRNP formation and/or stability, although it may of course contribute to the phenotype.

Assembly of U6 Mutant RNAs into U4/U6 and U4/U5/U6 snRNPs

Another potential explanation for the phenotype of lethal U6 mutants is defective snRNP-snRNP interactions. To test this possibility we took advantage of our previous demonstration that the three particles containing U6 (U6, U4/U6 and U4/U5/U6 snRNPs) can be separated by velocity sedimentation on glycerol gradients (Bordonné et al, 1990). Extracts prepared from heterozygous strains used in the Northern hybridization

experiments were fractionated on 10-30% glycerol gradients and the RNA was analyzed by Northern hybridization probing simultaneously for U4, U5 and U6 snRNAs.

The results are shown in Figure 5 (panels A-E). The control extract was made from a strain containing both wild type U6 and chimeric U6-5'Sp genes. As can be seen in panel A, three different particles are resolved: free U6 snRNP (fractions 17-21), U4/U6 snRNP (fractions 13-15) and U4/U5/U6 snRNP (fraction 1-5). Most U6 is found as free snRNP or in the U4/U5/U6 snRNP. Curiously, despite the fact that the U6-5'Sp RNA is found at 3 fold lower levels than the wild type U6 RNA in fractions 17-21 containing free U6 snRNP, it is present in equimolar amounts in fractions containing the U4/U5/U6 snRNP (fractions 1-5); the reason for this is unknown.

As expected from the Northern analysis, the ratios of mutant to pseudowildtype RNA in the free U6 snRNP fractions of the gradients of lethal U6 mutants (panels B-E) are consistent with a range of defects in stable snRNP formation, with C48G (panel B) exhibiting the greatest difference and U80G (panel E) being expressed as well as the pseudowildtype. Despite these differences, one can assess the ability of a given mutant to form multi-snRNP complexes on a "per molecule" basis by comparing the ratio of mutant to pseudowildtype RNA in fractions containing free U6, U4/U6 and U4/U5/U6 snRNPs.

The extreme instability of the C48G mutant (Figure 4B, lane 7) makes the interpretation of the gradient analysis of this mutant difficult. An overexposure of the autoradiogram is shown in Figure 5, panel B. Some mutant RNA can be observed in the U4/U6 and U4/U5/U6 snRNP-containing fractions; however, the ratio of mutant to pseudowildtype RNA is lower than that found in the free U6 snRNP-containing fractions (compare lanes 1-5 with 17-21), suggesting some defect in snRNP-snRNP interaction(s) in this mutant. An identical pattern was observed for another relatively unstable mutant A49G (data not shown).

Another mutant in the ACAGAG region, A51C (panel C) appears to retain the ability to interact with U4 and U5 (witness the ratio of mutant to pseudowildtype RNA in

fractions 1-3, 9-13 and 15-19), as does the stem I mutant G60U (panel D). Analysis of the G50A and G52A mutants as well as for the stem I mutants Δ A59 and G60C indicate that these mutants are similarly assembled into U4/U6 and U4/U5/U6 particles (data not shown). In contrast, the lethal mutant in the terminal base-pair of stem II (U80G), which is expressed as well as the pseudowildtype internal control, exhibits a severe defect in snRNP-snRNP interaction. This mutant barely forms appreciable amounts of U4/U6 or U4/U5/U6 snRNPs in heterozygous extracts (panel E; compare ratios of U6 RNA found in fractions 1-5 and 17-21).

In summary, these results indicate that most mutants in the ACAGAGA motif and the stem I region still retain the ability to form U4/U6 and U4/U5/U6 snRNPs despite varying degrees of stable RNA accumulation; thus, they may be defective in steps downstream of the formation of the U4/U5/U6 snRNP. It is therefore of interest to determine whether these mutant snRNPs are assembled into the spliceosome.

Unfortunately, we have been unable to assess this parameter because of the difficulty in isolating sufficient quantities of yeast splicing complexes to quantitatively analyze mutant and wild type RNA composition by Northern hybridization.

The efficiency of the second step of the splicing reaction is decreased in the G50A mutant.

In order to assess the defective function of U6 snRNAs harboring temperature-sensitive mutations, we have examined their activities in vitro. Splicing was examined in extracts prepared from strains carrying one of three temperature-sensitive alleles, G50A, G50U or G52U, as their sole copy of U6. Particularly interesting was the mutant G50A which shows a severe growth defect, even at permissive temperature (Figure 3). Incubation of radioactive actin mRNA precursor in a splicing extract prepared from this strain results in successful completion of the first step of splicing, but a drastic decrease in the efficiency of the second step of the reaction (3' splice site cleavage and exon ligation) both at 15°C (compare the ratio of lariat to lariat intermediate in Figure 6, lanes 3 in panels A,B) and at 23°C (lane 6, panel A). In contrast, the efficiency of splicing in an extract prepared from

G50U and G52U strains (lanes 4,5,7 and 8 in panel A, lane 5 in panel B) is comparable to that found for a wild type extract (lane 1 in panel A, lane 2 in panel B). This correlates with the superior growth phenotypes of G50U and G52U compared to the G50A mutant. Identical results were obtained with an independent G50A extract (lane 4 in panel B), indicating that the decrease in the efficiency of the second step of splicing is not due to variation in extract preparation. The defect of the G50A extract can be complemented with a U6-containing, snRNP-enriched fraction (fraction I; Cheng and Abelson, 1986) from a wild type extract (lane 9 in panel A). The slight decrease in the amount of lariat intermediate observed in the G50A extract compared to wild-type (compare lanes 3 and 6 to lane 1 in panel A) is also ameliorated by the addition of fraction I (lane 9), suggesting that the G50A mutant may have a small effect on the first step in addition to its substantial defect in the second step of the splicing reaction.

Discussion

Mutagenesis Identifies Twelve Critical Residues in U6 snRNA

Of the five RNAs required for the splicing of mRNA precursors (U1, U2, U4, U5, and U6 snRNAs), only two have been assigned specific functions: in both yeast and mammals, the U1 and U2 snRNAs interact with the intron substrate, in part by Watson-Crick base-pairing (see Introduction for references). In contrast, little is known regarding the roles of the U4, U5 and U6 spliceosomal RNAs. Of these three, U6 is by far the most conserved in size and sequence, implying strong functional constraints; it is therefore a particularly attractive target for genetic studies. Previous functional analysis of yeast spliceosomal RNAs by site-directed mutagenesis revealed a surprising tolerance to point mutations, even when phylogenetically invariant nucleotides were altered. Examples include the dispensability of the conserved loop IV sequence of U2 (Shuster and Guthrie, 1990), the flexibility of the highly conserved A(U3-6)G Sm binding site in U5 snRNA (Jones and Guthrie, 1990) and the viability of most point mutations in the invariant loop of U5 snRNA (B. Patterson, D. Frank and C.G., unpublished results). Finally, even several mutants in the invariant 5' end of U1 snRNA, which interacts directly with the intron by base-pairing, are viable (Siliciano and Guthrie, 1988; Séraphin et al., 1988). This apparent tolerance may reflect subtle contributions of particular invariant residues, or redundant interactions. Conversely, the clusters of lethal point mutations identified at the 5' end of U1 snRNA or in the branchpoint recognition domain of U2 snRNA reflect critical and highly-constrained interactions between these snRNAs and the intron (Siliciano and Guthrie, 1988; Séraphin et al., 1988; Parker et al., 1987; T. Simmons, J. Milligan and C.G., unpublished).

Because of the difficulty in identifying critical nucleotides in spliceosomal RNAs by site-directed mutagenesis, we have first employed a genetic screen to identify lethal point mutations in the yeast U6 snRNA. By coupling a generally applicable strategy for uniformly mutagenizing the U6 gene with such a screen, and then performing further

site-directed mutagenesis, we have succeeded in identifying 12 positions in the U6 snRNA at which substitution or deletion of a single nucleotide is a lethal or temperature-sensitive event. Six of these positions lie in the U4/U6 interaction domain while the other six cluster in an invariant hexanucleotide upstream of the interaction domain. Further genetic and biochemical analyses of these mutant RNAs suggest that the sensitivity of these particular conserved residues to mutation reflects important roles for U6 at multiple points in the splicing pathway.

A Point Mutation in Stem II Blocks Formation of the U4/U6 snRNP

We have shown by Northern analysis and velocity sedimentation experiments that most mutants in the conserved hexanucleotide and in stem I of U6 are stable and retain the ability to assemble into U4/U6 and U4/U5/U6 snRNPs. In contrast, a point mutation in the terminal base-pair of stem II of the U4/U6 interaction domain (U80G), while producing stable U6 RNA, almost completely abolishes formation of U4/U6 and U4/U5/U6 snRNPs, implicating this conserved residue in the association of U4 and U6 snRNAs during the splicing cycle. The defect in U80G seems unlikely to be due merely to disruption of the U4/U6 base-pairing interaction, however, since three mutants that are predicted to reduce base-pairing in stem II to an equal or greater degree are fully viable (Table 1). Further genetic analysis, including the testing of the effect of a compensatory mutation in U4 that restores base pairing with this mutant, is needed to resolve this issue.

Asymmetric Roles for U4 and U6 in Stem I

We have found that stem I of the U4/U6 interaction domain harbors crucial residues on the U6 side of the helix in the conserved trinucleotide AGC (positions 59-61). Strikingly, the presumptively base-paired residues in U4 are not required for function in vivo despite the fact that two of these are phylogenetically invariant. Furthermore, compensatory mutations in U4 that restore base-pairing with lethal or conditional lethal U6 mutants fail to suppress the biological phenotypes. We conclude that those residues in U6 play a role in splicing independent of base-pairing with U4. Since lethal mutants in this

region produce stable U6 RNA, and the mutant U6 snRNPs associate with U4 and U5 snRNPs, we propose that the invariant AGC trinucleotide functions in critical interactions downstream of the formation of the U4/U5/U6 snRNP (see below).

The observation that all eight mutations at positions 58-60 in stem I of U4 are tolerated, together with the finding that three point substitutions in stem II in U6 are viable, suggests that the precise structural character of the U4/U6 base-pairing interaction may be relatively flexible. Indeed, inspection of the structure of the U4/U6 helices from various species reveals some variation in helix lengths and placement of bulges; however, the overall extent of base-pairing remains relatively constant, suggesting that it is the main functional parameter (Guthrie and Patterson, 1988). Given the asymmetry between U4 and U6 described above, one role for the base-pairing interaction may be to attach U6 to U4 for delivery to the spliceosome via interactions between U4 and other factors. This is consistent with the observation that the 5' stem-loop of U4, which is required for the binding of the PRP4 protein (Xu et al., 1990) is also required for the association of the U4/U6 snRNP with the U5 snRNP (Bordonné et al, 1990).

A Mutation in the ACAGAG Hexanucleotide is Defective in a Late Step of Splicing

Construction of all possible nucleotide substitutions in the ACAGAG hexanucleotide revealed that all positions are required for U6 function; interestingly, in several cases, different changes at a single nucleotide gave rise to different biological phenotypes. For instance, changing A47 to a C is lethal, a G is temperature-sensitive, and a U is viable (Figure 3). Notably, this pattern of phenotypes does not correlate with ability of A47 to engage in Watson-Crick base-pairing; in that case both C and U changes would be equally deleterious. In this regard, it is useful to consider our data in the terms of a model proposed by McPheeters et al. (1989), that proposes base-pairing between a conserved region of U2 snRNA just downstream of the branchpoint interaction domain and the ACAGAG region in U6. The appeal of this hypothesis is that it would juxtapose highly conserved regions of U6 with the intron branchpoint. However, as the pattern of

mutant phenotypes in the ACAGAG hexanucleotide (at positions 47, 50, and 52) does not correlate with the expected disruption in base-pairing, our data do not lend immediate support to this model.

While mutants at positions 48 and 49 accumulate very low levels of U6 RNA, perhaps reflecting disruption of a protein-RNA interaction required for U6 snRNP formation, those at positions 47, 50, 52 and to a lesser extent position 51 produce more stable RNA and, where tested, appear to retain the ability to interact with U4 and U5 snRNPs. This result is consistent with that of Bindereif et al. (1990) who have demonstrated that a mutant human U6 RNA that contains a deletion of the first 52 nucleotides, which includes the invariant ACAGAG region, is efficiently assembled into U4/U6 particles in an in vitro system. Finally, we show here that a strain carrying the G50A mutation in U6 exhibits a significant decrease in the efficiency of the second step of the splicing reaction in vitro. Since the first step is efficiently completed, all previous steps of spliceosome assembly, including the destabilization of U4 must also occur.

Possible Implications

As described in the Introduction, these studies were motivated by the hypothesis that U4 functions to deliver U6 to the spliceosome and to sequester functionally important residues in U6. Considering the simplest form of the hypothesis, one predicts the existence of residues in U6 that reside in the interaction domain that cannot be altered without abolishing their function; in contrast, their partners in U4 should be relatively insensitive to mutation, provided that the overall stability of the base-pairing interaction is maintained. Indeed this prediction is satisfied by the asymmetric phenotypes exhibited by the mutations in stem I described above. Secondly, as expected of residues whose (primary) function is in catalysis, most lethal mutants in U6 accumulate stable RNA and assemble into U4/U5/U6 snRNPs. Furthermore, one of these mutants, G50A, must be assembled into the spliceosome as it completes the first step of the splicing reaction in vitro.

While the genetic and biochemical behavior of these mutants satisfy several important predictions of the hypothesis outlined above, we can by no means rule out the alternative interpretation that the essential residues identified by lethal point mutations function primarily as protein binding sites. Genetic suppression studies may help to distinguish between these models. Ultimately, of course, high-resolution structural studies will be required to determine whether these residues are part of the active site(s) of the spliceosome or play a more indirect role.

It is, however, provocative to consider our results in the context of the discovery of mRNA-type introns in U6 snRNAs. Based on the identification of a single insertion event in stem I of *S. pombe* U6 (Tani and Ohshima, 1989), it was proposed that this region of U6 is in close proximity to the intron during the actual splicing reaction (Brow and Guthrie, 1989). According to this view, residues in U6 flanking the intron insertion point are predicted to play a functionally important role in the reaction. Indeed, we have shown that the AGC trinucleotide adjacent to the insertion site in stem I exhibits asymmetric behavior with respect to U4 and that mutations in these invariant residues must affect a step(s) in the pathway downstream of formation of the triple snRNP. While this correlation might have been argued to be purely coincidental, we now find a remarkable concordance with the location of a second intron in the conserved ACAGAG hexanucleotide in the yeast *Rhodospiridium dactyoidum* (Tani and Ohshima, pers. comm.). Taken together, these observations are consistent with the hypothesis that the nucleotides in stem I and the upstream hexanucleotide not only serve critical roles, but are also good candidates for residues that participate directly in the splicing reaction.

Experimental Procedures

Yeast strains, plasmids and genetic methods

The strain YHM1 (MATa ura3 his3 lys2 trp1 leu2 snr6::LEU2 YCp50-SNR6) is a haploid strain carrying a disruption of the chromosomal copy of the SNR6 gene in which the U6 coding sequence (nts -10 to +122, Brow and Guthrie, 1988) is replaced by the yeast LEU2 gene. The wild type U6 gene is carried on a YCp50 (CEN, URA3) plasmid. The strain YKS2 (MATa ura3 his3 lys2 trp1 ade2 snr14::TRP1 YCp50-SNR14) was described previously (Bordonné et al, 1990). The shuttle vectors (pSE358, 360 and 362) used in this study were obtained from S. Elledge. pSE358 is a precursor of pUN10; pSE360 and pSE362 are identical to pUN50 and pUN90, respectively (Elledge and Davis, 1988). All yeast manipulations were performed according to standard methods (Rose et al., 1989). The phenotypes of the U6 and U4 mutations were determined by the plasmid shuffle method (Boeke et al, 1987).

Construction of a Library of Mutant SNR6 Genes

Introduction of Restriction Sites Flanking the U6 Coding Sequence

A 1.4 Kb EcoRV-HpaI subclone containing the U6 gene (Brow and Guthrie, 1988) was cloned into the EcoRV site of the pBluescript (-) vector (Stratagene). Sph I and Xho I sites were introduced in the region flanking the coding sequence of SNR6 by oligonucleotide-directed mutagenesis using the Kunkel method (Kunkel et al., 1987; McClary et al., 1989). The SphI site was introduced at the 5' end of the U6 gene by mutation of the nucleotides ACT (positions -7 to -5) to TGC. The Xho I site was created by making an A to C change at position +122. This mutated DNA fragment was excised from the vector using the Bam HI and Sal I restriction sites present in the polylinker. Bam HI linkers were added according to standard methods (Sambrook et al., 1989), and the resulting insert fragment was gel-purified. The yeast-E. coli shuttle vector pSE358 (CEN,

TRP1) was digested with Sph I and Bam HI, Bam HI linkers were added, and the resulting DNA was gel-purified. Ligation of vector and insert resulted in the production of the plasmid pSX6. Yeast strains carrying this plasmid as sole source of U6 exhibited no growth defect compared to the parental strain, indicating that the Eco RV-Hpa I genomic clone containing the Sph I and Xho I sites could fully complement a disruption of SNR6 .

Synthesis and Cloning of the U6 Coding Sequence from Degenerate Oligonucleotides

Two 82 nt oligonucleotides were synthesized. Oligo 182 encodes the sense strand of SNR6 from nts -13 to +69 (Brow and Guthrie, 1988). Oligo 282 encodes the antisense strand of SNR6 from nts +130 to +49. The two oligonucleotides overlap by 21 nts. They differ from the wild type sequence in that Oligo 182 carries an Sph I site at its 5' end and oligo 282 contains an Xho I site at its 3' end; these sites are identical to those introduced above. Both oligonucleotides were synthesized at a low level of degeneracy (99.84% correct, 0.16% mixture of the three incorrect nucleotides) throughout their length. The oligonucleotides were annealed by heating to 75°C and cooling slowly (1°C/min) to room temperature in a 0.5 ml mixture containing 10 mM Tris-HCl pH 7.5, 50 mM NaCl, 10 mM MgCl₂, 5 mM DTT, 33 mg/ml BSA, and of 400 ng each oligonucleotide. Following annealing, dATP, dCTP, dGTP and dTTP were added to a final concentration of 250 μM along with 300 units of the Klenow fragment of E. coli DNA polymerase I in a final reaction volume of 0.6 ml. Following incubation at 23 °C for 1 hour, the mixture was extracted with phenol and chloroform, precipitated with ethanol and digested with 300 U of Sph I and 600 U of Xho I in a volume of 0.1 ml. The reaction mixture was then extracted with phenol and chloroform, precipitated with ethanol, resuspended in 10 mM Tris-HCl pH 8.0, 1 mM EDTA and chromatographed on Sephadex G-50 to remove the short end oligonucleotides created by restriction digestion. The flow-through fraction represents a pool of degenerate DNA fragments that correspond to the coding sequence of the U6 gene.

The plasmid pSX6 (1μg) described above was digested with Sph I and Xho I. The large fragment lacking the SNR6 coding sequence was gel-purified and ligated to the pool

of degenerate U6 DNA fragments described above using T4 DNA ligase. The reaction mixture was treated with GeneClean (Bio 101) according to the manufacturer's recommendations, and the DNA was introduced into the E. coli strain DH5a (Hanahan, 1983) by electroporation (Dower et al., 1988). We made the assumption that the two-fold higher level of degeneracy in the region where the two oligonucleotides overlap is corrected by mismatch repair in E. coli. We have detected no bias either for or against mutations in the overlap region (see Table 1). A small amount of the transformation mixture was plated in serial dilutions to assess transformation efficiency; the rest was used to inoculate a 1 liter culture for the preparation of plasmid DNA. The serial dilutions revealed that there were approximately 2×10^5 transformants.

Expected and Observed Frequencies of Single Nucleotide Substitutions

The expected fraction of mutants in the library containing a single nucleotide substitution was calculated using the formula $F(P) = n! P^{n-r} (1-P)^r / (n-r)! r!$ where $F(P)$ is the fraction of oligonucleotides that contain r changes in a sequence of length n , and where $1-P$ is the level of degeneracy (Sambrook et al., 1989). In our case, considering single changes ($r=1$) in the SNR6 coding sequence ($n=112$) where the level of degeneracy is 0.0016, the fraction of molecules containing a single change is equal to 0.15. Sequencing of 43 randomly-selected clones from the mutant library revealed six (14%) that contained a single change in the SNR6 coding region, in reasonable agreement with the 15% value predicted (data not shown). Since there are $112 \times 3 = 336$ possible single nucleotide substitutions in SNR6, each mutation will be represented once, on average, in 2240 clones ($336/0.15$). Therefore, by screening 5000 colonies, each single nucleotide substitution would be expected to be represented 2.2 times on average. Again, this is approximately equal to the observed value of 2.0 (calculated from values listed in Table 1).

Isolation and Analysis of Mutant Plasmids

Plasmid DNA were isolated from yeast using the glass bead/ phenol method (Hoffman and Winston, 1987), treated with GeneClean and introduced into E. coli by electroporation (Dower et al., 1988). Mutant plasmids were digested with Sph I and Xho I and fractionated on 2% agarose gels. Those that contained inserts that were approximately the same size as wild type were analyzed further. The coding region sequence of the U6 mutants was determined by dideoxynucleotide sequencing using Sequenase (U.S. Biochemicals). The phenotype of each mutant was confirmed using the plasmid shuffle assay as described above.

Site-Directed Mutagenesis of SNR6 and SNR14

Oligonucleotide-directed mutagenesis of the 5' stem loop and the ACAGAGA regions of the U6 gene and of stem I of both U4 and U6 was performed using the Kunkel method (Kunkel et al., 1987; McClary et al., 1989). By using two degenerate oligonucleotides, we obtained 12 multiple mutants and 15 single point substitutions in the ACAGAGA motif of the U6 gene. Five other mutants of this region were a generous gift from Patrizia Fabrizio (California Institute of Technology). The U6 mutants were subcloned into pSE358, the U4 mutants into pSE362.

Northern Hybridization, Velocity Sedimentation Analysis and In vitro Splicing

Total yeast RNA was prepared using the guanidinium thiocyanate method (Wise et al., 1983). Electrophoresis, transfer and hybridization conditions as well as glycerol gradient analysis were performed as described previously (Bordonné et al., 1990). Yeast whole cell extract preparation, synthesis of actin precursor, and in vitro splicing conditions were performed according to Lin et al. (1985).

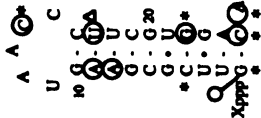
Acknowledgements

We gratefully acknowledge Karen Shannon who generated and analyzed several stem I mutants as well as the U4 deletion strain used in this study. Whole cell extract for performing in vitro transcription assays was kindly provided by David Brow, and Fraction 1 was a gift from Beate Schwer. We thank Patrizia Fabrizio and John Abelson for exchanging ACAGAGA box mutants and freely discussing unpublished results. We also thank Ian Mattaj and Albrecht Bindereif for helpful discussions. Paul Bates provided invaluable advice on gene synthesis and library construction. We are also indebted to members of the laboratory for lively discussion and helpful comments on the manuscript. Lucita Esperas provided excellent technical assistance. H.D.M. is a trainee of the Medical Scientist Training Program. R.B. was supported by grants from the C.N.R.S. and the Philippe Foundation. This work was supported by a grant to C.G. from the N.I.H (GM21119).

Figure 1. *S. cerevisiae* U4/U6 Structure and Location of Mutants

The location and phenotypes of mutants (designated in the inset) are summarized in the context of the U4/U6 secondary structure (Brow and Guthrie, 1988). Shown are the results of the strategy described in Figure 2 (summarized in Table 1) as well as further site-directed mutagenesis (Figure 3 and Table II). Viable substitutions or deletions represent changes that are viable in the context of either a single or multiple mutant (see Table I). Invariant nucleotides (marked by an asterisk) are those that are identical in mammalian, fly, bean, *S. cerevisiae*, trypanosome (Guthrie and Patterson, 1988) and *S. pombe* (Tani and Ohshima, 1989) U6 snRNAs. The two arrows indicate the sites of intron insertion in *R. dacyroidum* and *S. pombe*, respectively (Tani and Ohshima, 1989; pers. comm.).

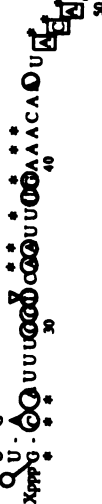
5' stem loop



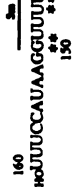
3' terminal domain



central domain



160



yeast U6

stem II

stem I

yeast U4

160



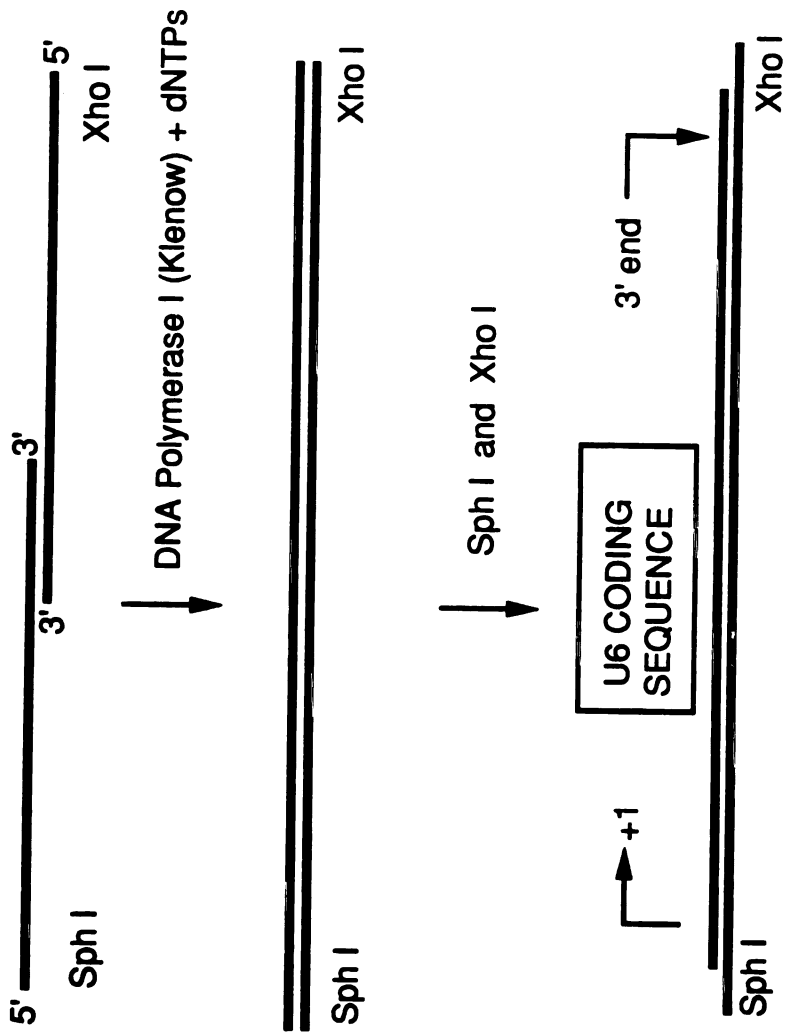
- (O) viable substitution;
- (⊖) viable deletion;
- (Δ) lethal deletion;
- (□) lethal substitution;
- (●) temperature-sensitive substitution;
- (⊙) cold-sensitive deletion.

Figure 2. Scheme for Isolation of U6 Mutants.

(A). Synthesis of SNR6 from degenerate oligonucleotides. Black lines at top represent two degenerate 82 nt oligonucleotides synthesized as described in the Experimental Procedures. The sense strand oligonucleotide corresponds to nts -13 to +69 in the numbering system of Brow and Guthrie (1988). The antisense strand oligonucleotide corresponds to nts +130 to +49 (5' to 3'). The oligonucleotides overlap by 21 nt. In addition, each oligonucleotide contains mutations near their 5' ends that introduce restriction sites for Sph and Xho I, respectively. Identical sites were introduced into a genomic SNR6 clone (producing pSX6). Following annealing and filling-in reactions, the double-stranded product was digested with Sph I and Xho I and ligated to pSX6 via the two restriction sites.

Electroporation of *E. coli* resulted in the production of a library of 2×10^5 clones.

(B). Genetic screen for SNR6 mutants based on the plasmid shuffle method (Boeke et al., 1987). DNA from the library described in (A) was used to transform a strain harboring a deletion of the chromosomal SNR6 coding sequence which is complemented by a URA3-marked plasmid containing a wild type SNR6 gene. Cells that contain an introduced plasmid harboring a lethal mutation are identified by replica-plating of transformants onto plates containing 5-fluoroorotic acid (FOA), which selects for loss of the URA3-marked plasmid. Inability to grow on FOA reflects a lethal mutation in the introduced copy of SNR6.



SELECT AGAINST WILD-TYPE STREAKING COLONIES ON 5-FLUOROOROTIC ACID PLATES

INTRODUCE MUTANT U6 ALLELES

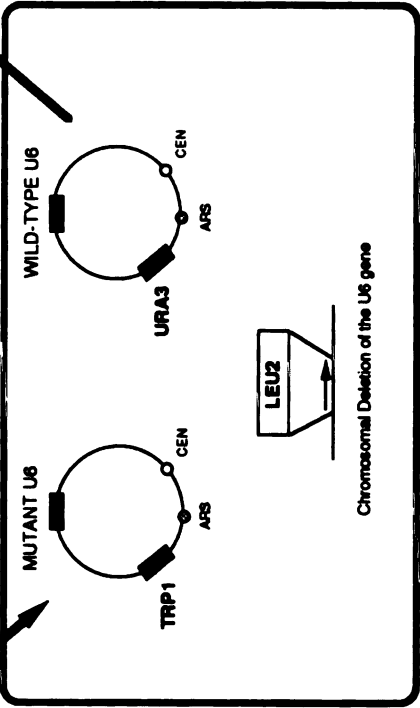


Figure 3. Phenotypes of Mutations in the Invariant ACAGAGA Motif.

The phenotypes of the U6 mutant were determined using the plasmid shuffle method as described in Figure 2B. -, lethal at all temperatures; +, viable at all temperature; NT, not tested.








	47	48	49	50	51	52	53
	A	C	A	G	A	G	A
A		-		sick 23° -30.37°		-	
G	sick 37°	-	-		-		+
C	-		-	+	-	-	+
U	+	-	-	+ 23° sick 30° - 37°	-	sick 37°	N.T.

Figure 4. Northern Analysis of U6 Mutants.

A) Schematic representation of the heterozygous strains carrying both the pseudo wild type U6-5'Sp chimera and various U6 mutants (U6*).

B) Northern blot of total RNA prepared from heterozygous strains. The probe is complementary to nts 92-112 of yeast U6. Lanes marked wt, 5'Sp and wt+5'Sp correspond to strains carrying only wild type U6 gene, the U6-5'Sp gene, and both wild type and U6-5'Sp U6 genes, respectively. Mutants are listed above each lane.

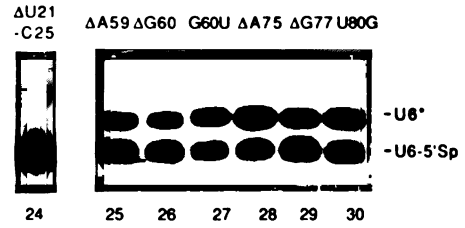
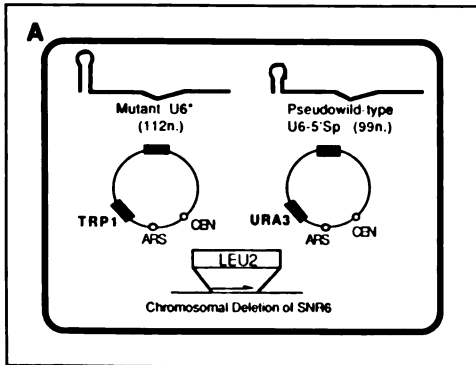
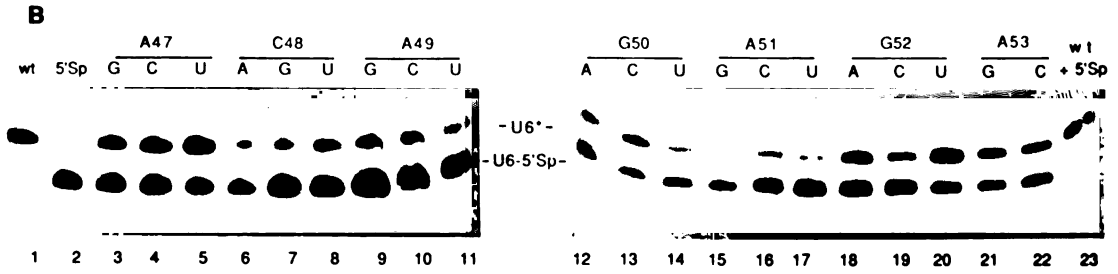


Figure 5. Velocity Sedimentation Analysis of U6 Mutants.

Splicing extracts were prepared from heterozygous strains carrying both the pseudowildtype U6-5'Sp chimera and either a wild type U6 gene (panel A) or the indicated mutant (panels B-E). The extracts were fractionated on 10-30% glycerol gradients, without prior incubation with ATP and in the absence of precursor mRNA as previously described (Bordonné et al., 1990). RNA present in odd numbered fractions was analyzed by Northern hybridization using probes complementary to yeast U4, U5 and U6 snRNAs. The RNA species, the positions of U6, U4/U6 and U4/U5/U6 snRNPs as well as the direction of sedimentation are indicated.

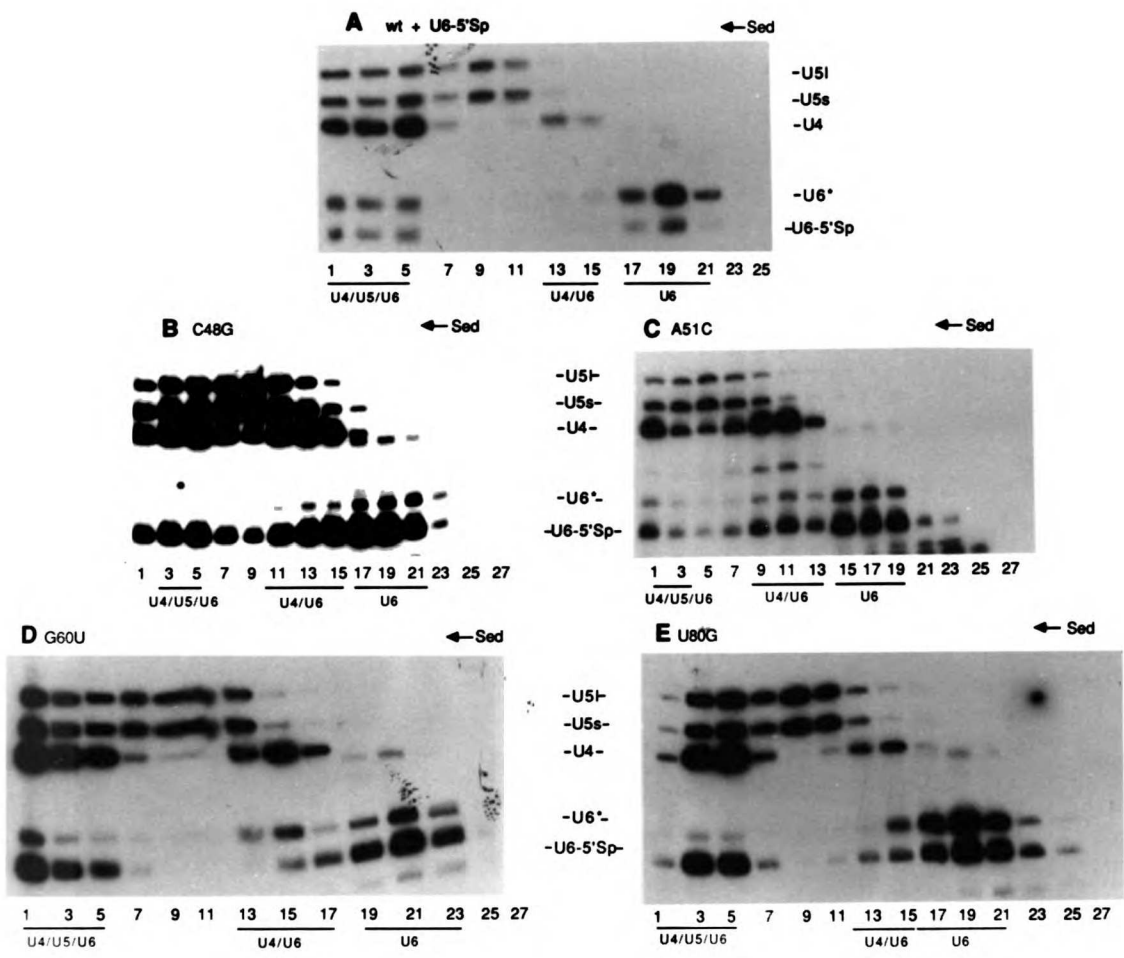


Figure 6. Splicing Activity of Mutant U6 Extracts.

Extracts prepared from wild type, G50A, G50U and G52U strains were assayed for splicing at 15°C for 60 min or at 23°C for 30 min under standard splicing conditions (Lin et al, 1985) using a ³²P-labeled in vitro transcribed yeast actin pre-mRNA. Reaction products were separated on 6% denaturing polyacrylamide gels. The identity of the reaction products is shown. "Pre" indicates precursor RNA incubated without splicing extract. (A) The autoradiogram is an overexposure in order to observe the lack of intron lariat in lanes 3 and 6. The complementation experiment (lane 9) was performed by mixing 4 ul of G50A extract with 1 ul of Fraction 1 from a wild type extract. The reaction was initiated by the addition of the other components of the splicing reaction. Lane 10, splicing reaction performed with 2 ul of Fraction 1 only. The lack of mature mRNA in G50A extracts is shown in panel (B). Lanes 3 and 4 in panel B represent two independent G50A splicing extract preparations.

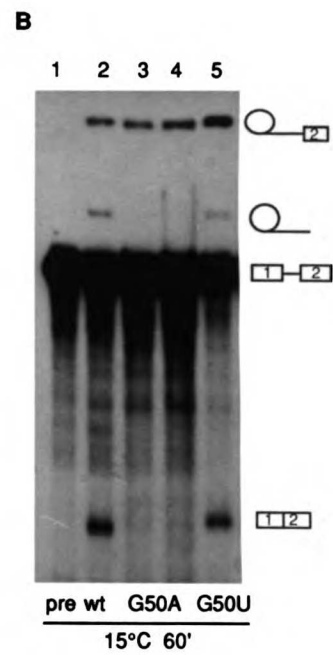
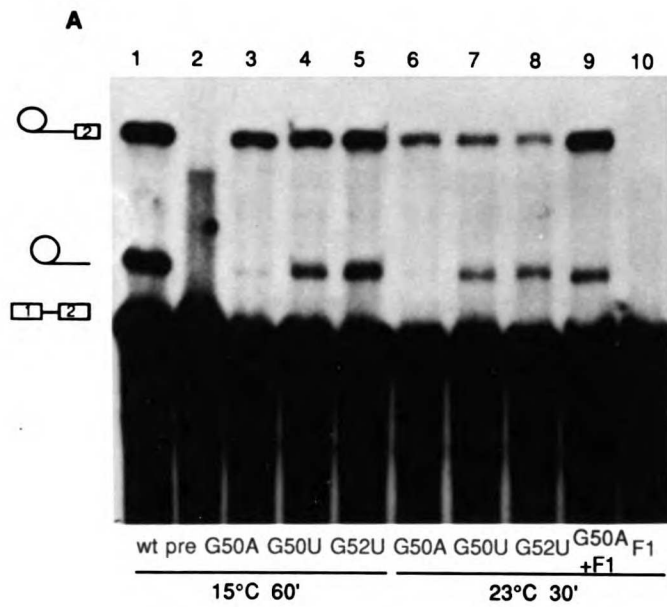


Table I. U6 Mutants.

The phenotype and location of mutants isolated in the screen described in Figure 2 are summarized. Nomenclature is as follows: for a point substitution, the wild type nucleotide and its position are followed by the mutant nucleotide; nucleotide deletions are designated by a "Δ" preceding the wild type nucleotide and position; insertions of a nucleotide is indicated by an "i" following the mutant nucleotide. Only single nucleotide substitutions and deletions are listed for lethal and conditional lethal mutants with the exception of three conditional deletion mutants involving more than one nucleotide (see text). For viable mutants, both single and multiple mutants are shown. The multiple mutants are duplicated, appearing in all columns corresponding to the region of each change (marked in boldface) found in that mutant. Randomly selected clones from the mutant library, previously constructed site-directed mutants (*), and mutants that initially screened as "lethal" but were found to be viable upon retesting (**) account for those mutants listed under "viable". The number in parenthesis indicate the number of independent isolates obtained for a particular mutation.

	5' Stem-Loop (nt 1-25)	Central Domain (nt 26-53)	Stem I (nt 54-62)	Stem II (nt 63-80)	3' Terminal Domain (nt 81-112)
Lethal		AC48 C48A (2) C48U (3) AA49 A49G (1) G52A (1)	AA59 AG60 G60U (2)	AA75 AG77 U80G (2)	
Temperature Sensitive	AU21-C25	AA47	C61G (3)		
Cold Sensitive	AG1 AU3-G7 AU21-C25				AU80-U98
Viabile	A8U A9C** G1A1 C14A AU17 G22U C25U*	A26U* G30A G31A** AU32 A34U G39A ΔC72 A34C C68G C92U A35U A35U U109C U38A A45C* A45U*		ΔC69 A34U G39A ΔC72 A34C C68G C92U	ΔC84 AU88-U90 A34C C68G C92U A35U U109C

Table 1

Table II. Phenotypes of Mutations in Stem I of U4 and U6.

Columns represent SNR6 alleles; rows correspond to SNR14 alleles. The intersection of the two describes the phenotype of that combination of alleles: +, fully viable; -, lethal; ts, temperature-sensitive. Blank boxes represent combinations not tested. Note that strains containing both mutant SNR6 and SNR14 alleles also contain the chromosomal wild type copy of SNR14.

U4 allele	U6 allele			
	WT	G60U	C60C	C61G
WT	+	-	-	ts
G58A	+			ts
G58C	+			ts
G58U	+			ts
C59A	+	-	-	
C59G	+	-	-	
C59U	+	-	-	
U60A	+			
U60C	+			

CHAPTER 2

A Novel Base-Pairing Interaction Between U2 and U6 snRNAs Suggests a Mechanism for the Catalytic Activation of the Spliceosome

Summary

Prior to the chemical steps of mRNA splicing, the extensive base-pairing interaction between the U4 and U6 spliceosomal snRNAs is disrupted. Here, we use a mutational analysis in yeast to demonstrate a conserved base-pairing interaction between the U6 and U2 snRNAs that is mutually exclusive with the U4/U6 interaction. In this novel pairing, conserved sequences in U6 interact with a sequence in U2 that is immediately upstream of the branchpoint recognition region. Remarkably, the residues in U6 that can be consequently juxtaposed with the intron substrate include those which have been proposed previously to be catalytic. Both the first and second steps of splicing are inhibited when this base-paired structure is mutated. These observations, together with the high conservation of the U2/U6 structure, lead us to propose that it might be a component of the spliceosomal active site.

Introduction

The chemical pathway that accomplishes the removal of introns from nuclear mRNA precursors involves two sequential transesterifications (reviewed in Green, 1991; Guthrie, 1991). Cleavage at the 5' splice site is accompanied by the formation of a 5'-2' phosphodiester linkage between the 5' end of the intron and an adenosine in the intron. In the second step of the reaction, the 3' splice site is cleaved with the concomitant formation of the ligated exons and the excision of the intron as a lariat structure. Since this chemistry is shared by Group II self-splicing introns, it has been suggested that nuclear mRNA splicing is fundamentally an RNA-catalyzed process (Sharp, 1985; 1991; Cech, 1986).

Much attention has been devoted to the five evolutionarily conserved small nuclear RNAs (U1, U2, U4, U5 and U6 snRNAs) that are required for nuclear mRNA splicing (reviewed in Green, 1991; Guthrie, 1991), partly because of their potential role as direct mediators of the reaction. Packaged by proteins into small nuclear ribonucleoprotein particles (snRNPs), the RNAs assemble onto an intron-containing substrate in an ordered pathway to form the spliceosome, in which the chemical steps of the reaction take place. In yeast and mammals, recognition of the 5' splice site and intron branchpoint are mediated in part through Watson-Crick base-pairing with U1 and U2 snRNAs, respectively (reviewed in Green, 1991; Guthrie, 1991). Recent studies suggest that, like U1 and U2, U5 also interacts with the pre-mRNA, in this case with the 5' and 3' exons (Newman and Norman, 1991; 1992).

In contrast to U1, U2 and U5, little is known about the specific functions of the U4/U6 snRNP. These RNAs are found base-paired to each other forming a single particle (Bringmann et al., 1984; Hashimoto and Steitz, 1984; Siliciano et al., 1987; Brow and Guthrie, 1988). U6 is unusual among the spliceosomal snRNAs in its high degree of phylogenetic conservation, the yeast molecule being 80 percent identical to its human homolog over half its length (Brow and Guthrie, 1988). On the basis of phylogenetic

comparisons, it has been proposed that the U4/U6 base-pairing interaction consists of two intermolecular helices termed stem I and stem II (Figure 1; Brow and Guthrie, 1988); the stem I interaction had been previously observed in a psoralen crosslinking study (Rinke et al., 1985). Studies in yeast and metazoan systems have provided strong evidence for this model and demonstrated that both stems are required for the formation of the U4/U6 snRNP (Hamm and Mattaj, 1989; Bindereif et al., 1990; Vankan et al., 1990; Shannon and Guthrie, 1991). Despite its stability, the U4/U6 base-pairing interaction is dynamic: after the assembly of the spliceosome, the interaction is disrupted, and upon native gel electrophoresis U4 is released from the spliceosome (Pikielny et al, 1986; Cheng and Abelson, 1987; Lamond et al., 1988). Complexes that lack U4 are the first in which splicing intermediates and products are found (Pikielny et al, 1986; Konarska and Sharp, 1987; Cheng and Abelson, 1987; Lamond et al., 1988). Importantly, U4 snRNA apparently does not participate in the subsequent chemical steps of splicing, since a spliceosomal intermediate that lacks U4 has been shown to be functional (Yean and Lin, 1991).

(1) The temporal correlation between the release of U4 and the appearance of reaction intermediates, (2) the dispensability of U4 prior to the chemical steps of splicing, and (3) the remarkable size and sequence conservation of U6 are consistent with the hypothesis that U6 participates directly in catalysis, and that a primary function of U4 is to sequester U6 in an inert conformation (Guthrie and Patterson, 1988). The disruption of the U4/U6 interaction would then liberate specific residues in U6 to function directly in splicing. By postulating dual constraints on residues in U6 (base-pairing with U4 and participation in catalysis), this model explains why nucleotides in U6 that base-pair with U4 are more conserved than their partners in U4 (Guthrie and Patterson, 1988; Figure 1). It has also been suggested that the mRNA-type introns that interrupt a handful of fungal U6 snRNA genes arose through reverse splicing accidents in which introns integrated

into a proximal component of the catalytic machinery, namely U6 snRNA (Brow and Guthrie, 1989; Tani and Ohshima, 1991; reviewed in Guthrie, 1991; Figure 1).

We have previously conducted a genetic analysis of the U6 molecule in the yeast *Saccharomyces cerevisiae* (Madhani et al., 1990). By combining mutagenesis of the U6 gene with a screen for mutants that are deleterious for cell growth, we identified two stretches of nucleotides that are particularly sensitive to point mutations: the ACAGAG hexanucleotide in the central domain (nts 47-52) and the AGC sequence (nts 59-61) in stem I of the U4/U6 interaction domain (Madhani et al., 1990; Figure 1). The modest disruption of the U4/U6 base-pairing interaction caused by point mutants in the stem I region was shown not to be responsible for the lethal phenotypes of these mutants since analogous mutants in the stem I region of U4 have no effect on cell growth (nts 58-60; see Figure 1); moreover, compensatory mutants in U4 designed to restore base-pairing fail to suppress the lethality of the U6 mutants (Madhani et al., 1990). We thus concluded that nucleotides in the stem I region of U6 have a role(s) in addition to base-pairing with U4. A mutational analysis of the yeast U6 snRNA has also been described by Fabrizio and Abelson (1990). Using a cell free system to assay the splicing activities of synthetic U6 mutant RNAs, they identified a virtually identical set of nucleotides as being important for U6 function in vitro (Fabrizio and Abelson, 1990). In addition, these studies revealed that while most functionally important nucleotides are required at or prior to the first chemical step of splicing, mutants at four positions lead to varying degrees of inhibition of the second chemical step of splicing (Fabrizio and Abelson, 1990; asterisks in Figure 1).

These studies of the yeast U6 snRNA and similar analyses of metazoan U6 snRNAs (Vankan et al., 1990, 1992; Bindereif and Green, 1990; Wolff and Bindereif, 1992) have identified regions of the molecule required at multiple steps of the splicing pathway, including spliceosome assembly and the two chemical steps of the reaction; however, the specific molecular interactions that underlie these requirements have yet to

be elucidated. In particular, two key mechanistic questions remain: 1) what is the function of the dynamically unstable U4/U6 base-pairing interaction and 2) what are the specific roles of the mutationally-sensitive nucleotides in U6 snRNA? Here we report experiments which provide important insight into these issues. Based on genetic suppression analyses, we propose a structural model for the active site of the spliceosome, in which previously proposed catalytic residues of U6 (ACAGAG and AGC) are directly juxtaposed with the branchpoint recognition region of U2. The predominant feature of this structure is an intermolecular helix, whose formation requires the displacement of U4 snRNA from U4/U6 stem I and its replacement by a highly conserved sequence in U2. Biochemical experiments described herein and elsewhere (Fabrizio and Abelson, 1990; D. McPheeters and J. Abelson, pers. comm.) indicate that residues that form this U2/U6 helix are important for both chemical steps of splicing in vivo and in vitro.

Results

U2/U6 Base-Pairing Model

Starting with the premises that the essential nucleotides in U6 are components of the spliceosomal active site and that the release of U6 from U4 activates U6 for participation in catalysis, we searched for base-pairing interactions between U6 and other snRNAs that would juxtapose these residues of U6 with the intron. We noticed that nucleotides in the stem I region of U6 (nts 54-61 in yeast) are complementary to a highly conserved region of U2 snRNA (nts 21-30 in yeast) which is itself immediately upstream of the sequence in U2 that is known to base-pair with the intron branchsite region (Figure 2; Parker et al., 1987). The resulting structure comprises two intermolecular helices (labeled helix Ia and helix Ib in Figure 2) connected by a two-nucleotide bulge. This structure is distinct from a previously identified base-pairing interaction between a more 5' region of U2 and the 3' end of U6 (which we refer to below as U2/U6 helix II; Hausner et al., 1990; Wu and Manley, 1991; Datta and Weiner, 1991). U2/U6 helix I can closely juxtapose essential residues in U6 with the intron branchpoint (Figure 2). Its functional requirement would also explain our previous genetic results that suggest a dual role for nucleotides in U6 that participate in U4/U6 stem I (Madhani et al., 1990). If the deleterious phenotypes of mutants in this region of U6 are due to the disruption of base-pairing with U2, then their effects on growth would be predicted to be suppressed by supplying cells with compensatory mutants in U2 that restore Watson-Crick complementarity.

Phenotypes of U6 snRNA Mutants Can Be Suppressed by Restoring Complementarity with U2 snRNA

To test the U2/U6 helix I model, we employed a haploid *S. cerevisiae* strain (YHM1) that contains 1) a wild-type U6 gene on a centromere-bearing plasmid marked with the *URA3* gene and 2) a deletion of the chromosomal U6 coding sequence (Figure 3A; Madhani et al., 1990). This strain can be transformed with plasmids encoding

various alleles of U6 and U2, and the growth phenotypes of transformants can be assayed by streaking colonies onto 5-fluoroorotic acid-containing plates (5-FOA), which select for cells that have lost the wild-type *URA3*-marked plasmid (Figure 3; Boeke et al., 1987). This strain also contains a wild-type chromosomal copy of U2; since compensatory mutations are expected to be gain-of-function alleles, they should be dominant over the (endogenous) wild-type gene. For each U6 mutant described below, we first examined the growth phenotype over a range of temperatures (25-37 °C), and then tested the effects of compensatory U2 mutants under conditions where a given U6 mutant is lethal. In order to determine whether or not suppression reflected the restoration of base-pairing per se, we also examined the effects of non-compensatory U2 mutants. If base-pairing is occurring, one predicts only compensatory mutants to act as suppressors. As described below in detail (and summarized in Table 1), in each of seven cases, we were successful in suppressing the phenotype of a given U6 mutant with the predicted compensatory mutant in U2. Conversely, in none of 29 cases tested did a non-compensatory mutant or wild-type U2 have effects at all temperatures tested. Some "noncognate" U2 mutants can actually act as weak suppressors by partially restoring base-pairing (e.g. through the restoration of one of two disrupted base-pairs); however, at higher temperatures, suppression is only seen with the true cognate U2 allele. For purposes of clarity, only data from the most stringent conditions (i.e. the highest temperature at which suppression was observed) are presented below.

Positions 56 and 57

Since previous mutagenesis data indicated that single point mutations at nts 56 and 57 in U6 had relatively mild effects on splicing in vitro (Fabrizio and Abelson, 1990), we decided to construct double point mutations at these positions. Changing nucleotides 56 and 57 from AU to UA (U6-A56U, U57A) results in lethality at 30 °C (Figure 4A). This phenotype can be suppressed by a U2 mutant that restores base-pairing (U2-A27U, U28A) as predicted by the model (Figure 4B); the observed growth is equivalent to that

seen with the parental wild-type strain (data not shown). On the other hand, suppression is not observed with four non-compensatory U2 mutants (U2-A27C, U28G; U2-A27G, U28G; U2-U23C; U2-U23G; Figures 4C-F). Importantly, the failure of the noncognate U2 alleles to suppress is not due to their inability to function per se since each of them can suppress their cognate mutation in U6 (see below). As expected, the introduction of an additional wild-type U2 gene has no effect on the growth of U6-A56U, U57A or any other U6 mutant (Table 1).

A different mutant combination at the same dinucleotide (U6-A56C, U57C) is lethal at 33 °C (Figure 4G). Introduction of the U2 compensatory mutant (U2-A27G, U28G) suppresses the growth defect (Figure 4H). However, U2-A27U, U28A, which could suppress U6-A56U, U57A, fails to suppress this mutant (Figure 4I). Likewise, three other non-compensatory mutant (U2-A27C, U28G; U2-U23C; U2-U23G) also fail to suppress (Figures 4J-L).

Finally, changing positions 56 and 57 in U6 from AU to CG (U6-A56C, U57G) is also lethal at 33 °C (Figure 4M). Again, the appropriate compensatory U2 mutant (U2-A27C, U28G) suppresses the growth defect of the U6 mutant (Figure 4N). However, four noncognate U2 alleles (U2-A27U, U28A; U2-A27G, U28G; U2-U23C; U2-U23G) do not suppress (Figures 4O-R).

Position 58

Mutation of C58 to a U results in lethality at 37 °C (Figure 5A). As before, we attempted to suppress this defect using the compensatory mutant in U2 (U2-G26A); however, no suppression was observed (data not shown). Considering the possibility that the suppressor was inadequately expressed or assembled, we placed U2-G26A on a high-copy plasmid. As shown in Figure 5B, U2-G26A on a high-copy plasmid suppresses the growth defect of U6-C58U. This effect is also allele-specific since wild type U2 as well as two non-cognate suppressors, U2-U23C and U2-U23G (on high-copy plasmids) do

not suppress U6-C58A (Figures 5C, 5D). The latter mutants (U2-U23C and U2-U23G) do, however, suppress their cognate U6 mutants (data not shown).

We also constructed a different mutant at position 58, C58A. This mutant is lethal under all conditions tested (Figure 5E; data not shown). Introduction of the compensatory U2 mutant (on a low-copy plasmid), G26U, allows growth at 31.5 °C. However, two non-compensatory mutants in U2 fail to suppress (U2-U23C; U2-U23G), again demonstrating the specificity of the interaction (Figures 5G, 5H).

Position 59

Mutation of A59 to C is lethal at 35 degrees (Figure 6A). It can be suppressed by the compensatory mutant U2-U23G (Figure 6B). In contrast, three non-compensatory U2 mutants (U2-U23C; U2-A27U, U28A; U2-A27C, U28G) do not have any effect (Figures 6C-E). Similarly, mutation of A59 to a G is lethal under all conditions tested (Figure 6F shows a plate incubated at 30 °C; data not shown). We found that the U2 suppressor, U2-U23C, suppresses this growth defect at all temperatures (Figure 6G shows suppression at 30 °C). On the other hand, three non-compensatory U2 mutants (U2-U23G; U2-A27U, U28A; U2-A27C, U28G) fail to show any effect at any temperature tested (Figures 6H-J show plates incubated at 30 °C).

Positions 60 and 61

Mutation of G60 to a U or a C is lethal under all conditions (Madhani et al., 1990). Introduction of the cognate U2 suppressors (U2-C22A; U2-C22G) fails to suppress the lethality of these mutants (Table 1). In one case tested (U2-C22A), suppression is still not observed when the U2 mutant is placed on a high-copy plasmid (Table 1). Similarly, C61G, which is lethal at 37 °C (Madhani et al., 1990), is also not suppressed by U2-G21C either on a low-copy plasmid or on a high-copy plasmid (Table 1).

Comparison of the Growth Phenotypes of U2 and U6 Mutants

There are several potential explanations for why suppression was not observed at positions 60 and 61, including poor expression of the U2 suppressors or a lack of a base-pairing requirement at these positions. Another possibility is that the U6 residues have essential roles in addition to base-pairing with U2 (or vice-versa). To begin to address this issue, we examined the growth phenotypes of strains that contained comparable U2 and U6 mutants in helix Ia and Ib as their sole copy of the respective gene. We reasoned that if the only roles of two nucleotides were to base-pair with each other, then mutation of either should have an equally deleterious effect on cell growth. However, if a particular nucleotide has an additional role, then its alteration should have a more severe effect than an analogous change in its base-pairing partner.

Two strains were used. The U6 mutants were assayed as above in YHM1. The U2 mutants were assayed in an analogous strain (YHM111) that contains a deletion of the chromosomal U2 gene and a wild-type U2 gene on a *URA3*-marked centromere plasmid. As before, the phenotypes of mutants were assessed by first transforming these strains with U6 and U2 mutants that disrupt helix Ia or Ib (Figure 2) and then observing the growth of transformants streaked to 5-FOA plates and incubated at 25, 30 or 37 °C.

As shown in Table 2, mutants that disrupt helix Ia, have similar phenotypes regardless of whether the alteration is in U6 or in U2. For instance, U6-A56U, U57A and U6-A57C, U58G are lethal at each temperature tested, and the analogous mutants in U2 (U2-A27U, U28A; U2-A27C, U28G) exhibit the same phenotype. Likewise, U6-A56C, U57C grows poorly at 25 , well at 30, but not at 37 °C, and the comparable mutant in U2 (U2-A27C,U28C) shows the identical pattern (Table 2). Finally, mutants in U6-C58 and its predicted pairing partner have similar effects on growth. Note that the C58U mutant, which results in a U-G “wobble” base-pair, exhibits a relatively mild (temperature-sensitive) phenotype (Table 2).

We observed a different pattern in helix Ib. As described above, mutants at position 59 in U6 are lethal or temperature-sensitive (Table 2) and can be suppressed by

the predicted compensatory changes in U2 at position 23. In striking contrast, we observed that the mutants at position 23 in U2 (U2-U23C; U2-U23G) have no effect on growth on their own (Table 2). It is also notable that the U6-A59G mutant, which should allow the formation of a G-U base-pair with U2-U23, exhibits a more deleterious phenotype than A59C which completely disrupts base-pairing; this suggests that something in addition to the stability of base-pairing with U2 at this position is important for cell growth.

At position 60 in U6, mutants are lethal (Table 2) but cannot be suppressed by compensatory mutants at position 22 in U2 (see above); the U2 mutants at this position exhibit no growth defects on their own (Table 2). Finally, the most complex situation is observed at position 61 in U6 and its predicted pairing partner, position 21 in U2. We observed that while mutation of either is deleterious, changing U6 (U6-C61G) results in temperature-sensitive growth while the U2 mutant (U2-G21C) is cold-sensitive (Table 2).

In summary, while mutants in U2/U6 helix Ia exhibit similar phenotypes regardless of whether the alteration is made in U6 or in U2, we observe a marked asymmetry in phenotypes of helix Ib. In particular, changes to nts 59 and 60 in U6 are much more deleterious than changes in their predicted base-pairing partners, nts 22 and 23 in U2.

Mutants in U2 Inhibit Both Steps of Splicing In Vivo

In a previous *in vitro* study of mutants in the yeast U6 molecule, it was found that while most deleterious mutants in U4/U6 stem I affect the first step of splicing, mutation of two nucleotides (nts 58 and 59) inhibit the second chemical step of the reaction (Fabrizio and Abelson, 1990). In light of our model, it seemed likely that mutants in residues in U2 that engage in base-pairing with these nucleotides in U6 would also affect both steps of splicing *in vivo*. Indeed, independent experiments by McPheeters and Abelson (pers. comm.) indicated that this was the case *in vitro*.

To test this *in vivo*, we constructed a yeast strain that contains a wild-type U2 gene that is under the control of the *GAL1-10* UAS, which allows one to regulate the transcription of U2 by growing cells in different carbon sources (Figure 7A). This strategy has been used previously to regulate snRNA expression (Patterson and Guthrie, 1987; Séraphin and Rosbash, 1989; Miraglia et al., 1991). Into this strain, we introduced either wild-type U2 or U2 mutants at positions 21, 23, 26 and 27-28. Cultures of these transformants were shifted from galactose-containing media to glucose-containing media for 15 hrs., which causes transcriptional repression of the *GAL*-regulated U2 gene and, as a consequence, depletion of (the regulated) wild-type U2 snRNP from the cell (see Experimental Procedures). We then harvested total RNA from these strains and analyzed the splicing of endogenous transcripts by a primer-extension method.

We first examined the splicing of the intron-containing *SNR17A* and *SNR17B* genes, which each encode the nucleolar U3 snRNA (Myslinski et al., 1990). By using a single ³²P-end-labeled primer that is complementary to the second exons of both genes, we were able to measure the levels of unspliced U3A and U3B RNAs. The reactions also included a primer complementary to U5 snRNA as an internal control for the amounts of RNA analyzed in each reaction. The results are shown in Figure 7B and are quantitated in Table 3.

In the control sample, we examined RNA from depleted cells that contained an additional copy of a wild-type U2 gene. This allowed us to determine the background levels of unspliced pre-U3A and pre-U3B RNAs (Figure 7B, lane 8). The U2 mutants are shown in lanes 1-7. Three mutants (U2-G26U; U2-A27U, U28A; U2-A27C, U28G) show a two- to seven- fold accumulation of pre-U3A and U3B (Figure 7B; Table 3). A slight increase in pre-mRNA levels is also seen in U2-G21C (Figure 7B; Table 3). However, no discernible accumulation is seen in U2-U23C, U23G or G26A (Figure 7B).

Because of the architecture of the *SNR17* genes, the band produced by primer-extension of the U3 lariat intermediates (the product of the first step of splicing)

comigrates with mature U3 snRNA (Myslinski et al., 1990). Therefore, in order to determine whether the second step of splicing was affected by the U2 mutants, we examined the splicing of a different gene, *RP51A*, which encodes a ribosomal protein (Teem and Rosbash, 1983). The RNA samples used in the experiment described above were analyzed using primers complementary to the intron and 3' exon of this gene (Figures 7C and 7D). The levels of pre-mRNA and lariat-intermediate for the wild-type control are shown in lane 8. Strikingly, mutants at positions 21, 23, and 26 cause the accumulation of lariat-intermediate (Figures 7C and 7D; Table 3), indicating inhibition of the second step of splicing. In addition, several mutants exhibit increases in the level of unspliced *RP51A* pre-mRNA (Figure 7C; Table 3). Curiously, the mutants that show the most pronounced effect on the levels of this pre-mRNA (G21C, U23C, U23G) exhibit little or no accumulation of pre-U3 (Table 3). Differences in the response of different pre-mRNAs to perturbations of the spliceosome have been observed previously (e.g. Patterson and Guthrie, 1987); however, their bases have yet to be elucidated.

In summary, these data indicate that residues U2-G21, U2-U23 and U2-G26 are particularly important for the second step of splicing *in vivo*. In addition, mutations at positions 21, 23, 26 and 27-8 can also inhibit the first step of splicing, as manifested by the accumulation of unspliced pre-mRNA.

Discussion

A Novel U2/U6 Base-Pairing Interaction

We have identified a novel base-pairing interaction between the stem I region of yeast U6 snRNA and the sequence just upstream of the branchpoint interaction region in yeast U2 snRNA (U2/U6 helix I; Figure 2). In seven instances, we have been able to suppress the growth phenotypes of U6 mutants that disrupt the predicted base-pairing interaction with compensatory U2 mutants that restore base-pairing (Figures 4-6).

Conversely, in each of the 29 cases tested, non-compensatory U2 mutants (as well as wild-type U2) do not suppress the phenotypes of the U6 mutants. These data provide strong evidence for the structural model presented in Figure 2. Biochemical data (Figure 7) show that the integrity of this helix is required for efficient splicing *in vivo*.

Although many of the nucleotides in U2/U6 helix I can be altered as long as base-pairing is maintained, several observations suggest that particular nucleotides have additional functions. First, suppression is almost never complete. As described in the Results, specific suppression by compensatory U2 mutants can be achieved for many U6 mutants (positions 56-59) but only at certain temperatures, above which growth can not be observed. For other mutants, such as those at positions 60 and 61 in U6, we do not observe suppression under any conditions. Although we can not rule out the possibility that there is no base-pairing requirement at these positions, the potential for base-pairing between U6 nts 60-61 and U2 nts 21-22 is universally conserved. This fact and the evidence for base-pairing at the adjacent position (U6-A59 and U2-U23) lead us to favor the alternative interpretation, namely that nts 60 and 61 in U6 engage in base-pairing but also have an additional, essential role.

Second, in contrast to U2/U6 helix Ia, mutants in U2/U6 helix Ib exhibit a marked asymmetry in phenotypes. For example, while our data indicate base-pairing between U6-A59 and U2-U23, mutants in U6-A59 are either lethal or temperature-sensitive, while

altering U2-U23 has no effect on growth (Table 2). This observation can be rationalized by proposing that U6-A59 has a function in addition to base-pairing with U2-U23.

Since the residues in U6 that participate in U2/U6 helix I also base-pair with U4 (Figure 1), this may explain some of the observations described above. However, point mutants in U4 that disrupt the U4/U6 stem I interaction do not affect cell growth (Madhani et al., 1990); thus, it is likely that residues in U6 that are involved in the U4/U6 stem I and U2/U6 helix I interactions also engage in other functionally important interactions that have yet to be identified.

U2/U6 Helix I May Be A Component of the Spliceosomal Active Site

The requirement of U2/U6 helix I for cell growth and splicing raises the question of whether the structure participates directly in catalysis or plays an indirect role, promoting the formation of a spatially or temporally distant active site. Below we describe characteristics of the U2/U6 structure that lead us to favor the former possibility.

Potential Juxtaposition of Candidate Catalytic Residues in U6 with Intron

The potential position in space of U2/U6 helix I relative to the intron is consistent with it being a component of the active site. That is, the U2/U6 structure can directly juxtapose two key regions of U6 (the ACAGAG hexanucleotide in the central domain and the AGC sequence in U4/U6 stem I) with the intron branchpoint (Figure 2). Indeed, we and others have previously proposed that these two regions of U6 contain particularly attractive candidates for catalytic residues based on their mutational sensitivity, the biochemical properties of mutants in these sequences, and their coincidence with intron insertion sites (Madhani et al., 1990; Fabrizio and Abelson, 1990; reviewed in Guthrie, 1991).

Is the U2/U6 helix formed at a time consistent with a role in catalysis? As discussed in detail below, the U2/U6 interaction likely forms after assembly of the spliceosome but prior to catalysis, consistent with a direct role. Presumably, for U2/U6 helix I to be juxtaposed with the intron branchpoint, it must occur simultaneously with

the U2-branchpoint region interaction. The timing of this U2-intron interaction has not been precisely established. Recently, however, crosslinks between U2 and the branchpoint region have been observed in fully assembled spliceosomes; these were induced by either UV light (Sawa and Shimura, 1992) or a psoralen reagent (Wassarman and Steitz, 1992). Crosslinks between U6 and the intron were also identified in these experiments. These have been localized to a region just upstream of the ACAGAG hexanucleotide in U6 and to a sequence downstream of the 5' splice site (Sawa and Shimura, 1992; H. Sawa and J. Abelson, pers. comm.; Wassarman and Steitz, 1992). The potential simultaneous formation of U2/U6 helix I and the U2-branchpoint region helix would offer a structural basis for the observed proximity between U6 and the 5' splice site.

Phylogenetic Conservation

U2/U6 helix I exhibits extraordinary phylogenetic conservation, consistent with the view that it is an active site element. Virtually all of the nucleotides in the structure are identical in all organisms for which sequences are available, including the highly divergent kinetoplastid protozoa (Guthrie and Patterson, 1988; C.G., S. Mian and H. Roiha, unpublished). Two nucleotides in helix Ia, U6-U54 and U6-C58, are not universally conserved (Figure 2); however, these nucleotides covary to just one other pattern (to A54 and U58) among all species examined (Guthrie and Patterson, 1988; Roiha et al., 1989; C.G., S. Mian and H. Roiha, unpublished). In fact, the U6 molecules of all metazoans for which sequences are available display the A54, U58 pattern, which results in a U2/U6 helix Ia that is one base-pair shorter than in *Saccharomyces* (and replaces the U6-C58/U2-G26 base-pair with a U6-U58/U2-G26 pair). The only other nonconserved nucleotide, U2-U24, is found in the two nucleotide bulge between U2/U6 helix Ia and helix Ib (Figure 2). It varies only to an A in all characterized metazoans (Guthrie and Patterson, 1988; C.G., S. Mian and H. Roiha, unpublished).

Residues in U2/U6 Helix I Are Important for Both Steps of Splicing

Nucleotides in U6 that we have shown here to be in U2/U6 helix I have been demonstrated previously to be important for both steps of splicing *in vitro* (Fabrizio and Abelson, 1990). Based on our model, one might expect that mutants in residues in U2 that participate in the structure would also inhibit both chemical steps of splicing. This was borne out in our *in vivo* analysis (Figure 7). Notably, we observed that mutation of positions 21, 23 and 26 in U2 results in the accumulation of lariat-intermediate *in vivo*, while changes at positions 27-28 result only in the accumulation of unspliced pre-mRNA. Some mutants that inhibit the second step of splicing also exhibit an accumulation of unspliced pre-mRNA. Our results with U2 are in general agreement with recent experiments that demonstrate that alteration of position 26 and, to a lesser extent, position 27 in yeast U2 inhibit the second step of splicing *in vitro* (D. McPheeters and J. Abelson, pers. comm.). Although we do not observe any accumulation of lariat-intermediate in mutants that change position 27, this apparent discrepancy may reflect differences in the assays employed (*in vitro* vs. *in vivo*). Mutants at position 23 in U2 have yet to be tested for activity *in vitro* (D. McPheeters and J. Abelson, pers. comm.).

Given the potential proximity to the intron and strong phylogenetic conservation of U2/U6 helix I, the requirement of these base-paired residues for both steps of splicing could reflect the direct involvement of this helix in the catalysis of both reactions. If true, this raises the question of why some residues are particularly important for the first chemical step of splicing, while other, adjacent nucleotides are more important for the second step. A parsimonious explanation would be that the catalytic sites for the two steps are largely overlapping, but also contain distinct components specific to each step. Such a model is consistent with the fact that the nucleophiles that participate in the transesterification reactions (a 2' hydroxyl in the first step and a 3' hydroxyl in the second step), are similar but not identical. This hypothesis may also account for the observed differences in the importance of the 2' hydroxyl groups that lie adjacent to the cleaved phosphodiester bonds at the 5' versus 3' splice sites (Moore and Sharp, 1992).

Structural Similarity with Domains 5 and 6 of Group II Self-Splicing Introns

In addition to similarities in the chemistry of splicing between Group II autocatalytic introns and the spliceosome, two specific structural analogies have been suggested to support an evolutionary relationship between these systems. The first involves recognition of the intron branchpoint. In Group II introns the branchpoint adenosine is specified in part by being bulged out of an intramolecular helix termed domain 6 (Figure 8; Schmelzer and Schweyen, 1986). Similarly, in the spliceosome, the branchpoint adenosine is also found bulged out of a helix, in this case an intermolecular helix involving U2 snRNA (Figure 8; Parker et al., 1987; Wu and Manley, 1989; Zhaung and Weiner, 1989). The second analogy arises from studies demonstrating that the conserved loop of U5 snRNA can base-pair with exon sequences immediately adjacent to the 5' and 3' splice sites (Newman and Norman, 1992). These authors suggest that the U5 loop is analogous to the D3 loop in Group II introns, which is also known to base-pair with the 5' and 3' exons (Newman and Norman, 1992; Jacquier and Michel, 1987; Jacquier and Jacquesson-Breuleux, 1991). While these analogies suggest similarities in the mechanism of splice site selection between the two systems, neither of these examples involves highly conserved sequences in Group II introns, such as those that one might expect to be involved in catalysis.

In light of the results described in this manuscript, we considered whether there might be additional structural similarities between the two systems involving highly conserved sequences. A good candidate for a catalytic element in Group II introns is domain 5, which is the most conserved domain of these introns. It immediately precedes domain 6 (the branchpoint region helix), and its integrity is essential for self-splicing (Jarrell et al., 1988; Koch et al., 1992). Domain 5 consists of two helices connected by a two nucleotide bulge; it is also highly conserved in primary sequence (Figure 8; Michel et al., 1989). In our model of the spliceosomal snRNAs, the branchsite helix is also immediately preceded by a helix-2 nt bulge-helix structure that involves residues that are

virtually phylogenetically invariant (Figure 8). There is also some limited sequence identity between helix Ib and the potentially analogous region in domain 5 (indicated by asterisks in Figure 8). These structural similarities suggest the possibility that the U2/U6 structure and the U2-branchpoint interaction represent homologs of Group II intron domains 5 and 6, respectively. Further evaluation of the similarities between the two systems will likely come from an understanding of the specific tertiary contacts that position the branchpoint adenosine as well as the 5' and 3' splice sites within the respective conserved core structures.

RNA Structural Rearrangements: A General Paradigm for Spliceosome Assembly

Although the dynamic nature of the extensive U4/U6 base-pairing interaction has been known for some time (Pikielny et al., 1986; Cheng and Abelson, 1987; Konarska and Sharp, 1987; Lamond et al., 1988), the purpose of its cyclical disruption and reformation has been enigmatic. In that the novel U2/U6 structure described here and stem I of the U4/U6 base-pairing interaction are mutually exclusive (Figure 9), we propose that an important function of the unwinding of U4/U6 is to allow the formation of U2/U6 helix I. Since the U4/U6 interaction is known to be disrupted after the assembly of the spliceosome, but prior to the chemical steps of the reaction (Pikielny et al., 1986; Cheng and Abelson, 1987; Lamond et al., 1988), it is reasonable to propose that the U2/U6 interaction forms during the window of time after U4/U6 destabilization but prior to (or concomitant with) the chemical steps of the reaction.

The U2/U6 helix I structure involves sequences in U6 which are (initially) part of stem I of the U4/U6 interaction. In principle, the U4/U6 stem II interaction could be maintained after formation of the U2/U6 structure. However, since U4 can be released from functional spliceosomes prior to catalysis (Yean and Lin, 1991), stem II is presumably also disrupted prior to the first step of splicing. A rearrangement involving stem II is supported by phylogenetic covariation analyses, which indicate base-pairing between the first few nucleotides of the stem II region and the beginning of the 3'

terminal domain (C.G., S. Mian, H. Roiha, unpublished). An intramolecular U6 helix that incorporates this observation is depicted in Figure 9; this pairing is mutually exclusive with stem II of the U4/U6 interaction. This stem-loop has also been proposed by Brow and coworkers as part of a larger secondary structure model for "free" (non-spliceosomal) U6 snRNP based on chemical modification studies (R. Troy and D. Brow, pers. comm.). Interestingly, we have previously described a mutant whose biochemical properties may be explained by this structure. The lethal mutant U6-U80G is apparently blocked in the transition from the free U6 snRNP to the U4/U6 snRNP (Madhani et al., 1990; see Figure 1). This mutation would affect the U that bulges out of the intramolecular U6 helix in Figure 9. Replacing U80 with a G would permit base-pairing with the C on the other side of the bulge, increasing the stability the putative hairpin structure (Figure 9). Since the unwinding of this structure would be necessary to re-form the U4/U6 stem II interaction, the hyperstabilization of the intramolecular helix caused by the U6-U80G mutation potentially explains the failure of this mutant U6 to associate with U4. Further experiments will be necessary to test this model; specifically, mutations that disrupt the intramolecular U6 helix are predicted to suppress the phenotypes of U6-U80G. Indeed, it has been recently shown that the phenotype of a different hyperstabilizing mutant can be suppressed by a destabilizing mutant elsewhere in the helix (D. Fortner and D. Brow, pers. comm.).

According to this view, the unwinding of the U4/U6 snRNAs could promote two RNA rearrangements: a U4/U6 stem I to U2/U6 helix I isomerization and a U4/U6 stem II to U6 intramolecular stem isomerization. As proposed above, the former transition could serve to juxtapose candidate catalytic residues in U6 with the intron. In addition, the base-pairs in U2/U6 helix I and in the intramolecular U6 structures may also have another role. Once the base-pairs that hold together U4 and U6 are disrupted, some alternative interaction is presumably necessary to prevent the immediate reassociation of

the unwound strands. The formation of alternative base-pairs in U2/U6 helix I and the U6 intramolecular helix may be significant in this regard.

The region of U2 snRNA in U2/U6 helix I is thought to participate in an intramolecular stem (Figure 9; Keller and Noon, 1985). In addition to the conserved complementarity of bases in the two halves of the stem, the existence of this hairpin is suggested by Watson-Crick covariation of the sequence of one base-pair in the top part of the structure (Guthrie and Patterson, 1988) and the inaccessibility of this region of RNA to oligonucleotide probes (Lamond et al., 1989). Evidence that this structure may be dynamic comes from observations in mammals that demonstrate base-pairing involving the 5' half of the U2 stem-loop and the 3' terminal domain of U6 (U2/U6 helix II in Figure 9). This interaction, which was first inferred from a psoralen crosslinking study (Hausner and Weiner, 1990), requires the unwinding of the U2 5' stem-loop. Its functional importance was subsequently demonstrated in transfected mammalian cells (Wu and Manley, 1991; Datta and Weiner, 1991). However, since this pairing can be disrupted without detectable effect in yeast (Fabrizio et al., 1989; Madhani et al., 1990; Bordonné and Guthrie, 1992), its role in this organism may be a more subtle one, perhaps serving to assist in the opening up of the U2 5' stem to facilitate interaction between its 3' half and the helix I region of U6. This may be reflected in the relatively low primary sequence conservation of U2/U6 helix II (Figure 9). Interestingly, in mammalian nuclear extracts, the accessibility of the U2 5' stem-loop to oligonucleotide hybridization is increased when a 2'O-methyl RNA oligonucleotide is annealed to the branchpoint region interaction domain of U2 (Lamond et al., 1989). A provocative interpretation of this observation is that the U2-branchpoint region interaction promotes the formation of the U2/U6 interaction during spliceosome assembly by activating the unwinding of the U2 5' stem loop.

In summary, the current evidence suggests (a minimum of) three RNA conformational rearrangements that occur during spliceosome assembly. Presumably,

these events must be reversed in order for the snRNPs to be recycled and used in the next round of splicing. How are these events accomplished and regulated? Two families of known or suspected RNA-dependent ATPases that also share homology to ATP-dependent RNA helicases are required for splicing in yeast (reviewed in Guthrie, 1991; Schmid and Linder, 1992); to date no physiological RNA substrate for any of these proteins has been identified. Similarly, an RNA binding (RNP consensus) protein family member, PRP24, has been implicated in regulation of the U4/U6 base-pairing cycle (Shannon and Guthrie, 1991); its binding sites have yet to be elucidated. The dynamic RNA-RNA interactions described above constitute excellent candidate substrates for these proteins. The requirements for ATP hydrolysis at many steps of spliceosome assembly could in part reflect a need for energy to facilitate such RNA rearrangement reactions. In turn, the ordered nature of spliceosome assembly argues that these reactions are tightly regulated with respect to timing and directionality.

Experimental Procedures

Yeast Methods and Strains

All yeast procedures including plasmid shuffle assays were performed using standard methods (Guthrie and Fink, 1991). YHM1 (*MATa ura3 his3 lys2 trp1 leu2 snr6::LEU2 YCp50-SNR6*) has been described previously (Madhani et al., 1990). YHM111 (*MATa trp1 ura3-52 ade2-101 his3 lys2 snr20::LYS2 pSE360-SNR20*) was constructed by transforming the diploid strain ES218 (Shuster and Guthrie, 1988) with a plasmid encoding the wild-type U2 gene, followed by sporulation. Both YHM1 and YHM111 are descendants of S288C. The *GAL-U2* strain (YHM113) was created by 1) transformation of YHM111 with p*GAL-U2* (see below) followed by 2) removal of the wild-type U2 plasmid by the streaking of transformants to 5-fluoroorotic acid-containing plates.

U6 and U2 Plasmids

The low-copy shuttle vectors used in this study, pSE358 (*TRP1*, CEN) and pSE362 (*HIS3*, CEN), were obtained from S. Elledge (Baylor University). pSE358 is a precursor to pUN10 and pSE362 is identical to pUN90 (Elledge and Davis, 1988). For high copy experiments, U2 mutants were subcloned into the 2 μ -based *HIS3* vector, pRS423 (a gift from Joachim Li).

We have previously introduced Sph I and Xho I restriction sites just upstream and downstream of the U6 coding sequence in order to facilitate mutagenesis (Madhani et al., 1990). The plasmid pSX6 contains this U6 gene derivative cloned into pSE358 (Madhani et al., 1990). For mutagenesis of U2, we used a U2 derivative that contains 1) a single nucleotide insertion at its 5' end that creates an Eco RI site and 2) a Bam HI linker in place of a segment of the large non-essential domain of yeast U2 (see Figure 1 in Shuster and Guthrie, 1990). pES143 contains the Sal I-Sma I fragment containing this derivative in pBluescript (Stratagene Cloning Systems, La Jolla, CA). In this study we employed a derivative, pES143 Δ B, which contains a deletion of a Bam HI site in the pBluescript

polylinker. Construction of *GAL* UAS-regulated U2 gene was accomplished by replacement of the *Sal* I-*Dra* III fragment of pES143, which contains all U2 sequences upstream of the putative TATA box, with the *Sau* 3A-*Dde* I fragment of the *GAL1-GAL10* intergenic region (Schnieder and Guarente, 1991). The *Sal* I-*Sac* I fragment was cloned into pSE358 to yield p*GAL*-U2.

Mutagenesis Strategy

Mutants in U6 and U2 derivatives described above were created by polymerase chain reaction amplification of the respective DNAs using primers that contained the desired nucleotide changes. For the U2 mutants this was accomplished in one step using primers that overlapped the *Eco* RI site at the 5' end of the modified U2 gene in pES143 (5' primer spans positions +1 to +36 relative to the transcription start site of the sense strand) and the *Bam* HI site that is downstream of the U2 Sm site (3' primer spans +266 to +227 on the antisense strand). For the U6 mutants, a two-step protocol was used. In the first amplification reaction, we used a mutagenic primer that extends from positions +21 to +62 on the sense strand of the (relative to the transcription start site) and a 3' primer that extends from positions +129 to +96 on the antisense strand. One tenth of this reaction was used in a second amplification using a 5' primer spanning positions -12 to +33 and the same 3' primer as used before. Reaction conditions were as follows: 1uM primers, 200 uM dNTPs, 0.06 U/ul Amersham Hot Tub Polymerase, 2ng/ul template DNA (pSX6 or pES143ΔB) in 1X buffer supplied with Hot Tub polymerase. Total volume was 50 ul. After an initial denaturation at 94 °C for 3 min., and an annealing step at 35 C for 2 min, amplifications were performed for 20 cycles using a two-temperature step protocol: 1 min. at 50 °C and 45 sec. at 94 °C.

The resulting reaction products were precipitated with ethanol and resuspended in 40 ul of water. For the U6 mutants, the DNA was treated with *Sph* I and *Xho* I and was cloned into the *Sph* I and *Xho* I sites of pSX6. For the U2 mutants, the DNA was treated with *Eco* RI and *Bam* HI and used to replace the same fragment in pES143ΔB. A

fragment containing the U2 gene was then cloned into the polylinker of pSE362 using Sac I and Sal I. In all cases, the amplified region was sequenced to confirm that the identity of each mutant

Depletion of U2 snRNA Using GAL-U2

The GAL-U2 strain (and derivatives) was grown to mid-log phase in minimal media containing 2% galactose and 2% sucrose. Cells were pelleted by centrifugation and resuspended in minimal media containing 2% glucose. Cultures were maintained in mid-log phase (OD₆₀₀=0.1 to 1.0) by dilution with glucose-containing media. After 15 hrs., cells were pelleted and frozen prior to subsequent RNA isolation.

RNA Isolation and Analysis

Total RNA was isolated from yeast using the hot phenol method (Kohrer and Domdey, 1991). RNA was analyzed using the primer-extension protocol described by Patterson and Guthrie (1991). The following ³²P-end-labeled primers were used:

SNR17A and *SNR17B* (U3 snRNA; Myslinski et al., 1990): 5'-

CCAAGTTGGATTCAGT-3' (complementary to exon 2 of both genes).

RP51A (Teem and Rosbash, 1983): 5'-GTATGACTTTATTGCGCATGTCTGACTC-3'

(intron primer) and 5'-CGCTTGACGGTCTTGGTTC-3' (exon 2 primer).

SNR7 (U5 snRNA; Patterson and Guthrie, 1987): 5'-

AAGTTCCAAAAAATATGGCAAGC-3'.

The sizes of the extension products shown in Figures 7B, 7C and 7D that are generated by primer-extension of the endogenous RNAs are as follows. *SNR17* exon 2 primer: pre-U3A = 237 nts; pre-U3B = 210 nts; and lariat-intermediate and U3 snRNA = 81 nts. *RP51A* intron primer: pre-mRNA = 93, 103 nts; lariat intermediate and excised lariat = 73 nts. *RP51A* exon 2 primer: lariat-intermediate = 87 nts; mRNA = 49, 59 nts. *SNR7* primer: U5 = 180 nts.

Acknowledgements

We thank D. Fortner, R. Troy, and D. Brow; D. McPheeters, H. Sawa and J. Abelson; and D. Wassarman and J. Steitz for communicating results prior to publication. We are grateful to J. Li for plasmids; S.M. Noble, J.G. Umen and P. Raghunathan for helpful criticism of the manuscript; S.M. Noble for synthesis of the oligonucleotides used in this study; and H. Roiha, L. Esperas and C. Pudlow for technical support. H.D.M. is a recipient of a UCSF Chancellor's Fellowship. This work was supported by a grant to C.G. from the National Institutes of Health (GM21119). C.G. is an American Cancer Society Research Professor of Molecular Genetics.

Figure 1. *S. cerevisiae* U4 and U6 snRNAs.

Phylogenetically invariant residues are shown in uppercase and bold (based on alignments of Guthrie and Patterson, 1988; and C.G., S. Mian, and H. Roiha, unpublished). Asterisks mark residues specifically required for the second step of splicing in vitro (Fabrizio and Abelson, 1990). Arrows mark the locations of mRNA-type introns in the U6 genes of *S. pombe* (Tani and Ohshima, 1989) and *R. dactyoidum* (Tani and Ohshima, 1991). The essential ACAGAG and AGC sequences mentioned in the text span positions 47-52 and 59-61, respectively.

Figure 2. U2/U6 Base-Pairing Model.

Shown is the Watson-Crick complementarity between nts 54-61 of yeast U6 snRNA and nts 21-30 of yeast U2 snRNA. Also depicted is the established interaction between nts 33-39 of yeast U2 and the yeast intron branchpoint region consensus, UACUAACA (Parker et al., 1987). The branchpoint adenosine is shown attacking the 5' splice site during the first chemical step of splicing. In yeast, the 5' splice site consensus sequence is GUAUGU. The 3' splice site (YAG) is usually 30-50 nts downstream of the branchpoint.

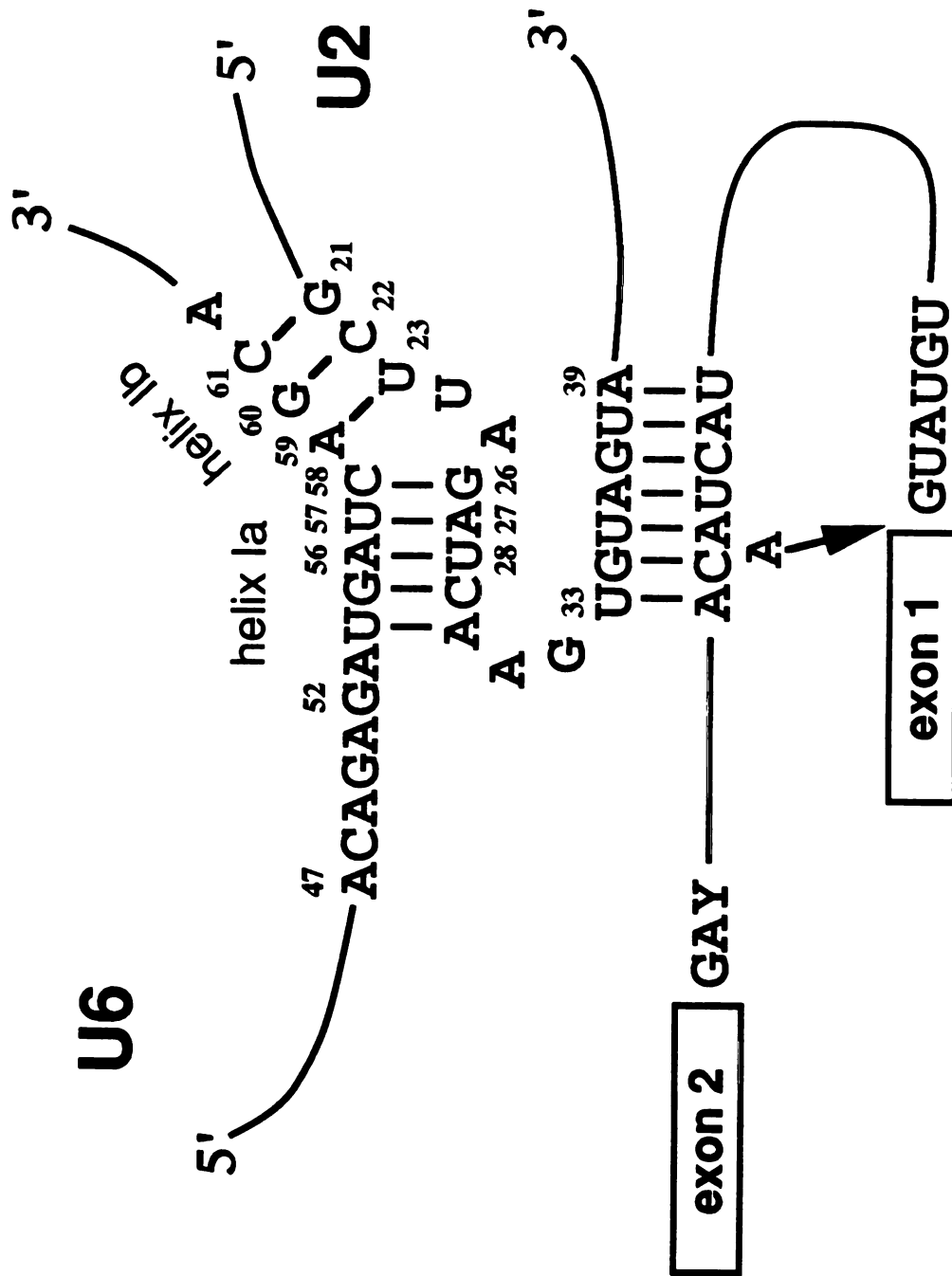


Figure 3. Plasmid Shuffle Assay for Mutants.

This yeast strain YHM1 is depicted (Madhani et al., 1990). This strain contains a deletion of the chromosomal U6 coding sequence that is complemented by a wild-type U6 gene carried on a centromeric plasmid marked with the yeast *URA3* gene. U6 mutants, either alone or in combination with U2 compensatory mutants or non-compensatory mutants, can be introduced by transformation. The phenotype of the introduced U6 mutant can then be assessed by streaking transformants to plates containing 5-fluoroorotic acid (5-FOA), which selects for loss of the *URA3*-marked plasmid (Boeke et al., 1987).

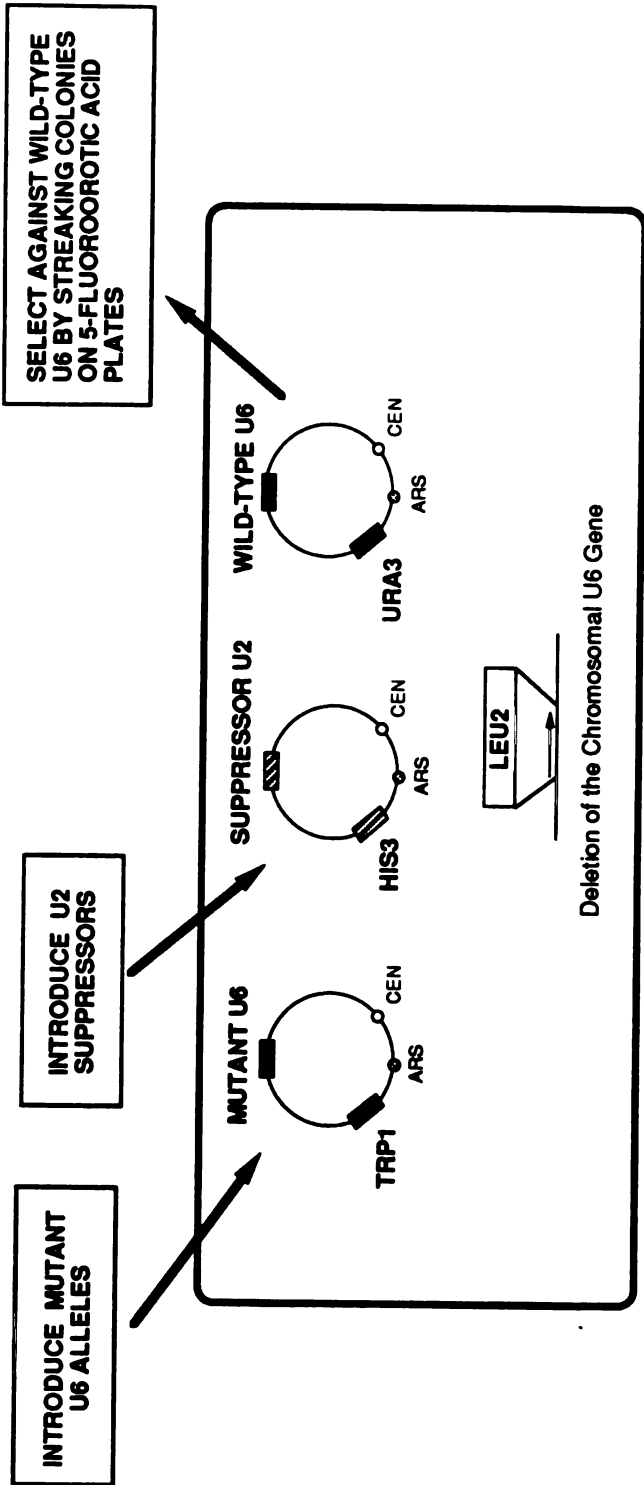


Figure 4. Specific Suppression of U6 Mutants at Positions 56-57 by Compensatory U2 Mutants.

Shown is the growth on 5-FOA of YHM1 derivatives containing the indicated U6 mutant either on its own (A, G, M), in the presence of the predicted compensatory mutant in U2 that restores base-pairing according to Figure 2 (B, H, N) or in the presence of non-compensatory U2 alleles (C-F, I-L, O-R). Plates shown in A-F (U6-A56U,U57A) were incubated at 30 °C for three days. Those shown in G-R (U6-A56C,U57C; U6-A56C,U57G) were incubated at 33 °C for three days.

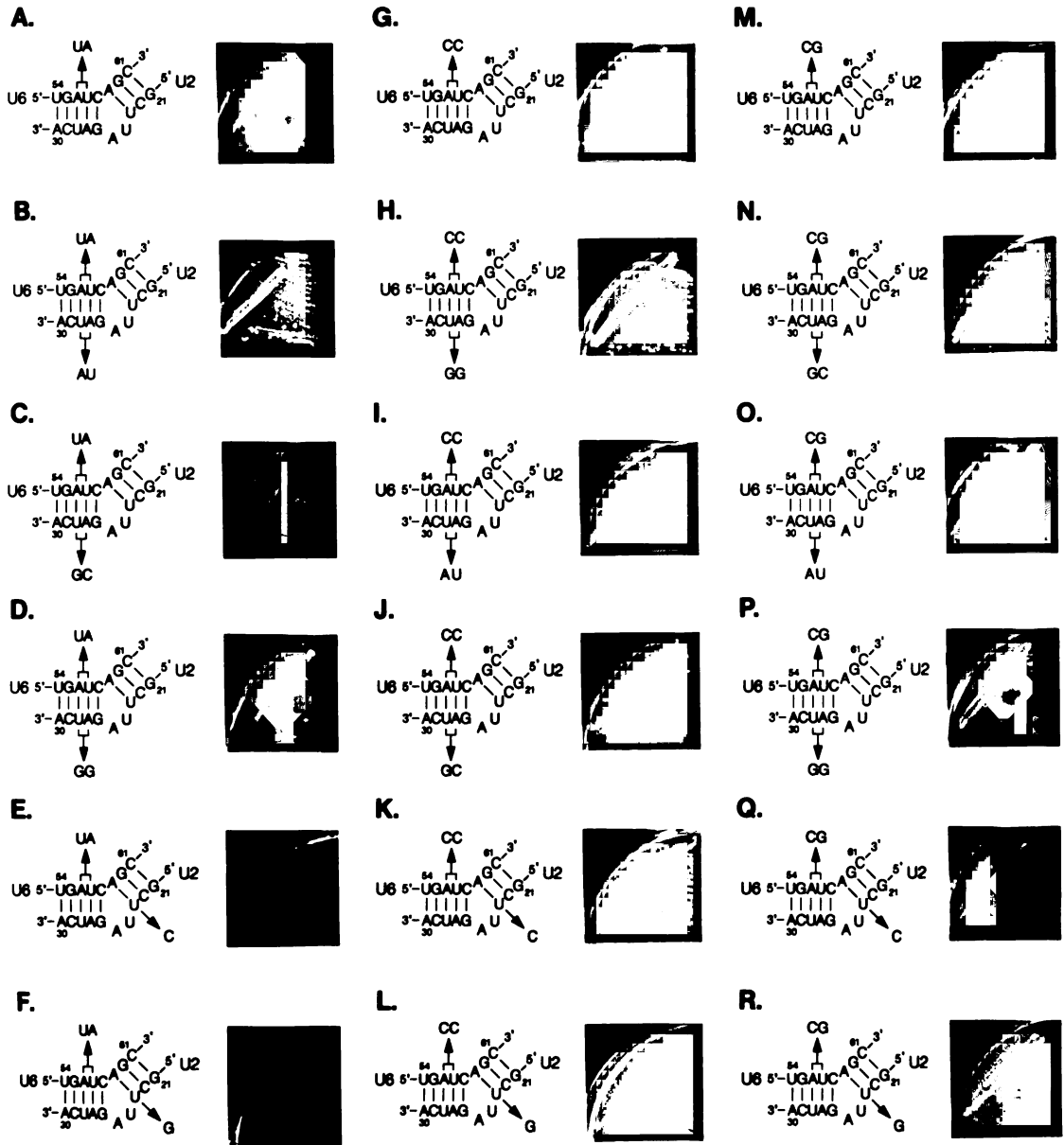


Figure 5. Specific Suppression of U6 Mutants at Position 58 by Compensatory U2 Mutants.

The growth of the indicated mutants at position 58 in U6 was assayed as in Figure 4. Mutants were assayed their own (A, E), in the presence of compensatory mutants in U2 that are predicted to restore base-pairing (B, F), or in the presence of non-compensatory U2 alleles (C, D, G, H). Plates shown in A-D (U6-C58U) were incubated at 37 °C for three days; those in E-H (U6-C58A) were incubated at 31.5 °C for three days. U2 mutants used in B-D were carried on high-copy plasmids (see Table 1).

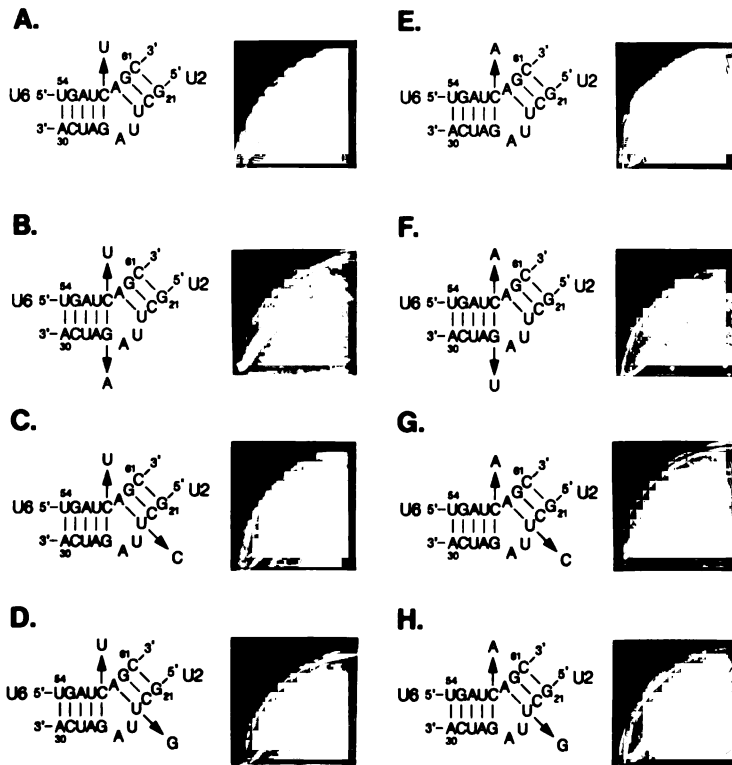


Figure 6. Specific Suppression of U6 Mutants at Position 59 by Compensatory U2 Mutants.

The growth of the indicated mutants at position 59 in U6 was assayed as in Figure 4. Mutants were assayed on their own (A, F), in the presence of compensatory mutants in U2 that are predicted to restore base-pairing (B, G), or in the presence of non-compensatory U2 alleles (C-E, H-J). Plates shown in A-E (U6-A59C) were incubated at 35 °C for three days; those shown in F-J (U6-A59G) were incubated at 30 °C for three days.

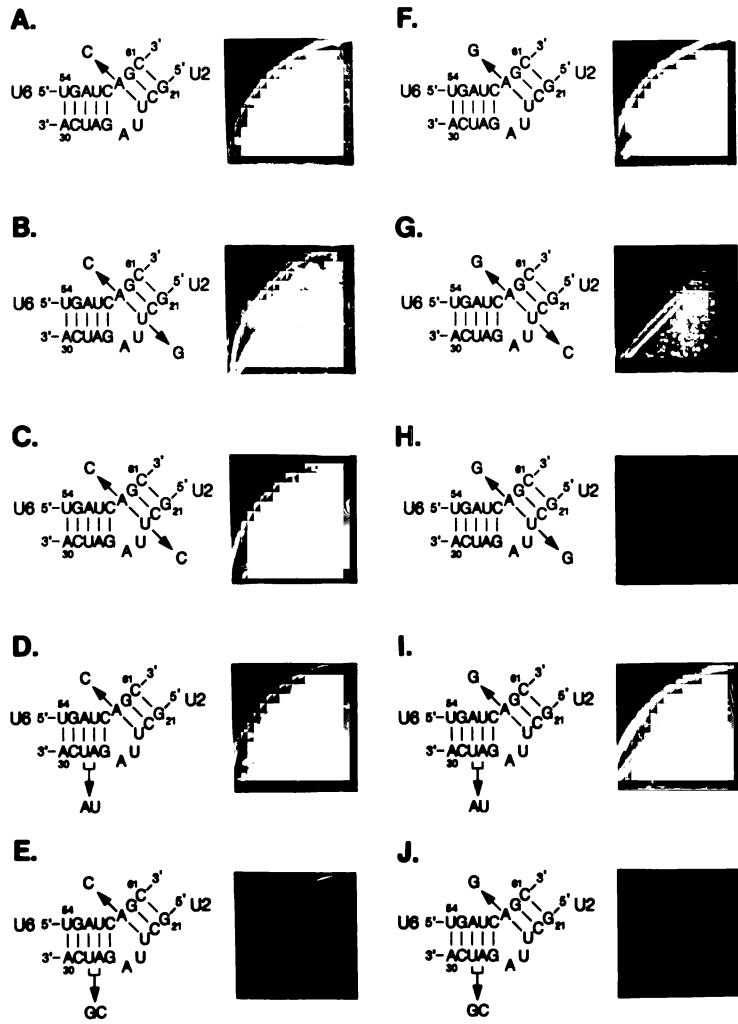


Figure 7. Mutants in U2 Inhibit Both Steps of Splicing In Vivo.

A. Strain Used for Analysis.

A strain (YHM113) containing a deletion of the chromosomal U2 gene that is complemented by a *GAL* UAS-regulated U2 gene is depicted. Plasmids that encode mutant U2 alleles or wild-type U2 were individually introduced into this strain by transformation. Cultures of the resulting strains were shifted from galactose media to glucose media for 15 hrs. to deplete cells of wild-type U2 snRNP.

B. Analysis of In Vivo Splicing Defects: *SNR17A* and *SNR17B*.

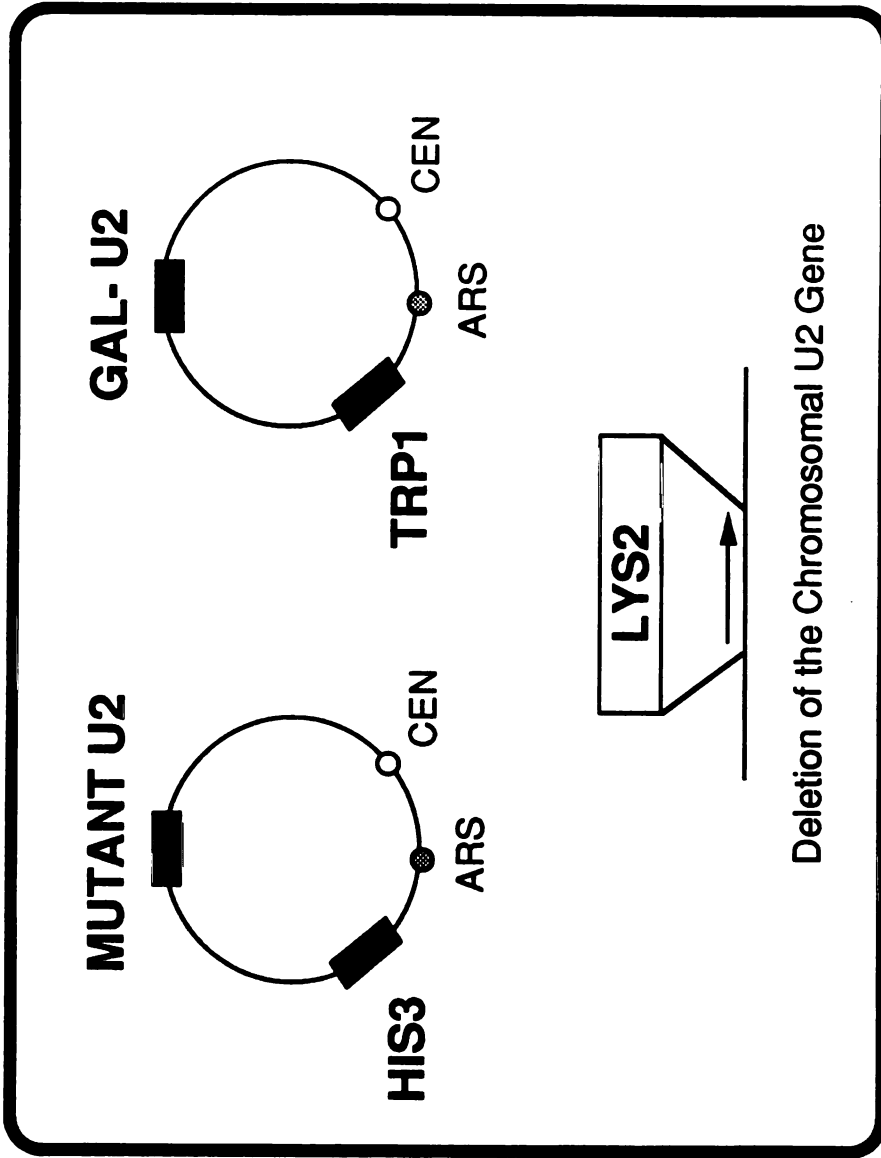
Total RNA from the strains described in A was analyzed by a primer-extension method using a ³²P-end-labeled oligonucleotide complementary to the second exons of the yeast *SNR17A* and *SNR17B* genes (Myslinski et al., 1990). A labeled oligonucleotide complementary to U5 snRNA was also included in the reaction as an internal control for the amounts of RNA in each reaction. The products were analyzed by electrophoresis through a 6% denaturing acrylamide gel followed by autoradiography. Bands that correspond to unspliced pre-U3A, pre-U3B, mature U3 and U5 snRNAs are indicated. U3 lariat-intermediate comigrates with mature U3 snRNA. Boxes indicate exon sequences, and lines depict intron sequences. The band (marked by an asterisk) below that which corresponds to full-length U5 is the result of a reverse transcriptase "strong stop" due to secondary structure in U5 snRNA. "M" indicates markers (pBR322/HpaII). The U2 alleles analyzed are indicated above each lane.

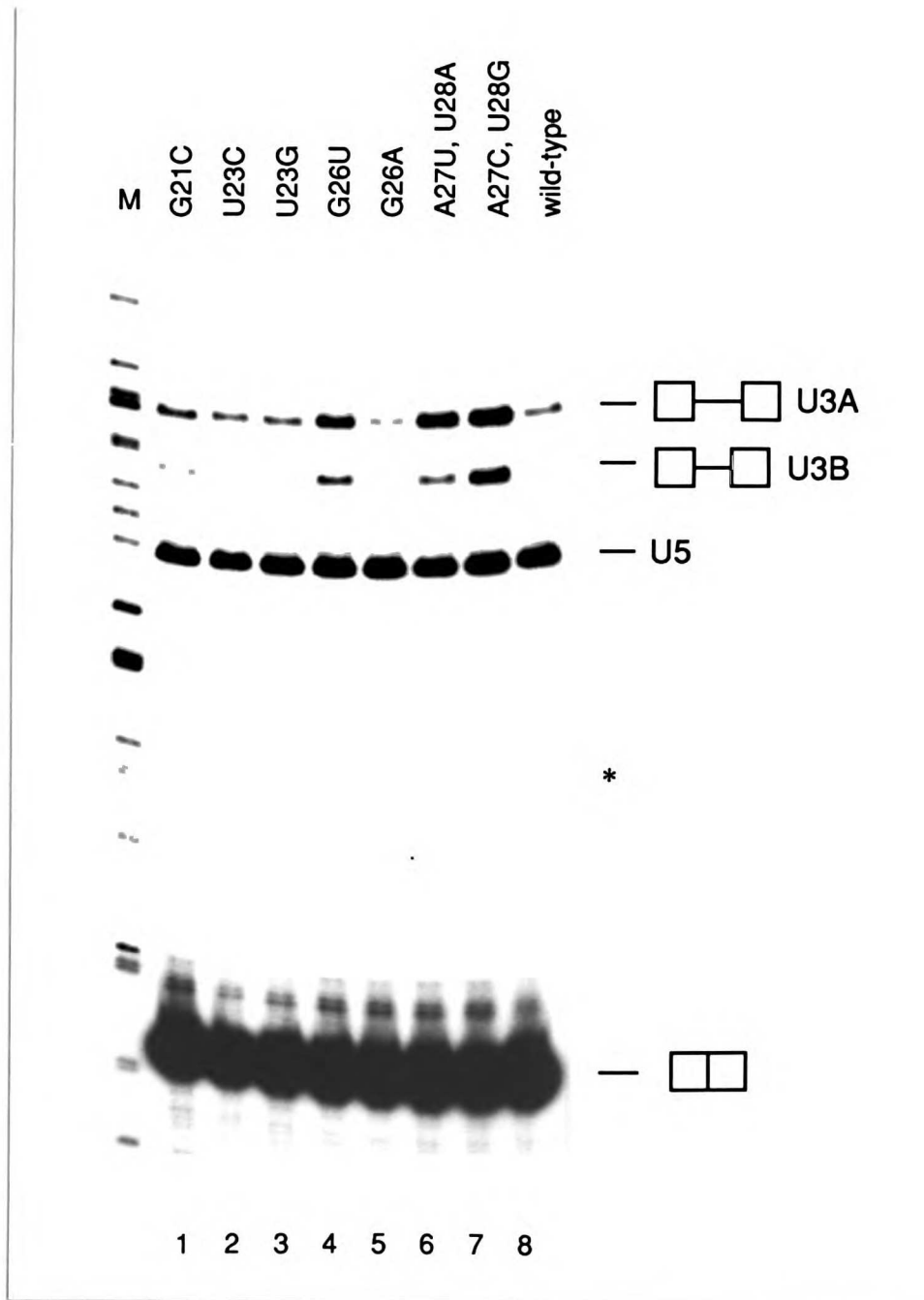
C and D. Analysis of In Vivo Splicing Defects: *RP51A*.

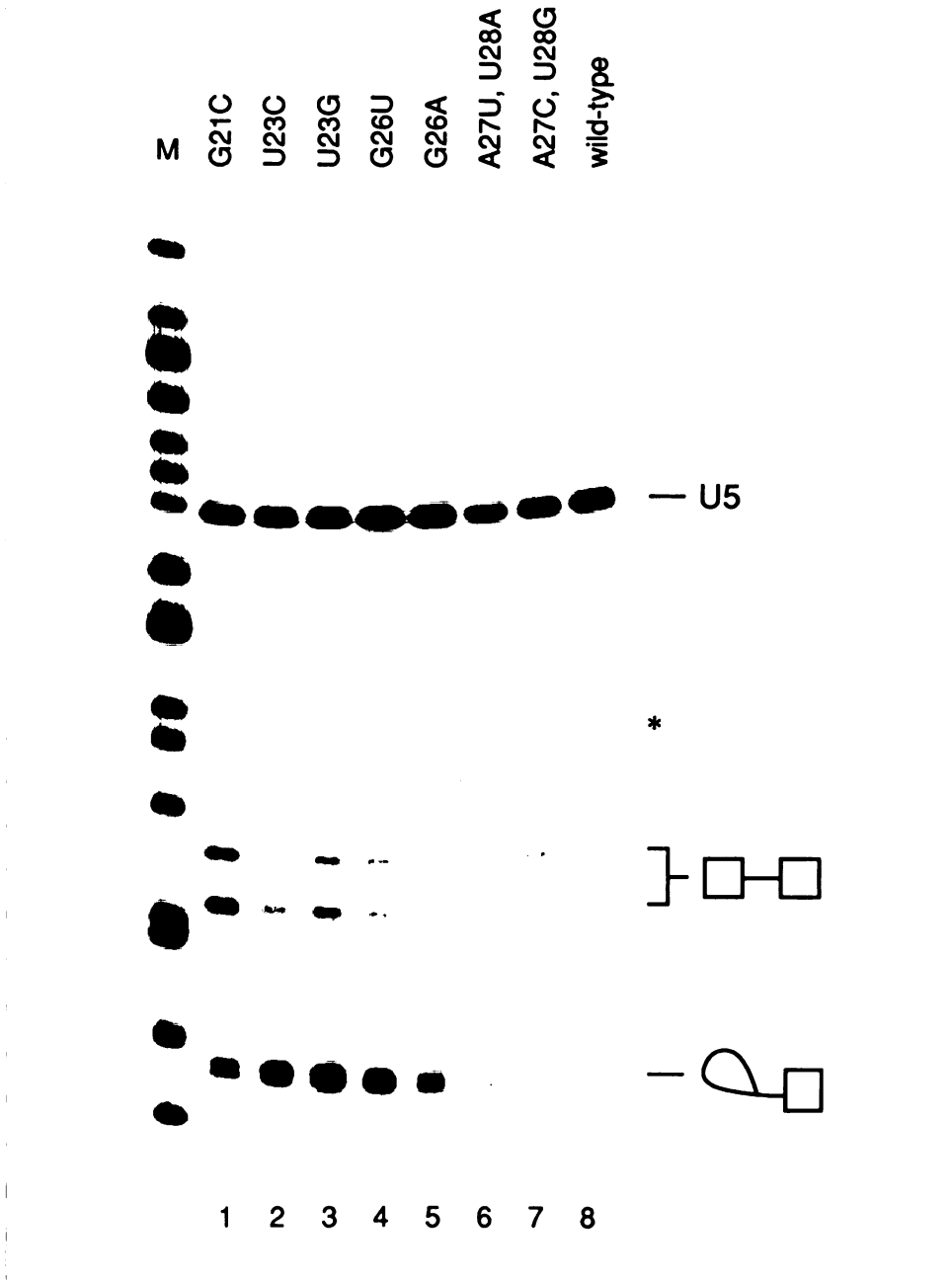
In panel C, the RNA samples used in B were analyzed using an oligonucleotide complementary to the intron of the yeast *RP51A* gene (Teem and Rosbash, 1983). Bands that correspond to unspliced pre-mRNA (note there are two transcription start sites for the *RP51A* gene), lariat-intermediate and the U5 internal control are indicated. Since the intron primer can, in principle, also hybridize to the excised intron lariat, we examined several of the same RNA samples using a primer complementary to the second exon of

RP51A (panel D) and confirmed that the observed signal is due to the accumulation of lariat-intermediate (bands not designated in panel D are probable reverse transcriptase "strong stops" commonly seen with this primer).

A







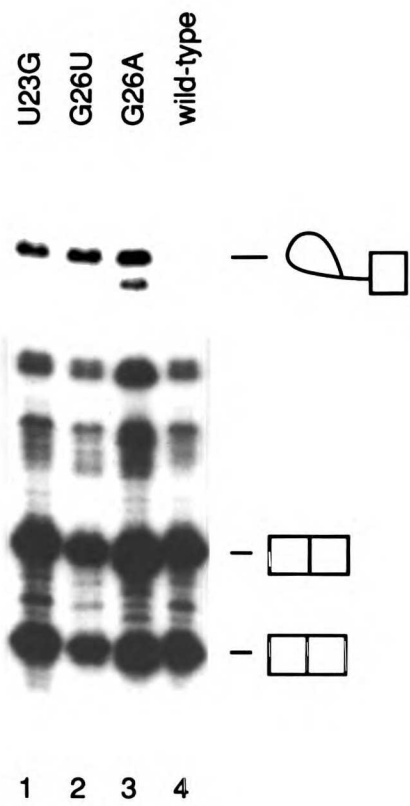
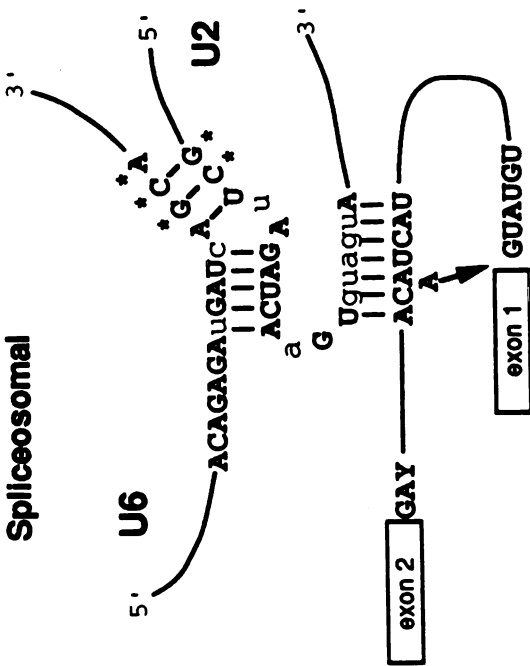


Figure 8. Structural Similarity Between the Spliceosome and Group II Introns.

On the left, U2 and U6 snRNAs are shown together with a yeast consensus intron as in Figure 2 (phylogenetically invariant residues are indicated in uppercase bold). The consensus sequence for domains 5 and 6 of Group IIA introns is shown on the right (Michel et al., 1989). Highly conserved nucleotides in Group IIA introns are shown in uppercase bold; conserved purines and pyrimidines are denoted by 'r' and 'y', respectively; and variable sequences are denoted by 'n'. Asterisks next to nucleotides in both structures indicate a limited identity in primary sequence.

Spliceosomal



Group IIA

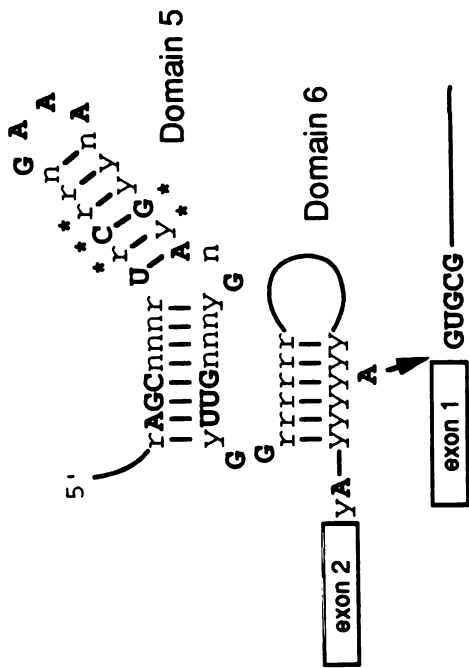


Figure 9. Conformational Isomers and Phylogenetic Conservation of U2, U4 and U6 snRNAs.

Base-pairing interactions between U4 and U6, U2 and U6 as well as intramolecular structures are shown. Uppercase bold nucleotides represent those which are phylogenetically invariant (Guthrie and Patterson, 1988; C.G., S. Mian, and H. Roiha, unpublished). Nucleotides in the U4/U6 structure and in the U2 intramolecular structure that engage in base-pairing in the U2/U6 structure are colored accordingly. Structural domains of the molecules discussed in the text are indicated.

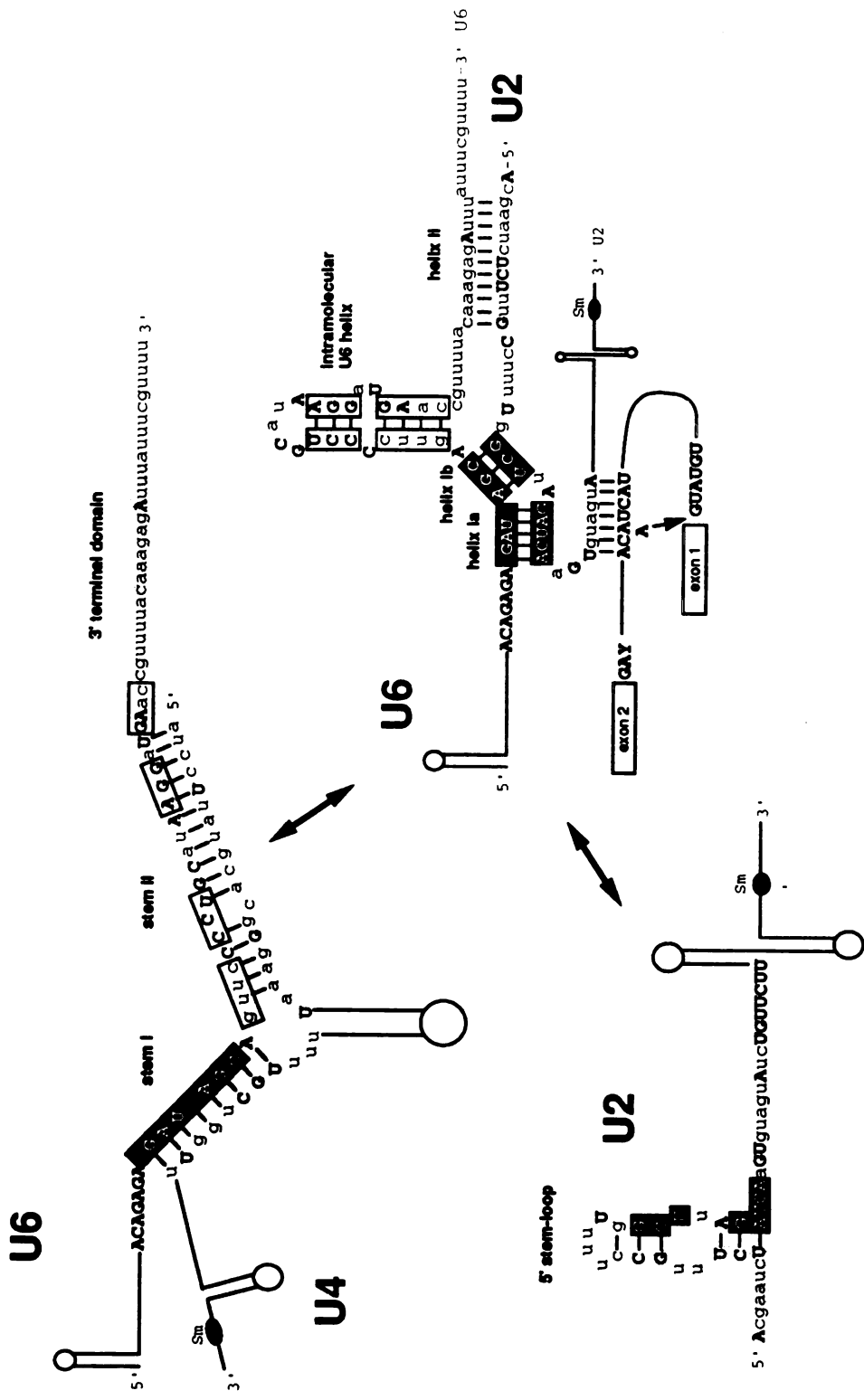


Table 1. Summary of Genetic Suppression Experiments.

Mutants in the *S. cerevisiae* U6 and U2 snRNAs are indicated by the wild-type nucleotide and its position followed by the identity of the mutant nucleotide. ^aAdditional copy of U2 snRNA introduced into YHM1. "Null" refers to the introduction of a vector plasmid containing no U2 gene. ^bCEN indicates a centromeric (low copy) yeast vector; 2 μ indicates a high-copy yeast vector. ^cExcept for U6-A56U, U57A and U6-A59G, suppression was generally much poorer or not observed at temperatures higher than that indicated. ^dGrowth of the YHM1 derivatives on 5-fluoroorotic acid plates after three days.

Table 1

U6 allele	U2 allele ^a	U2 vector ^b	temperature ^c	growth ^d
A56U, U57A	null	CEN	30	-
	WT	CEN	30	-
	A27U, U28A	CEN	30	+
	A27C, U28G	CEN	30	-
	A27G, U28G	CEN	30	-
	U23C	CEN	30	-
	U23G	CEN	30	-
A56C, U57C	null	CEN	33	-
	WT	CEN	33	-
	A27G, U28G	CEN	33	+
	A27U, U28A	CEN	33	-
	A27C, U28G	CEN	33	-
	U23C	CEN	33	-
	U23G	CEN	33	-
A56C, U57G	null	CEN	33	-
	WT	CEN	33	-
	A27C, U28G	CEN	33	+
	A27U, U28A	CEN	33	-
	A27G, U28G	CEN	33	-
	U23C	CEN	33	-
	U23G	CEN	33	-
C58U	null	2 μ	37	-
	WT	2 μ	37	-
	G26A	2 μ	37	+
	U23C	2 μ	37	-
	U23G	2 μ	37	-
C58A	null	CEN	31.5	-
	WT	CEN	31.5	-
	G26U	CEN	31.5	+
	U23C	CEN	31.5	-
	U23G	CEN	31.5	-
A59C	null	CEN	35	-
	WT	CEN	35	-
	U23G	CEN	35	+
	U23C	CEN	35	-
	A27U, U28A	CEN	35	-
A59G	A27C, U28G	CEN	35	-
	null	CEN	30	-
	WT	CEN	30	-
	U23C	CEN	30	+
	U23G	CEN	30	-
G60U	A27U, U28A	CEN	30	-
	A27C, U28G	CEN	30	-
	null	CEN	18-37	-
	WT	CEN	18-37	-
	C22A	CEN	18-37	-
G60C	C22A	2 μ	18-37	-
	null	CEN	18-37	-
	WT	CEN	18-37	-
	C22G	CEN	18-37	-
C61G	null	CEN	37	-
	WT	CEN	37	-
	G21C	CEN	37	-
	G21C	2 μ	37	-

Table 2. Comparison of Phenotypes of U2 and U6 Mutants that Disrupt Helix I.
Mutants are designated as in Table 1. '+' indicates wild-type growth, '+/-' indicates poor growth, and '-' indicates no growth. Plates were scored after three days.

Table 2

growth							
U6 allele	25°C	30°C	37°C	U2 allele	25°C	30°C	37°C
null	-	-	-	null	-	-	-
wild-type	+	+	+	wild-type	+	+	+
A56U,U57A	-	-	-	A27U,U28A	-	-	-
A56C,U57C	-/+	+	-	A27C,U28C	-/+	+	-
A56C,U57G	-	-	-	A27C,U28G	-	-	-
C58A	-	-	-	G26A	-	-/+	-
C58U	+	+	-	G26U	-	-	-
A59C	+	+	-	U23G	+	+	+
A59G	-	-	-	U23C	+	+	+
G60C	-	-	-	C22G	+	+	+
G60U	-	-	-	C22A	+	+	+
C61G	+	+	-	G21C	-	-	+

Table 3. Splicing Defects Exhibited by U2 Mutants: Quantitation of Pre-mRNA and Lariat-Intermediate.

Radioactivity in the gels that correspond to the autoradiograms displayed in Figures 7B and 7C was quantitated using a Molecular Dynamics phosphor screen and a phosphorimager. The relative amounts of pre-mRNA, lariat intermediate and the U5 snRNA (internal control) was determined. The values for pre-mRNA and lariat-intermediate ("L-I") were then normalized for the amount of RNA analyzed in each reaction, as reflected by the levels of the U5 internal control. In the Table, the levels for wild-type is arbitrarily set at 1.0; the levels shown for the mutants therefore reflect "fold-increases" over wild-type.

Table 3

Relative Levels				
U2 allele	pre-U3A	pre-U3B	pre-RP51A	RP51A L-I
G21C	1.2	1.5	4.7	3.0
U23C	1.0	0.9	2.0	5.6
U23G	1.0	0.7	2.9	7.6
G26U	1.8	2.7	1.6	3.6
G26A	0.6	0.6	0.9	2.4
A27U, U28A	3.1	3.4	1.3	1.0
A27C, U28G	3.7	6.9	1.7	0.5
wild-type	1.0	1.0	1.0	1.0

**Randomization-Selection Analysis of snRNAs In
Vivo: Evidence for a Tertiary Interaction in the
Spliceosome**

Summary

Putative components of the spliceosomal active site include a bulged helix between U2 and U6 snRNAs (U2-U6 helix I) and the adjacent ACAGAG hexanucleotide in U6. We have developed an in vivo, bimolecular randomization-selection method to functionally dissect these elements. Although a portion of U2-U6 helix I resembles the G binding site of Group I introns, the data are inconsistent with an analogous functional role for this structure in the spliceosome. Instead, analysis of several novel covariants supports the existence of a structure in which the terminal residue of the U6 hexanucleotide (ACAGAG) engages in a tertiary interaction with the helix I bulge. Such a higher order structure, together with other known interactions, would juxtapose the two clusters of residues of the U2-U6 complex that are specifically required for the second chemical step of pre-mRNA splicing with the 3' splice site.

Introduction

The splicing of messenger RNA precursors (pre-mRNAs) occurs in the spliceosome, a large and dynamic ribonucleoprotein complex containing five small nuclear RNAs (U1, U2, U4, U5, and U6 snRNAs) and at least 50 proteins (for reviews see Moore et al., 1993; Rymond and Rosbash, 1992; Green, 1991; Guthrie, 1991). Similarities between the two-step chemical pathway of pre-mRNA splicing and that of Group II autocatalytic introns has led to the proposal that the former is also fundamentally an RNA-catalyzed process mediated by the snRNA components of the spliceosome (Sharp, 1985;1991; Cech, 1986; Guthrie, 1991). Indeed, a number of direct RNA-RNA interactions involving the pre-mRNA substrate and the spliceosomal snRNAs have been demonstrated. It is well-established that recognition of the 5' splice site and intron branchpoint involves Watson-Crick base-pairing with U1 and U2 snRNAs, respectively (reviewed in Moore et al., 1993; Rymond and Rosbash, 1992). More recent studies indicate that U5 also interacts with the pre-mRNA, in this case with the 5' and 3' exons (Newman and Norman, 1991; 1992; Wyatt et al., 1992; Sontheimer and Steitz, 1993). A non-Watson-Crick interaction between the guanosines at the 5' and 3' splice sites has been proposed to function in the second chemical step of splicing (Parker and Siliciano, 1993). Several of these interactions have potential counterparts in Group II self-splicing introns (reviewed in Weiner, 1993; Chanfreau and Jacquier, 1993).

Our studies have focused on the U6 spliceosomal snRNA (Madhani et al., 1990; Madhani and Guthrie, 1992). This highly conserved molecule is associated with U4 snRNA through an extensive base-pairing interaction, which is disrupted prior to the first chemical step of splicing (reviewed in Moore et al., 1993; Rymond and Rosbash, 1992; Green, 1991; Guthrie, 1991). We have previously used a mutational approach in yeast to demonstrate the existence of a conserved base-pairing interaction between U6 and U2 snRNAs that is mutually exclusive with the U4-U6 interaction (Madhani and Guthrie, 1992). In this pairing, termed U2-U6 helix I, a conserved sequence in U6 snRNA

interacts with sequences in U2 that are just upstream of the branchpoint recognition region of U2. As a result, highly conserved and functionally important residues in U6 can be juxtaposed with the intron branchpoint. Residues that participate in this structure have been shown to be required for cell viability (Madhani et al., 1990) as well as for both chemical steps of splicing *in vitro* and *in vivo* (Fabrizio and Abelson, 1990; Madhani and Guthrie, 1992; McPheeters and Abelson, 1992). These properties led us to propose a model for the active site of the spliceosome (Figure 1) in which U2-U6 helix I might participate directly in chemical steps of splicing (Madhani and Guthrie, 1992). Because this helix is mutually exclusive with stem I of the U4-U6 interaction, its formation offers a mechanistic rationale for the destabilization of U4-U6 prior to the chemical steps of splicing (Madhani and Guthrie, 1992). Further evidence consistent with a direct role for this structure in catalysis is suggested by *in vitro* crosslinking experiments (Sawa and Shimura, 1991; Wassarman and Steitz, 1992; Sawa and Abelson, 1992) and, more recently, genetic suppression experiments (Lesser and Guthrie, 1993; Kandels-Lewis and Séraphin, 1993) which demonstrate base-pairing between the highly conserved ACA sequence upstream of U2-U6 helix I and the 3' portion of the 5' splice site consensus (Figure 1A). Notably, the three RNA-RNA interactions depicted in Figure 1 provide a structural mechanism for juxtaposing the branchpoint nucleophile with the 5' splice site.

U2-U6 helix I exhibits intriguing similarities to structures in self-splicing introns (reviewed in Moore et al., 1993; Weiner, 1993). We have previously noted a resemblance to domain 5 of Group II introns: both structures are highly conserved, lie just upstream of helices involved in branchpoint recognition, and contain two nucleotide bulges that interrupt the 3' side of their respective helices (Madhani and Guthrie, 1992; Michel et al., 1989b). A different analogy was suggested by an *in vitro* mutational analysis of the AGA sequence in yeast U2 snRNA (McPheeters and Abelson, 1992; nts 25-27 in Figure 1). On the basis of structural and phenotypic similarities to the AGA sequence in the P7 helix of Group I introns, which contains the binding site for the guanosine (G) cofactor (Michel et

al., 1989a), it was proposed that the essential role of the AGA sequence in U2 snRNA in the second chemical step of pre-mRNA splicing is to bind to the conserved G found at the 3' splice site of nuclear introns (McPheeters and Abelson, 1992). This putative spliceosomal G binding motif has been cited as a possible case of convergent evolution (Weiner, 1993). Moreover, it has recently been proposed based on stereochemical studies that the spliceosome generates a Group I-like catalytic site to execute the second step of splicing (Moore and Sharp, 1993).

Evaluation of the possible roles of snRNAs in catalysis and their relationship to components in self-splicing introns will ultimately require knowledge of the higher order foldings of the structures in which they participate. In view of the large and dynamic nature of the spliceosome, a potentially powerful strategy for deriving such structural constraints is phylogenetic covariation analysis; this approach has already been applied successfully to diverse RNA molecules (Levitt, 1969; Woese et al., 1980; Noller et al., 1981; Michel et al., 1989b; Michel and Westhof, 1990; Romero and Blackburn, 1991). In the case of Group I introns (Michel and Westhof, 1990), sufficient long-range constraints have been obtained in the form of tertiary interactions to allow the determination of a robust three-dimensional structural model, key aspects of which have been confirmed experimentally (reviewed in Cech, 1993).

Unfortunately, almost all of the U2 and U6 residues involved in the proposed active site model of the spliceosome (Figure 1) are phylogenetically invariant, precluding a strictly analogous approach to the identification of tertiary structure (Guthrie and Patterson, 1988; C.G., S. Mian, and H. Roiha, unpublished). In other systems this limitation has been overcome through the generation of "artificial phylogenies:" novel functional variants selected in vitro from pools of randomized sequences (reviewed in Szostak and Ellington, 1993; Gold et al., 1993) This approach has been exploited to identify functionally important tertiary RNA interactions in the Rev-responsive-element of human immunodeficiency virus type 1 (Bartel et al., 1991) and in the *sunY* Group I ribozyme

(Green et al., 1993). However, there are significant impediments to the application of such methods to the spliceosome. First, the region of interest (Figure 1) is derived from several different RNA molecules, yet current in vitro methods do not allow for the selection of functional pairs of variants (intermolecular covariants). Second, it is not feasible to efficiently reconstitute splicing in vitro with multiple synthetic RNAs, nor to select in vitro for functional variants.

In order to circumvent these limitations, we have employed a method that allows for the single-step selection in vivo of functional covariants of two interacting molecules from gene pools containing synthetically randomized residues. We have applied this procedure to functionally dissect residues in the U2-U6 helix I region that are involved in the second chemical step of splicing (Figure 1). The properties of the selected variants do not conform to those predicted by the G binding site model for the AGA sequence in U2. Instead, analysis of several novel variants support the existence of a structure in which the terminal residue of the U6 hexanucleotide (ACAGAG) forms a tertiary interaction with the helix I bulge. To our knowledge, it represents the first evidence for higher order RNA structure in the spliceosome. We discuss its implications for the active site involved in the second chemical step of splicing.

Results

Randomization-Selection Strategy

Our strategy is summarized in Figure 2 (see Experimental Procedures for details). We first constructed libraries of yeast U6 and U2 genes in which particular residues had been randomized through chemical synthesis. These were used to cotransform a yeast strain, YHM118, in which both chromosomal copies of U2 and U6 are deleted and complemented by a single *URA3*-marked centromere plasmid that contains both wild-type genes. The cotransformants were then replica-plated to media containing 5-fluoroorotic acid (5-FOA), which selects against the *URA3*-marked wild-type U2-U6 plasmid (Boeke et al., 1987). Colonies that grow on 5-FOA contain U2 and U6 functional covariants which can then be isolated and analyzed by DNA sequencing. In deciding what residues to randomize in the libraries, we assumed that residues involved in the same step of splicing would be the most likely to interact with each other. In the U2 and U6 libraries described here, regions that encompass residues involved in the second chemical step of splicing were randomized (Figure 1; nts 51, 52, 58, 59 in U6 and nts 23-26 in U2). In addition, since two of the U2 residues randomized are thought to participate in an alternative intramolecular structure, U2 stem I (Guthrie and Patterson, 1988), their putative base-pairing partners were also randomized (nts 9-10).

We selected for functional cotransformants on 5-FOA under two different conditions, which represent arbitrary (but experimentally convenient) thresholds. First, we isolated non-temperature sensitive (non-ts) variants by demanding growth after 2 days at 30 °C and screening replica plates for temperature-sensitivity at 37 °C. Second, we reduced the stringency of selection by isolating temperature-sensitive (ts) variants. This was accomplished by selecting positives after 4 days, followed by screening of replica plates at 37 °C. The 60 individual variant pairs (25 non-ts and 35 ts) obtained are listed in Figures 3. Diagrams showing the nucleotides recovered at each randomized position are shown in Figure 4. These sequences were visually inspected for nucleotide covariations.

Analysis of the Selected Variants

In the conserved hexanucleotide in U6, the last two positions were randomized (ACAGAG; positions 51 and 52). In all variants, the wild type A residue was observed at position 51 (Figure 4). In contrast, all three possible nucleotide changes were observed at position 52. This observation was unexpected, since two of the changes, U6-G52A and U6-G52C, are unconditionally lethal as single mutations (Madhani et al., 1990). We will return to the basis for this result in the next section .

In helix I, the residues in U2 and U6 flanking and including the two-nucleotide bulge that separates helix Ia and helix Ib were randomized. We have previously reported evidence for base-pairing between U6-C58 and U2-G26 as well as between U6-A59 and U2-U23 (Figure 1; Madhani and Guthrie, 1992). The role of U2-G26 is of particular interest since this residue is the most critical in the proposed G binding site described in the Introduction (McPheeters and Abelson, 1992). In the case of the G binding site of Group I introns, the identity of the G in the AGA sequence is phenotypically more important than base-pairing because of its critical role in substrate binding (Michel et al., 1989a; Yarus et al., 1991a). Therefore, it was of interest to determine whether this was the case in the selected variants. Extensive Watson-Crick covariation was observed between U6 nt 58 and U2 nt 26 (Table 1), strongly supporting the occurrence of base-pairing at this position. To examine in detail the base-pairing requirements at this position, we constructed yeast strains that contained all possible nucleotide combinations at these two positions, using U2 and U6 alleles created by site-directed mutagenesis. These were assayed at 25, 30, and 37 °C. The phenotypes of these strains are summarized in Table 2 and shown in Figure 5A, for plates incubated at 30 °C. As can be seen by examining the diagonals in both Figure 5A and Table 2, all Watson-Crick appositions support cell growth under the conditions tested. Both G-U wobble pairs are functional, though one (U6-C58U/U2-G26) is ts at 37 °C (Figure 5A, Table2). One of the two A-C appositions confers slow, ts growth (Figure 5A, Table 2); interestingly, rare A-C pairs that replace G-U pairs in rRNA phylogeny are

always found at helical junctions (Gutell, 1993). No other nucleotide apposition is functional at this position under any of the condition tested (Figure 5A, Table 2).

Previously, it was shown that double mutants that affect both G26 and A27 in U2 result in a more severe phenotype in vitro than single mutations at either position ; indeed, a complete inhibition of the second step of splicing was observed (McPheeters and Abelson, 1992). This observation was rationalized in terms of a recent "axial" G binding site proposal for Group I introns in which both the G and 3' A of the AGA sequence interact with the G substrate (McPheeters and Abelson, 1992; Yarus et al., 1991a; 1991b). However, given the results described above, an alternative possibility is that the severe defect of double mutants at nts 26 and 27 in U2 might be due instead to a defect in base-pairing with U6. To test this possibility, we constructed and analyzed a double transversion at these positions (U2-G26C, A27U). As expected, in the presence of wild-type U6, this mutant is lethal at 25, 30 and 37 °C (Figure 5B shows plates incubated at 30 °C). In contrast, in the presence of a U6 allele that restores base-pairing (U6-U57A, C58G), wild-type growth is restored under all conditions tested (Figure 5B). Moreover, suppression between the U2 and U6 alleles is mutual since the U6 allele is also lethal in the presence of wild-type U2 (Figure 5B). Taken together with the results shown in Figure 5A and summarized in Table 2, the data indicate that base-pairing at these positions, rather than specific sequence, is crucial for cell viability and, presumably, the second step of splicing.

The other base-pair randomized consists of U6 nt 59 and U2 nt 23. We previously demonstrated that the deleterious growth phenotypes of U6-A59G, a lethal allele, and U6-A59C, a ts allele, can be specifically suppressed by U2-U23C and U2-U23G respectively. However, in the presence of wild-type U6, the U2 mutations have no effect on cell growth, although they exhibit a measurable defect in the second step of splicing in vivo (Madhani and Guthrie, 1992). Thus, base-pairing at this position, while demonstrable, is not essential for cell growth. We expected, therefore, that the selected variants containing the wild-type nucleotide at U6 position 59 would contain all possible nts at position 23 in U2,

while those that contained U6-A59G would only be found in combination with the compensating U2-U23C mutation . This is what we observed (Figures 3 and 4; Table 3). The U6-A59C mutation was not found among the non-ts variants even in combination with the predicted compensatory mutant U2-U23G (Table 3). It does appear in the ts variants, but not always in combination with U2-U23G (Table 3). This latter result is expected since in the presence of wild-type U2, U6-A59C exhibits a deleterious effect on growth only above the 30 °C temperature used in our selection experiments (Madhani and Guthrie, 1992).

In an effort to understand better the structural requirements at this base-pair, we used site-directed mutants to construct YHM118 strains containing all possible appositions between U6 nt 59 and U2 nt 23. The growth phenotypes of these strains on 5-FOA are shown in Table 4. Specific suppression of U6-A59C by U2-U23G and of U6-A59G by U2-U23C was observed (Table 4), confirming the occurrence of base-pairing at this position. Since the U6-A59C/ U2-U23G combination supports growth at all temperatures tested, the reason for its absence in the non-ts selected variants is unknown but could reflect a defect that becomes apparent only in combination with other changes found in the variants. The U6-A59U site-directed mutation, which was also absent from the selected variants, was found to be inviable, even in combination with the compensatory mutation U2-U23A. The observation that base-pairing is not sufficient to confer growth is consistent with our previous suggestion for an additional role for U6-A59 (Madhani and Guthrie, 1992).

Analysis of the variants revealed that the two-nucleotide bulge (U2 nts 24-25) that separates helix Ia and helix Ib can be replaced by a wide variety of dinucleotides (15/16 of the possible dinucleotides are found; Figures 3 and 4). To further delineate the minimal features of the bulge required for growth, we constructed single and double nucleotide deletions of the bulge in addition to all possible single nucleotide substitutions. As expected from the selection data, all substitutions in U2 nts 24 and 25 were fully viable

(Table 5). Single nucleotide deletions are tolerated, whereas deletion of both nts 24 and 25 is lethal (Table 5). Finally, we engineered single nucleotide insertions in U6 at the kink (between nts 58 and 59) opposite the bulge; all 4 insertions are lethal (Table 7). Thus, the bulge appears to be moderately tolerant to mutational insult.

In addition to the regions described above, U2 nts 9 and 10 were randomized in the U2 library to test the importance of base-pairing in the lower portion of U2 stem I. However, since many functional variants are unpaired at either or both randomized positions (Figure 3), it appears that neither the U2-C9/G26 pair nor the U2-U10/A25 pair is essential for growth. Indeed, one variant (TS 109) contains a deletion that encompasses this region. These observations are in agreement with previous *in vitro* results in which no requirement for base-pairing in the lower part of the stem was observed (McPheeters and Abelson, 1992).

Unexpected variants containing lethal mutations at U6 position 52

As mentioned above, several unexpected ts variants were isolated from the libraries. These contain either an A or a C at nt 52 in U6, which we have shown previously to be lethal as single mutations (Madhani et al., 1990). This discrepancy is not due to a difference in the yeast strains employed in the two studies since, as single changes, G52A and G52C are lethal at all temperatures tested in YHM118 in the presence of wild-type U2 (data not shown). Therefore, in the viable variants, the lethality of G52A and G52C is being suppressed by additional mutations. Since U6-A51 does not deviate from wild-type in any of the variants, mutations in the bulge region or in U2 nts 9-10 must be responsible for suppression, since they are the only other randomized residues in the libraries. A single variant was isolated that contains U6-G52A; nine isolates contain U6-G52C. We describe an analysis of the U6-G52A-containing variant first.

The sequences of U2 and U6 in the randomized region of the single U6-G52A variant is shown in Figure 6A. In addition to G52A, this variant contains a transversion of the U6-C58/ U2-G26 base-pair (a flip to U6-C58G/ U2-G26C), mutations in the helix I

bulge region as well as mutations in nts 9 and 10 in the 5' region of U2 stem I. In order to determine which of the additional mutations were responsible for suppression we performed two different additional selection experiments (secondary selections). We first cotransformed YHM118 with plasmid DNA encoding U6-G52A together with the U2 library and selected for functional variants at 30 °C for 4 days on 5-FOA media, as in the initial selection experiment (see Experimental Procedures for details). However, no functional variants were obtained. We reasoned that this failure might be due to a requirement for the flip in the U6-C58/ U2-G26 base-pair. Indeed, when we attempted to select variants by cotransforming YHM118 with the double U6 mutant (U6-G52A, C58G) and the U2 library, positives were easily obtained. All are ts at 37 °C. Eighteen were analyzed by DNA sequencing (Figure 6B). Strikingly, all 18 contain a G residue at nt 25 in the helix I bulge but no consistent changes at nts 9, 10, or 24. As expected, all contain a G26C change in U2 that maintains base-pairing with U6-C58G. These results demonstrate that three changes are necessary for suppression of U6-G52A: U2-A25G and the flip of the U6-C58/ U2-G26 base-pair. To confirm these requirements using site-directed mutations, we constructed YHM118 strains containing U2 and U6 mutants in which U6-G52A was combined with either U2-A25G, the transversion or both. While neither U2-A25G nor the flip alone is able to support growth on 5-FOA of U6-G52A under any condition tested (25-37 °C), the combination of both results in slow growth at 25, 30, and 33 °C (data not shown). In order to test whether or not gross alterations of the bulge could suppress U6-G52A, we combined it with each of the viable bulge mutations listed in Table 5, including the two single nucleotide bulge deletions. In none of the eight cases was suppression observed (data not shown).

In our initial screen, we identified nine variants containing U6-G52C. In this case two classes of variants can be discerned based on shared sequence motifs (Figure 7A). Class I can be divided into three subsets (IA, IB and IC), all of which are characterized by the occurrence of one or more G residues in the helix I bulge. The four class IA variants all

contain U2-U23C and U2-A25G; the former change disrupts the first base-pair in U2-U6 helix Ib. The two class IB variants also contain U2-U23C, but instead of a G at nt 25 in U2, they contain a G at nt 24 and a U at nt 25 (Figure 7A). The single class IC variant contains, among other changes, U2-A25G, and a flip of the U6-C58/ U2-G26 base-pair. In these respects, it mimics the U6-G52A suppressors. The two members of the class II G52C-containing variants are grouped together because they share a subset of changes: both contain U2-A25C, a flip of the U6-C58/ U2-G26 base-pair as well as either a transition or a transversion in the U6-A59/ U2-U23 base-pair (Figure 7A).

We performed a secondary selection, starting with U6-G52C. YHM118 was cotransformed with this mutant and the U2 library, and functional variants were selected on 5-FOA at 30 °C. Based on our initial classification, we expected to obtain representatives of only class IA and class IB, since the other classes contain a flip of the U6-C58/ U2-G26 base-pair. Twelve functional variants, all of which are ts at 37 °C, were analyzed (Figure 7B). As predicted, eleven out of the twelve match the consensus from class IA (U23C and A25G); the single exception contains U23C and U24G, and therefore mimics class IB. Three of the class IA-like are also labeled class IB since these variants contain a G residue at the first position of the bulge. Further analysis of the class IC variant will be described below.

To attempt to dissect the class II G52C-containing variants, we constructed a pair of U2 and U6 alleles that contained the nucleotide substitutions common to the two members of this class (U6-G52C; C58G; U2-A25C, G26C). This combination proved to be inviable (data not shown), indicating that additional changes, likely the alterations in the U6-A59/ U2-U23 base-pair, are necessary for growth.

Specificity of suppression

In principle, the mutations in the bulge region of helix I could function in suppression directly by affecting a physical interaction between this region and nt 52 in U6, or more indirectly, by forming or disrupting a different interaction. To address this issue,

we asked whether or not bulge-region variants that suppress U6-G52C could also suppress U6-G52A and vice versa. Since the G52A-containing variants mimic the structure of the class IC U6-G52C-containing variants, we expected that the former class of bulge-region variants might at least weakly support growth in combination with U6-G52C (and vice versa). In contrast, we expected that the class IA, IB and II U6-G52C-containing variants would not support growth when combined with U6-G52A, since these did not contain the required flip of the U6-G58/U2-G26 base-pair found in the G52A-containing variants.

We constructed YHM118 strains in which we combined representative bulge-region variants with all possible nucleotides at U6 position 52 and examined growth of these derivatives on 5-FOA at 25, 30, 33, 35, and 37 °C. Table 6 summarizes these results and Figure 8 shows the growth of representative combinations at 30 °C. As expected, bulge-region variants originally identified in combination with G52A also support growth in combination with G52C; however, in each case, they suppress G52A more strongly than G52C (Table 6, rows 2-6). For example, the variant shown in Figure 9B suppresses G52A but not G52C at 30 °C, but at lower temperatures, weak suppression of G52C is observed (Table 6, row 2). None of these bulge-region variants affect the growth of G52U, a ts mutant (Table 6, rows 2-6; Figure 8B). The results for the G52C containing variants are simpler. Each member tested of the class IA, IB and II G52C-containing variants supports growth in the presence of G52C and but not in the presence of G52A under any condition tested (Table 6, rows 7-11, 13; Figures 8C, 8D, 8F). Interestingly, the class IA and IB suppressors are lethal in combination with G52U (Table 6, rows 7-11; Figures 8C and 8D). This temperature sensitivity of G52U is slightly exacerbated by the class II bulge variant tested (Table 6, row 13; Figure 8D). As predicted from its structure, the single class IC variant tested suppresses both G52C and G52A, albeit poorly (Table 6, row 7).

In summary, a restricted and specific set of bulge-region variants suppress U6-G52A and U6-G52C. The class I G52C suppressors and all of the G52A suppressors are

characterized by the appearance of a G residue in the helix I bulge. In addition to specific substitutions within the bulge, alterations in at least one of the base-pairs that flank the bulge are required for growth. Variants isolated initially in combination with G52A preferentially suppress this U6 mutation. However, as expected from their similarity to the class IC G52C-containing variants, weak suppression of G52C was also observed. In contrast, three of the four classes of G52C-containing bulge-region variants are highly allele-specific. That is, no detectable suppression of G52A was observed; moreover, these variants exacerbate the phenotype of G52U. The other class (IC) of G52A-containing variants structurally mimics the G52A-containing variants and, can support growth of G52A.

Discussion

Creating an "Artificial Phylogeny" of Spliceosomal snRNAs in Yeast

The constraints of higher order folding are essential to the development of robust models for three-dimensional structure. To seek tertiary interactions among putative active site components of the spliceosome (Figure 1), we employed a method that allowed us to select in vivo for functional covariants of two interacting molecules from gene libraries that contain randomized residues (Figure 2). This method allowed us to create an "artificial phylogeny" of the U2-U6 helix I region (Figures 3 and 4). This method differs from in vitro randomization-selection methods (reviewed in Szostak and Ellington, 1993; Gold et al., 1993) in several important ways that affect its applicability. First, unlike current in vitro methods, in vivo selection permits the isolation of functional pairs of covariants versus variants of a single molecule. Secondly, these variants can be isolated in a single selection step; in vitro methods are generally iterative because they are limited by the enrichment obtainable in a single cycle of biochemical selection. Moreover, because our selection method is based on a genetic phenotype, its potential usefulness can be extended to molecules other than RNA and to situations where biochemical selections are impractical. Finally, a limitation of our method is that many fewer variants can be introduced into cells (10^6) than can be manipulated in vitro (10^{15} ; Bartel and Szostak, 1993), thereby limiting the number of residues that can be analyzed in a single experiment. If one desires to analyze all possible variants, selection in vitro raises the number of residues that can be randomized from approximately 10 to 25 ($4^{10}=10^6$; $4^{25}=10^{15}$). Of course, in both cases, decreasing the level of degeneracy would permit the analysis of larger sets of residues (e.g. Green and Szostak, 1992).

Does the AGA Sequence of U2 Function as a Group I Intron-like G Binding Site?

As expected, our analysis of the selected variants revealed Watson-Crick covariation at two positions previously proven to engage in base-pairing (Tables 1 and 3; Madhani and Guthrie, 1992). Of particular interest are the data that relate to the U6-C58/

U2-G26 base-pair. As discussed in the Introduction, U2-G26 has been proposed to function as part of a Group I intron-like G binding site for the conserved G at the 3' splice site of nuclear introns (McPheeters and Abelson, 1992). Such a model would be consistent with the recent proposal, based on stereochemical studies, that the spliceosome generates a Group I-like catalytic site to execute the second chemical step of splicing (Moore and Sharp, 1993). In Group I introns, analysis of the putatively homologous base-pair (G264-C311 in the Tetrahymena rDNA intron) indicates that the identity of the G at position 264 is more important for G binding than is base-pairing of this residue with its partner, C311 (Yarus, 1991a). This asymmetry is expected because G264 forms hydrogen bonds with the G substrate (Michel et al. 1989a). In contrast, detailed analysis of the U2-G26/ U6-C58 base-pair (Figure 5A, Tables 1 and 2) demonstrates that the identity of U2-G26 can be varied to any other nucleotide so long as base-pairing is maintained. These data are reinforced by our analysis of a double mutant (U2-G26C, A27U), which was shown previously to completely inhibit the second step of splicing in vitro (McPheeters and Abelson, 1992). This severe block was proposed to result from the disruption of all hydrogen bonds with the G at the 3' splice site according to a recent "axial" G binding site model for Group I introns, in which G is bound by hydrogen bonding to A265 as well as G264 (McPheeters and Abelson, 1992; Yarus, 1991a; 1991b). However, the growth defect of this U2 allele can be fully suppressed by the U6 double compensatory mutant (Figure 6B). Thus, our data do not support the hypothesis that the AGA sequence in U2 snRNA functions as a Group I-like G binding site; rather, the critical role of this sequence appears to be a base-pairing interaction with U6 snRNA.

Evidence for a Tertiary Interaction

In addition to providing further insight into the roles of established RNA-RNA interactions, our approach permits the identification of nucleotide covariations indicative of previously unknown secondary and/or tertiary interactions. Below we summarize

evidence, based on the analysis of several novel variants, for a tertiary interaction between U6-G52 and the helix I bulge.

Novel Variants Containing Lethal Substitutions in the ACAGAG Hexanucleotide

We isolated ts variants from the randomized libraries that contained otherwise lethal mutations, G52A and G52C, in the terminal residue of the ACAGAG hexanucleotide. We demonstrated that specific changes in the bulge region of U2-U6 helix I suppress the lethality of these substitutions. In the case of U6-G52A, an A to G substitution in the second nucleotide of the bulge together with a flip of the adjacent base-pair of helix Ia are necessary and sufficient to suppress its lethal phenotype. In the case of U6-G52C, two classes of suppressors could be discerned based on common sequence motifs. Class I contains three subsets (IA, IB, IC), all of which contain a G residue in one of the two residues of the bulge. Class IA and class IB suppressors contain, in addition, a U2-U23C mutation which disrupts the first base-pair of helix Ib. Class IC instead contains a flip of the U6-C58/ U2-G26 base-pair and therefore mimics the structure of the G52A-containing variants. The class II bulge variants found in association with G52C are more complex, containing changes in both base-pairs that flank the bulge as well as changes in the bulge itself.

Specificity of Suppression Suggests a Direct Interaction

An important question is whether suppression reflects the formation of a direct tertiary interaction between U6 nt 52 and the helix I bulge, or a more indirect interaction. To address this issue, we examined the specificity of suppression. We found that variants isolated initially in combination with G52A preferentially suppress this U6 mutation. However, as expected from their similarity to the class IC G52C-containing variants, weak suppression of G52C was also observed. In contrast, three of the four classes of G52C-containing bulge-region variants exhibit dramatic specificity: no detectable suppression of G52A was observed; moreover, these variants exacerbate the ts phenotype of G52U. The other class (IC) of G52C-containing variants structurally mimics the G52A-containing

variants and, as expected, can support growth of G52A. The substantial specificity of suppression can most simply be explained by proposing a direct interaction between U6 nt 52 and the helix I bulge. In this scenario, the examples of incomplete allele specificity (i.e. the G52A and G52C class IC variants) could be accounted for by the existence of a common element to the physical interaction in the different cases of suppression. Concordant with the latter notion is the observation that several classes of suppressors are characterized by the occurrence of one or two G residues in the helix I bulge; the exception is the more complex G52C-containing class II suppressors. It should be noted that a specific interaction between U6-G52 and the bulge is not absolutely essential for cell growth since when nt 52 is wild-type, the sequence requirements in the bulge are completely flexible. This pattern is reminiscent of the U6-A59/U2-U23 base-pair where a direct Watson-Crick interaction can be demonstrated only when U6-A59 is mutated to a G or a C (Table 4).

Model for Suppression

Any model that accounts for the novel variants described above must rationalize for the following observations: 1) the ability of highly specific changes in the bulge region to suppress otherwise lethal mutations in U6 nt 52; 2) a requisite G residue in the two-nucleotide bulge in the majority of both G52C and G52A-containing variants; 3) the requirement for alterations in one of the base-pairs flanking the bulge; and 4) substantial but partially overlapping specificity of suppression. Although the complexity of the suppressors make it difficult to derive a single structural model that accounts for all of the data, the following model provides a simple explanation which can account for the four observations summarized above.

We propose that U6-G52 forms a symmetrical heteropurine base-pair with U2-A25 (Figure 9A). Such a base-pair is found at the junction of the anticodon and D stems in yeast tRNA^{Phe} (reviewed in Saenger, 1984). We further propose that the identity of flanking residues influences the stability of this interaction. In this scenario, the G52A

suppressors result in an isosteric flip of the U6-G52/U2-A25 base-pair (Figure 9B). The required flip of the adjacent base-pair could reflect a necessity for optimal stacking between the proposed U6-G52/ U2-A26 base-pair and the adjacent base-pair, additional hydrogen bonding interactions, or a steric incompatibility between the U6-G52A/ U2-A25G apposition with the wild-type base-pair in helix Ia. Several studies have documented the influence of flanking residue sequence context on the thermodynamic stability of hydrogen bonding interactions in RNA, including tertiary interactions (reviewed in Turner and Bevilacqua, 1993). Michel et al. (1990) have observed cooperative interactions between adjacent tertiary interactions (base-triples) in the catalytic core of Group I introns.

The Class IA, IB, and IC G52C-containing variants can be rationalized by a Watson-Crick G52C-A25G pair which would be a similar but not isomorphous replacement of the original heteropurine apposition (Figure 9C). Such substitutions have been observed in ribosomal rRNA phylogeny and are consistent with the similarities in symmetry and backbone geometry between symmetric heteropurine pairs and Watson-Crick pairs (Gutell, 1993; Saenger, 1984). In the case of class IB suppressors, which contain a G residue at the first position of the bulge, we suggest that it (U2 nt 24) pairs with U6-G52C instead. Again, how the flanking residues influence suppression is unclear; one possibility is that the unpairing of the first base-pair in helix Ib caused by the U2-U23C change found in the class IA and IB variants augments the flexibility of the sugar-phosphate backbone to allow the closer approach required in the Watson-Crick pair (Figure 9C). Alternatively, the selection for U2-U23C might reflect an additional stacking or hydrogen bonding interaction. The class II suppressors, however, are not readily rationalized by this model; they may represent a fundamentally different structural solution to the same functional problem. Such novel replacements of tertiary interactions have been observed in Group I introns and in tRNA (Green et al., 1993; Hou et al., 1993; Peterson et al., 1993).

How does the proposed U6-G52/U2-A25 pairing explain the partially overlapping pattern of suppression specificity (Table 6)? According to the model, the majority of the G52C-containing and all of the G52A-containing variants involve a direct interaction between U6 nt 52 and U2-A25G. The fact that one of the base-pairing partners (U2-A25G) is the same in both cases offers a structural rationale for why the same change in the bulge can, in certain contexts, contribute to suppression of both G52A (by a heteropurine swap) and G52C (by a Watson-Crick replacement). The differential requirement for specific flanking residues could then account for why some suppressors are highly specific, while others are less so (Table 6).

We have tested the structural feasibility of a direct tertiary interaction between U6-G52 and U2-A25 by constructing an atomic ball-and-stick physical model of the U2-U6 helix I region that includes the upstream ACAGAGA sequence (see Experimental Procedures). We found that a U6-G52/U2-A25 pair could be accommodated in the context of helix I by requiring that nt 53 in U6 cross the major groove of U2-U6 helix Ia. Short loops capable of crossing the major groove of an A-form helix have been proposed for and observed in H-type RNA pseudoknots (Puglisi et al., 1990; Wyatt et al., 1990; reviewed in ten Dam et al., 1992). A computer graphic rendition of this model is shown in Figure 9D. This arrangement was chosen to illustrate that stacking of the G-A pair onto the U6-C58/U2-G26 pair would be sterically permissible (see above). Given the current constraints, other configurations are of course possible. Nonetheless, this exercise illustrates that these two regions can be readily juxtaposed.

Functional Implications

The model for a direct interaction between U6-G52 and U2-A25 explains the bulk of the experimental data and is structurally reasonable. Given the complexity of the suppression data, however, it seems likely that this depiction of the interaction is oversimplified. As with other examples of tertiary interactions proposed on the basis of functional covariation data (Michel et al, 1990; Bartel et al., 1991; Green et al., 1993),

high-resolution structural studies will be necessary to understand its details. Nonetheless, it is interesting to consider a direct interaction between U6-G52 and the helix I bulge in the context of other recent observations. As described in the Introduction, two clusters of residues in U2 and U6 are specifically required for the second chemical step of splicing in diverse species (circled in Figure 1A; see Introduction for references). One cluster involves nt 51 and 52 in U6, the other involves the residues that immediately flank the helix I bulge. Notably, a direct interaction between U6-G52 and U2-A25 would closely juxtapose these two groups of residues. Especially in light of other recent results, it is provocative to consider the possibility that this long-range interaction reflects the formation of an active site involved in the second chemical step. First, crosslinking studies performed in mammalian extracts demonstrate proximity between the second nucleotide of the intron and the equivalent of A51 in U6 prior to and/or during the second step of splicing (Sontheimer and Steitz, 1993). Second, a non-Watson-Crick interaction between the conserved G's at the 5' end 3' ends of the intron has been shown to be important for the second step of splicing (Parker and Siliciano, 1993). If these interactions occur simultaneously such that the 5' and 3' splice sites are juxtaposed and placed in proximity to A51 in U6 (Figure 10), then an interaction between U6-G52 and U2-G25 would facilitate the recruitment of the second cluster of residues critical for the second step of splicing to this region. Thus, we suggest that the tertiary interaction proposed here might function in a network of RNA-RNA interactions that together form an active site involved in 3' splice site cleavage and exon ligation.

Experimental Procedures

Strain Construction

Yeast procedures used in this study have been described previously (Guthrie and Fink, 1991). YHM118 (a *leu2 lys2 trp1 his3 ura3 ade2 snr6::LEU2 snr20::LYS2* pU2U6U[*SNR6 SNR20 URA3 CEN*]) was constructed as follows. Two parental strains were employed. One contains a disruption of the chromosomal U6 gene, YHM2 (α *leu2 lys2 trp1 his3 ura3 ade2 snr6::LEU2* pSX6U[*SNR6 URA3 CEN*]) and one contains a disruption of the chromosomal U2 gene YHM111 (a *lys2 trp1 his3 ura3 ade2 snr20::LYS2* pU2U[*SNR20 URA3 CEN*]). Each contains a complementing URA3-marked plasmid containing the wild-type snRNA gene. YHM2 and YHM111 were mated, and diploids were selected on 5-FOA which also cures them of both wild-type plasmids. These were transformed with pU2U6U, which contains the wild-type U2 and U6 genes on a single URA3-marked plasmid. Following sporulation, haploid progeny were identified which contained both U2 and U6 gene disruptions and the complementing plasmid. Growth of this strain on 5-fluoroorotic acid (5-FOA), which selects against the wild-type U2 and U6 genes, was shown to be dependent on the introduction of a functional copy of U2 and a functional copy of U6.

Construction of U2 and U6 Gene Libraries Containing Randomized Residues

U2 and U6 DNA fragments containing randomized residues were created by polymerase chain reaction of U2 and U6 DNAs using synthetic oligonucleotide primers that were fully degenerate at specified positions. These fragments were used to replace the respective wild-type sequences in snRNA gene-containing plasmids that contain restriction sites that either flank the coding sequence of U6 (pSX6; Madhani et al., 1990) or the conserved region of U2 (pES143 Δ B; Madhani and Guthrie, 1992). The total number of residues randomized (in U2 and U6) was limited to 10. If only one combination of these nucleotides is functional we expect it to be represented once in approximately 10^6 variant pairs, which approaches the upper limit of what is practical to screen in yeast (see below).

Oligonucleotide synthesis was performed on a 0.05 umol scale on a Cylcone DNA synthesizer (Milligen) using reagents and conditions recommended by the manufacturer. Due to the differential reactivities of the nucleoside phosphoramidites, a biased mixture of 30% A, 30% C, 20 %T, and 20 % G phosphoramidites was used at the randomized positions; this ratio has been observed to result in an equal incorporation (25% each) of the 4 monomers (D. Bartel, personal communication; see below).

To construct the U2 fragment, a 5' primer was used that spans positions +1 to +36 of the U2 gene in pES143ΔB (with respect to the transcription start site) in the sense strand and contains randomized residues at positions 9, 10, 23, 24, 25, and 26. The 3' primer used spans residues +266 to +227 on the antisense strand (Madhani and Guthrie, 1992). Amplification was performed exactly as before (Madhani and Guthrie, 1992) except that 1 ng of a template that corresponds to an inviable U2 allele (U2-G26U) was used and 35 cycles of amplification were performed. A mutant template was used so as to avoid any possible contamination with wild-type U2 sequences. To generate more DNA, a second amplification was performed using the same primers. This consisted of two 100 ul reactions in which 20 ul of the first reaction was amplified for 20 cycles.

To construct the U6 fragment, we used a mutagenic primer that spans positions +21 to +62 on the sense strand of the U6 gene in pSX6 and contains randomized residues at positions 51, 52, 58 and 59. The 3' primer spans residues +129 to +96 on the antisense strand. These two primers were used in a first round of PCR in which 1ng of a mutant template (U6-C60G) was amplified for 35 cycles as above. 40 ul of this reaction was further amplified in two 100 ul reactions for 20 cycles using the same 3' primer and a 5' primer that spanning positions -12 to +33 (Madhani and Guthrie, 1992).

The U2 and U6 fragments were extracted with phenol/chloroform to remove the polymerase and spin chromatographed twice on 1 ml columns G-25 Sephadex equilibrated in TE buffer (10mM Tris-HCl pH 8, 0.1 mM EDTA) to remove unincorporated nucleotides. The U2 fragment were treated with 200 U each of BamHI and EcoRI for 5

hours at 37 °C. The U6 fragment was treated with 40 U of SphI and 200 U of XhoI for 5 hours at 37 °C. These were then heated to 70 °C for 20 min. to inactivate the endonucleases and spin chromatographed twice on G-50 Sephadex equilibrated in TE in order to remove the short end oligonucleotides produced by restriction endonuclease digestion. Samples were precipitated with ethanol and resuspended in 50 ul of TE.

In order to avoid contamination with wild-type sequences, the vectors pSX6 and pES143ΔB were modified so that the wild-type snRNA sequences between the introduced restriction sites were removed and replaced with unrelated stuffer DNA. The resulting derivatives, pΔSX and pΔES, contain 1.6 and 1.3 kb stuffer fragments, respectively, that are derived from the yeast gene *PRP16*. pΔSX was digested with SphI and XhoI; similarly, pΔES was digested with EcoRI and BamHI. The vector fragments were separated from the stuffer fragments by agarose gel electrophoresis. DNA was recovered from gels using GeneClean (Bio 101).

Libraries were constructed by ligation of 200 ng of gel-purified vector DNA with 50 ng of the appropriate insert fragment in a volume of 20 ul containing 50 mM Tris pH 7.6, 10 mM MgCl₂, 5 mM DTT, 50 ug/ml BSA, 0.1 U/ul T4 DNA ligase, and 1 mM ATP. Following incubation for 16 hrs. at 16 °C, the reactions were heated to 70 °C for 5 min., cooled on ice. Reaction products were introduced into *E. coli* strain DH5α via electroporation (Dower et al., 1988). The resulting U6 library contains 2.8×10^5 independent clones (each variant represented 1×10^3 times); the U2 library contains 4.1×10^5 independent clones (each variant represented 1×10^2 times). Control ligations lacking insert indicated negligible background. Unlike ΔSX, pΔES cannot replicate in yeast. Therefore, the U2 library was subcloned en masse into the yeast vector pSE362 (*HIS3*, *CEN*) using Sal I and Sac I sites that flank the U2 gene. Little, if any, complexity was lost during this subcloning step since $>10^6$ transformants were recovered. DNA sequencing of the pool DNA revealed that the appropriate residues had been randomized. Moreover, at

these positions, we observed an even distribution of nucleotides except for G, which was underrepresented approximately two-fold.

Selection Experiments

For transformation, competent YHM118 was prepared from 1 L of an exponentially-growing culture using a modification of the lithium acetate method (Schliestl et al., 1989). Cells were pelleted by centrifugation, washed once with 20 ml of 0.1 M lithium acetate in TE and finally resuspended in 1 ml of 0.1 M lithium acetate in TE to form a concentrated paste. Prior to use, 0.5 mls of 50% glycerol was added and the cells were frozen by an overnight incubation at -70 °C. The use of highly concentrated, frozen cells was found to increase cotransformation efficiency approximately 10-fold. In the initial selection experiments, 1 ml of thawed competent cells were transformed with 5 ug of each library. Transformants (10^5) were selected on 10 SD -HIS -TRP plates at 30 °C for 3 days. These were replica-plated to pre-warmed 5-FOA plates which were then incubated for either 2 or 4 days at 30 °C. Approximately 0.5 and 2% of the transformants, respectively, grew on 5-FOA. These were replica-plated to pre-warmed YEPD plates which were then incubated at 37 °C for 2 days in order to test for temperature-sensitivity. Non-ts variants that grew initially after 2 days on 5-FOA and ts variants that grew after 4 days on 5-FOA were selected for further analysis. Following colony-purification, the U2 and U6 plasmids were recovered from the variants using standard methods (Guthrie and Fink, 1991), and used to retransform YHM118 in order to verify the growth phenotype. The DNA sequences of the randomized regions of a total of 60 U2 functional variants and their 60 U6 partners were determined.

Secondary selections in which specific lethal U6 mutants were used in combination with the U2 library were accomplished by cotransformation of YHM118 followed by selection of the resultant transformants on 5-FOA for 4 days at 30 °C. In these cases, approximately 3% of the transformants grew on 5-FOA. These were analyzed as above.

Model Construction

Parts for the RNA physical model were purchased from Maruzen, Inc (Tokyo). Helices were constrained into A-form using spacers and supports supplied by the manufacturer. A model was built that corresponds to the sequences shown in Figure 1. To examine the tertiary interaction suggested by the results, we assumed the symmetric G-A pair between U6 nt 52 and U2 nt 25 discussed above. This was found to be sterically feasible in many different conformations including one in which the base-pair is stacked on the end of helix Ia. Computer modeling was done using the interactive modeling program SYBYL (Tripos Associates). In this case, only helix I and the upstream AGA sequence were modeled.

Acknowledgments

We thank David Bartel, Alan Frankel, Rachel Green, Robin Gutell, and members of our laboratory for helpful discussions. We are grateful to Suzanne Noble, Jim Umen, Andrew Murray, Ira Herskowitz, and Sean Burgess for critical comments on the manuscript. We also thank Uli Schmitz for help with computer modeling and Lucita Esperas, Carol Pudlow, and Heli Roiha for technical assistance. H.D.M. is a trainee of the University of California Medical Scientist Training Program. C.G. is a American Cancer Society Research Professor of Molecular Genetics. This work was supported by a grant from the NIH.

Figure 1:

RNA-RNA Interactions Between the Intron, U2 and U6 snRNAs.

S. cerevisiae snRNA sequences are shown. Intron sequences are the S. cerevisiae consensus. Depicted are the U2-branchpoint region helix (Parker et al., 1987; Zhaung and Weiner, 1989; Wu and Manley, 1989), U2-U6 helix I (Madhani and Guthrie, 1992), and the U6-5' splice site helix (Wassarman and Stetiz, 1992; Sawa and Abelson, 1992; Lesser and Guthrie, 1993; Kandels-Lewis and Séraphin, 1993). Residues in U2 and U6 required prior to the first chemical step of splicing and underlined; those involved in step 2 are circled (Fabrizio and Abelson, 1990; Madhani and Guthrie, 1992; McPheeters and Abelson, 1992).

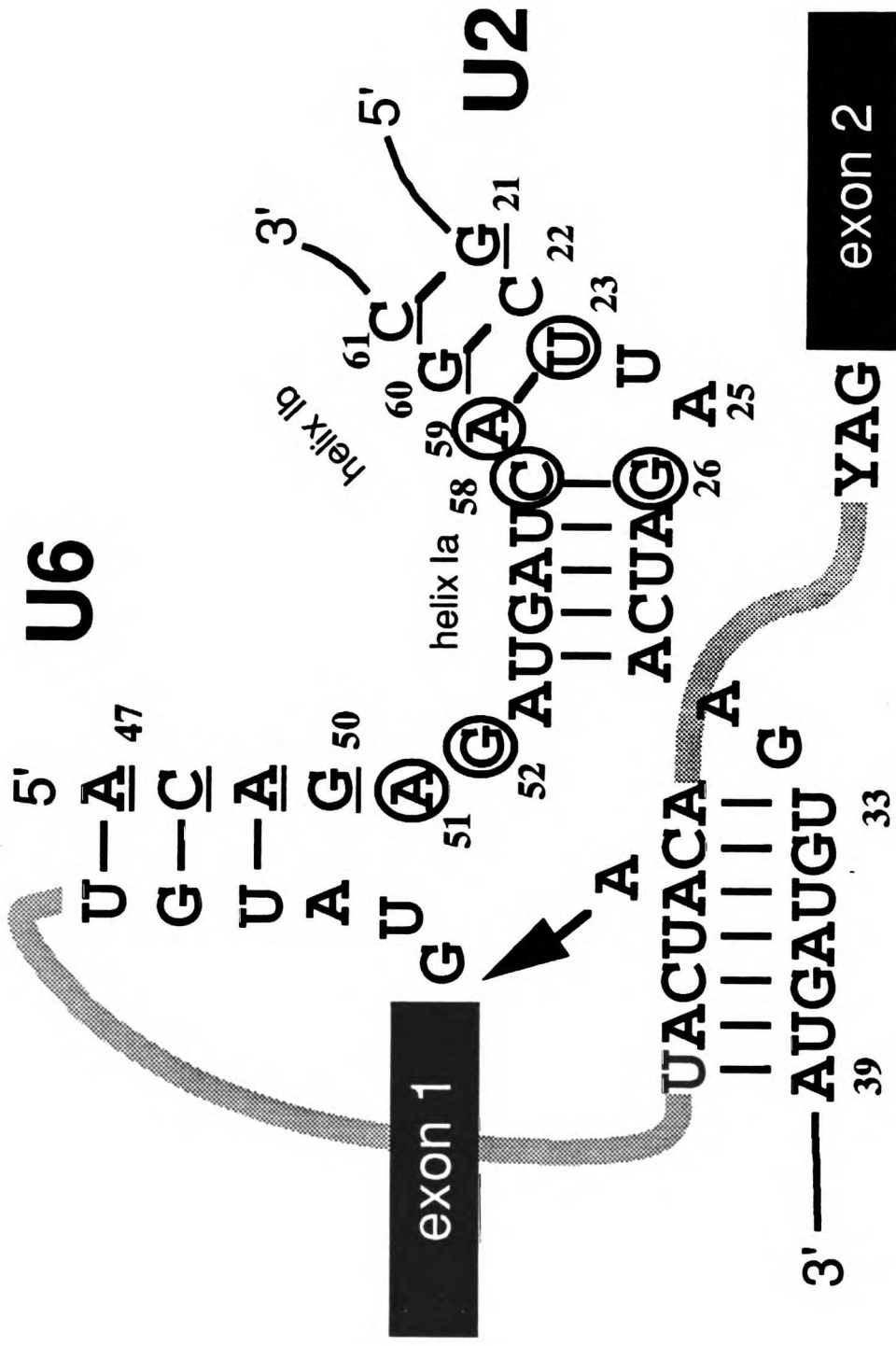
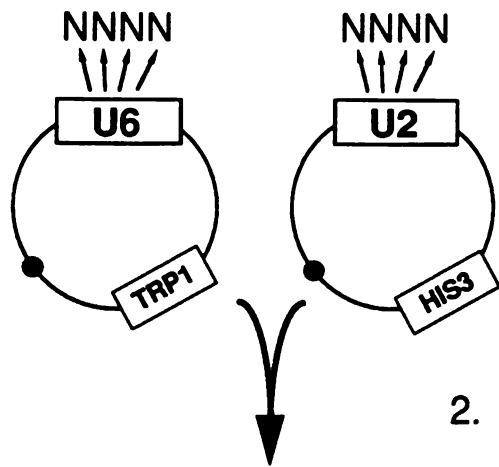


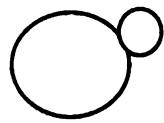
Figure 2:

Strategy for In Vivo Selection of Functional Covariants of Two Interacting Molecules (see Experimental Procedures for details).

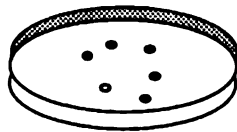


1. Construct libraries of U2 and U6 genes containing randomized residues at specific positions

2. Cotransform yeast with both libraries



3. Select for Functional Molecules



4. Recover & Sequence Plasmids

5. Analyze for Covariations

Figure 3:

Selected Variant Pairs.

A. Sequences of non-ts variant pairs selected after 2 days on 5-FOA at 30 °C. B.

Sequences of ts variant pairs selected from the U2 and U6 libraries after 4 days on 5-FOA at 30 °C. Bold indicates changes from wild-type. Asterisks indicate variants containing otherwise lethal mutations at U6 nt 52. Prime (') entries are ts variants selected originally selected after 2 days on 5-FOA at 30 °C.

Figure 4:

Recovered Nucleotides of Variant Pairs.

A. Shown in the context of the U2-U6 structure are the nucleotides recovered at each randomized position in the variants shown in Figure 3A. Large font indicates that only the wild-type nucleotide was recovered at that position. **B.** Nucleotides recovered at each randomized position in the variants shown in Figure 3B.

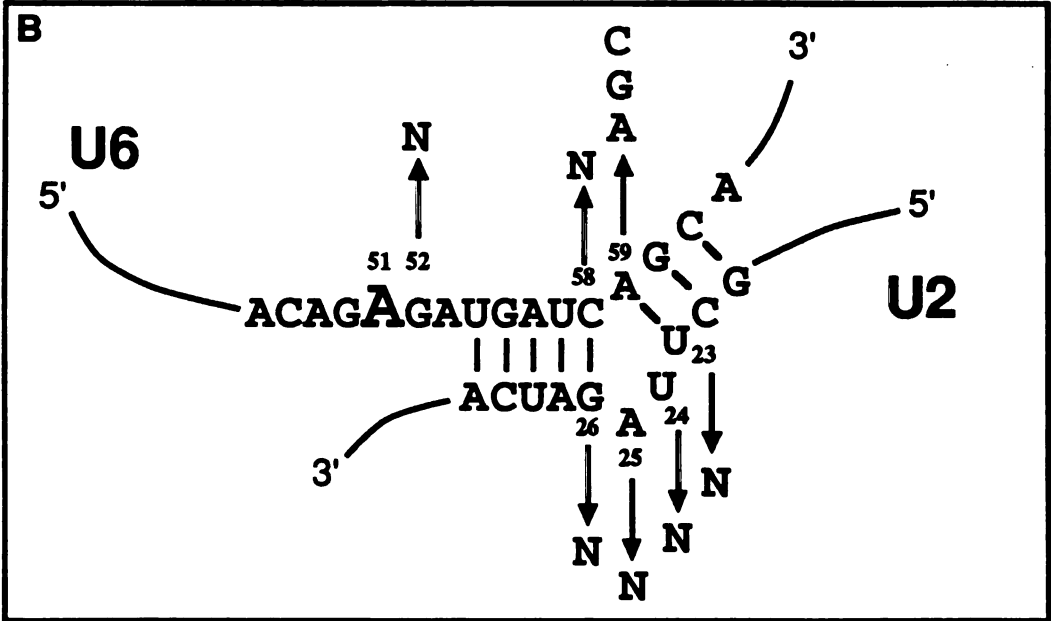
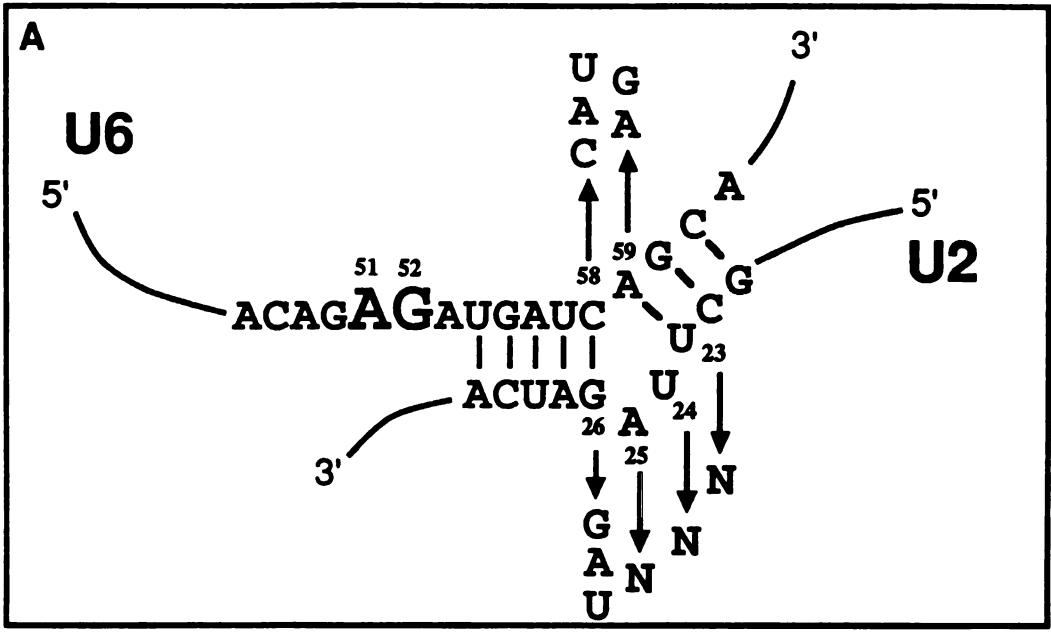


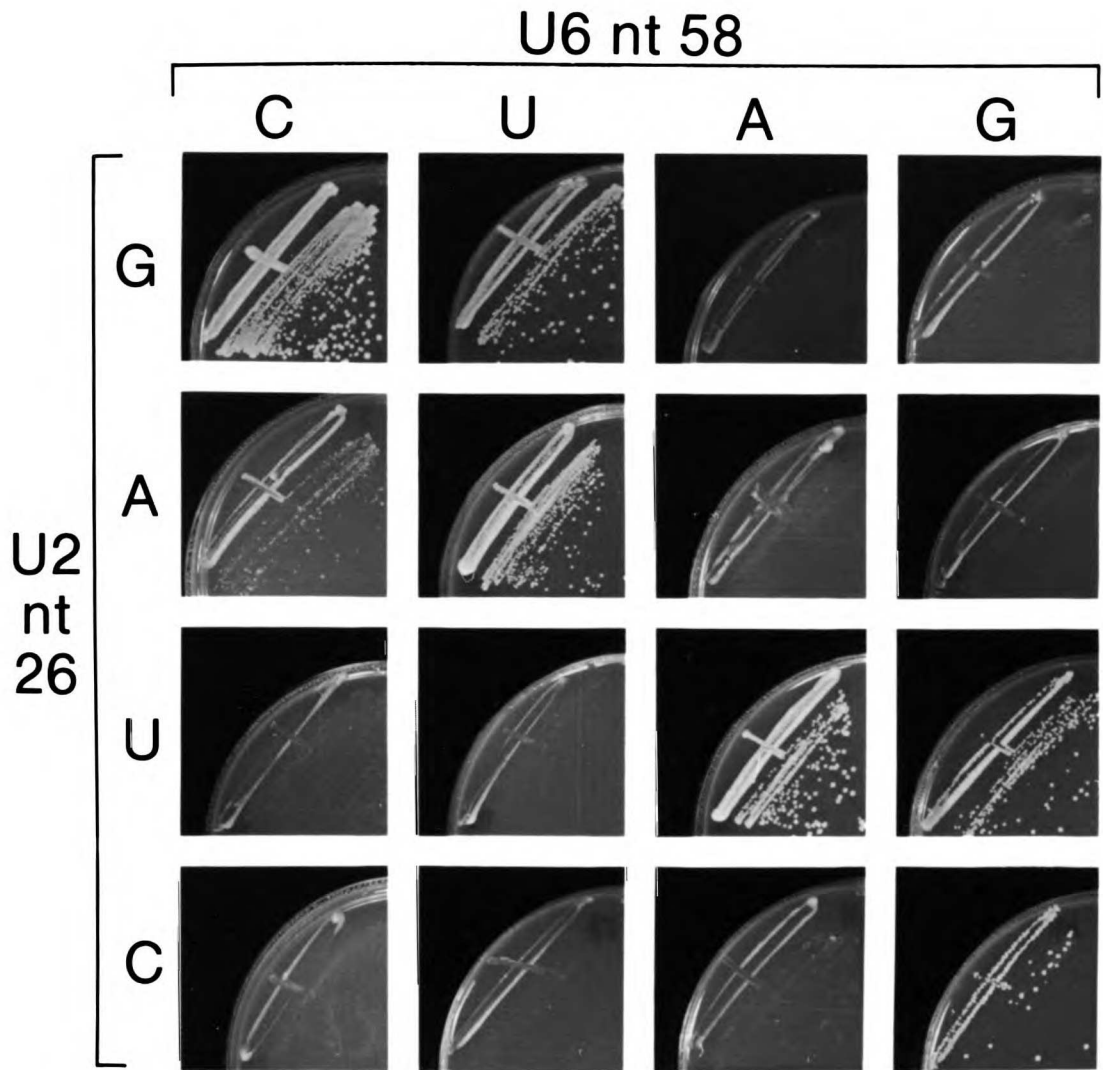
Figure 5

A. Analysis of the U6-C59/ U2-G26 Base-Pair.

Growth on 5-FOA of YHM118 derivatives harboring the indicated U2 and U6 alleles at nts 26 and 58, respectively. Plates were incubated at 30 °C for 3 days.

B. Analysis of Double Mutants in U2-U6 Helix Ia.

Growth on 5-FOA of YHM118 derivatives harboring the indicated U2 and U6 alleles at nts 26-27 and 57-58, respectively. Plates were incubated at 30 °C. for 3 days.



1000 900 800 700 600 500 400 300 200 100 0

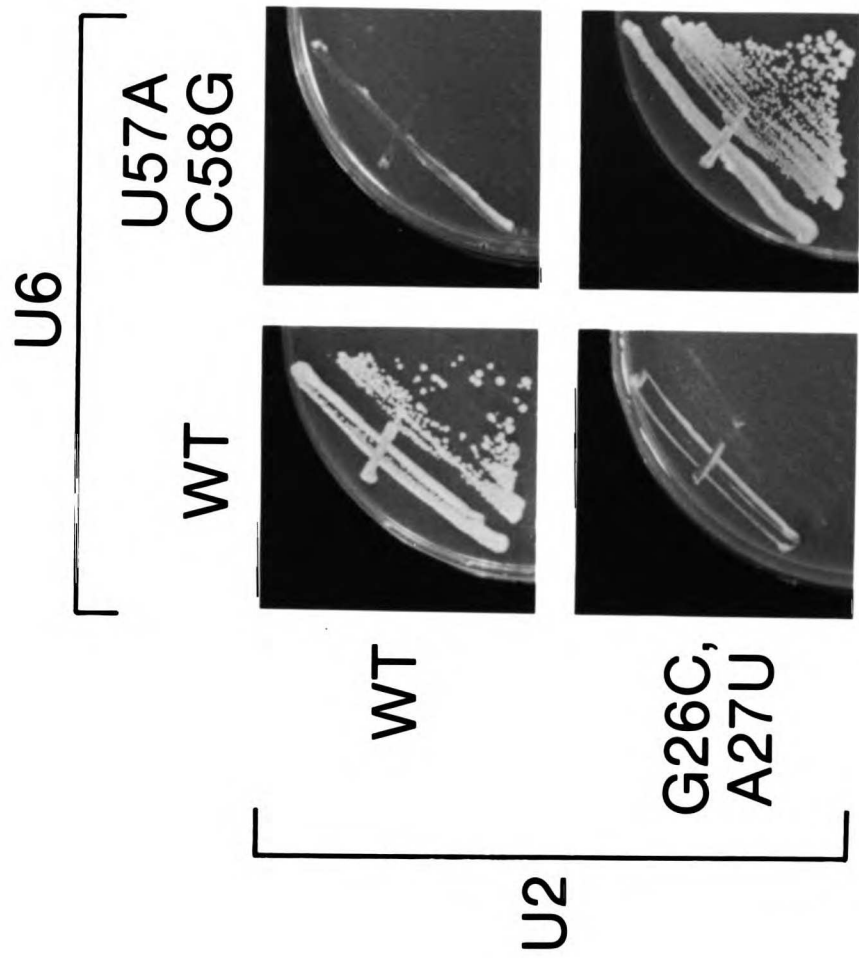


Figure 6.

Analysis of G52A-Containing-Variants.

A. The single variant pair isolated from the U2 and U6 B libraries that contains the lethal G52A mutation. B. U2 alleles isolated from the U2 B library after cotransformation of YHM118 with U6-G52A, C58G and selection at 30 °C for 4 days on 5-FOA plates.

A.
U6 51 52 58 59 9 10 23 26
 ** ** ** ** ** ** ** ** ** **
U2 TS043 ACAGAAUGAUGAGCA TS100 UACUUGCCUUUUUGGCCUAGCAUC

B.
U2 9 10 23 26
 ** ** **
 A52SUP01 UCAUUGCCUUUUUGGCCUAGCAUC
 A52SUP02 UUAUUGCCUUUUUGGCCUAGCAUC
 A52SUP03 UCAUUGCCUUUUUGGCCUAGCAUC
 A52SUP04 UCUUUGCCUUUUUGGCCUAGCAUC
 A52SUP05 UCAUUGCCUUUUUGGCCUAGCAUC
 A52SUP06 UCCUUGCCUUUUUGGCCUAGCAUC
 A52SUP07 UAUUUGCCUUUUUGGCCUAGCAUC
 A52SUP08 UCAUUGCCUUUUUGGCCUAGCAUC
 A52SUP09 UCUUUGCCUUUUUGGCCUAGCAUC
 A52SUP10 UAAUUGCCUUUUUGGCCUAGCAUC
 A52SUP11 UGCUUGCCUUUUUGGCCUAGCAUC
 A52SUP12 UCUUUGCCUUUUUGGCCUAGCAUC
 A52SUP13 UCUUUGCCUUUUUGGCCUAGCAUC
 A52SUP14 UUAUUGCCUUUUUGGCCUAGCAUC
 A52SUP15 UCAUUGCCUUUUUGGCCUAGCAUC
 A52SUP16 UCAUUGCCUUUUUGGCCUAGCAUC
 A52SUP17 UCCUUGCCUUUUUGGCCUAGCAUC
 A52SUP18 UCAUUGCCUUUUUGGCCUAGCAUC
 invariant **GC**

Figure 7.

Analysis of G52C-Containing Variants

A. Four classes of variants isolated from the U2 and U6 B libraries that contains the lethal G52C mutation. B. U2 alleles isolated from the U2 B library after cotransformation of YHM118 with U6-G52C and selection at 30 °C for 4 days on 5-FOA plates.

A.

Class IA

U6

51 52 58 59 23 26
 ** ** ** **

TS029 ACAGACAUGAUCAGCA TS086 UUUUUGCCUUUUGGCCCGGAUC
 TS037 ACAGACAUGAUCAGCA TS094 UCGUUGCCUUUUGGCCAGGAUC
 TS048 ACAGACAUGAUAAGCA TS105 UUCUUGCCUUUUGGCCUGUAUC
 TS049 ACAGACAUGAUAAGCA TS106 UUUUUGCCUUUUGGCCAGUAUC
 invariant C C G

Class IB

U6

51 52 58 59 23 26
 ** ** **

TS031 ACAGACAUGAUCAGCA TS088 UCAUUGCCUUUUGGCCGUGAUC
 TS033 ACAGACAUGAUAAGCA TS090 UCAUUGCCUUUUGGCCGUAUC
 invariant C A CGU

Class IC

U6

51 52 58 59 23 26
 ** ** **

TS035 ACAGACAUGAUCAGCA TS092 UCAUUGCCUUUUGGCCUGGCAUC

Class II

U6

51 52 58 59 23 26
 ** ** **

TS032 ACAGACAUGAUCGCA TS089 UCUUUGCCUUUUGGCCGACCAUC
 TS047 ACAGACAUGAUGGCA TS104 UCAUUGCCUUUUGGCCUCCAUC
 invariant C C G

B.

U2

9 10 23 26
 ** ** **

C52SUP06 UCCUUGCCUUUUGGCCAGGAUC
 C52SUP07 UUUUUGCCUUUUGGCCCGGAUC
 C52SUP08 UCAUUGCCUUUUGGCCAGGAUC
 C52SUP09 UCAUUGCCUUUUGGCCAGGAUC
 C52SUP10 UCUUUGCCUUUUGGCCAGGAUC
 C52SUP11 UCCUUGCCUUUUGGCCCGGAUC
 C52SUP12 UCUUUGCCUUUUGGCCAGGAUC
 C52SUP13 UACUUGCCUUUUGGCCAGGAUC
 C52SUP14 UCUUUGCCUUUUGGCCAGGAUC
 C52SUP15 UUUUUGCCUUUUGGCCCGGAUC
 C52SUP16 UAAUUGCCUUUUGGCCCGGAUC
 C52SUP17 UCUUUGCCUUUUGGCCCGGAUC
 invariant C G CG

Class
 IA
 IA
 IA
 IA
 IA
 IA/IB
 IA
 IA
 IA
 IA/IB
 IA/IB
 IB
 IA
 IB

U(1) L(1)M(1)

Figure 8.

Specificity of Suppression.

Growth on 5-FOA of YHM118 containing all possible nts at U6 position 52 and the indicated bulge variants in U2-U6 helix I. Plates were incubated at 30 °C for 4 days.

U6 nt. 52

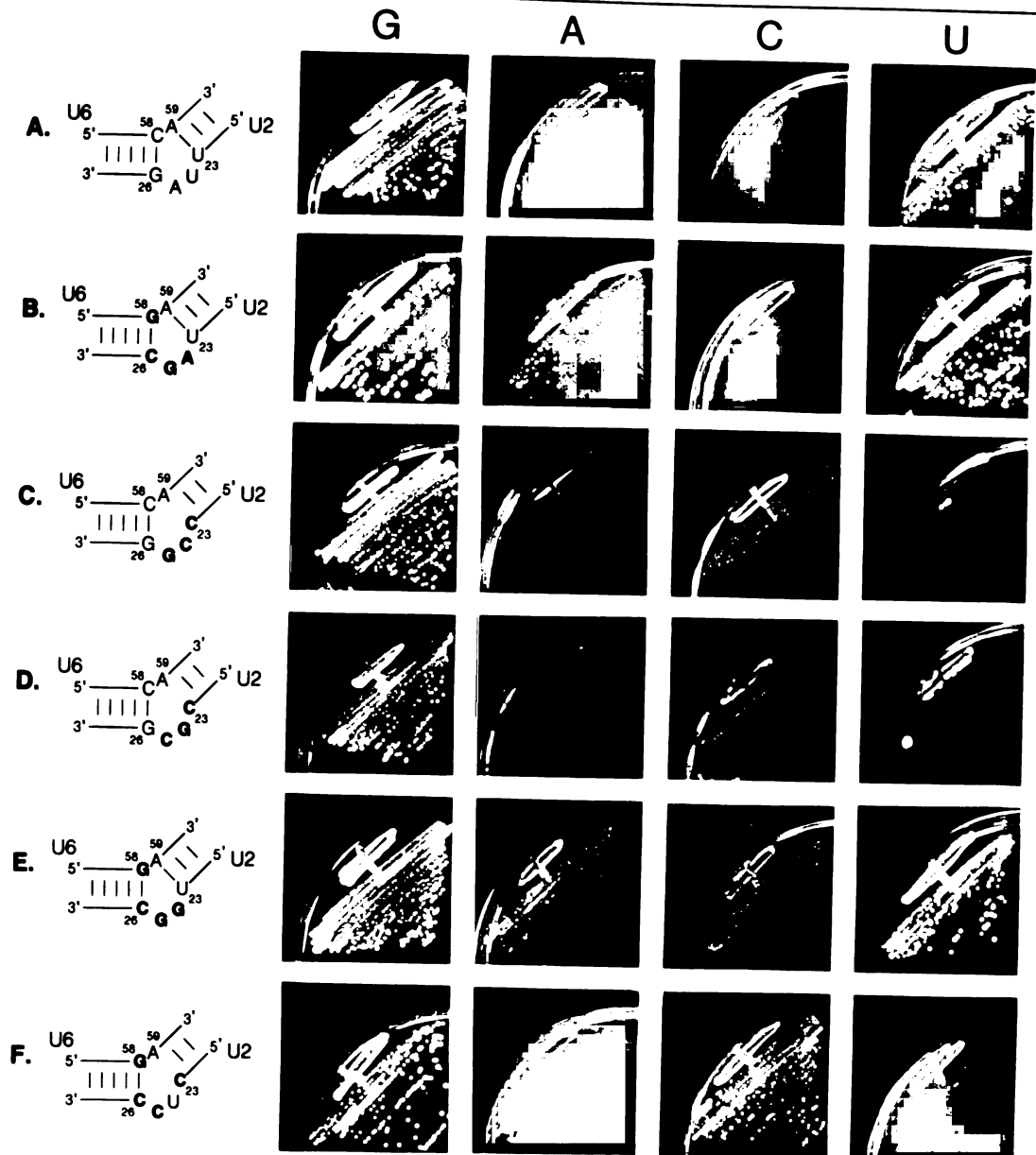


Figure 9

Comparison of symmetric G-A (panel A), A-G (panel B) and C-G (panel C) base-pairs

(Saenger, 1984). D. Graphic depiction of the proposed heteropurine pair in the context of U2-U6 helix I.

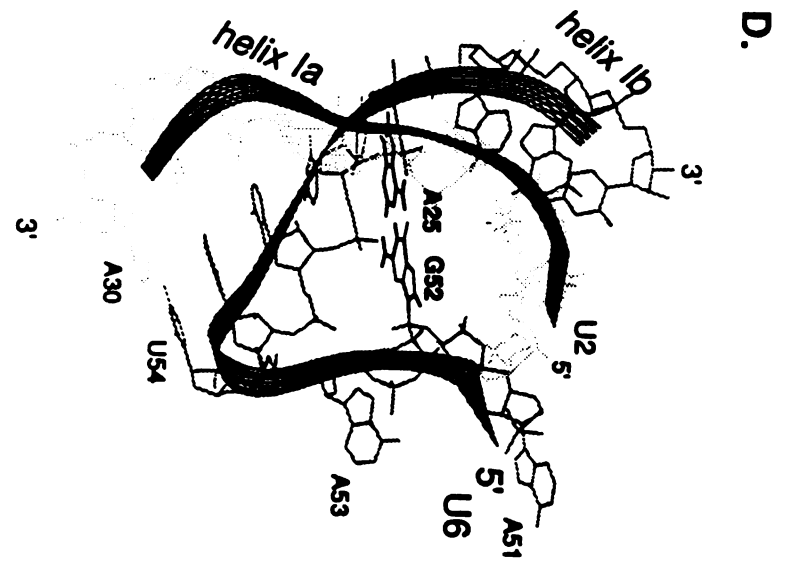
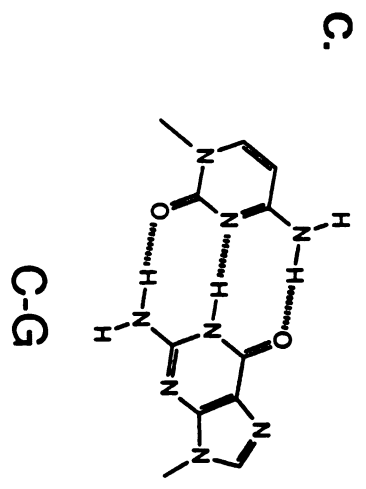
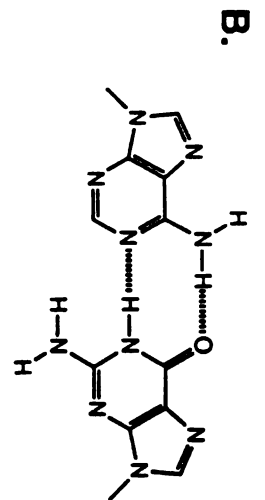
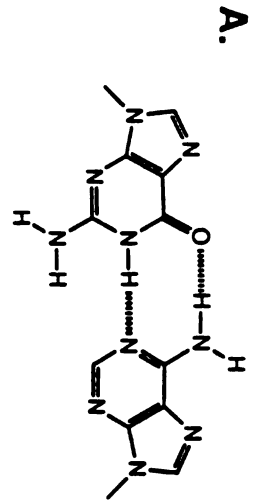


Figure 10

Network of RNA-RNA Interactions Involving the 3' Splice Site.

The intron is shown in lariat-intermediate form. In addition to the interactions shown in Figure 1, this figure depicts the non-Watson Crick between the guanosines at the 5' and 3' splice site (Parker and Siliciano, 1993), a site-specific crosslink between the second residue of the 5' splice site and U6-A51 (Sontheimer and Steitz, 1993), U5-exon interactions (Newman and Norman, 1992; Wyatt et al., 1992; Sontheimer and Steitz, 1992), and proposed tertiary interaction between U6-G52 and the bulge of U2-U6 helix I.

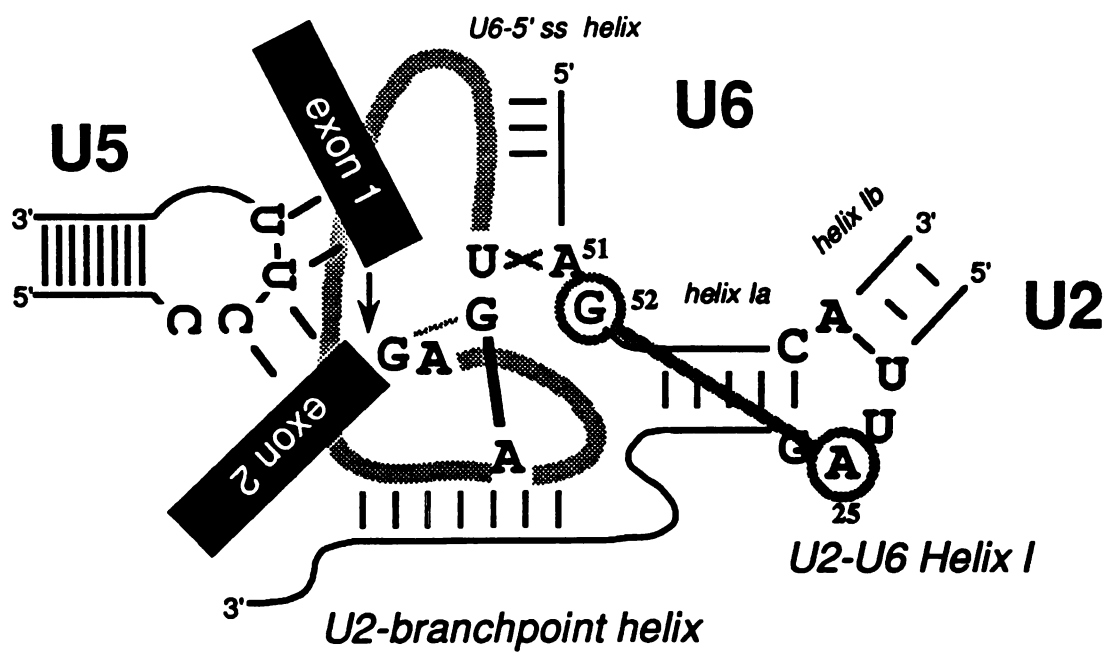


Table 1:

Types of Base Appositions Seen Between U6 nt 58 and U2 nt 26 in Functional Variants

Shown in Figure 3. Entries refer to the number of covariants of each type.

^aall are U2-G26A/ U6-C58

Table1.

Variant class	Watson-Crick	G-U wobble	Other ^a
non-ts variants	25	0	0
ts variants	26	5	4

Table 2:

Phenotypes of Base Appositions Between U6 nt 58 and U2 nt 26.

YHM118 derivatives containing the indicated U2 and U6 allele combinations assayed on 5-FOA after 3 days at 25, 30 and 37 °C. +: wild-type growth at 25, 30 and 37 °C. -: no growth at 25, 30 and 37 °C. ts^a: wild-type growth at 25 and 30 °C and no growth at 37 °C. ts^b: slow growth at 25 and 30 °C and no growth at 37 °C. The wild-type nucleotides are indicated in bold.

Table 2

		U6 nt 58			
		C	U	A	G
U2 nt 26	G	+	ts ^a	-	-
	A	ts ^b	+	-	-
	U	-	-	+	+
	C	-	-	-	+

Table 3:

Base Appositions Seen Between U6 nt 59 and U2 nt 23 in Functional Variants Shown in Figure 3.

Table 3

identity of U6 nt 59	W-C	other
A (wild-type)	21	24
G	6	0
C	1	8
U	0	0

UWU FIDW 100

Table 4:

Phenotypes of base appositions between U6 nt 59 and U2 nt 23. YHM118 derivatives containing the indicated U2 and U6 allele combinations assayed on 5-FOA after 3 days at 25, 30 and 37 °C. +: wild-type growth at 25, 30 and 37 °C. -: no growth at 25, 30 and 37 °C. ts^a: wild-type growth at 25 and 30 °C and no growth at 37 °C. The wild-type nucleotides are indicated in bold.

Table 4

		U6 nt 59			
		C	U	A	G
U2 nt 23	G	+	-	+	-
	A	-	-	+	-
	U	ts ^a	-	+	-
	C	-	-	+	+

Table 5

Phenotypes of mutants in the bulge region of U2-U6 helix I.

YHM118 derivatives containing the indicated U2 or U6 allele assayed on 5-FOA after 3 days at 25, 30 and 37 °C. U2 mutants assayed in combination with wild-type U6; U6 mutants assayed in combination with wild-type U2. +: wild-type growth at 25, 30 and 37 °C. -: no growth at 25, 30 and 37 °C. i58 represents the insertion of the indicated nucleotide after U6 nt 58.

Table 5

mutant	growth
U2-U24C	+
U2-U24A	+
U2-U24G	+
U2-A25G	+
U2-A25C	+
U2-A25U	+
U2- Δ U24	+
U2- Δ A25	+
U2- Δ U24, Δ A25	-
U6-i58G	-
U6-i58A	-
U6-i58U	-
U6-i58C	-

Table 6.

Specificity of suppression of G52A and G52C by bulge-region variants.

The highest temperature and degree of growth of the indicated allele combination was observed is shown (relative to wild-type). Bold entries refer to cognate combinations.

^aThe U6 entries refer to the sequence of the bulge region only (U6 nt 52 varies depending upon the column on the right side of the table). The U2 entries refer to the actual variant used in the experiment (see Figures 6 and 7 for sequences).

Table 6

bulge region sequence ^a			U6 nt 52				
U6	U2	Isolated as a suppressor of	G	A	C	U	
WT	WT	N.A.	wt +++++	-	-	35 +	
C58G	TS100	G52A	wt	30 ++	25 +/-	33 +	
C58G	A52SUP1	G52A	wt	33 +++	30 +	35 +	
C58G	A52SUP17	G52A	wt	30 +++	30 +/-	35+	
C58G	A52SUP4	G52A	wt	30 ++	25 +	35 +	
C58G	A52SUP9	G52A	wt	35 +/-	30 +	35 +	
WT	TS086	G52C (IA)	wt	-	30 ++	-	
WT	C52SUP10	G52C (IA)	wt	-	33 +/-	-	
WT	C52SUP15	G52C (IA)	wt	-	35 +/-	-	
WT	C52SUP17	G52C (IB)	wt	-	33 +	-	
WT	TS088	G52C (IB)	wt	-	30 ++	-	
C58G	TS092	G52C (IC)	wt	30 +	30 +	33 ++	
C58G	TS104	G52C (II)	wt	-	35 +	30 +/-	

**Genetic Interactions Between the RNA Helicase
Homolog Prp16 and Spliceosomal snRNAs Identify
Candidate Ligands for the Prp16 RNA-dependent
ATPase**

Abstract

Pre-mRNA splicing occurs in a large and dynamic ribonucleoprotein complex, the spliceosome. Several protein factors involved in splicing are homologous to a family of RNA-dependent ATPases, the so called DEAD/DEAH proteins. A subset of these factors exhibit RNA helicase activity in vitro. These proteins are thought to mediate RNA conformational rearrangements during spliceosome assembly. However, the RNA ligands for these factors are currently unknown. Here, we present genetic evidence in *S. cerevisiae* for a functional interaction between the DEAH protein Prp16, and the U6 and U2 spliceosomal snRNAs. Using a library of mutagenized U6 snRNA genes, we have identified fourteen strong suppressors of the cold-sensitive (*cs*) allele, *prp16-302*. Remarkably, each suppressor contains a single nucleotide deletion of one of the six residues that lie immediately upstream of a sequence in U6 that interacts with the 5' splice site. Analysis of site-directed mutants revealed that nucleotide substitutions in the adjacent U2-U6 helix I structure also suppress *prp16-302*, albeit more weakly. The U6 suppressors partially reverse the phenotype of two other *cs* alleles, *prp16-1* and *prp16-301*, but not the four temperature-sensitive (*ts*) alleles tested. Finally, overexpression of each *cs* allele exacerbates its recessive growth phenotype and confers a dominant negative *cs* phenotype. We propose that the snRNA suppressors function by destabilizing an interaction between the U2-U6 complex and a hypothetical factor (X), which is trapped by *cs* mutants of *PRP16*. The phenotypes of overexpressed *prp16* alleles are consistent with the model that this trapped complex inhibits the dissociation of Prp16 from the spliceosome. We discuss the intriguing possibility that factor X is Prp16 itself.

Introduction

Introns are removed from messenger RNA precursors within a large and dynamic ribonucleoprotein complex, the spliceosome, in which the two chemical steps of the splicing reaction take place (reviewed in Moore, Query, and Sharp, 1993; Rymond and Rosbash, 1992; Green, 1991). The spliceosome is formed by the ordered assembly of the four small nuclear ribonucleoprotein particles (U1, U2, U5, U4-U6 snRNPs), together with numerous extrinsic protein factors, onto the intron-containing substrate. Similarities in chemistry between nuclear pre-mRNA splicing and Group II autocatalytic splicing have led to the proposal that the former is fundamentally an RNA-catalyzed process performed by the snRNA components of the spliceosome (Sharp, 1985; Cech, 1986). Indeed, numerous RNA-RNA interactions involving the pre-mRNA substrate and the spliceosomal snRNAs have been identified (reviewed in Moore, Query, and Sharp, 1993; Weiner, 1993; Rymond and Rosbash, 1992; Green, 1991).

Our studies have focused on the role of the highly conserved U6 snRNA (Madhani, Bordonné and Guthrie, 1990; Madhani and Guthrie, 1992). We have previously employed a mutational approach in *Saccharomyces cerevisiae* to demonstrate a base-pairing interaction between U2 and U6 snRNAs that is mutually exclusive with the extensive U4-U6 base-pairing interaction (Madhani and Guthrie, 1992). In this novel pairing, termed U2-U6 helix I, a conserved sequence in U6 snRNA interacts with sequences in U2 that are immediately upstream of the branchpoint recognition region of U2. As a result, functionally important residues in U6 can be juxtaposed with the intron branchpoint. Residues that form this structure have been shown to be required for cell viability (Madhani, Bordonné, and Guthrie, 1990; Madhani and Guthrie, 1992) and for both chemical steps of splicing *in vitro* and *in vivo* (Fabrizio and Abelson, 1990; Madhani and Guthrie, 1992; McPheeters and Abelson, 1992). These properties led us to propose a model for the active site of the spliceosome (Figure 1) in which U2-U6 helix I might participate directly in chemical steps of splicing (Madhani and Guthrie, 1992). Because it

is mutually exclusive with the U4-U6 interaction, the existence of U2-U6 helix I offers a mechanistic rationale for the destabilization of the U4-U6 interaction that occurs prior to the chemical steps of splicing (reviewed in Moore, Query, and Sharp, 1993; Rymond and Rosbash, 1992). Other biochemical and genetic studies, which indicate a direct interaction between the ACA sequence in U6 snRNA (nts 47-49) and a portion of the 5' splice site consensus sequence (Figure 1), are also consistent with the view that U2-U6 helix I is an active site component of the spliceosome (Sawa and Shimura, 1992; Wassarman and Steitz, 1992; Sawa and Abelson, 1992; Lesser and Guthrie, 1993; Kandels-Lewis and Séraphin, 1993).

The prominent role of dynamic RNA-RNA interactions in splicing suggests that one important class of functions for the estimated >50 proteins required for splicing is likely to be the catalysis and regulation of these RNA structural rearrangements. Of particular interest are a family of RNA-dependent ATPases which mediate many of the ATP-dependent steps of splicing (reviewed in Schmid and Linder, 1992). These factors (Prp2, Prp 5, Prp16, Prp28), which were identified through the use of genetics in *Saccharomyces cerevisiae*, have been classified into two subfamilies on the basis of conserved sequence motifs (DEAD and DEAH box families). Members of these families are involved in diverse biological processes; several have been shown to exhibit ATP-dependent RNA helicase activity in vitro (reviewed in Schmid and Linder, 1992; see also Lee and Hurwitz, 1993). However, of the tested DEAD/DEAH splicing factors (Prp2, Prp16 and Prp28), none exhibit RNA helicase activity (Schwer and Guthrie, 1991 and unpublished; Kim et al., 1992, E. Strauss and C.G, unpublished). A reasonable explanation is that the DEAD/DEAH splicing factors are capable of unwinding activity only when bound to specific RNA ligands in the spliceosome. An major step towards testing this hypothesis would be the identification of such ligands.

Prp16, the prototypical member of the DEAH box family (Burgess, Couto and Guthrie, 1990), is required at or prior to the second chemical step of splicing and is known

to interact transiently with the spliceosome (Schwer and Guthrie, 1991). The original allele of *PRP16*, *prp16-1*, was isolated as a dominant suppressor of an intron branchpoint mutation (Couto et al., 1987). More recent studies have demonstrated that the rate of ATP hydrolysis by Prp16 influences the accuracy of branchpoint recognition by regulating the use of a discard pathway for aberrant lariat intermediates (Burgess and Guthrie, 1993). Other experiments demonstrate that ATP hydrolysis by Prp16 directly or indirectly causes a conformational change in the spliceosome that leads to the protection of the 3' splice site from oligonucleotide-directed RNase H cleavage (Schwer and Guthrie, 1992a). Finally, the original branchpoint suppressor allele, *prp16-1*, has been shown to exhibit a dominant negative phenotype when overexpressed (Schwer and Guthrie, 1992b). This allele exhibits a recessive cold-sensitive (*cs*) defect when expressed on a low-copy vector (Schwer and Guthrie, 1992b). The molecular basis for the dominant negative phenotype was revealed by *in vitro* studies that demonstrated that the purified Prp16-1 protein is capable of binding to the spliceosome, but is deficient in ATP hydrolysis and release from the spliceosome (Schwer and Guthrie, 1992b). Indeed, Prp16-1 functions as a dose-dependent dominant inhibitor of splicing *in vitro* (Schwer and Guthrie, 1992b). These studies have allowed us to uncouple three functions of Prp16: 1) binding to the spliceosome, 2) nucleotide hydrolysis required for a conformational change and 3) release from the spliceosome. While the outlines of the Prp16 cycle have been formulated, its precise function is not understood, in part because its RNA ligand in the spliceosome remains unknown.

The requirement for specific residues of U2 and U6 snRNAs in the second chemical step of splicing (see above) suggests these RNAs as possible candidates for RNA ligands of Prp16. Here we describe studies aimed at detecting a functional interaction between the U2-U6 complex and Prp16. We reasoned that mutants in an RNA ligand for Prp16 might suppress the defect of a *PRP16* mutant by either 1) decreasing the stability of a target RNA-RNA duplex and thus easing the requirement for helicase activity or 2) disrupting an RNA-protein interaction that becomes rate-limiting in the protein mutant. We

report the isolation and characterization of mutants in the U2 and U6 snRNAs that suppress cs but not temperature-sensitive (ts) mutations of *PRP16*. The data can be most simply accommodated by a model in which the snRNA suppressors function by destabilizing an interaction between the U2-U6 complex and a hypothetical factor (X), which is trapped in cold-sensitive mutants of *PRP16*. The effects of overexpressed *PRP16* alleles are consistent with the hypothesis that such a trapped interaction inhibits the dissociation of Prp16 from the spliceosome. In the simplest case, factor X is Prp16 itself.

Materials and methods

Yeast methods: All yeast genetic manipulations including media preparation, crosses, plasmid shuffle assays, plasmid recovery and transformations were performed according to published methods (Guthrie and Fink, 1991). Strain genotypes, derivations and sources are summarized in Table 6.

Plasmid Construction: Conditional *PRP16* alleles on centromere-containing plasmids have been described previously, with the exception of *prp16-302*. This allele was transferred to a plasmid vector by gap repair of a wild-type *PRP16* gene in a *prp16-302* strain. YSN131, a gift from S. Noble, was transformed with a fragment of pSB62 (*PRP16 HIS3 CEN*) that was missing the 5' two-thirds of the *PRP16* coding sequence. Of 13 *HIS*⁺ transformants assayed, all were *Cs*⁻, suggesting that the *prp16-302* mutation is located in the N-terminal two thirds of the protein. A plasmid recovered from one of these strains was shown to confer cold-sensitivity when used to replace the wild-type *PRP16* allele in YS78 using the plasmid shuffle method. This allele was also subcloned into pSE358 (*TRP1 CEN*) using the *EcoRI* and *SphI* site that flank the *PRP16* fragment. The resulting plasmid was used in the experiments described in the text. Overexpression constructs encoding conditional *PRP16* alleles were made by swapping the *SacI-SacI* fragment of pG16 (pG1-*PRP16*) with the same fragment from the centromere plasmid-borne alleles.

U6 Mutant Library: The U6 mutant library used has been described previously (Madhani, Bordonné and Guthrie, 1990). This library was constructed through degenerate chemical synthesis of the U6 coding sequence. It is highly representative, containing mutants in all regions of U6 (Madhani, Bordonné and Guthrie, 1990; H.D.M and C.G., unpublished; P. Raghunathan and C.G., unpublished). In addition to containing nucleotide substitutions, the library also contains single nucleotide deletions at a lower frequency as determined by DNA sequencing of randomly-selected isolates.

Site-Directed Mutagenesis: U2 and U6 site-directed mutants were either obtained from our published collection (Madhani, Bordonné and Guthrie, 1990; Madhani and Guthrie, 1992) or created using synthetic oligonucleotides and a polymerase chain reaction-based strategy described previously (Madhani and Guthrie, 1992).

Results

Since Prp16 interacts transiently with the spliceosome (Schwer and Guthrie, 1991), we reasoned that mutant versions of Prp16 that retain the ability to bind the spliceosome might be the most useful for genetic suppression studies involving snRNAs. As described above, the dominant negative phenotype of overexpressed *prp16-1* can be rationalized by its ability to bind the spliceosome but not function in a subsequent step. To identify similar alleles, we tested our existing collection of plasmid-borne conditional lethal *PRP16* alleles for this phenotype. Three cs (*prp16-1* [Couto et al., 1987; Schwer and Guthrie, 1992b]; *prp16-301* [Burgess and Guthrie, 1993]; *prp16-302* [S. Noble and C.G, unpublished]) and four ts alleles of *PRP16* (*prp16-2* [Vijayraghavan, Company and Abelson, 1989; Schwer and Guthrie, 1991; Burgess and Guthrie, 1993]; *prp16-201*, *-202*, *-205* [Burgess, 1993]) were cloned into pG1 (pGPD, *TRP1*, 2 μ), the vector used previously to overexpress *prp16-1* (Schwer and Guthrie, 1992b; Schena et al. 1991). These plasmids were introduced into a yeast strain, YS78, in which the chromosomal *PRP16* gene is disrupted and complemented by the wild-type *PRP16* gene on a *URA3*-marked centromere plasmid (Burgess, 1993). As controls, the recessive phenotype of each allele was assayed in parallel.

Table 1 summarizes the growth phenotypes of each allele at various temperatures when 1) expressed on a centromere plasmid as the sole copy, 2) overexpressed in the absence of wild-type *PRP16*, or 3) overexpressed in the presence of wild-type *PRP16* (to assay for dominant negative phenotypes). Two patterns of phenotypes are apparent. First, all of the cs, but none of the ts alleles of *PRP16* exhibit a dominant negative effect when overexpressed in the presence of wild-type *PRP16* (Table 1). Second, the growth defects of cs alleles expressed in the absence of wild-type *PRP16* are consistently exacerbated by overexpression; in contrast, each of the four ts alleles tested is at least partially self-suppressed by overexpression (Table 1). Curiously, in the cases of the cs alleles, the severity of the dominant negative effect of a particular allele does not correlate precisely

with the severity of its cold-sensitivity in the absence of wild-type *PRP16*. For example *prp16-301* and *prp16-302* result in a more pronounced cs defects than *prp16-1*, but less dramatic dominant negative phenotypes.(Table 1).

Thus, based on the criterion of dominant negativity, the cs alleles of *PRP16* appeared to be the most likely to retain some ability to interact with the spliceosome. For our initial experiments, we chose the *prp16-302* allele because it exhibited the tightest cs defect. As a source of snRNA mutants, we employed a library of U6 alleles created previously through degenerate chemical synthesis of the entire coding sequence (Madhani, Bordonné and Guthrie, 1990). This highly representative bank exists on a *TRP1*-marked centromere plasmid. Since snRNA mutant alleles have often been observed to be poorly expressed when required to compete with the wild-type allele (E. Shuster and C.G, unpublished ; Madhani, Bordonné and Guthrie, 1990), our experiments were designed to permit the recovery of recessive suppressors in U6 of *prp16-302*. We constructed a haploid yeast strain, YHM145, which contains *prp16-302*, a disruption of the chromosomal U6 gene, and a wild-type copy of the U6 gene on a *URA3*-marked centromere plasmid. Using this strain, we could replace the wild-type U6 allele with mutant versions using the plasmid shuffle technique (Boeke and Fink, 1987). In this method, mutants are introduced by transformation, and the wild-type *URA3*-containing plasmid is selected against using 5-fluoroorotic acid (5-FOA).

Into YHM145, we introduced the U6 mutant library by transformation. Approximately 10^4 transformants were selected at 30 °C on SD -TRP plates. These were then replica-plated to 5-FOA-containing plates and placed at 30 °C for two days in order to select for cells that lacked the wild-type U6 plasmid. Finally, colonies that grew on 5-FOA were replica-plated to YEPD plates which were placed at a non-permissive temperature for *prp16-302*, 16 °C, in order to select for suppressors. Colonies that grew after 7 days of incubation were purified by streaking onto YEPD plates followed by incubation at 18 °C. The U6 plasmids were recovered from these candidates for further analysis. Fourteen

plasmids were identified that suppressed the *cs* defect of *prp16-302* upon retransformation of YHM145. The relative growth of these alleles is shown in Figure 2. As can be seen, the suppressors substantially alleviate the *cs* defect of *prp16-302*, restoring growth close to wild-type levels (Figure 2). The sequence of the U6 coding region was determined for each mutant (Figure 3). Remarkably, all 14 suppressors contain a single nucleotide deletion of one of the 7 nucleotides that lie upstream of the 5' splice site binding sequence in U6 snRNA (Figure 3; see also Figure 1). This region exhibits high phylogenetic conservation, but contains few invariant residues (Guthrie and Patterson, 1988; C.G., S. Mian, and H. Roiha, unpublished). Four of the mutants contain additional changes. It is unlikely that these account for the suppressor phenotype, however, since in each case we recovered other suppressors that contain the same single residue deletion in nts 41-46 of U6 in the absence of the additional alterations (Figure 3). The isolation of point deletions is significant since nucleotide substitutions in this region can suppress *prp16-302*, but much more poorly so (data not shown).

Since the suppressor screen required that the U6 alleles be fully functional (we demanded growth on 5-FOA after two days at 30 °C prior to selecting for suppressors), we considered the possibility that slow-growing and/or conditional-lethal U6 alleles in the region might also function as suppressors but would have been selected against in the screen. We took advantage of our collection of site-directed mutants (Madhani, Bordonné and Guthrie, 1990; Madhani and Guthrie, 1992; H.D.M., unpublished) to determine whether or not mutations in the adjacent ACAGAGA sequence or in the U2-U6 helix I region of U6 and U2 snRNAs (Figure 1) could also suppress *prp16-302*. We constructed a haploid *prp16-302* strain, YHM187, that contains disruptions of both the chromosomal U2 and U6 genes complemented by a single *URA3*-marked centromere plasmid that carries both wild-type genes. We used this strain to replace the wild-type U2 gene or the wild-type U6 gene with mutant versions using the plasmid shuffle technique. In the case of the mutant U6 alleles, YHM187 was simultaneously transformed with a U6 mutant and a wild-

type U2 gene prior to streaking on 5-FOA. Similarly, to assay U2 mutants, these were introduced together with wild-type U6 prior to streaking on 5-FOA. The resulting strains were assayed for growth in the cold (Table 2). Several alterations in the conserved ACAGAGA sequence in U6 (in nts 47, 50, 52, and 53) result in very low levels of suppression (Table 2). Interestingly, double substitutions in U2-U6 helix Ia confer moderate levels of suppression, both in the case of alterations to U6 (G55C, A56U; A56G, U57G) and U2 (A27C, U28C; U28A, C29G; Table 2). The U2 alleles, however, are weaker suppressors than the U6 alleles.

As described in the Introduction, one mechanism by which we expected that suppression of mutant *PRP16* alleles might occur is through the weakening of a target helix. It was therefore of interest to determine whether the reduction in stability of helix Ia was responsible for suppression in these cases. Consequently, we assayed the effects of combinations of U2 and U6 alleles that disrupt base-pairing in helix Ia, restore wild-type stability, or increase the predicted stability of helix Ia. Nine different combinations were tested, including wild-type. Figure 4 shows the predicted structure of helix Ia in each of these allele combinations. Next to each is shown the growth of the corresponding YHM187 derivative on YEPD plates at 18 °C after 9 days. In contrast to our expectations, each of the variants suppresses *prp16-302*, irrespective of the predicted stability of the helix (Figure 3, compare B-E with F-I). Thus, alterations in the sequence of helix Ia, not its stability, underlies the observed suppression. We note that our analysis of U2 was limited to site-directed mutants in the U2-U6 helix I region; it is therefore possible that suppressors in other regions of U2 exist.

Our suppressor screens were based on the assumption that snRNA mutants capable of suppressing *PRP16* mutants would function better in the absence of competition from the wild-type snRNA allele; however, for technical reasons (see below), it was desirable to have alleles that functioned dominantly. To this end, we tested representative U6 alleles from the recessive screen for their ability to suppress *prp16-302* in the presence of a wild-

type U6 allele. We employed a YS78 derivative in which the wild-type copy of *PRP16* was replaced by *prp16-302*. This strain, which contains a wild-type chromosomal copy of the U6 gene, was transformed with five strong U6 suppressor alleles. As shown in Table 3, each allele is capable of dominantly suppressing *prp16-302*. In two of five cases (U6- Δ C43 and U6- Δ A44), dominant suppression is as effective as recessive suppression, and produces close to wild-type growth. However, the other three U6 suppressors function more weakly in the presence of wild-type U6 than in its absence (Table 3).

This observation facilitated tests of a different question: is suppression specific for the *prp16-302* allele or are other alleles also suppressed? The availability of dominant U6 suppressors allowed us to test their effects on isogenic *prp16* strains created using the plasmid shuffle method. The analysis above demonstrated that cs versions of Prp16 produce dominant negative effects when overexpressed, consistent with some ability to interact with the spliceosome, whereas overexpression of ts alleles does not have this effect. This disparity suggests that the two types of conditional alleles are blocked at different steps. Therefore, we expected that snRNA suppressors of *prp16-302* would suppress other cs *PRP16* alleles but not ts alleles. To test this hypothesis, we constructed YS78 derivatives containing of each of the ts and cs *PRP16* alleles on pSE358 (*TRP1*, *CEN*) as the sole copy in the presence or absence of one of two strong suppressors, U6- Δ C43 and U6- Δ A44. As shown in Table 4, U6- Δ C44 partially suppresses *prp16-1* and *prp16-301* in addition to *prp16-302*. U6- Δ C43 suppresses *prp16-301* and *prp-302* but not *prp16-1*. The inability of U6- Δ C43 to suppress *prp16-1* likely reflects its being a weaker suppressor in general compared to U6- Δ A44 (Table 4). In contrast, no suppression by either U6 mutant of ts alleles of *PRP16* alleles was observed (Table 4).

Finally, we asked whether or not overexpressed cs alleles of *PRP16* can be suppressed by U6- Δ C43 or U6- Δ A44. YS78 derivatives containing pG1-borne *prp16-1*, *prp16-301* and *prp16-302* as the sole copy of *PRP16* were transformed with either a vector control, or one of the two U6 alleles. In the case of *prp16-1* and *prp16-301*, no

suppression was observed (Table 5). Slight suppression of the *cs* defect of *prp16-302* was seen at 18 °C but not at 16 °C (Table 5). Thus overexpression of *cs* alleles of *PRP16* somehow antagonizes suppression. This result could be due to the general increase in the severity of the *cs* phenotype caused by overexpression (see above), or it could reflect a more direct effect on suppression.

Discussion

This study was motivated by the recent realization that the assembly and function of the spliceosome is accompanied by a series of RNA rearrangements. These findings (reviewed in Weiner, 1993; Moore, Query and Sharp, 1993) suggest that a key role for at least one class of protein factors involved in splicing is in the mediation and control these RNA conformational transitions. Members of the DEAD/DEAH family of helicase-like proteins are good candidates for such factors. However, despite an increasing understanding of their temporal action in the splicing pathway, nothing is known regarding their specific biological ligands.

Prp16, the prototype of the DEAH family, has been particularly well-characterized (Couto et al., 1987; Burgess, Couto, and Guthrie, 1990; Schwer and Guthrie, 1991; 1992a; 1992b; Burgess and Guthrie, 1993). Prp16 binds to the spliceosome prior to the second step of splicing, subsequently performs a function that requires ATP hydrolysis, and is then apparently released from splicing complexes prior to or concomitant with the second chemical step of splicing. Given that the purified protein is an RNA-dependent ATPase (Schwer and Guthrie, 1991), Prp16 presumably interacts with one or more RNA molecules in the spliceosome. We hypothesized that U6 and U2 snRNAs might interact with Prp16 because specific residues on both RNAs are critical for the second chemical step of splicing. Consequently, we set out to hunt for functional interactions between these RNAs and Prp16.

We took advantage of an existing collection of conditional lethal alleles of *PRP16* for these studies. One mutant protein, Prp16-1, is known to bind spliceosomes in vitro but not function in a subsequent step (Schwer and Guthrie, 1992b). As expected from this in vitro behavior, this allele also causes a dominant negative phenotype over wild-type *PRP16* when overexpressed in vivo (Schwer and Guthrie, 1992b). Reasoning that alleles capable of interacting with the spliceosome would be the most useful for detecting functional interactions with snRNAs, we identified two additional cs alleles of *PRP16* that also exhibit

a dominant negative phenotype when overexpressed (*prp16-301* and *prp16-302*; Table 1). By analogy to *prp16-1*, we expect that these mutant proteins also retain some ability to bind the spliceosome but are deficient in a subsequent activity; confirmation of this notion will require the purification and in vitro analysis of these mutant molecules. Assuming this to be the case, the most severe *cs* allele, *prp16-302*, was chosen for a mutant hunt to identify suppressors in U6 snRNA.

Using a synthetically mutagenized library of U6 genes, we identified 14 *cs*⁺ suppressors of *prp16-302*. Remarkably, each contains a single nucleotide deletion in one of the seven residues upstream of the 5' splice-site binding sequence in U6 snRNA (Figures 1-3; nts 40-46). Further analysis identified somewhat weaker suppressors of *prp16-302* in U2-U6 helix Ia (Figure 1, Table 2). We had initially considered the notion that cold-sensitivity might be due to the inability of a mutant Prp16 to unwind a target helix. However, suppression cannot be due to the disruption of helix Ia, because both mutants that destabilize helix Ia and mutants that hyperstabilize helix Ia were found to result in suppression (Figure 4). Therefore, suppression is due to changes to the sequence, not the stability, of helix Ia (Figure 4). We found that all three of the *cs PRP16* alleles could be suppressed by one or both of the two strong U6 suppressor alleles tested, suggesting that these alleles share a common defect. In contrast, *ts* alleles of *PRP16* were not suppressed. Finally, we observed that overexpression of *cs PRP16* alleles exacerbates their recessive growth defect (Table 1) and antagonizes suppression by the U6 suppressors (Table 5).

The observation that mutations in many different nucleotides in U6 and U2 snRNAs in the U2-U6 helix I region (Figure 1) lead to suppressor activity suggests that disruption of an interaction involving these residues is responsible for suppression. Shown in Figure 5A is a model in which a factor, X, is proposed to interact with the U2-U6 complex, induce a change in its conformation, and then be released. We suggest that the release step becomes rate-limiting for cell growth in the cold in the presence of a *cs* mutant of Prp16. Disruption of this RNA-protein interaction would overcome this block

and allow splicing to proceed. In this model, X could be a protein, an RNA, or Prp16 itself.

In the first two cases (X= another protein or RNA), the results can be rationalized by proposing that Prp16 competes with the U2-U6 complex for X. Cs mutants of Prp16 would be defective in binding X (which could be a consequence of a defect in ATPase activity) and would result in the accumulation of a U2-U6-X complex. The suppressors would function by weakening the interaction between U2-U6 and X which, as a result, would partially restore the equilibrium with Prp16. This model is similar to one proposed to explain genetic and biochemical interactions among U4, U6 and the U6 snRNP protein Prp24 (Shannon and Guthrie, 1991). In that study it was observed that mutations that destabilized the U4-U6 base-pairing interaction result both in a cs growth defect and the accumulation of a U4-U6-Prp24 complex, a likely intermediate in assembly of the U4-U6 snRNP (A. Jandrositz and C.G., unpublished). The cold-sensitivity produced by this bottleneck can be partially suppressed *in vivo* by mutations in the U6 gene or in an RNA-binding motif in *PRP24* that each demonstrably disrupt the U6-Prp24 interaction. Based on these results, it was suggested that the destabilization of the U6-Prp24 interaction partially restores an equilibrium with the weakened U4-U6 complex, allowing the formation of sufficient U4-U6 snRNP to promote cell growth (Shannon and Guthrie, 1991). However, when applied to the current situation, this model does not explain why overexpression of cs versions of Prp16 exacerbates cold-sensitivity. Indeed, one might expect the opposite to be the case, namely that overexpression would improve the ability of mutant versions of Prp16 to compete for X*.

*It should be noted that the nt 40-46 region has also been implicated as a binding site for Prp24 in free (non-spliceosomal) U6 snRNP (Shannon and Guthrie, 1991; A. Jandrositz and C.G., unpublished).

Whether Prp24 could function as factor X is unclear, there is currently no evidence either for or against a role for Prp24 in the spliceosome. However, mutations in *PRP24* that weaken the Prp24-U6 interaction

A second possibility is that X is Prp16 itself. As shown in Figure 5B, Prp16 binds the spliceosome prior to the second chemical step of splicing and, upon ATP hydrolysis, induces a conformational change in the spliceosome that leads to protection of the 3' splice site (Schwer and Guthrie, 1991; 1992a). At some point, the protein is released from the spliceosome so that it can function in the next splicing cycle (Schwer and Guthrie, 1991). The *cs* alleles of Prp16 would be defective in release of the protein from the U2-U6 complex. The U2 and U6 mutations would destabilize this direct interaction, promoting the dissociation of Prp16. This model can also explain why overexpression of *cs PRP16* alleles exacerbates their phenotype. In this scenario, high levels of the mutant Prp16 protein would promote its rebinding to the U2-U6 complex following its initial release and prior to the subsequent step. As a result, the primary defect of these alleles, release from the spliceosome, would be antagonized.

In addition to rationalizing several important aspects of the genetic data, this second model makes several testable predictions. First, release of Prp16 from spliceosomes should be defective in the *cs* alleles. For Prp16-1, it is known that the protein binds the spliceosome but is blocked in a subsequent step prior to its release (Schwer and Guthrie, 1992b). However, whether the release step per se or a prior step is defective has not been determined. Second, the observed in vitro RNA-dependent ATPase defect of the purified Prp16-1 protein (Schwer and Guthrie, 1992b) is predicted to be due, at least in part, to a defect in RNA release as opposed to defects in ATP binding or the chemical step of nucleotide hydrolysis. Defects in RNA release would manifest themselves as a defect in the apparent steady-state rate of ATP hydrolysis if dissociation of the protein from RNA is required in order to initiate a second ATPase cycle. More sophisticated kinetic studies will

(Shannon and Guthrie, 1991) fail to suppress *prp16-302* (H.D.M. and C.G., unpublished). Moreover, no suppressors of *prp16-302* were isolated with changes in a second region implicated in Prp24 binding in the 3' terminal domain of U6 (Figure 3; Shannon and Guthrie, 1991).

be required to determine whether this is the case. Finally, if the snRNA suppressors act by destabilizing an interaction with Prp16, one predicts that the same ends could be achieved by a different means: amino acid changes in Prp16 that destabilize the interaction with RNA. Indeed, such intragenic suppressors of the *cs* defect of *prp16-1* can easily be isolated; of four analyzed, all contain different additional amino acid changes in the helicase-related domain of Prp16 (S. Burgess and C.G., unpublished).

Although several aspects of the data can most simply be explained by proposing that Prp16 interacts directly with the U2-U6 complex, additional experiments will be required to critically test this model. Nonetheless, it is interesting to consider what the function of such an interaction might be. Of particular importance is the function of ATP hydrolysis by Prp16. Burgess and Guthrie (1993) have demonstrated that the rate of ATP hydrolysis by Prp16 influences the accuracy of intron branchpoint recognition by regulating the use of a discard pathway for aberrant lariat intermediates. In their kinetic model, ATP hydrolysis plays an additional, but unspecified, role in the productive branch of the pathway (Burgess and Guthrie, 1993). One possibility is that the energy of ATP hydrolysis is converted into RNA binding energy so as to activate Prp16 for binding to the U2-U6 complex. Consistent with this notion, recent experiments demonstrate that ATP hydrolysis by the DEAD box family member eIF4A leads to a form of the protein that exhibits greatly increased affinity for RNA (Pause and Sonnenberg, 1993). If, as we have proposed, the U2-U6 complex functions as part of a spliceosomal active site (Madhani and Guthrie, 1992), such an activated form of Prp16 could serve 1) to stabilize the structure in a conformation required for catalysis during second chemical step of splicing or 2) to promote an RNA conformational rearrangement required prior to the second chemical step. Either possibility would be consistent with the observed Prp16-dependent protection of the 3' splice observed during *in vitro* splicing (Schwer and Guthrie, 1991a). Additionally, release of the Prp16 from the U2-U6 complex would occur concomitant with or prior to the second step of splicing. Understanding the precise function of the RNA-dependent

ATPase activity of Prp16 will require a description of the changes in active site structure that are likely to occur between the two chemical steps of splicing (Moore and Sharp, 1993), and the relationship between these conformational shifts and the nucleotide-regulated states of Prp16.

Acknowledgments

We are grateful to S.M. Noble for providing the *prp16-302* *cs* allele and for helpful discussions. We thank , S.M. Burgess, I. Herskowitz, A.W. Murray, S.M. Noble and J.G. Umen, and Y. Wang for critically reading this manuscript.. H.D.M. is a trainee of the University of California at San Francisco Medical Scientist Training Program. C.G. is an American Cancer Society Research Professor of Molecular Genetics. This work was supported by a grant from the National Institutes of Health.

Figure 1.

RNA-RNA interactions between U2 snRNA, U6 snRNA, and the pre-mRNA.

Shown are the U2-branchpoint interaction (Parker et al., 1987), U2-U6 helix I (Madhani and Guthrie, 1992) and the U6-5' splice site interaction (Wassarman and Steitz, 1992; Sawa and Shimura, 1992; Sawa and Abelson, 1992; Lesser and Guthrie, 1993; Kandels-Lewis and Séraphin, 1993). The sequences for the snRNAs are from *S. cerevisiae*, and the intron sequences reflect the *S. cerevisiae* consensus. "Y" indicates a pyrimidine.

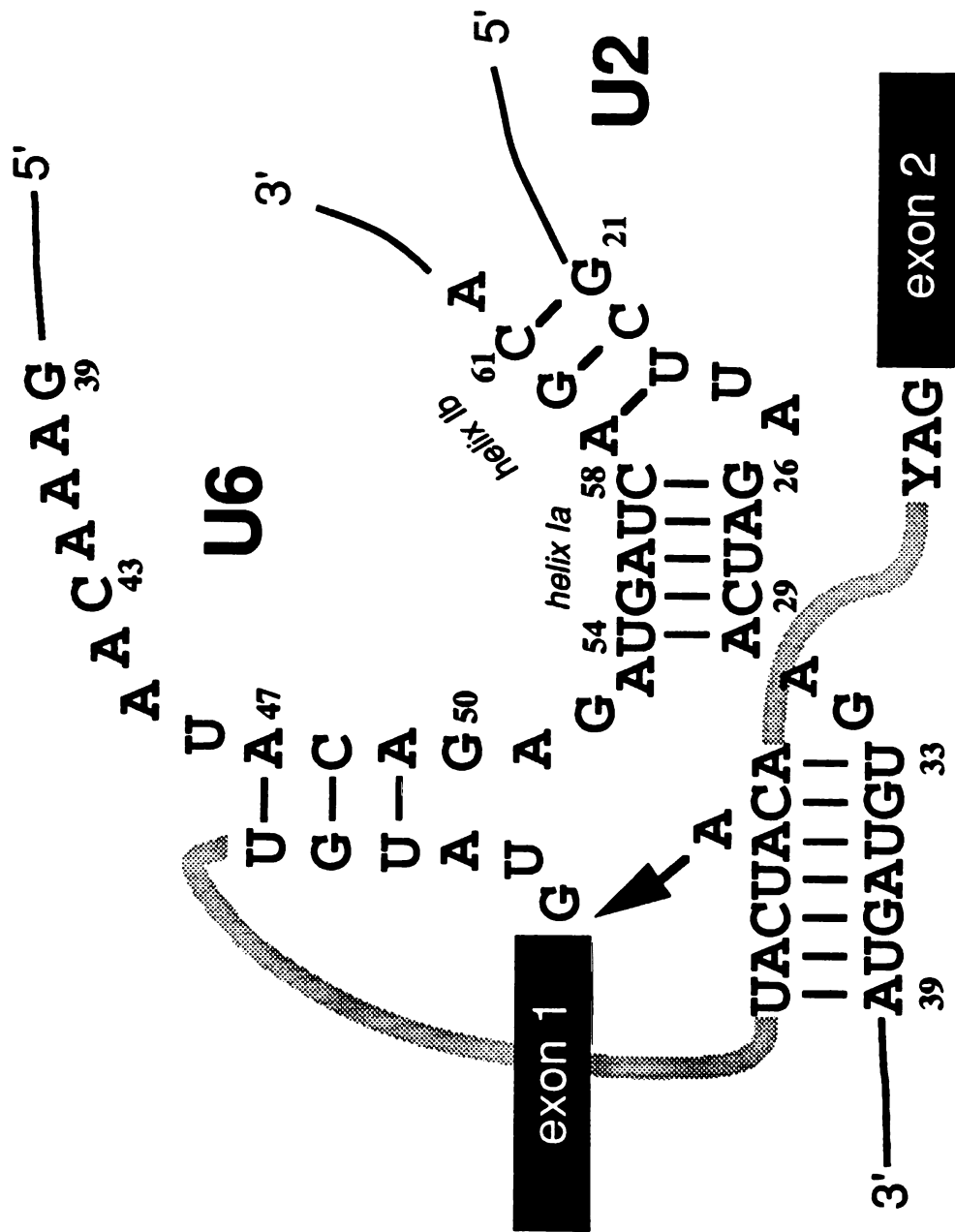


Figure 2.

Suppressors of *prp16-302*.

Growth of YHM145 derivatives containing (as their sole copy of U6) the 14 suppressors isolated from the U6 mutant library (panels B-N). Panel O shows the growth of YHM145 transformed with a vector control. Panel P shows the growth of a wild-type sister spore (YHM146). YEPD plates were incubated at 18°C for 5 days.

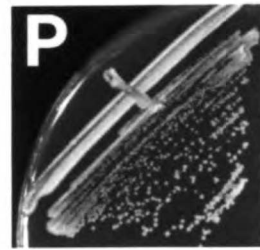
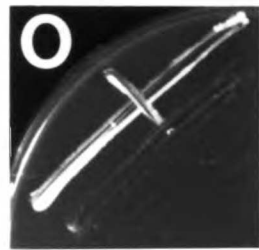
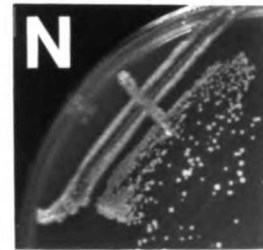
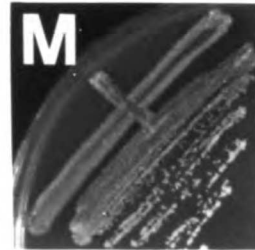
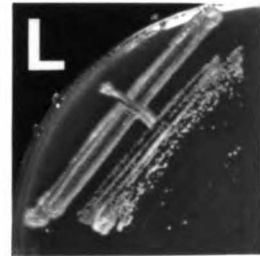
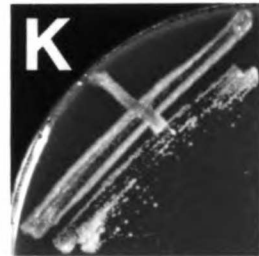
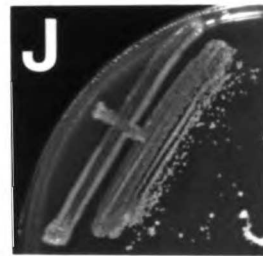
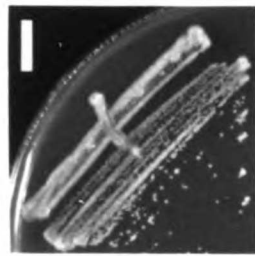
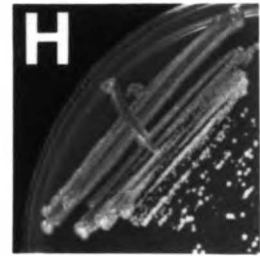
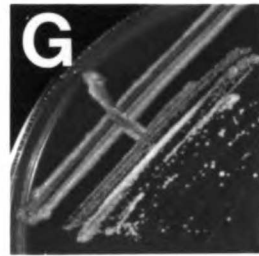
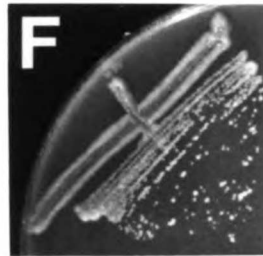
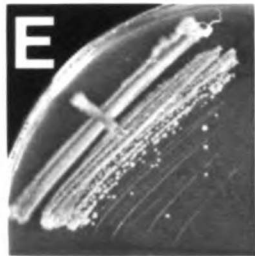
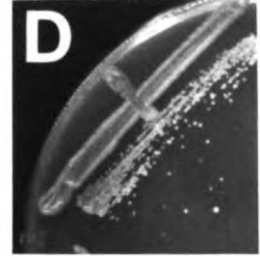
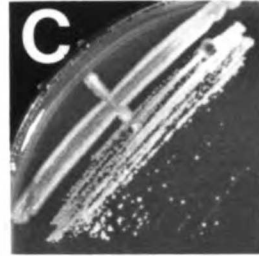
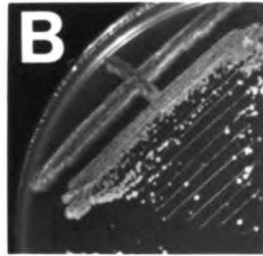
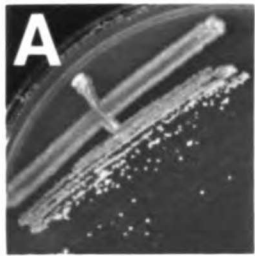


Figure 3.

Sequence of the U6 coding sequence for the suppressor alleles shown in Figure 2.

Sequences 1-14 correspond to suppressors shown in Figure 2, panels B-N, respectively.

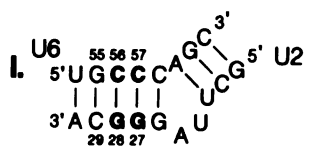
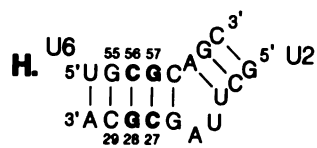
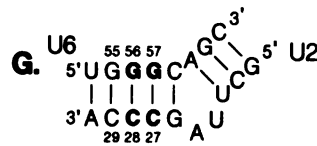
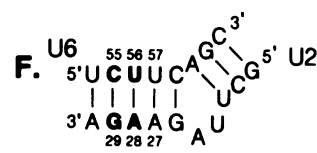
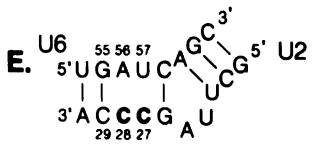
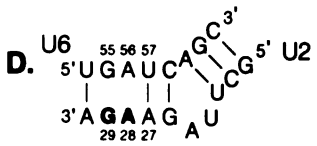
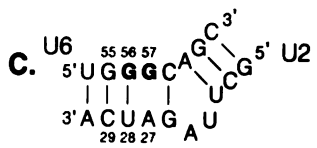
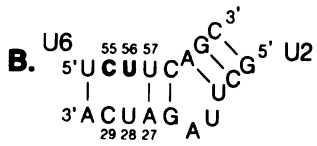
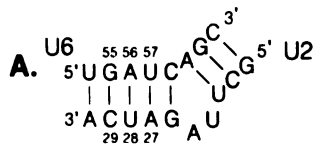
Note that each of the 14 suppressors contains a point deletion in nts 40-46 (underlined), which lie immediately 5' to the conserved ACAGAGA sequence (lowercase). By convention, deletions in nucleotide runs are referred to by the most 5' residue.

	1		10		20		30		40		50
			•		•		•		•		•
	GTUCCGCGAAGUAACCCUUCGUGGACAUTUUGGUCAAUTUGAAACAAUacagagaUGA										
1								Δ	
2								G.Δ	
3									Δ
4								Δ	
5									Δ
6					Δ				Δ
7									Δ
8	GGC								Δ
9									Δ
10									Δ
11										Δ
12									Δ
13									Δ
14									Δ
		60		70		80		90		100	110
		•		•		•		•		•	•
	UCAGCAGUUCGCCUGCAUAAGGAUGAACCGUUUACAAGAGAUUUAUUUCGUUUU										
1
2
3
4					G.				
5
6										G.
7
8					U.				
9
10
11
12
13
14

Figure 4.

Growth of YHM187 derivatives containing the indicated alterations in U2-U6 helix Ia.

Growth on YEPD was assessed after 9 days at 18 °C. A longer incubation time was used with this strain compared to YHM145 because the *prp16-302* phenotype is slightly more severe in this background.



J. + wild-type PRP16



Figure 5.

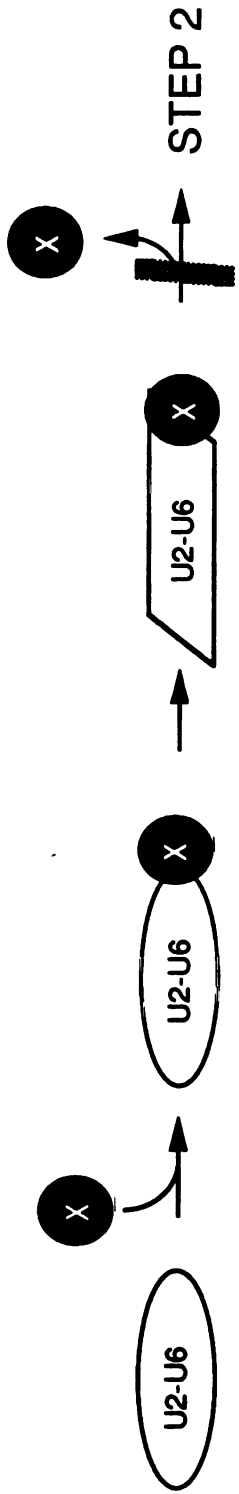
A. Model for suppression.

A factor, X, is proposed to interact with the U2-U6 complex and mediate a conformational change (depicted as a change from an ellipse to a parallelogram). In *cs PRP16* alleles, it is proposed that the release of X from the U2-U6 complex becomes rate-limiting in the cold. Mutants in U2 and U6 suppress this *cs* defect by weakening the interaction with X, promoting its release. X could be Prp16, another protein, or an RNA.

B. Prp16 Cycle.

Depicted is the binding of Prp16 to the spliceosome (Schwer and Guthrie, 1991), a conformational change induced by ATP hydrolysis (Schwer and Guthrie, 1992a) -- represented a change in shape of the spliceosome (ellipse to parallelogram)-- and dissociation of Prp16 from the spliceosome prior to or concomitant with the second chemical step of splicing (Schwer and Guthrie, 1991).

A.



blocked in prp16cs

B.

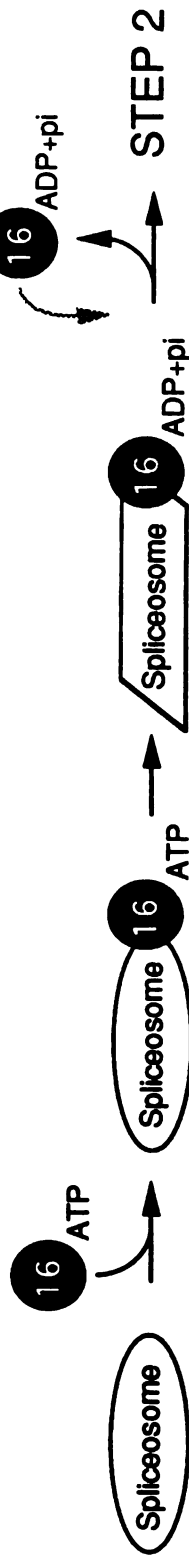


Table 1.

Growth of YS78 derivatives containing alleles of *PRP16*.

The first set of columns describes the growth at various temperatures of strains containing conditional *PRP16* alleles on pSE358 (*TRP1*, *CEN*) as the sole allele. The second set of columns describes the growth of strains containing pG1-borne alleles (*TRP1*, 2 μ) as the sole copy. The third set of columns, in which dominant negative effects are shown, describes the growth of strains in which the indicated pG1-borne allele is in a strain containing wild-type *PRP16* on a centromere vector. Growth in the first two sets of columns was assayed on 5-FOA at 25, 30, 33, 35, and 37 °C. For the assessment of growth in the cold, transformants were cured of the wild-type plasmid on 5-FOA at 30 °C, and then streaked to YEPD plates which were incubated for the 5 days at 18 °C or 12 days at 16 °C. This resulted in more sensitive and reproducible results. To test for dominant negative phenotypes, transformants were assayed on SD -TRP -URA to select for both the pG1-borne allele and the wild-type allele, which is on pSE360 (*URA3*, *CEN*). **Bold** indicates differences with the data in the first set of columns.

Table 1

	<i>prp16</i> (CEN-ARS) <i>prp16::LYS2</i>								<i>Pgpp-prp16</i> (2+) <i>prp16::LYS2</i>								<i>Pgpp-prp16</i> (2+) <i>prp16::LYS2</i> <i>PRP16</i> (CEN-ARS)							
	16°C	18	25	30	33	35	37		16	18	25	30	33	35	37		16	18	25	30	33	35	37	
allele	+++	+++	+++	+++	+++	+++	++	+++	+++	+++	+++	+++	+++	+++	++	+++	+++	+++	+++	+++	+++	+++	++	
<i>PRP16</i>	+++	+++	+++	+++	+++	+++	++	+++	+++	+++	+++	+++	+++	+++	++	+++	+++	+++	+++	+++	+++	+++	++	
<i>prp16-2</i>	NT	+++	+++	+++	++	++	-	NT	NT	+++	+++	+++	+++	+++	++	+++	+++	+++	+++	+++	+++	+++	++	
<i>prp16-201</i>	NT	+++	+++	+++	++	++	-	NT	NT	+++	+++	+++	+++	+++	++	+++	+++	+++	+++	+++	+++	+++	++	
<i>prp16-202</i>	NT	+++	+++	+++	++	++	-	NT	NT	+++	+++	+++	+++	+++	++	+++	+++	+++	+++	+++	+++	+++	++	
<i>prp16-205</i>	NT	+++	+++	+++	++	++	-	NT	NT	+++	+++	+++	+++	+++	++	+++	+++	+++	+++	+++	+++	+++	++	
<i>prp16-1</i>	-/+	++	+++	+++	+++	+++	++	-/+	+	+++	+++	+++	+++	+++	++	-/+	-/+	+++	+++	+++	+++	+++	++	
<i>prp16-301</i>	-	+	+++	+++	+++	+++	+	.	-/+	+++	+++	+++	+++	+++	++	+++	+++	+++	+++	+++	+++	+++	++	
<i>prp16-302</i>	-	-/+	+++	+++	+++	+++	++	.	-	+++	+++	+++	+++	+++	++	-/+	-/+	+++	+++	+++	+++	+++	++	

Table 2.

Growth of YHM187 derivatives containing site-directed mutants in U6 or U2 snRNAs as the sole copy of the respective gene.

YEPD plates were incubated for 9 days at 18 °C. WT indicates wild type. ^a Control: YHM187 containing WT U6, WT U2, and pSB2 (*PRP16 URA CEN*).

Table 2

U6 allele	U2 allele	Growth
WT	WT	-
Δ A47	WT	-/+
A47U	WT	-
G50C	WT	-/+
G52U	WT	-/+
A53C	WT	-/+
A53G	WT	-/+
U54A	WT	-
G55C	WT	-/+
G55C, A56U	WT	++
A56G, U57G	WT	++
C58U	WT	-
A59C	WT	-
C61U	WT	-
WT	G21U	-
WT	C22A	-
WT	U23C	-
WT	U23G	-
WT	A27C, U28C	-/+
WT	U28A, C29G	+
WT	C29G	-
WT	A30U	-
Control ^a	Control ^a	++++

Table 3.

Comparison of dominant versus recessive suppression of *prp16-302* by U6 suppressor alleles.

YHM187 derivatives were cotransformed with the indicated alleles, and growth was assessed after 9 days at 18 °C. ^aGrowth of YHM187 derivatives containing indicated U6 and U2 alleles that have not been cured of the wild-type U2-U6 plasmid. SD -URA plates were incubated for 9 days at 18 °C. ^bGrowth of YHM187 derivatives containing indicated U6 and U2 alleles that have been cured of the wild-type U2-U6 plasmid. SD -TRP plates were incubated for 9 days on at 18 °C. ^cControl: YHM187 containing WT U6, WT U2, and pSB2 (*PRP16 URA CEN*).

Table 3

U6 allele	U2 allele	Recessive Suppression ^a	Dominant Suppression ^b
WT	WT	-	-
ΔA40	WT	+++	+
ΔC43	WT	+++	+++
ΔA44	WT	+++	+++
ΔU46	WT	+++	++
A56G, U57G	WT	++	+
Control ^c	Control ^c	++++	++++

Table 4.

Allele-specificity of suppression.

Shown are the effects on growth at various temperatures of U6 suppressor alleles on YS78 derivatives containing mutant alleles of *PRP16* on pSE358 (*TRP1*, *CEN*) as the sole allele. Assays were performed as in Figure 1. Bold indicates differences with the data in the first set of columns.

Table 4

allele	pSE358 (vector) <i>ppr16</i> (CENARS) <i>ppr16::LYS2</i>								U6AA43 (CENARS) <i>ppr16</i> (CENARS) <i>ppr16::LYS2</i>								U6AA44 (CENARS) <i>ppr16</i> (CENARS) <i>ppr16::LYS2</i>							
	16°C	18	25	30	33	35	37		16	18	25	30	33	35	37		16	18	25	30	33	35	37	
<i>PRP16</i>	+++	+++	+++	+++	+++	+++	++	+++	+++	+++	+++	+++	+++	+++	++	+++	+++	+++	+++	+++	+++	+++	++	
<i>ppr16-2</i>	NT	+++	+++	+++	++	++	-	NT	+++	+++	+++	+++	++	++	-	NT	+++	+++	+++	+++	++	++	-	
<i>ppr16-201</i>	NT	+++	+++	+++	++	++	-	NT	+++	+++	+++	+++	++	++	-	NT	+++	+++	+++	+++	++	++	-	
<i>ppr16-202</i>	NT	+++	+++	+++	++	++	-	NT	+++	+++	+++	+++	++	++	-	NT	+++	+++	+++	+++	++	++	-	
<i>ppr16-205</i>	NT	+++	+++	+++	++	++	-	NT	+++	+++	+++	+++	++	++	-	NT	+++	+++	+++	+++	++	++	-	
<i>ppr16-1</i>	-/+	++	+++	+++	+++	+++	++	-/+	++	+++	+++	+++	+++	+++	++	+	++	+++	+++	+++	+++	+++	++	
<i>ppr16-301</i>	-	+	+++	+++	+++	++	+	-	+++	+++	+++	+++	+++	++	+	-	+++	+++	+++	+++	+++	+++	+	
<i>ppr16-302</i>	-	-/+	+++	+++	+++	+++	++	-	+	+++	+++	+++	+++	+++	++	-/+	+++	+++	+++	+++	+++	+++	++	

Table 5.

Overexpression of cs PRP16 alleles antagonizes suppression by U6 mutants.

Depicted is the growth of YS78 derivatives containing the indicated PRP16 allele on pG1 as the sole copy. Compared is the effects of vector, U6- Δ C43 and U6- Δ A44. **Bold** indicates differences from the "vector" columns.

Table 5

		Plasmid Borne U6 Gene					
		None		U6- Δ C43		U6- Δ A44	
allele	vector type	16°C	18°C	16°C	18°C	16°C	18°C
<i>prp16-1</i>	<i>2</i> μ	-/+	+	-/+	+	-/+	+
<i>prp16-1</i>	<i>CEN</i>	-/+	++	-/+	++	+	++
<i>prp16-301</i>	<i>2</i> μ	-	-/+	-	-/+	-	-/+
<i>prp16-301</i>	<i>CEN</i>	-	+	-	++	-	++
<i>prp16-302</i>	<i>2</i> μ	-	-	-	-/+	-	-/+
<i>prp16-302</i>	<i>CEN</i>	-	-/+	-	+	-/+	++

Table 6

Strain	Genotype	Derivation	Source
YS78	a <i>ade2 his3 leu2 lys2 prp16::LYS2 trp1 ura3 pSB2 (PRP16 URA3 CEN)</i>		Burgess, 1993
YSN131	α <i>ade2 his3 leu2 lys2 prp16-302 ura3</i>		S. Noble, unpublished
YSN132	α <i>ade2 his3 leu2 prp16-302 ura3</i>		S. Noble, unpublished
YHM1	a <i>ade2 his3 leu2 lys2 trp1 ura3 snr6::LEU2 pSX6U (SNR6 URA3 CEN)</i>		Madhani, Bordonné and Guthrie, 1990
YHM145	a <i>ade2 his3 leu2 lys2 prp16-302 trp1 ura3 snr6::LEU2 pSX6U (SNR6 URA3 CEN)</i>	YSN132 X YHM1	This study
YHM111	a <i>ade2 his3 lys2 ura3 snr20::LYS2 pU2U(SNR20 URA3 CEN)</i>		Madhani and Guthrie, 1992
YHM151	α <i>ade2 his3 leu2 lys2 prp16-302 ura3 snr20::LYS2 pU2U(SNR20 URA3 CEN)</i>	YSN131 X YHM111	This study
YHM187	α <i>ade2 his3 leu2 lys2 prp16-302 snr20::LYS2 snr6::LEU2 ura3 pU2U6U (SNR6 SNR20 URA3 CEN)</i>	YHM145 X YHM151	This study

EPILOGUE

**Dynamic RNA-RNA Interactions in the Pre-mRNA
Splicing Mechanism: A Principle of Spliceosomal
Design**

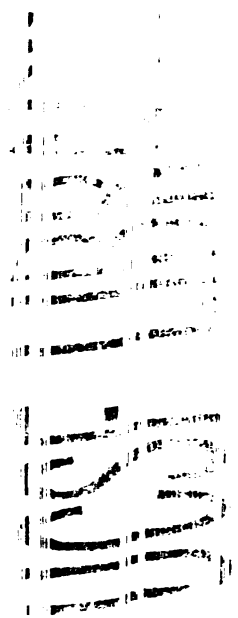
The central questions that surround the pre-mRNA splicing mechanism can be viewed from two vantage points, that of the substrate or that of the splicing apparatus. The chemistry of splicing defines the task at hand. Knowledge of the components of the spliceosome and the assembly pathway give us a "parts list" and assembly instructions. However, a conceptual gap exists between our understanding of the chemical mechanism of splicing on the one hand and the machinery responsible for the execution of this pathway on the other. Without having designed the machine ourselves, we are left to struggle to make these connections. In Chapters 1-4, I described progress towards elucidating some of these correspondences. Below, I review these and other RNA-based interactions that underlie many key aspects of spliceosomal function.

U1 snRNA-Intron Base-Pairing Interactions: Defining the Splice Sites

The first snRNA-intron interaction was proposed 14 years ago based on sequence complementarity between the 5' end of U1 snRNA and the 5' splice site consensus (Lerner et al., 1980; Rogers and Wall, 1980; Figure 1). Several years later, binding of U1 snRNP to the 5' splice site was demonstrated in vitro (Mount et al., 1983). Subsequently, it was shown that the integrity of sequences at the 5' end of U1 snRNA is essential for splicing (Kramer et al., 1984). Genetic proof of base-pairing came in the form of elegant experiments performed in mammalian cells in which the splicing of an intron containing a mutation in the 5' splice site could be rescued by a compensatory mutation in the 5' end of U1 snRNA (Zhuang and Weiner, 1986). Similar studies in yeast (Seraphin et al., 1988; Siliciano and Guthrie, 1988; Seraphin and Rosbash, 1990) yielded evidence for an additional role for the 5' splice site. Alterations of the fifth nucleotide of two different yeast introns result in the activation of nearby aberrant cleavage sites, the site and efficiency of cleavage depending on the intron assayed (Parker et al., 1985; Jacquier et al., 1985; Fouser and Friesen, 1986). Surprisingly, compensatory mutations that restore base-pairing with the intron fail to suppress cleavage at the aberrant sites; instead, cleavage at both the normal and aberrant sites is increased (S eraphin et al., 1988; Siliciano and Guthrie, 1988; S eraphin

and Rosbash, 1990). These results suggest that the fifth position of the intron likely engages in an additional, unidentified interaction (see below). Finally, experiments employing duplicated 5' splice sites have provided evidence that the U1-5' splice site interaction plays a primary role in choosing the 5' splice site in *S. cerevisiae* (Goguel et al, 1991). This observation is consistent with the observed early hierarchic role for U1 in spliceosome assembly and commitment to the splicing pathway (Ruby and Abelson, 1988; Séraphin and Rosbash, 1989; 1991).

In the original model for the U1-5' splice site interaction, it was proposed that the conserved AG dinucleotide at the 3' end of nuclear introns also base-pairs with the invariant CU sequence that lies next to the 5' splice site binding domain of U1 (Figure 1). This model is particularly attractive since it offers a mechanism for a concerted identification of the 5' and the 3' splice site. Evidence for this base-pairing interaction has come recently from studies of a class of introns (so called AG-dependent introns) which, for unknown reasons, require the integrity of the AG at the 3' splice site for the first step of splicing to occur (Reed, 1989). Reich et al.(1992) reasoned that this dependency might be due to the U1-3' splice site interaction proposed previously. This was shown to be the case by experiments performed in the yeast *S. pombe* in which mutations in the AG dinucleotide were shown to be suppressible by compensatory mutations in U1 snRNA (Reich et al., 1992). Moreover, the U1 residues involved in base-pairing were demonstrated to be essential for cell growth in *S. pombe* (Reich et al., 1992). It is important to note that only the block to the first step of splicing is relieved by the U1 compensatory mutations, indicating a different role for the AG dinucleotide during the second step of splicing. The U1-3' splice site interaction appears not to play a critical role in *S. cerevisiae* where the same mutations in U1 snRNA have no effect on cell growth (Séraphin and Kandels-Lewis, 1993; J.G. Umen and C.G., unpublished). The dispensability of these U1 sequences is consistent with the observation that mutations in the



AG dinucleotide at the 3' splice site of *S. cerevisiae* introns block the second chemical step of splicing but not the first (Vijayraghavan et al., 1986).

Base-Pairing with U2 snRNA Defines the Intron Branchpoint

Early biochemical experiments suggested that U2 snRNP interacts with sequences that include the intron branchpoint (Black and Steitz, 1985). Potential sequence complementarities between U2 and the branchpoint region (Keller and Noon, 1985; Ares, 1986) led to compensatory base-change experiments in *S. cerevisiae* that demonstrated the U2-branchpoint interaction shown in Figure 1 (Parker et al., 1987). In this model, the branchpoint adenosine nucleophile is bulged out of a U2-intron duplex (Figure 1). Elegant experiments using chemically engineered pre-mRNAs containing modifications of specific ribose sugars in the branchpoint region indicate that the bulging of this residue is required for its usage (Query et al., 1993). The consensus for the branchpoint sequence is considerably more degenerate in mammals compared to yeast, indicating a more flexible nucleotide sequence requirement. Nonetheless, through the use of sensitive splice site competition constructs, it has been possible to demonstrate a role for base-pairing with U2 snRNA in mammals (Zhuang and Weiner, 1989; Wu and Manley, 1989). Importantly, these studies also show how modulating the site of the U2-branchpoint interaction can influence the choice of 5' or 3' splice sites, because the architecture of the pre-mRNAs employed resulted in a coupling of splice site choice to branch site choice.

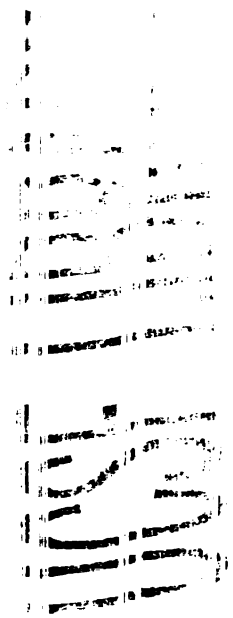
In yeast and in mammals, binding of U2 snRNP to the branchpoint requires multiple protein factors and ATP (Konarska and Sharp, 1987; Cheng and Abelson, 1987; Ruskin et al., 1988; Zamore and Green, 1989; Abovich et al., 1990; Krämer and Utans, 1991; LeGrain et al., 1993; Brosi et al., 1993; Ruby et al., 1993; Arenas and Abelson, 1993). The mechanism by which these proteins assist the assembly of U2 snRNP into the spliceosome remains elusive. Analysis of U2 snRNA has identified a stem-loop 3' to the branchpoint recognition region (stem IIA) that is necessary for this event: mutations that weaken stem IIA prevent binding of U2 snRNP to the pre-mRNA (Ares and Igel, 1990;

Zavanelli and Ares, 1991). Intriguingly, in vivo structure probing experiments demonstrate that these mutations result in the formation of an alternative RNA structure whose potential to form is conserved phylogenetically (Zavanelli and Ares, 1991). These authors suggest that interconversion between the alternative structure and stem IIA might be important for the binding of U2 snRNP to the pre-mRNA. The function of such an rearrangement has yet to be elucidated.

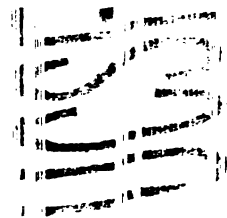
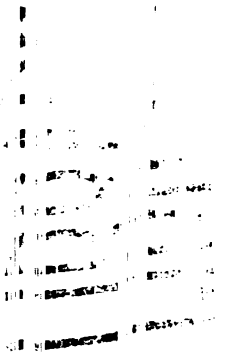
Why does the binding of U2 snRNP to the intron branchpoint region require the action of multiple proteins and an additional RNA structure? One possibility is that these factors communicate with components, such as U1 snRNP, that recognize different elements in the intron. This is clearly the case for one factor required for the U2-branchpoint region interaction, U2AF, which interacts with the conserved pyrimidine tract that lies just downstream of the mammalian branchpoint (Ruskin et al., 1988; Zamore and Green, 1989). U2AF might assist U2 binding through interactions with the protein factors involved in U2 snRNP binding mentioned above, or through a direct interaction with U2 snRNA. The U1-5' splice-site and U1-3' splice site interactions described above, which could occur simultaneously, may also be an example of communication between distinct informational elements in the intron, in which different features of the intron (in this case at each end of the intron) are assessed in concert (Reich et al., 1992). Such mechanisms might enhance the fidelity of splicing by demanding the coupled recognition of multiple intron elements.

Mutually Exclusive Base-Pairing Interactions Involving U4, U6 and U2 snRNAs: A Model for the Catalytic Activation of the Spliceosome

Among the five snRNAs required for pre-mRNA splicing, U6 stands out in terms of its significant size and sequence conservation. In both yeast and mammalian cell extracts, U6 is found to be extensively base-paired with U4 snRNA (Hashimoto and Steitz, 1984; Rinke et al., 1984; Brow and Guthrie, 1988). Isolation of the *S. cerevisiae* U6 snRNA allowed phylogenetic comparisons that led to a model for the U4-U6 interaction



(Brow and Guthrie, 1988; Figure 2). This model has since been proven in several experimental systems (Bindereif et al., 1990; Vankan et al., 1990; Shannon and Guthrie, 1991). Phylogenetic conservation of sequence in the base-paired regions is strikingly asymmetric, with much more variability in the U4 sequence (Guthrie and Patterson, 1988; C.G., S. Mian, and H. Roiha, unpublished; Figure 2). This pattern of conservation suggests that there are more stringent functional constraints on U6 than U4 (Guthrie and Patterson, 1988). Despite the high in vitro stability of this interaction ($T_m = 52$ °C in yeast; Brow and Guthrie, 1988), the U4-U6 interaction is destabilized in the spliceosome: U4 is released from or at least less tightly bound to splicing complexes prior to the chemical steps of the reaction (Konarska and Sharp, 1987; Cheng and Abelson, 1987; Lamond et al., 1988; Blencowe et al., 1989; Yean and Lin, 1991). This temporal correlation together with the aforementioned properties of U6 led to speculation that the destabilization of the U4-U6 interaction might activate U6 for participation in catalysis (Guthrie and Patterson, 1988). The subsequent discovery of rare mRNA-type introns in the U6 genes of unrelated fungi was suggested reflect splicing accidents in which excised introns integrate into a catalytic component of the splicing machinery, namely U6 snRNA (Brow and Guthrie, 1989; Tani and Ohshima, 1989; 1991). One prediction of this model is that the regions interrupted by these introns (presumptive active site residues) should be functionally important. This was borne out by two mutational studies of the yeast U6 snRNA (Madhani et al., 1990; Fabrizio and Abelson, 1990). In one case, a library of U6 mutants was screened that was constructed through degenerate synthesis of the coding sequence for mutants that are deleterious to cell viability (Madhani et al., 1990). In the other, an in vitro reconstitution assay was used to examine the effects of a large collection of site-directed mutants on splicing (Fabrizio and Abelson, 1990). While many residues in U6 were found to be dispensable for function, single point mutations in two regions were found to have dramatic effects on cell viability and splicing: a short sequence in U4-U6 stem I (CAGC) that is interrupted by an intron in *S. pombe* and a second stretch (ACAGAG) that is



interrupted by an mRNA-type intron in *R. dactyoidum* (Tani and Ohshima, 1991; Figure 2). The in vitro studies demonstrated that while some of these residues are important prior to the first step of splicing, others are only required for the second step of the reaction (Fabrizio and Abelson, 1990). Studies in frog oocytes demonstrated an important role for these two clusters of residues in *Xenopus* U6 snRNA as well (Vankan et al., 1990). Further studies in yeast and in frog oocytes indicated that those U6 residues that participate in U4-U6 stem I have a role independent of base-pairing with U4 (Madhani et al., 1990; Vankan et al., 1990).

The nature of this additional interaction was made clear by the discovery of a base-pairing interaction between U2 and U6 snRNAs that is mutually exclusive with the extensive U4-U6 interaction (Madhani and Guthrie, 1992). In this novel pairing, termed U2-U6 helix I, a conserved sequence in U6 interacts with sequences in U2 that lie immediately upstream of the branchpoint recognition domain (Figure 3). Consequently, the putative active site residues in U6 described above can be closely juxtaposed with the intron branchpoint. The residues in U6 were shown previously to be important for both chemical steps of splicing (Fabrizio and Abelson, 1990). As predicted by the model, the U2 residues were found also to play a role in both chemical steps in vivo and in vitro (Madhani and Guthrie, 1992; McPheeters and Abelson, 1992). U2-U6 helix I exhibits extraordinary phylogenetic conservation, suggesting that its formation is not unique to *S. cerevisiae*. Indeed, the importance of the homologous U6 residues in metazoans for both chemical steps of splicing has been demonstrated in human and nematode cell-free splicing systems (Wolff et al., 1993; Yu et al., 1993). Taken together, these properties are consistent with the notion that U2-U6 helix I functions as a central component of the spliceosomal active site (reviewed in Weiner, 1993).

Ultimate understanding of the possible roles of U2-U6 helix I in catalysis will require a detailed understanding of the three-dimensional structure of the spliceosome. In the cases of tRNAs and Group I introns, the elucidation of tertiary (or "long range")

contacts through phylogenetic covariations has facilitated the accurate prediction of three-dimensional structure (Levitt, 1969; Michel and Westof, 1989). A similar approach aimed at identifying tertiary interactions in the U2-U6 helix I region has recently been described (Madhani and Guthrie, in prep). Because of the high conservation of this region, a novel bimolecular randomization-selection procedure was employed to generate "artificial phylogenies" (Madhani and Guthrie, in prep.). This study provides evidence for a long range interaction in which the terminal residue of the hexanucleotide (ACAGAG) forms a direct contact with the bulge in U2-U6 helix I. Such a higher order interaction can juxtapose the two clusters of residues of the U2-U6 complex that are known to be required for the second chemical step of pre-mRNA splicing. Further application of this method in studies that involve randomization of conserved intron sequences in the pre-mRNA, in addition to snRNA sequences, should identify further structural constraints, the goal being a detailed picture of the three-dimensional architecture of the spliceosomal active sites.

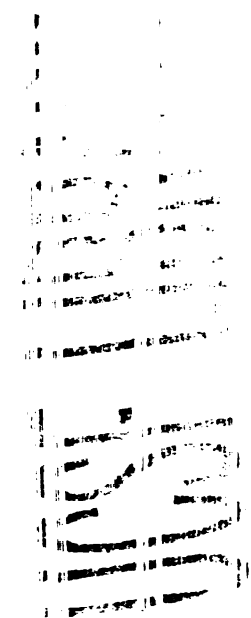
Because it is mutually exclusive with the U4-U6 interaction, U2-U6 helix I offers a molecular explanation for the disruption of U4-U6 prior to catalysis and supports the original suggestion that this destabilization event is central to the catalytic activation of the spliceosome. However, U2-U6 helix I is mutually exclusive with only a portion of the U4-U6 interaction, U4-U6 stem I. Since U4 can be released from splicing complexes prior to catalysis (Yean and Lin, 1991), U4-U6 stem II is presumably also disrupted. On the basis of phylogenetic covariations, we previously proposed an intramolecular U6 stem-loop as a conformational alternative to U4-U6 stem II (Figure 4; Madhani and Guthrie, 1992; C.G., S. Mian and H. Roiha, unpublished). Recent studies are consistent with the notion that this structure might indeed play a role in the active spliceosome (Wolff and Bindereif, 1993). Similarly, residues in U2 that form U2-U6 helix I are also thought to participate in an intramolecular structure, U2 stem I (Figure 4; Keller and Noon, 1985; Guthrie and Patterson, 1988; McPheeters and Abelson, 1992). Thus, multiple

conformational rearrangements are likely to occur upon the destabilization of the U4-U6 interaction (Madhani and Guthrie, 1992).

The RNA rearrangements involving U2, U4 and U6 snRNAs are presumably mediated and regulated by spliceosomal proteins. Of particular interest are five helicase-like proteins that are involved in splicing (Prp2, Prp5, Prp16, Prp22, Prp28; reviewed in Schmid and Linder, 1992). Based on conserved sequence motifs, these proteins fall into one of two subfamilies (DEAD and DEAH). A major gap in our understanding of these proteins is the identity of their RNA ligands. This has hindered efforts aimed at elucidating the specific roles of these factors in the known RNA-based events of spliceosome assembly and disassembly. It is therefore notable that recent genetic suppression studies indicate a functional interaction between the DEAH box splicing factor Prp16 and the U2 and U6 snRNAs (Madhani and Guthrie, in prep.). Several aspects of the genetic data can be explained by proposing that the U2-U6 complex might interact directly with Prp16. These data encourage biochemical efforts aimed at detecting a physical interaction between the U2-U6 complex and Prp16. A combination of genetic and biochemical experiments should prove fruitful in analyzing the role of other members of this protein family.

U6-5' Splice Site Base-Pairing: Aligning the Substrate for Cleavage

A direct interaction between U6 snRNA and the intron-containing substrate is suggested by several crosslinking studies. Using a UV crosslinking method, Sawa and Shimura (1992) reported an association of U6 snRNA with the pre-mRNA and lariat-intermediate during *in vitro* splicing in human cell extracts. These crosslinks were roughly mapped to the vicinity of the 5' end of the intron and the ACAGAG sequence in U6 (Sawa and Shimura, 1992). Subsequently, psoralen-induced crosslinks between U6 and the pre-mRNA were mapped more precisely and led to a specific base-pairing model (Wassarman and Steitz, 1992), which is shown in the context of other known interactions in Figure 5. In this model, the ACA sequence in U6 base-pairs with the last two (in mammals) or three (in *S. cerevisiae*) residues of the 5' splice site consensus. Precise mapping of UV-induced



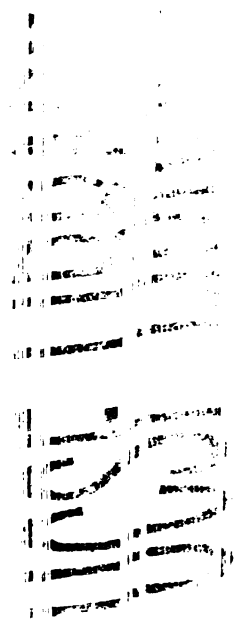
crosslinks between U6 and the lariat intermediate in a yeast in vitro system led to a slightly different model, in which sequences 5 residues upstream of the ACA sequence interact with the 5' splice site (Sawa and Abelson, 1992). More recently, a crosslink between the second residue of the intron (in lariat-intermediate form) and the penultimate residue of the ACAGAG hexanucleotide has also been induced using a chemically modified pre-mRNA containing a photoactivatable 4-thiouridine group at the second position of the intron (Sontheimer and Steitz, 1993).

While these studies indicate proximity between U6 and the 5' splice site, they do not address the question of whether or not this interaction is functionally important. Two groups have now obtained strong evidence for a role for this interaction in aligning the 5' splice site for cleavage in *S. cerevisiae* (Lesser and Guthrie, 1993; Kandels-Lewis and Séraphin, 1993). As mentioned above, mutations in the fifth position of two different yeast introns result in the appearance of upstream aberrant cleavage sites. Since the restoration of complementarity with U1 snRNA does not suppress the occurrence of aberrant cleavage, a second molecule is likely to interact with this sequence. The model shown in Figure 5 proposes that the C48 in U6 interacts with the fifth nucleotide of the intron and raises the possibility that aberrant cleavages induced by intron position 5 mutants are due to a weakening of base-pairing with U6 snRNA. If true, then one expects that restoring base-pairing by mutation of U6 should suppress cleavage at the aberrant site and increase cleavage at the normal site. Kandels-Lewis and Séraphin (1993) demonstrated this expectation to be the case in the yeast *RP51A* gene: the C48U and C48A mutations in U6 can partially suppress aberrant cleavage resulting from a G5A and G5U mutations in this intron, respectively. Lesser and Guthrie (1993) demonstrated that increasing complementarity between U6 and the intron in nonconserved sequences that flank the proposed interaction (intron positions 7 and 8; U6 positions 45 and 46) can suppress aberrant cleavage induced by G5A and G5C mutations in the yeast actin intron. Interestingly, a mutation predicted to stabilize the alternative register proposed by Sawa and

Abelson (1992) results in an increase in aberrant cleavage, suggesting that a realignment of the 5' splice site on U6 might determine the site of aberrant cleavage events in intron position 5 mutants (Lesser and Guthrie, 1993).

It is worthwhile to consider the implications of the three RNA-RNA interactions shown in Figure 5. Taken together, they provide a mechanism for bringing together the nucleophile in the first chemical step of the splicing reaction, the branchpoint adenosine, and its target phosphate at the 5' splice site. At the same time, these interactions juxtapose conserved residues in U2-U6 helix I that are required for both steps of splicing with these reaction partners, and is consistent with the proposal that helix I functions as a component of the spliceosomal active site. Finally, it is important to note that the U6-5' splice site interaction is mutually exclusive with the U1-5' splice site interaction, which implies the existence of a handing-off process in which the 5' splice site is transferred from U1 to U6. Indeed, in a model mammalian in vitro system, binding of RNA oligonucleotides containing a 5' splice site consensus sequence to U1 snRNA was found to be mutually exclusive in vitro with its ability to induce the formation of and to bind to a U2-U4-U6-U5 snRNP (Konforti et al., 1993). It seems likely that the activation of aberrant cleavage sites in yeast reflects the ease with which the transfer of the 5' splice site from U1 to U6 can be disrupted. This process is likely to be more difficult in organisms in which both cis- and trans-splicing occur, such as nematodes. In trans-splicing, the 5' splice site is likely to be delivered to U6 not by U1, but by the spliced leader (SL) snRNP (for review see Agabian, 1990). Consequently, in nematodes, the splicing machinery must accommodate two different mechanisms for transferring the 5' splice site to U6, one involving U1 and the other involving SL. Such plasticity might explain the remarkable occurrence of splicing accidents in nematode extracts in which the branchpoint nucleophile attacks sequences in U6 instead of the 5' splice site (Yu et al., 1993).

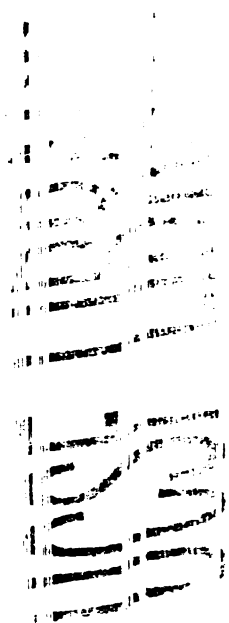
U5 snRNA-Exon Interactions



As might be expected from the fact that exons must encode diverse sequences, conserved information at the 5' and 3' splice sites resides almost completely in intron sequences (reviewed in Stephens and Schnieder, 1992; Penotti, 1991). However, limited conservation of exon sequences is evident. For example, in mammals, there is a moderate preference for an A at position -2 and a G at position -1 with respect to the 5' splice site; a weaker preference for a G at position +1 and a U at position +2 downstream of the 3' splice site is also observed. (Stephens and Schnieder, 1992; Penotti, 1991). This raises the issue of what recognizes these sequences. Below, we summarize genetic and biochemical experiments that implicate the conserved loop of U5 snRNA in exon binding during both chemical steps of splicing. We discuss models for the functional roles of these interactions.

5' Exon Interactions

An important advance into the possible functions of U5 snRNA in splicing came as a result of genetic experiments performed in *S. cerevisiae* in which a single nucleotide substitution in the conserved loop of U5 snRNA was isolated as a dominant suppressor of an intron position 1 mutant (Newman and Norman, 1991). Suppression was shown to be due to the activation of a nearby cryptic splice site. A detailed mutational analysis revealed that the activation of the cryptic site by the U5 mutant is a consequence of the creation of Watson-Crick complementarity of exon sequences upstream of the cryptic site (exon positions -2 and -3) and positions 5 and 6 of the loop of U5 snRNA (Newman and Norman, 1992; Figure 6). Several other cryptic sites are induced by other U5 loop variants that create complementarities with different nearby sequences in the pre-mRNA (Newman and Norman, 1992). The activation of the cryptic splice sites was dependent on the presence of the mutant 5' splice site: complete deletion of the mutant 5' splice site or its replacement with a wild-type 5' splice site prevents the induction of cryptic splice sites by mutations in the U5 loop (Newman and Norman, 1991; Newman and Norman, 1992). These studies demonstrated that the loop of U5 snRNA can base-pair with the 5' exon and



influence the site of cleavage according to Watson-Crick rules when the first nucleotide of the intron is mutated. Analogous experiments have recently been performed in cultured mammalian cells using substrates mutated at the first position of the intron, with similar, albeit more complex, results (Cortes et al, 1993).

Site-specific crosslinking studies have demonstrated that the penultimate residue of the 5' exon in the pre-mRNA can be crosslinked to the loop of U5 during *in vitro* splicing in human extracts (Wyatt et al., 1992). Remarkably, the register of the major crosslink (between exon position -2 and U5 loop position 5) correlates precisely with that proposed to explain the yeast genetic suppression data (Wyatt et al., 1992; Newman and Norman, 1992; Figure 6). This result indicates proximity between the 5' exon and the U5 loop in the context of a wild-type intron, arguing against the model that the observations made in yeast are unique to a mutant situation. More recently, site-specific crosslinking experiments involving the terminal residue of the 5' exon have also identified an interaction between this residue (exon residues -1) and position 4 of U5 loop in both the pre-mRNA and the excised 5' exon (Figure 6). Interestingly, crosslinks induced between U5 and the pre-mRNA can be chased through both steps of splicing upon further incubation (Sontheimer and Steitz, 1993). This experiment demonstrates that a covalent interaction between the U5 loop and the 5' exon does not interfere with the subsequent steps of splicing, eliminating the possibility that this crosslink is merely detecting a dead-end product (Sontheimer and Steitz, 1993).

3' Exon Interactions

The activation of cryptic 5' splice sites through the creation of base-pairing between the U5 loop and the 5' exon motivated Newman and Norman (1992) to search for interactions with the 3' exon. They were rewarded by the finding that an AG to AA change in the 3' splice site dinucleotide can be suppressed by U5 loop mutations (at positions 3 and 4) that increase complementarity with the first two residues of the 3' exon (Newman and Norman, 1992). In this case, the register of the interaction with respect to the cleavage site

differs by one nucleotide when compared to the 5' exon base-pairing interaction, such that U5 loop position 4 interacts both with 5' exon residue -1 and 3' exon residue +1 (Figure 6). These data have been extended by site-specific crosslinking studies in which the first residue of the 3' exon was crosslinked to the U5 loop during *in vitro* splicing human cell extracts (Sontheimer and Steitz, 1993).

Function of the U5 Loop During Splicing of Wild-Type Pre-mRNAs

Because exon sequences are highly variable (and must be to encode diverse polypeptides), it has been suggested that the interactions with the U5 loop are unconventional (Newman and Norman, 1992; Wyatt et al., 1992; Sontheimer and Steitz, 1992). In this model, the preponderance of uridine residues in the loop is rationalized by their ability to base-pair promiscuously. This lack of specificity would in turn require that U5 be positioned onto exon sequences by other elements, such as U1 snRNA, that recognize conserved information in the intron (Newman and Norman, 1992). Once fixed, it might function to hold the cut-off 5' exon between the two chemical steps of splicing (Sontheimer and Steitz, 1993). The existence of nonspecific base-pairing between the U-rich loop of U5 and exon sequences is difficult to prove since functional interactions between the two are only evident when the two are complementary. However, the fact that the consensus sequences for the last two positions in the 5' and the first two positions of the 3' exons are not perfect Watson-Crick complements of the U5 loop sequences with which they interact (see above) argues strongly against the alternative model that the loop sequences function instructively to specify the site of 5' or 3' splice site cleavage. Consequently, the limited conserved information contained in exon sequences is likely to be recognized by other factors. Indeed, 5' exon sequences do contribute to the recognition of the 5' splice site by Watson-Crick base-pairing with U1 snRNA in both mammals and yeast (Aebi et al., 1987; Seraphin and Kandels-Lewis, 1993; Figure 1). Candidates for factors that function (perhaps instructively) in concert with the U5 loop are encoded by the *SLU* genes, which were identified in a genetic screen that was designed to uncover factors

1950
1951
1952
1953
1954
1955
1956
1957
1958
1959
1960
1961
1962
1963
1964
1965
1966
1967
1968
1969
1970
1971
1972
1973
1974
1975
1976
1977
1978
1979
1980
1981
1982
1983
1984
1985
1986
1987
1988
1989
1990
1991
1992
1993
1994
1995
1996
1997
1998
1999
2000
2001
2002
2003
2004
2005
2006
2007
2008
2009
2010
2011
2012
2013
2014
2015
2016
2017
2018
2019
2020
2021
2022
2023
2024
2025
2026
2027
2028
2029
2030
2031
2032
2033
2034
2035
2036
2037
2038
2039
2040
2041
2042
2043
2044
2045
2046
2047
2048
2049
2050
2051
2052
2053
2054
2055
2056
2057
2058
2059
2060
2061
2062
2063
2064
2065
2066
2067
2068
2069
2070
2071
2072
2073
2074
2075
2076
2077
2078
2079
2080
2081
2082
2083
2084
2085
2086
2087
2088
2089
2090
2091
2092
2093
2094
2095
2096
2097
2098
2099
2100

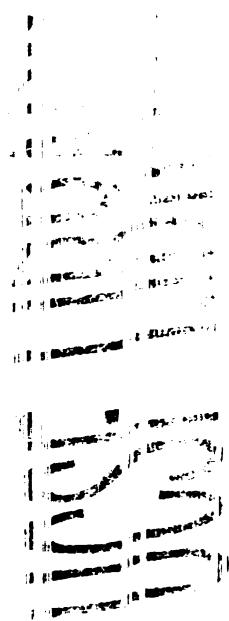
that act redundantly or together with the U5 loop (Frank et al., 1992; Frank and Guthrie, 1992). Of particular interest is *SLU7*, which encodes an essential splicing factor involved in the second step of splicing. Its sequence contains a potential RNA binding motif related to the zinc knuckle found in nucleic acid-binding retroviral *gag* proteins (Frank and Guthrie, 1992).

Recognition of the AG dinucleotide at the 3' Splice Site

While a great deal of information exists regarding the mechanism of 5' splice site and branchpoint recognition, comparatively little is known about how the conserved AG dinucleotide at the 3' splice site is recognized during the second chemical step of splicing. In this reaction, the phosphate at the 3' splice site must be brought into proximity with the 3' hydroxyl of the 5' exon. In principle, such a juxtaposition could be accomplished through an interaction between the 5' and 3' splice sites. This notion motivated Parker and Siliciano (1993) to search for an interaction between the terminal guanosines of the yeast actin intron. Both a G to A change (A1) in the first residue of the intron and a G to C mutation in the 3' most residue of the intron (C303) are known to result in severe blocks to the second chemical step of splicing in *S. cerevisiae*. Remarkably, the combination of these two mutations in a single intron results in the substantial alleviation of these defects (Parker and Siliciano, 1993). This mutual suppression is largely allele-specific: A303 results in the production of low levels of mRNA in combination with A1, but other 3' splice site mutations are inactive for suppression. These data can most simply be explained by proposing a direct interaction between the guanosines at the 5' and 3' splice sites prior to and/or during the second chemical step of splicing. This conclusion is reinforced by the rare occurrence of naturally-occurring introns that contain the equivalent of the A1-C303 combination (Jackson, 1991).

Roles for Base-Pairing in snRNP-snRNP Interactions

The ordered nature of spliceosome assembly makes it likely that snRNPs interact with each other during the splicing process. In the case of the U4-U6 interaction, the



structural basis is well established as a direct RNA-RNA interaction (Bringmann et al., 1984; Hashimoto and Steitz, 1984; Rinke et al., 1985; Brow and Guthrie, 1988). More recently, a base-pairing interaction between U2 and U6 snRNA that occurs in human cell extracts (i.e. in the absence of spliceosomes) has been identified through psoralen crosslinking experiments (Hausner et al., 1990). This interaction, now termed U2-U6 helix II, involves base-pairing between the 5' end of U2 snRNA and the 3' terminal domain of U6 snRNA (see Figure 4). U2-U6 helix II is important for splicing in mammalian cells (Datta and Weiner, 1991; Wu and Manley, 1991), but is dispensable in yeast (Fabrizio et al., 1989; Madhani et al., 1990; H.D.M. and C.G., unpublished). Mutations in human U6 snRNA that are predicted to disrupt U2-U6 helix II prevent spliceosome assembly subsequent to the binding of U2 snRNA to the pre-mRNA (Wolff and Bindereif, 1992).

Recent data demonstrate that the formation of the U4-U6 interaction is antagonized by the intramolecular U6 stem-loop described above (see Figure 4). Two groups have demonstrated that mutations that hyperstabilize this intramolecular structure inhibit the formation of the U4-U6 snRNP in vitro (Wolff and Bindereif, 1993) and in vivo (Fortner et al., 1993). A yeast protein, Prp24, has been implicated in the assembly of the U4-U6 snRNP (Shannon and Guthrie, 1991; J. Abelson, pers. comm.). Interestingly, mutants that hyperstabilize the intramolecular U6 stem can also be suppressed by mutants that destabilize the Prp24-U6 interaction (Fortner et al., 1993). This observation is consistent with the notion that Prp24 stabilizes the intramolecular U6 structure and fits well with the observation that the protein is associated exclusively with the fraction of U6 snRNA that is not associated with U4 snRNA in wild-type yeast extracts (Shannon and Guthrie, 1991). Although the observations described above argue that the Prp24 competes with U4 for binding to U6, this picture is likely to be oversimplified since destabilization of the U4-U6 interaction results in the accumulation of a Prp24-U4-U6 complex, which is not observed

in wild-type extracts (Shannon and Guthrie, 1991). This has been suggested to be a possible intermediate in the annealing of U4 to U6 (Shannon and Guthrie, 1991).

Assembly of the U4-U6 snRNP requires the two RNAs to interact. Based on modification interference experiments, it has been suggested that the 5 nucleotide loop of the intramolecular U6 structure functions as a nucleation site for the annealing of U4 to U6 (Wolff and Bindereif, 1993), analogous to the reaction involved in the first step of antisense regulation of the Col E1 replicon (reviewed in Tomizawa, 1993). In the latter case, the rate-limiting step in duplex formation between the sense and antisense RNAs is a "kissing" reaction involving intermolecular base-pairing between the loops of complementary stem-loops. This interaction is stabilized by the protein factor, Rom, which consequently enhances duplex formation (reviewed in Tomizawa, 1993). It will be interesting to see whether Prp24 plays a similar role in the annealing of U4 and U6 snRNAs. Particularly informative should an analysis of a putative annealing intermediate described above, the Prp24-U4-U6 complex (Shannon and Guthrie, 1991).

Reprise: Comparison With Autocatalytic Group II Introns

The obvious similarities in chemical mechanisms of nuclear pre-mRNA splicing and Group II self-splicing raise the question of whether the two mechanisms are mediated by analogous RNA structures. An initial observation that suggested that this might be the case involves the intron branchpoint. In nuclear pre-mRNAs, the branchpoint is in part identified through a base-pairing interaction with U2 snRNA in which the adenosine nucleophile is bulged out of the U2-pre-mRNA duplex (Parker et al., 1987; Zhuang and Weiner, 1989; Wu and Manley, 1989; Query et al., 1993). Similarly, in Group II introns, the branchpoint adenosine is also found bulged out of a duplex, termed domain 6 (Schmelzer and Schweyen, 1987; Figure 7).

Domain 6 is immediately preceded by the most conserved feature of Group II introns, domain 5, a small helix interrupted by a two-nucleotide bulge on its 3' side (Michel et al., 1989). Domain 5 is essential for splicing (Jarrell et al., 1988; Koch et al., 1992),

11
12
13
14
15
16
17
18
19
20
21
22
23
24
25
26
27
28
29
30
31
32
33
34
35
36
37
38
39
40
41
42
43
44
45
46
47
48
49
50
51
52
53
54
55
56
57
58
59
60
61
62
63
64
65
66
67
68
69
70
71
72
73
74
75
76
77
78
79
80
81
82
83
84
85
86
87
88
89
90
91
92
93
94
95
96
97
98
99
100

and has recently been shown to be important for both chemical steps of the splicing reaction (Dib-Hajj et al., 1993). These properties suggest domain 5 as an excellent candidate for a component involved in catalysis. Similarly, in the spliceosome, the branchpoint helix is preceded by a highly conserved helix (U2-U6 helix I) required for both steps of splicing (Madhani and Guthrie, 1992; Figure 7). Like domain 5, U2-U6 helix I is interrupted by a two-nucleotide bulge on its 3' side (relative to U6); moreover, it exhibits limited sequence identity with domain 5 (Madhani and Guthrie, 1992).

Exons in Group II introns are recognized in part through base-pairing with the D3 loop in domain 1 (Figure 7). This sequence base-pairs with both the 5' and 3' exons. One established function of the D3 loop-5' exon interaction (termed the EBS1-IBS1 interaction) is to hold the liberated 5' exon between the two chemical steps of splicing (Jacquier and Rosbash, 1986; Jacquier and Michel, 1987). In addition, the EBS1-IBS1 interaction plays a central role in determining the specific site of 5' splice site cleavage (Jacquier and Jacquesson-Breuleux, 1991). In the spliceosome, the U5 loop also interacts with the 5' and 3' exons, in a manner highly reminiscent of the D3 loop-exon interactions of Group II introns (Newman and Norman, 1992; Figure 7). As discussed above, the U5-5' exon interaction may play a role in holding the free 5' exon; however, it is unlikely that the interaction with U5 has a critical instructive function in determining the site of 5' splice site cleavage during the splicing of wild-type pre-mRNAs.

Intronic sequences in Group II introns just downstream of the 5' splice site are recognized by an internal loop in domain 1. This so-called ϵ - ϵ' interaction, which involves base-pairing of the third and fourth positions of the intron, is important for both steps of splicing (Jacquier and Michel, 1990). In the spliceosome, the conserved ACA sequence in U6 snRNA (in the ACAGAG hexanucleotide) has been proposed to interact with the intron positions 4-6 (in yeast) or (5-6) in mammals by base-pairing (Figure 5 shows the model proposed by Wassarman and Stetiz, 1992). This interaction can influence the site of 5' splice site cleavage in yeast (Kandels-Lewis and Seraphin, 1993; Lesser and Guthrie,

1
2
3
4
5
6
7
8
9
10
11
12
13
14
15
16
17
18
19
20
21
22
23
24
25
26
27
28
29
30
31
32
33
34
35
36
37
38
39
40
41
42
43
44
45
46
47
48
49
50
51
52
53
54
55
56
57
58
59
60
61
62
63
64
65
66
67
68
69
70
71
72
73
74
75
76
77
78
79
80
81
82
83
84
85
86
87
88
89
90
91
92
93
94
95
96
97
98
99
100

101
102
103
104
105
106
107
108
109
110
111
112
113
114
115
116
117
118
119
120
121
122
123
124
125
126
127
128
129
130
131
132
133
134
135
136
137
138
139
140
141
142
143
144
145
146
147
148
149
150
151
152
153
154
155
156
157
158
159
160
161
162
163
164
165
166
167
168
169
170
171
172
173
174
175
176
177
178
179
180
181
182
183
184
185
186
187
188
189
190
191
192
193
194
195
196
197
198
199
200

1993). Whether or not it also plays a role in the second step of splicing has not been determined. Unlike the case of the ϵ - ϵ' pairing, the ACA sequence of U6 is not part of an internal loop, but instead lies in a single-stranded region upstream of U2-U6 helix I region of U6.

The interaction between the guanosines at the 5' and 3' end of the intron required for the second step of nuclear pre-mRNA splicing (Parker and Siliciano, 1993) motivated Chanfreau and Jacquier (1993) to look for a similar interaction in a Group II intron. However, instead of finding a strictly analogous interaction, data from genetic suppression experiments support an interaction between the guanosine at the 5' end of the intron and the penultimate residue at the 3' end of the intron, a conserved adenosine (Chanfreau and Jacquier, 1993). Thus while splicing in both systems involves interactions between the ends of the intron, the details appear to be different in the two cases.

These similarities between the spliceosome and Group II introns raise two important questions. First, do they reflect (at one extreme) a profound conservation of three-dimensional architecture and catalytic mechanism or are they only coincidental (at the other extreme)? A high resolution picture of active site structures in both systems will be required to answer this question definitively. Nonetheless, the numerous and striking similarities seem very unlikely to be due purely to chance. A second question relates to the origins of these resemblances. While it was originally proposed that the spliceosome and Group II introns might have a common ancestor (Cech, 1986), this view has been recently challenged based on the limited primary sequence conservation between the two systems (Weiner, 1993). The alternative suggestion is that relationships between the two systems convergent evolution, in which similar solutions to the same chemical problems arose independently (Weiner, 1993). Obviously, answers to both of these questions would have significant implications for the origins of introns and the spliceosome.

Concluding Remarks

Recent progress in RNA splicing has led to the view that a network of RNA interactions may form the structural foundation of the spliceosome. Solutions (or at least strong hints) to many of the central puzzles of pre-mRNA are coming into focus. RNA-RNA interactions underlie many of the known aspects of substrate recognition, reaction partner juxtaposition, and in all likelihood, catalysis. With the outlines of a model for the active site of the spliceosome, we can now begin to consider in detail how its structure might lead to the chemical events of the splicing reaction. The elucidation of additional interactions (especially tertiary contacts) will be needed to develop a robust three-dimensional structural model. Moreover, the current data hint that the ATP-dependent steps of splicing may reflect the work of helicase-like proteins in mediating RNA conformational isomerizations. Understanding the dialogue between these factors, other proteins, snRNAs and the pre-mRNA remains an important objective.

The dynamic nature of many of the RNA-RNA interactions can explain several of the conserved aspects of the spliceosome assembly pathway. The early, transient role of U1 in 5' splice site binding is rationalized by its displacement by U6. We suggest that U1 may function in concert with other commitment factors as an intron recognition particle to recognize the substrate before transferring it to the catalytic components of the spliceosome. Such a division of labor might reflect a fundamental evolutionary dichotomy since organisms that exclusively perform trans-splicing, such as trypanosomes, appear to lack U1 snRNA and instead rely on a spliced-leader snRNP to deliver the 5' exon to the catalytic machinery (such organisms contain a conserved set of U2, U4 and U6 snRNAs). Finally, the occurrences of U2-U6 helix I and the intramolecular U6 structure support the model that the release of U4 from U6 prior to the first nucleolytic event reflects the catalytic activation of the spliceosome. These and other RNA rearrangements give weight to a new and general principle for spliceosome assembly in which dynamic isomerizations of structure serve to build active sites for the two chemical steps. Such mechanisms offer

Figure 1

U1 and U2 snRNAs Interact with the Pre-mRNA via Watson-Crick Base-Pairing

Genetically proven base-pairing interactions between U1 and the 5' splice site, between U1 and the 3' splice site, and between U2 and the branchpoint region are depicted.

SnRNA and intron sequences from *Saccharomyces cerevisiae* are shown.

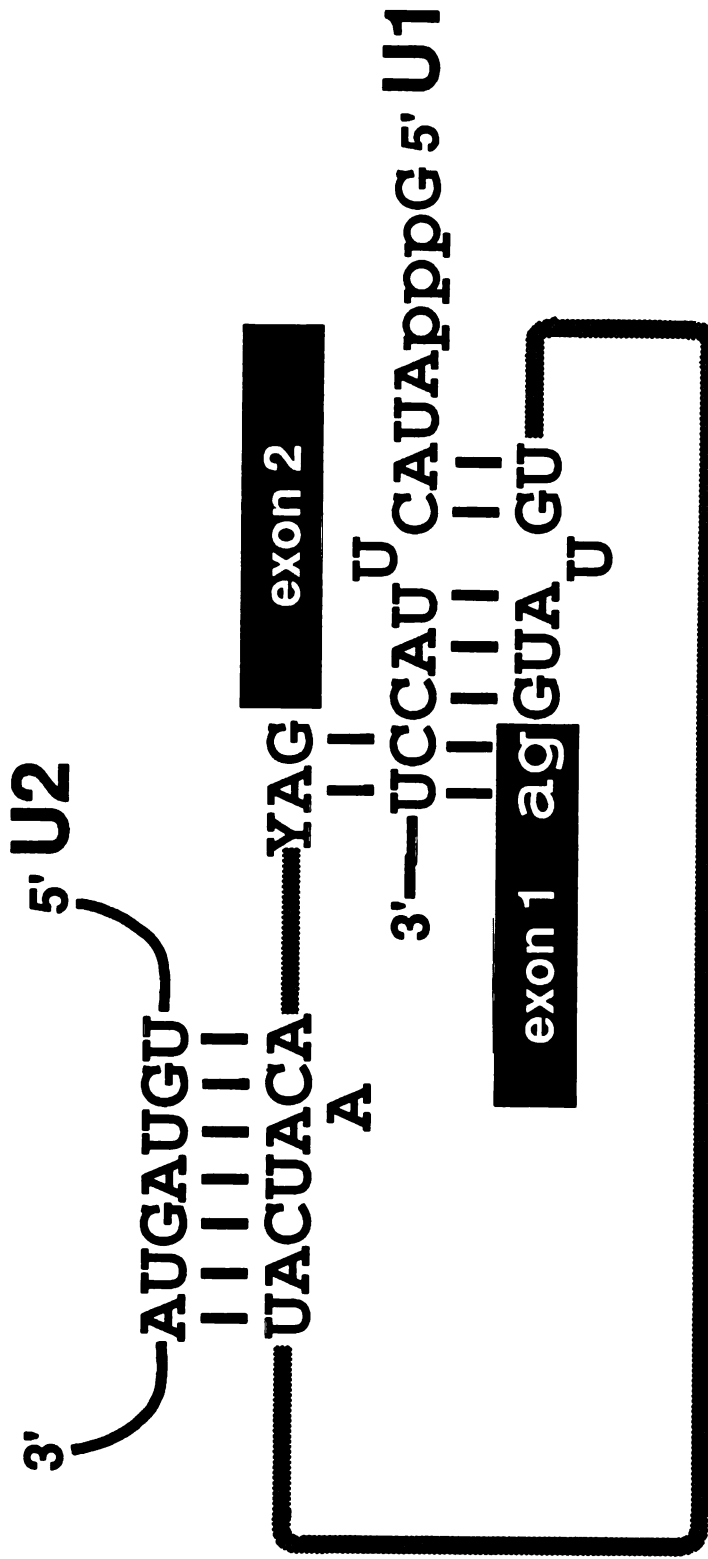


Figure 2.

U4 and U6 snRNAs Base-Pair with Each Other.

Phylogenetically invariant residues are shown in uppercase and bold (based on alignments of Guthrie and Patterson, 1988; and C.G., S. Mian, and H. Roiha, unpublished).

Asterisks mark residues specifically required for the second step of splicing *in vitro* (Fabrizio and Abelson, 1990). Arrows mark the locations of mRNA-type introns in the U6 genes of *S. pombe* (Tani and Ohshima, 1989) and *R. dactyoidum* (Tani and Ohshima, 1991). The essential ACAGAG and AGC sequences mentioned in the text span positions 47-52 and 59-61, respectively.

1. The first part of the document is a list of names and addresses of the members of the committee. The names are listed in alphabetical order, and the addresses are given in full, including the street name, city, and state.

2. The second part of the document is a list of the names and addresses of the members of the committee who have been elected to the office of chairman. The names are listed in alphabetical order, and the addresses are given in full, including the street name, city, and state.

1. The first part of the document is a list of names and addresses of the members of the committee. The names are listed in alphabetical order, and the addresses are given in full. The list includes the names of the members of the committee, the names of the members of the sub-committee, and the names of the members of the advisory committee. The addresses are given in full, including the street name, the city, the state, and the zip code.

2. The second part of the document is a list of the names and addresses of the members of the committee. The names are listed in alphabetical order, and the addresses are given in full. The list includes the names of the members of the committee, the names of the members of the sub-committee, and the names of the members of the advisory committee. The addresses are given in full, including the street name, the city, the state, and the zip code.

3. The third part of the document is a list of the names and addresses of the members of the committee. The names are listed in alphabetical order, and the addresses are given in full. The list includes the names of the members of the committee, the names of the members of the sub-committee, and the names of the members of the advisory committee. The addresses are given in full, including the street name, the city, the state, and the zip code.

Figure 3.

U2-U6 Helix I.

Shown is the Watson-Crick interaction between nts 54-61 of yeast U6 snRNA and nts 21-30 of yeast U2 snRNA. Also depicted is the base-pairing interaction between nts 33-39 of yeast U2 and the branchpoint region. Intron sequences conform to the consensus of *Saccharomyces cerevisiae*.

1
2
3
4
5
6
7
8
9
10
11
12
13
14
15
16
17
18
19
20
21
22
23
24
25
26
27
28
29
30
31
32
33
34
35
36
37
38
39
40
41
42
43
44
45
46
47
48
49
50
51
52
53
54
55
56
57
58
59
60
61
62
63
64
65
66
67
68
69
70
71
72
73
74
75
76
77
78
79
80
81
82
83
84
85
86
87
88
89
90
91
92
93
94
95
96
97
98
99
100

101
102
103
104
105
106
107
108
109
110
111
112
113
114
115
116
117
118
119
120
121
122
123
124
125
126
127
128
129
130
131
132
133
134
135
136
137
138
139
140
141
142
143
144
145
146
147
148
149
150
151
152
153
154
155
156
157
158
159
160
161
162
163
164
165
166
167
168
169
170
171
172
173
174
175
176
177
178
179
180
181
182
183
184
185
186
187
188
189
190
191
192
193
194
195
196
197
198
199
200

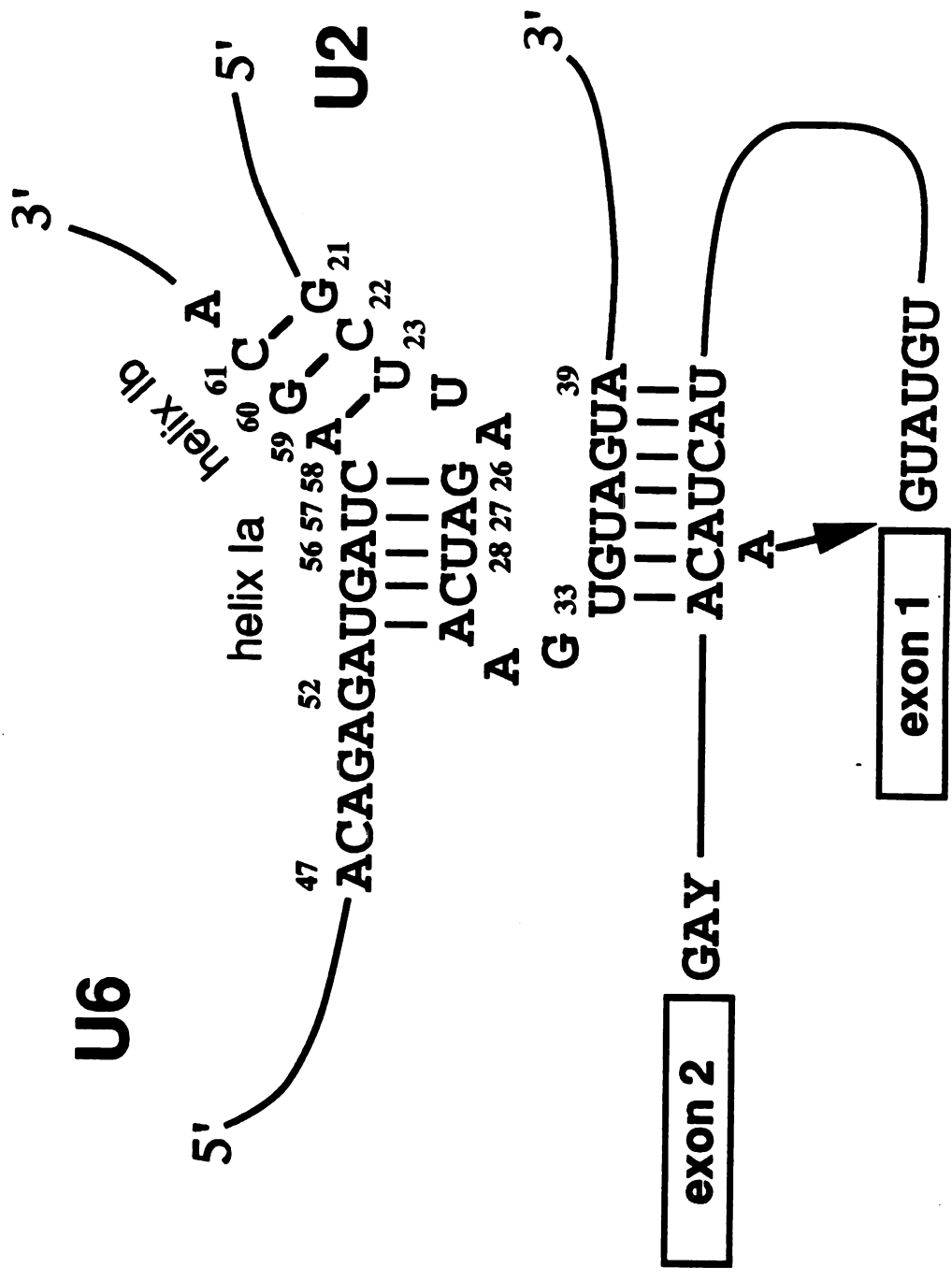


Figure 4.

Conformational Isomers and Phylogenetic Conservation of U2, U4 and U6 snRNAs. Base-pairing interactions between U4 and U6, U2 and U6 as well as intramolecular structures are shown. Uppercase bold nucleotides represent those which are phylogenetically invariant (Guthrie and Patterson, 1988; C.G., S. Mian, and H. Roiha, unpublished). Nucleotides in the U4-U6 structure and in the U2 intramolecular structure that engage in base-pairing in the U2-U6 structure are shaded accordingly. Structural domains of the molecules discussed in the text are indicated.

1
2
3
4
5
6
7
8
9
10
11
12
13
14
15
16
17
18
19
20
21
22
23
24
25
26
27
28
29
30
31
32
33
34
35
36
37
38
39
40
41
42
43
44
45
46
47
48
49
50
51
52
53
54
55
56
57
58
59
60
61
62
63
64
65
66
67
68
69
70
71
72
73
74
75
76
77
78
79
80
81
82
83
84
85
86
87
88
89
90
91
92
93
94
95
96
97
98
99
100

1. The first part of the document
 2. The second part of the document
 3. The third part of the document
 4. The fourth part of the document
 5. The fifth part of the document

6. The sixth part of the document
 7. The seventh part of the document
 8. The eighth part of the document
 9. The ninth part of the document
 10. The tenth part of the document

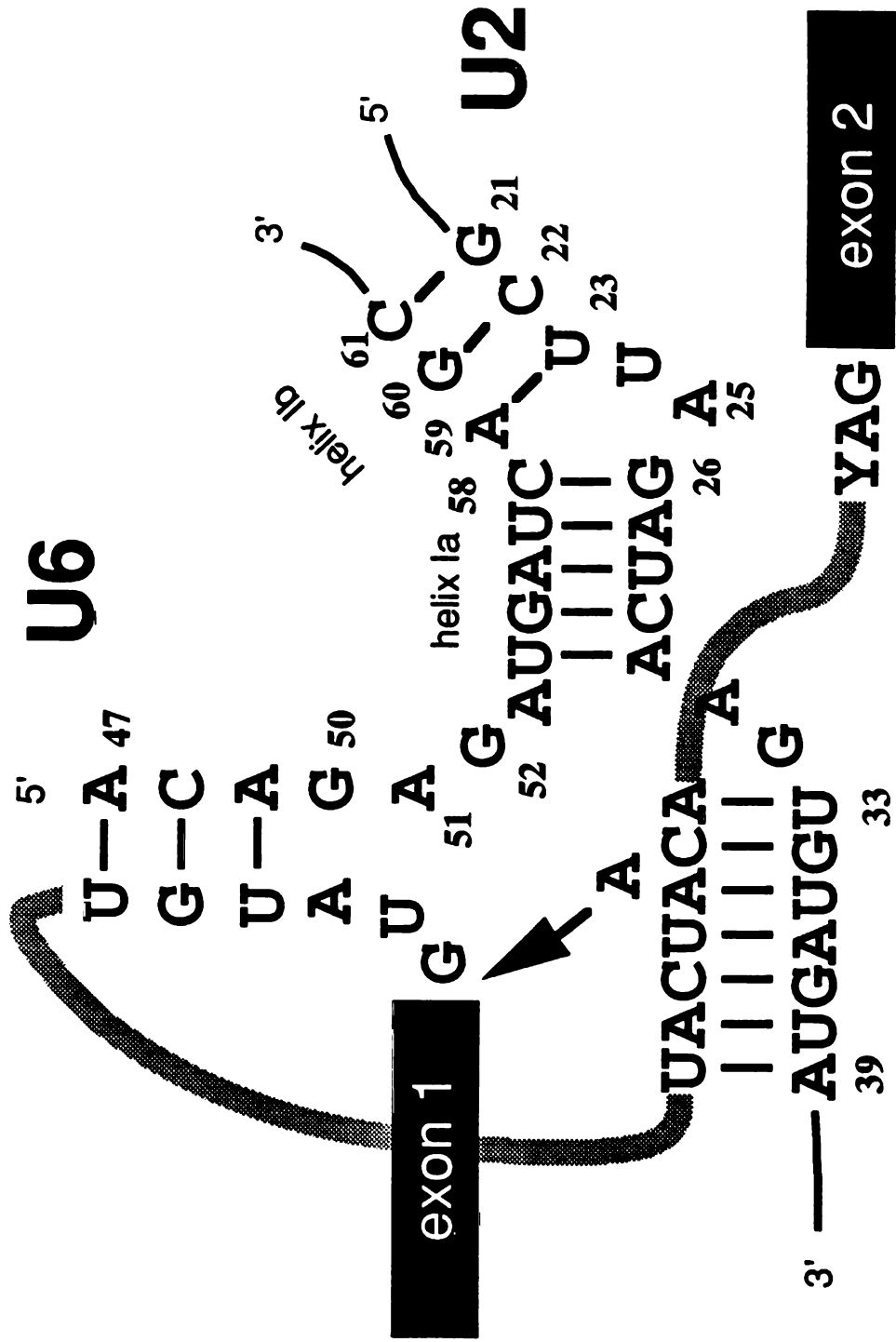
Figure 5.

U6-5' Splice Site Interaction.

Shown is Watson-Crick complementarity between U6 nts. 47-49 and the intron positions 3-6. Other interactions are as shown in Figure 5.

1
2
3
4
5
6
7
8
9
10
11
12
13
14
15
16
17
18
19
20
21
22
23
24
25
26
27
28
29
30
31
32
33
34
35
36
37
38
39
40
41
42
43
44
45
46
47
48
49
50
51
52
53
54
55
56
57
58
59
60
61
62
63
64
65
66
67
68
69
70
71
72
73
74
75
76
77
78
79
80
81
82
83
84
85
86
87
88
89
90
91
92
93
94
95
96
97
98
99
100

1
2
3
4
5
6
7
8
9
10
11
12
13
14
15
16
17
18
19
20
21
22
23
24
25
26
27
28
29
30
31
32
33
34
35
36
37
38
39
40
41
42
43
44
45
46
47
48
49
50
51
52
53
54
55
56
57
58
59
60
61
62
63
64
65
66
67
68
69
70
71
72
73
74
75
76
77
78
79
80
81
82
83
84
85
86
87
88
89
90
91
92
93
94
95
96
97
98
99
100





1
2
3
4
5
6
7
8
9
10
11
12
13
14
15
16
17
18
19
20
21
22
23
24
25
26
27
28
29
30
31
32
33
34
35
36
37
38
39
40
41
42
43
44
45
46
47
48
49
50
51
52
53
54
55
56
57
58
59
60
61
62
63
64
65
66
67
68
69
70
71
72
73
74
75
76
77
78
79
80
81
82
83
84
85
86
87
88
89
90
91
92
93
94
95
96
97
98
99
100



Figure 6.

U5-Exon Interactions

Shown is the highly conserved loop of U5 snRNA. The fourth and fifth positions of the loop are shown interacting with the last two residues of the 5' exon. The third and fourth positions of the loop are shown interacting with the first two residues of the 3' exon. Lines between the loop represent crosslinks or genetic suppression results.

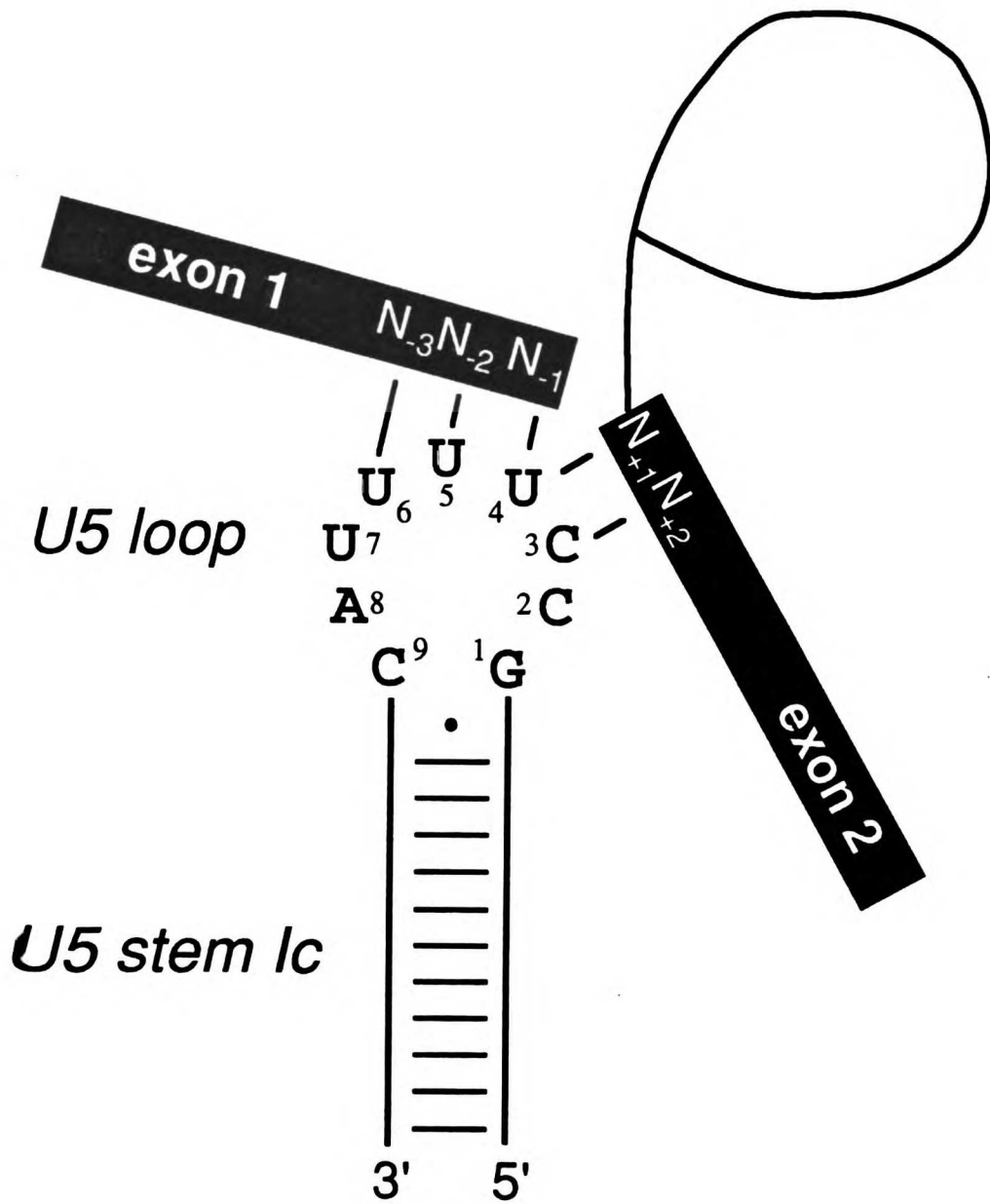
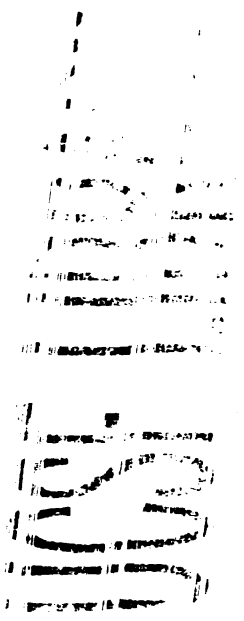


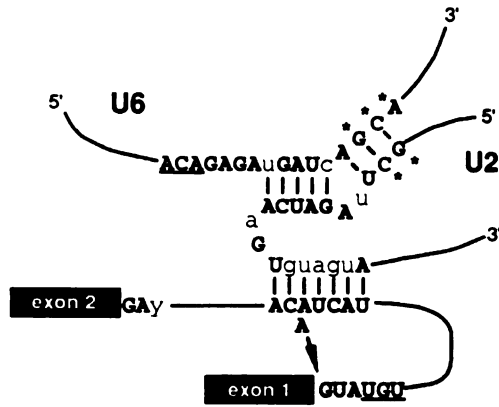
Figure 7.

Structural Similarities Between the Spliceosome and Group II Introns.

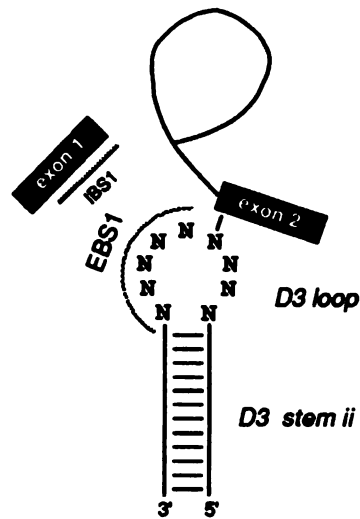
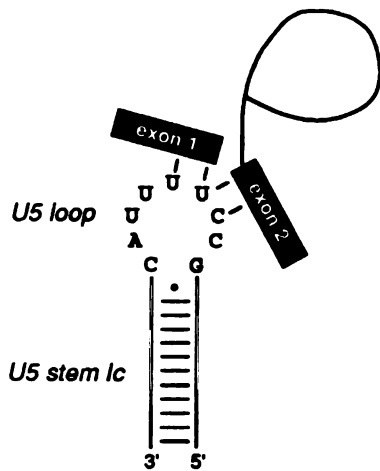
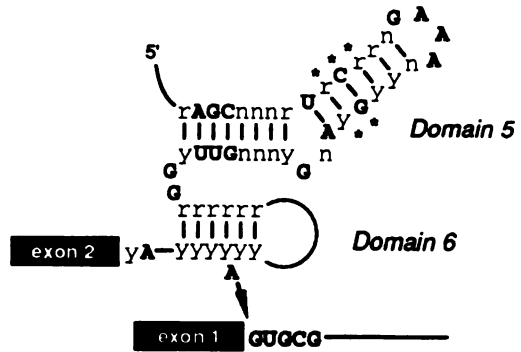
On upper the left, U2 and U6 snRNAs are shown together with a yeast consensus intron as in Figure 5 (phylogenetically invariant residues are indicated in uppercase bold). The consensus sequence for domains 5 and 6 of Group IIA introns is shown on the right (Michel et al., 1989). Highly conserved nucleotides in Group IIA introns are shown in uppercase bold; conserved purines and pyrimidines are denoted by 'r' and 'y', respectively; and variable sequences are denoted by 'n'. Asterisks next to nucleotides in both structures indicate a limited identity in primary sequence. Shown on the middle left are the U5-exon interactions as in Figure 7. Shown on the middle right are base-pairing interactions between the D3 loop in domain 1 of Group II introns and the 5' and 3' exons. EBS1 (exon binding sequence 1) and IBS1 (intron binding sequence 1) are specific designations for the interacting sequences in the D3 loop and 5' exon, respectively. The U6-5' splice site interaction is depicted on the lower left. Sequences that participate in this interaction are underlined in the diagram shown at the top left part of the figure. The ϵ - ϵ' interaction, which involves base-pairing between positions 3 and 4 of the 5' splice site and conserved sequences in an internal loop in domain C1 of Group II introns, is shown on the lower right.



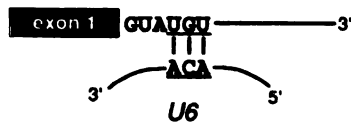
Spliceosomal



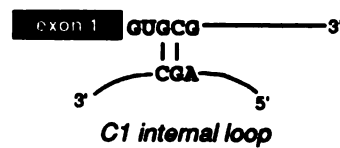
Group IIA



U6-5' splice site interaction



ϵ - ϵ'



APPENDIX 1

Randomization-Selection Analysis of Residues in the U2-U6 Helix I Region Required Prior to the First Chemical Step of Splicing

Summary

We analyzed residues in the U2-U6 helix I region required prior to the first chemical step of pre-mRNA splicing using the randomization-selection method described in Chapter 3. Characterization of the selected variants confirms previous data demonstrating the mutational sensitivity of the first four residues of the ACAGAG hexanucleotide and U6 residues in U2-U6 helix Ib. However, no covariations are apparent in the selected variants. Site-directed mutagenesis experiments performed under less stringent conditions, however, provide the first evidence for base-pairing between the terminal residues of helix Ib. The data also indicate that a mutually exclusive base-pairing interaction in U2 stem I is functionally important under some conditions, but not for cell growth in general.

Results and Discussion

In the U2-A and U6-A libraries, regions encompassing residues required at or before the first step of splicing were randomized (nts 47-50, 60-61 in U6 and nts 21-22 in U2). In addition, since several of the U2 residues randomized are thought to participate in an alternative intramolecular structure, U2 stem I, for which there is phylogenetic and functional evidence (Guthrie and Patterson, 1988; McPheeters and Abelson, 1992), their putative base-pairing partners were also randomized (U2 nts 13-14 in U2). We selected for functional cotransformants on 5-FOA using the same two conditions described in Chapter 3.

Variants obtained from these two conditions are shown in Figure 1A and 1B, respectively. The consensus sequences for these are shown in Figures 2A and 2B, respectively. In the ACAG sequence, the results are consistent with our previous mutational analysis which demonstrated that the majority of single nucleotide substitutions in this sequence are lethal (Madhani et al., 1990); indeed, in the non-ts variants, of the 4⁴ or 256 possible sequences, only the wild-type ACAG sequence was recovered (Figure 2A). A second region of interest randomized in the A libraries is in helix Ib (nts 60-61 in U6; nts 21-22 in U2). Consistent with previous mutational analyses, U6-G60 is conserved

among all of the variants, whereas, changes to U6-C61 are found in the ts variants (Figures 2A and 2B; Madhani et al., 1990). Unlike other positions in helix Ia and helix Ib, we were previously unable to demonstrate a role for base-pairing between U2 and U6 at these two phylogenetically invariant positions (Madhani and Guthrie, 1992). We had hoped to identify Watson-Crick covariations in these residues of helix Ib in the selected variants. However, although several different substitutions are seen at U6 nt 61 in the ts variants, no requirement for base-pairing with U2 nt 21 is apparent (Figure 1B).

Because of our interest in this region, we pursued the possibility that base-pairing might be evident under conditions different from those used in the selection experiments described above (30 °C). Using alleles created by site-directed mutagenesis, we found that the ts mutant U6-C61G can be suppressed by the compensatory mutant U2-G21C, when the latter contains an additional change, U2-C14G, that maintains the U2 stem I structure (Figure 1B; Table 1). Interestingly, U2-C14G also suppresses the cold-sensitive defect of the U2-G21C allele (Table 1). A different U2 allele at nts 14/21, U2-C14A, G21U, does not suppress U6-C61G, consistent with a requirement for a Watson-Crick interaction between U6 nt 61 and U2 nt 21 (Table 1). Suppression is much weaker at 30 °C (Table 1), the temperature used in our selection experiments, accounting for the inability to demonstrate a role for base-pairing in those experiments. Finally, despite the fact that base-pairing of in the upper part U2 stem I is necessary for suppression of U6-C61G by U2-G21C, neither the U2-G13/C22 nor the C14/G21 base-pair is essential for growth (Figure 1B; Table 2), indicating a flexible requirement for base-pairing.

Experimental Procedures

All procedures have been described in Chapter 3.

Figure 1:

Sequences of Selected Variants.

A. Non-ts variants selected after 2 days on 5-FOA at 30 °C. B. ts variants selected after 4 days on 5-FOA at 30 °C. Bold indicates changes from wild-type. Prime (') entries are ts variants initially selected after 2 days on 5-FOA at 30 °C.

A.**U6**

	47	50	60	61	13	14	21	22
	****		**	**	**	**	**	**
WT	ACAGAGAUGAUCAGCA				GCCUUUUGGC			
001	ACAGAGAUGAUCAGCA				CACUUUUGAC			
003	ACAGAGAUGAUCAGCA				GCCUUUUGGC			
004	ACAGAGAUGAUCAGCA				GACUUUUGCC			
006	ACAGAGAUGAUCAGCA				CCUUUUGAG			
008	ACAGAGAUGAUCAGCA				AGCUUUUGAA			
011	ACAGAGAUGAUCAGCA				UACUUUUGGU			
012	ACAGAGAUGAUCAGCA				CACUUUUGGA			
013	ACAGAGAUGAUCAGCA				AACUUUUGAC			
091	ACAGAGAUGAUCAGCA				GACUUUUGCC			
092	ACAGAGAUGAUCAGCA				CACUUUUGGC			
093	ACAGAGAUGAUCAGCA				CACUUUUGGU			
094	ACAGAGAUGAUCAGCA				UUCUUUUGGU			
095	ACAGAGAUGAUCAGCA				UCCUUUUGAG			
097	ACAGAGAUGAUCAGCA				UUCUUUUGAC			
102	ACAGAGAUGAUCAGCA				CCUUUUGAA			
103	ACAGAGAUGAUCAGCA				ACCUUUUGGU			
105	ACAGAGAUGAUCAGCA				CCUUUUGAG			
107	ACAGAGAUGAUCAGCA				CACUUUUGCC			
108	ACAGAGAUGAUCAGCA				UCCUUUUGGA			
109	ACAGAGAUGAUCAGCA				GUCUUUUGAA			
110	ACAGAGAUGAUCAGCA				GUCUUUUGAC			
111	ACAGAGAUGAUCAGCA				AGCUUUUGAA			
113	ACAGAGAUGAUCAGCA				AACUUUUGAG			
invr.	ACAG							GC

B.**U6****U2**

	47	50	60	61	13	14	21	22
	****		**	**	**	**	**	**
WT	ACAGAGAUGAUCAGCA				ACACAGAUGAUCAGCA			
TS001	ACACAGAUGAUCAGCA				ACACAGAUGAUCAGCA			
TS002	ACACAGAUGAUCAGCA				ACACAGAUGAUCAGCA			
TS003	ACACAGAUGAUCAGCA				ACACAGAUGAUCAGCA			
TS004	ACACAGAUGAUCAGCA				ACACAGAUGAUCAGCA			
TS005	ACACAGAUGAUCAGCA				ACACAGAUGAUCAGCA			
TS006	ACACAGAUGAUCAGCA				ACACAGAUGAUCAGCA			
TS007	ACACAGAUGAUCAGCA				ACACAGAUGAUCAGCA			
TS008	ACACAGAUGAUCAGCA				ACACAGAUGAUCAGCA			
TS009	ACACAGAUGAUCAGCA				ACACAGAUGAUCAGCA			
TS010	ACACAGAUGAUCAGCA				ACACAGAUGAUCAGCA			
TS011	ACACAGAUGAUCAGCA				ACACAGAUGAUCAGCA			
TS012	ACACAGAUGAUCAGCA				ACACAGAUGAUCAGCA			
TS013	ACACAGAUGAUCAGCA				ACACAGAUGAUCAGCA			
TS014	ACACAGAUGAUCAGCA				ACACAGAUGAUCAGCA			
TS015	ACACAGAUGAUCAGCA				ACACAGAUGAUCAGCA			
TS016	ACACAGAUGAUCAGCA				ACACAGAUGAUCAGCA			
TS017	ACACAGAUGAUCAGCA				ACACAGAUGAUCAGCA			
TS018	ACACAGAUGAUCAGCA				ACACAGAUGAUCAGCA			
TS019	ACACAGAUGAUCAGCA				ACACAGAUGAUCAGCA			
TS020	ACACAGAUGAUCAGCA				ACACAGAUGAUCAGCA			
TS021	ACACAGAUGAUCAGCA				ACACAGAUGAUCAGCA			
TS022	ACACAGAUGAUCAGCA				ACACAGAUGAUCAGCA			
TS023	ACACAGAUGAUCAGCA				ACACAGAUGAUCAGCA			
TS024	ACACAGAUGAUCAGCA				ACACAGAUGAUCAGCA			
TS025	ACACAGAUGAUCAGCA				ACACAGAUGAUCAGCA			
TS026	ACACAGAUGAUCAGCA				ACACAGAUGAUCAGCA			
TS027	ACACAGAUGAUCAGCA				ACACAGAUGAUCAGCA			
TS005'	ACACAGAUGAUCAGCA				ACACAGAUGAUCAGCA			
TS007'	ACACAGAUGAUCAGCA				ACACAGAUGAUCAGCA			
TS100'	ACACAGAUGAUCAGCA				ACACAGAUGAUCAGCA			
TS101'	ACACAGAUGAUCAGCA				ACACAGAUGAUCAGCA			
invr.	CA							G

Figure 2

Consensus sequences for variants

A. Consensus of variants shown in Figure 1A. B. Consensus of variants shown in Figure 1B.

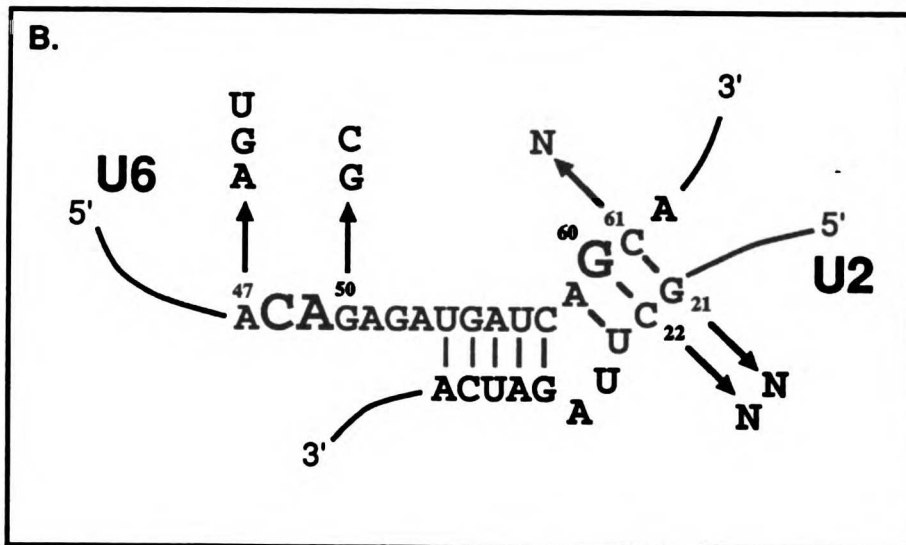
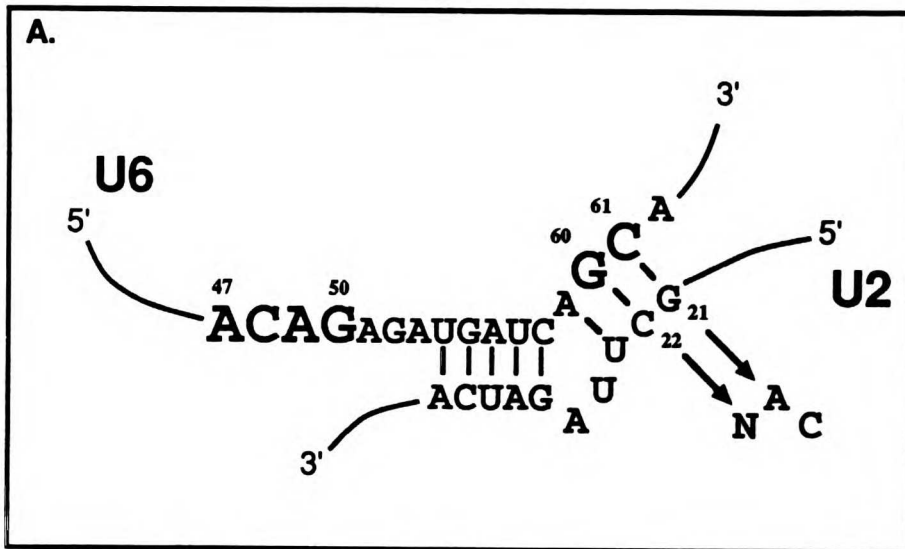


Table 1

		Growth		
U6 allele	U2 allele	25 °C	30 °C	37 °C
WT	WT	++++	++++	+++
C61G	WT	+	+/-	-
C61G	G21C	-	-	-
C61G	G21C, C14G	+++	+	-
C61G	G21U, C14A	+	+/-	-
WT	G21C	-	-	+++
WT	G21C, C14G	++++	++++	+++
WT	G21U, C14A	++++	++++	+++

11
12
13
14
15
16
17
18
19
20
21
22
23
24
25
26
27
28
29
30
31
32
33
34
35
36
37
38
39
40
41
42
43
44
45
46
47
48
49
50
51
52
53
54
55
56
57
58
59
60
61
62
63
64
65
66
67
68
69
70
71
72
73
74
75
76
77
78
79
80
81
82
83
84
85
86
87
88
89
90
91
92
93
94
95
96
97
98
99
100

101
102
103
104
105
106
107
108
109
110
111
112
113
114
115
116
117
118
119
120
121
122
123
124
125
126
127
128
129
130
131
132
133
134
135
136
137
138
139
140
141
142
143
144
145
146
147
148
149
150
151
152
153
154
155
156
157
158
159
160
161
162
163
164
165
166
167
168
169
170
171
172
173
174
175
176
177
178
179
180
181
182
183
184
185
186
187
188
189
190
191
192
193
194
195
196
197
198
199
200

Table 2

U2 Stem I Base-Pair	Watson-Crick	G-U/ U-G	Other
G13-C22	16	3	35
C14-G21	13	6	35

APPENDIX 2

Factors Required for the Synthesis and Function of U6 snRNA Identified Through a Genetic Screen for Synthetic Lethal Mutants

Summary

We employed a synthetic lethal screen for factors that interact functionally with the yeast U6 snRNA. Temperature-sensitive mutations in two genes, *SUD4* and *SUD5* were identified that produced an unconditional lethal phenotype when combined with a subset of temperature-sensitive alleles of U6 snRNA. These mutants also accumulate unspliced pre-mRNAs upon a shift to the nonpermissive temperature. Genomic clones that complement both the synthetic lethal and conditional defects of *sud4-1* and *sud5-1* were isolated. Genetic complementation and allelism tests demonstrate that *SUD4* is identical to *PRP6*, which encodes component of the U4-U6.U5 snRNP. DNA sequencing of the genomic clone that complements *sud5-1* revealed it to contain the previously characterized gene *BRF1*, which encodes an essential component of the general RNA polymerase III transcription factor TFIIIB. U6 is unique among the yeast spliceosomal snRNAs in that it is transcribed by RNA polymerase III instead of RNA polymerase II. Synthetic lethality with *sud5-1* is observed specifically in temperature-sensitive U6 mutants that exhibit defects in stable RNA accumulation. Thus, in this case, synthetic lethality is likely to be due to the combination of two biosynthetic, as opposed to functional, defects.

Results and Discussion

Mutant Isolation

To screen for synthetic lethal mutants, derivatives of the strain YHM1 (see Chapter 1) were constructed that contain a disruption of the chromosomal U6 allele, one of two temperature-sensitive U6 alleles (U6- Δ A47 or U6-C61G) on a *TRP1*, *CEN* plasmid and a wild-type U6 allele on a *URA3*, *CEN* plasmid. At permissive temperatures for the conditional U6 alleles, these strains can grow on 5-fluoroorotic acid (5-FOA) plates, which selects against the wild-type plasmid. These strains were heavily mutagenized with ultraviolet light (<1% survival) and plated on SD -TRP plates. Surviving colonies (30,000 for U6 Δ A47 and 40,000 for U6-C61G) were replica-plated to 5-FOA plates that were then incubated at room temperature (approximately 22 °C) for 4 days. Colonies that failed to

grow on 5-FOA were candidates for mutants that exhibit synthetic lethality with the U6 temperature-sensitive mutant. Of the 75 mutants 22 exhibited a conditional defect in the presence of wild-type U6 (temperature-sensitivity, cold-sensitivity or both). Because the conditional mutants are easier to analyze, these were chosen for further analysis. Backcrossing to the parental strain proved impractical because of very poor sporulation. This is not surprising in retrospect given the high level of mutagenesis used. After testing several strains, we were successful in backcrossing 14 of the mutants to the strain A364A twice, following only the conditional phenotype. These were then crossed to YHM1 or YHM2 to reintroduce the U6 gene disruption and transformed with the appropriate U6 mutant. Dependency on the wild-type plasmid at 22 °C was tested on 5-FOA. Of these, only two backcrossed mutants failed to grow on 5-FOA. These segregated as single gene defects and belonged to distinct complementation groups, *SUD4* and *SUD5* ("Six-U-Die"). Apparently, the other conditional mutants were not linked to the synthetic lethal defect (this was shown definitively to be the case for several of the complementation groups by isolating genomic clones that complemented the conditional defects but which failed to complement synthetic lethality). As with the sporulation problems, the high frequency of false positives may be related to the high amount of mutagenesis.

Mutant Characterization

In order to test whether *SUD4* and *SUD5* correspond to known genes involved in pre-mRNA splicing, complementation analysis was performed with the known temperature-sensitive splicing mutants (*prp2*, *prp3*, *prp4*, *prp5*, *prp6*, *prp8*, *prp9*, *prp11*, *prp16*, *prp17*, *prp18*, *prp19*, *prp21*, *prp22*, *prp24*, *prp26*, *prp27*). While *sud5-1* complemented all of these mutants at 37 °C (the nonpermissive temperature), *sud4-1* failed to complement the three different alleles of *PRP6* tested. Moreover, no recombinants were recovered after a cross between *sud4-1* and *prp6-6*, indicating genetic linkage (2 4-spore tetrads, 10 3-spore tetrads, and 8 2-spore tetrads were analyzed).

To analyze further the functional interaction between the Sud factors and U6, we examined the allele-specificity of synthetic lethality. *sud4-1* was initially isolated in combination with the U6-C61G temperature-sensitive alleles, whereas *sud5-1* was initially isolated in combination with U6-ΔA47. As shown in Table 1, *sud4-1* exhibits synthetic lethality with U6-C61G, but not with 4 other ts U6 alleles, including U6-ΔA47. In contrast, *sud5-1* exhibits synthetic lethality with U6-ΔA47 and U6-G50U, but not the other three U6 alleles, including U6-C61G.

To determine whether or not the *sud* mutants affected pre-mRNA splicing, we examined the effects of the *sud4-1* and *sud5-1* mutants on splicing in vivo. Cells were either grown at the permissive temperature (22 °C) or shifted to the nonpermissive temperature (37 °C) for 6 hours. RNA was harvested from these cells, and the splicing patterns of three endogenous transcripts (*SNR17A*, *SNR17B* and *MATa1*) were analyzed by a primer-extension method. *sud4-1* was found to exhibit a dramatic increase in levels of unspliced precursor for these three transcripts (data not shown). This was not surprising since it is an allele of the splicing gene *PRP6*. As shown in Figure 1, *sud5-1* also exhibits substantial accumulation of these pre-mRNAs as well. The splicing defect exhibited by *sud5-1*, together with the allele-specificity of synthetic lethality suggested strongly that *SUD5* participates in splicing through an interaction with U6 snRNA.

Genomic clones that complement the temperature sensitive phenotypes of *sud4-1* and *sud5-1* were isolated from a YCp50 (*URA3 CEN*) library (Rose et al., 1987). Two clones were isolated that complement *sud4-1* and a single clone was isolated that complements *sud5-1*. Complementing subclones were isolated and analyzed by partial DNA sequencing. As expected, both of the *SUD4* clones were found to contain the *PRP6* gene (LeGrain and Choulika, 1990). Similar analysis of a subclone that complements *sud5-1* revealed that this fragment had been sequenced previously and corresponds to the gene *BRF1*. This gene has been isolated by one group as a suppressor of a tRNA promoter mutation (Lopez-De-Leon et al., 1992) and by two others as a high copy

suppressor in the TATA-box Binding Protein, TBP (Colbert and Hahn, 1992; Buratowski and Zhou, 1992). All three groups demonstrated a role for Brf1 in transcription of tRNA and 5S RNA genes by RNA polymerase III. Subsequently, Brf1 has been shown to be a component of the general RNA polymerase III transcription factor TFIIB (Kassavetis et al., 1992). Brf1 is also required for the transcription of the U6 snRNA gene of *S. cerevisiae* by RNA Polymerase III in vitro (S. Hahn, personal communication).

Conclusions

Two genes *SUD4* and *SUD5* were identified in a genetic screen for factors that interact functionally with U6 snRNA. *SUD4* was shown to be identical to the pre-mRNA splicing gene *PRP6*. Little is known regarding the specific function of the Prp6 protein. Biochemical studies have demonstrated Prp6 to be a component of the U4-U6.U5 snRNP, but not of U4-U6 or free U6 snRNPs (Abovich et al., 1990; Gallison et al., 1993). The sequence of the *PRP6* gene predicts a large protein containing so-called TPR repeats which are thought to form amphipathic alpha helices and have been identified in a number of functionally diverse proteins, including the yeast transcriptional repression factor Ssn6 (Legrain and Choulika, 1990; reviewed in Goebel and Yanagida, 1991). The function of this motif is unknown. Future experiments should be directed at determining whether Prp6 interacts with U6 snRNA directly and at what point the protein functions in the spliceosome cycle. The availability of the cloned *PRP6* gene should aid such efforts.

The identity between *SUD5* and *BRF1* illustrates some of the pitfalls of genetic analysis. The *sud5-1* mutant exhibits many of the properties of a bona fide pre-mRNA splicing mutant, yet its effect is likely to be indirect. This conclusion is based on two pieces of evidence. First, Brf1 is required for the expression of all RNA polymerase III transcripts, including U6. Second, the U6 alleles that display synthetic lethality with *sud5-1* occur at positions 47 and 50 in the ACAGAG hexanucleotide. Of numerous deleterious mutants tested, mutants in the first four residues of this hexanucleotide exhibit the most dramatic defects in stable RNA accumulation (Madhani et al., 1990).

In hindsight, of course, one asks whether the isolation of a mutant that affects splicing indirectly could have been somehow avoided. In principle, *in vitro* heat-inactivation of splicing extracts prepared from the mutant can distinguish between direct and indirect effects (Lustig et al., 1986). In practice, however, this assay is not highly reproducible, and often requires complementation of the *in vitro* defect by the purified wild-type protein in order to be convincing. Another possibility in this case would have been to examine the levels of U6 snRNA in a *sud5-1* upon a shift to the nonpermissive temperature. However, this test is not as specific as it might first seem since mutants in several bona fide splicing factors, including the U6 snRNP protein Prp24, result in the destabilization of U6 at nonpermissive temperatures (Blanton et al., 1992). Consequently, given our current assays, it is difficult to see how the isolation of factors such as Brf1 can be avoided. Indeed, in independent experiments, Suzanne Noble in the laboratory has determined that the yeast gene *SLU1*, which was isolated in a screen for U5 synthetic lethal mutants (Frank et al., 1992), corresponds to a known sequence-specific DNA binding protein involved in the expression of many different genes in yeast (S. Noble, personal communication).

Experimental Procedures

All yeast genetic manipulations including media preparation, crosses, plasmid shuffle assays, complementation cloning, plasmid recovery and transformations were performed according to published methods (Guthrie and Fink, 1991).

Figure 1. *sud5-1* Exhibits the Accumulation of Unspliced Pre-mRNAs at the Nonpermissive Temperature.

Shown is a primer-extension analysis of the splicing patterns of the yeast U3A, U3B, and MATa1 genes. LI indicates lariat-intermediate. Analysis of RNA from cells grown under permissive conditions is shown in the lane indicated by U (unshifted). S, analysis of RNA from cells shifted to the nonpermissive temperature (37 °C) for 5 hours. M, molecular weight markers.

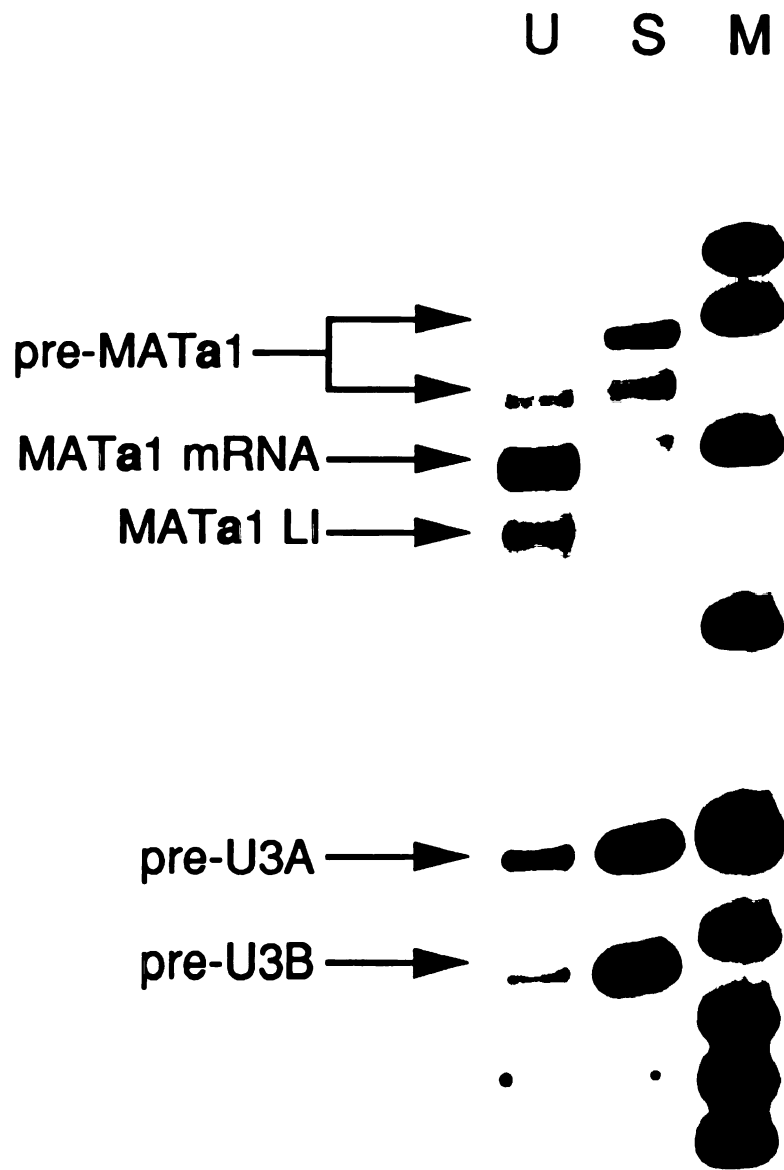


Table 1. Allele-Specificity of Synthetic Lethality.

Shown is the growth of *sud4-1* and *sud5-1* in combination with null or temperature-sensitive alleles of U6 snRNA.

Table 1

	U6 mutant						
<i>sud</i> mutant	null	WT	Δ A47	G50U	C58U	G59C	C61G
<i>sud4-1</i>	-	++	++	++	++	++	-
<i>sud5-1</i>	-	++	-	-	++	++	++

REFERENCES

Abovich, N., Legrain, P., and Rosbash, M. (1990). The yeast PRP6 gene encodes a U4/U6 small nuclear ribonucleoprotein particle (snRNP) protein, and the PRP9 gene encodes a protein required for U2 snRNP binding. *Mol Cell Biol* 10, 6417-25.

Aebi, M., Hornig, H., and Weissmann, C. (1987). 5' cleavage site in eukaryotic pre-mRNA splicing is determined by the overall 5' splice region, not by the conserved 5' GU. *Cell* 50, 237-46.

Agabian, N. (1990). Trans splicing of nuclear pre-mRNAs. *Cell* 61, 1157-60.

Arenas, J. E., and Abelson, J. N. (1993). The *Saccharomyces cerevisiae* PRP21 gene product is an integral component of the prespliceosome. *Proc Natl Acad Sci U S A* 90, 6771-5.

Ares, M. J. (1986). U2 RNA from yeast is unexpectedly large and contains homology to vertebrate U4, U5, and U6 small nuclear RNAs. *Cell* 47, 49-59.

Ares, M. J., and Igel, A. H. (1990). Lethal and temperature-sensitive mutations and their suppressors identify an essential structural element in U2 small nuclear RNA. *Genes Dev* 4, 2132-45.

Bartel, D. P., Zapp, M. L., Green, M. R., and Szostak, J. W. (1991). HIV-1 Rev regulation involves recognition of non-Watson-Crick base pairs in viral RNA. *Cell* 67, 529-36.

Bartel, D. P., and Szostak, J. W. (1993). Isolation of new ribozymes from a large pool of random sequences. *Science* 261, 1411-8.

Bindereif, A., and Green, M. R. (1987). An ordered pathway of snRNP binding during mammalian pre-mRNA splicing complex assembly. *EMBO J.* 6, 2415-2424.

Bindereif, A., Wolff, T., and Green, M. R. (1990). Discrete domains of human U6 snRNA required for the assembly of U4/U6 snRNP and splicing complexes. *EMBO J.* 6, 2415-2424.

Black, D. L., Chabot, B., and Steitz, J. A. (1985). U2 as well as U1 small nuclear ribonucleoproteins are involved in premessenger RNA splicing. *Cell* 42, 737-750.

Blanton, S., Srinivasan, A., and Rymond, B. C. (1992). PRP38 encodes a yeast protein required for pre-mRNA splicing and maintenance of stable U6 small nuclear RNA levels. *Mol Cell Biol* 12, 3939-47.

Blencowe, B. J., Sproat, B. S., Ryder, U., Barabino, S., and Lamond, A. I. (1989). Antisense probing of the human U4/U6 snRNP with biotinylated 2'-OMe RNA oligonucleotides. *Cell* 59, 531-539.

Boeke, J. D., Trueheart, J., Natsoulis, G., and Fink, G. R. (1987). 5-Fluoroorotic acid as a selective agent in yeast molecular genetics. *Methods Enzymol* 154, 164-75.

Bordonné, R., and Guthrie, C. (1992). Human and human-yeast chimeric U6 snRNA genes identify structural elements required for expression in yeast. *Nuc. Acids Res.* 20, 479-485.

Bordonné, R., Banroques, J., Abelson, J., and Guthrie, C. (1990). Domains of yeast U4 spliceosomal RNA required for PRP4 protein binding, snRNP-snRNP interactions, and pre-mRNA splicing in vivo. *Genes & Dev.* 4, 1185-1196.

Bringmann, P., Appel, B., Rinke, J., Reuter, R., Theissen, H., and Lührmann, R. (1984). Evidence for the existence of snRNAs U4 and U6 in a single ribonucleoprotein complex and for their association by intermolecular base pairing. *EMBO J* 3, 1357-63.

Brosi, R., Gröning, K., Behrens, S.-E., Lührmann, R., and Krämer, A. (1993). Interaction of Mammalian Splicing Factor SF3a with U2 snRNP and Relation of Its 60-kD Subunit to Yeast PRP9. *Science* 262, 102-105.

Brow, D. A., and Guthrie, C. (1988). Spliceosomal RNA U6 is remarkably conserved from yeast to mammals. *Nature* 334, 213-8.

Brow, D. A., and Guthrie, C. (1989). Splicing a spliceosomal RNA. *Nature* 337, 14-5.

Brow, D. A., and Guthrie, C. (1990). Transcription of a yeast U6 snRNA gene requires a polymerase III promoter element in a novel position. *Genes Dev* 4, 1345-56.

Buratowski, S., and Zhou, H. (1992). A suppressor of TBP mutations encodes an RNA polymerase III transcription factor with homology to TFIIB. *Cell* 71, 221-30.

Burgess, S., Couto, J. R., and Guthrie, C. (1990). A putative ATP binding protein influences the fidelity of branchpoint recognition in yeast splicing. *Cell* 60, 705-17.

Burgess, S. M., and Guthrie, C. (1993). A mechanism to enhance mRNA splicing fidelity: the RNA-dependent ATPase Prp16 governs usage of a discard pathway for aberrant lariat intermediates. *Cell* 73, 1377-91.

Burgess, S. M. (1993). Control of mRNA Splicing Fidelity by the RNA-dependent ATPase Prp16. Ph.D. Thesis, University of California, San Francisco.

Cech, T. R. (1986). The generality of self-splicing RNA: relationship to nuclear mRNA splicing. *Cell* 44, 207-10.

Chanfreau, G., and Jacquier, A. (1993). Interaction of intronic boundaries is required for the second step splicing efficiency of a group II intron. *EMBO J.*, in press.

Cheng, S.-C., and Abelson, J. (1986). Fractionation and characterization of a yeast mRNA splicing extract. *Proc. Natl. Acad. Sci.* 83, 2387-2391.

Cheng, S. C., and Abelson, J. (1987). Spliceosome assembly in yeast. *Genes Dev* 1, 1014-27.

Colbert, T., and Hahn, S. (1992). A yeast TFIIB-related factor involved in RNA polymerase III transcription. *Genes Dev* 6, 1940-9.

Cortes, J. J., Sontheimer, E. J., Seiwer, S. D., and Steitz, J. A. (1993). Mutations in the conserved loop of human U5 snRNA generate the use of novel cryptic 5' splice sites in vivo. *EMBO J.* submitted, .

Couto, J. R., Tamm, J., Parker, R., and Guthrie, C. (1987). A trans-acting suppressor restores splicing of a yeast intron with a branch point mutation. *Genes Dev* 1, 445-55.

Datta, B., and Weiner, A. M. (1991). Genetic evidence for base pairing between U2 and U6 snRNA in mammalian mRNA splicing. *Nature* 352, 821-4.

Dib-Hajj, S., Boulanger, S. C., Hebbar, S. K., Peebles, C. L., Franzen, J. S., and Perlman, P. S. (1993). Domain 5 interacts with domain 6 and influences the second transesterification reaction of group II intron self-splicing. *Nucleic Acids Res* 21, 1797-804.

Dower, W. J., Miller, J. F., and Ragsdale, C. W. (1988). High efficiency transformation of *E. coli* by high voltage electroporation. *Nucleic Acids Res* 16, 6127-45.

Elledge, S. J., and Davis, R. W. (1988). A family of versatile centromeric vectors for use in the sectoring-shuffle mutagenesis assay in *Saccharomyces cerevisiae*. *Gene* 70, 303-312.

Fabrizio, P., McPheeters, D. S., and Abelson, J. (1989). In vitro assembly of yeast U6 snRNP: a functional assay. *Genes Dev* 3, 2137-50.

Fabrizio, P., and Abelson, J. (1990). Two domains of yeast U6 small nuclear RNA required for both steps of nuclear precursor messenger RNA splicing. *Science* 250, 404-9.

Fortner, D., Troy, R., and Brow, D. (1993). A stem-loop in U6 snRNA defines a conformational switch required for pre-mRNA splicing. *Genes Dev.* in press .

Fouser, L., and Friesen, J. D. (1987). Effects on mRNA splicing of mutations in the 3' region of the *Saccharomyces cerevisiae* actin intron. *Mol. Cell. Biol.* 7, 225-230.

Frank, D., and Guthrie, C. (1992). An essential splicing factor, SLU7, mediates 3' splice site choice in yeast. *Genes Dev* 6, 2112-24.

Frank, D., Patterson, B., and Guthrie, C. (1992). Synthetic lethal mutations suggest interactions between U5 small nuclear RNA and four proteins required for the second step of splicing. *Mol Cell Biol* 12, 5197-205.

Galisson, F., and Legrain, P. (1993). The biochemical defects of *prp4-1* and *prp6-1* yeast splicing mutants reveal that the PRP6 protein is required for the accumulation of the [U4/U6.U5] tri-snRNP. *Nucleic Acids Res* 21, 1555-62.

Goebel, M., and Yanagida, M. (1991). The TPR snap helix: a novel protein repeat motif from mitosis to transcription. *Trends Biochem Sci* 16, 173-7.

Goguel, V., Liao, X. L., Rymond, B. C., and Rosbash, M. (1991). U1 snRNP can influence 3'-splice site selection as well as 5'-splice site selection. *Genes Dev* 5, 1430-8.

Gold, L., Tuerk, C., Allen, P., Binkley, J., Brown, D., Green, L., MacDougal, S., Schneider, D., Tasset, D., and Eddy, S. R. (1993). RNA: The Shape of Things to Come. In G. R. F. & A. J.F. (Eds.), *The RNA World* (pp. 497-510). Plainview, New York: Cold Spring Harbor Laboratory Press.

Gorbalenya, A. E., Koonin, E. V., Donchenko, A. P., and Blinov, V. M. (1988). A novel superfamily of nucleoside triphosphate-binding motif containing proteins which are

probably involved in duplex unwinding in DNA and RNA replication and recombination. FEBS Letters 235, 16-24.

Green, M. R. (1991). Biochemical mechanisms of constitutive and regulated pre-mRNA splicing. *Annu Rev Cell Biol* 7, 559-99.

Green, R., and Szostak, J. W. (1992). Selection of a ribozyme that functions as a superior template in a self-copying reaction. *Science* 258, 1910-5.

Green, R., and Szostak, J. W. (1993). In vitro genetic analysis of the hinge region between helical elements P5-P4-P6 and P7-P3-P8 in the sunY group I self-splicing intron. *J. Mol. Biol.* in press .

Gutell, R. R., Power, A., Hertz, G. Z., Putz, E. J., and Stormo, G. D. (1992). Identifying constraints on the higher-order structure of RNA: continued development and application of comparative sequence analysis methods. *Nucleic Acids Res* 20, 5785-95.

Gutell, R. (1993). Comparative studies of RNA: inferring higher-order structure from patterns of sequence variation. *Current Opinions in Structural Biology* 3, 313-322.

Guthrie, C., and Patterson, B. (1988). Spliceosomal snRNAs. *Annu Rev Genet* 22, 387-419.

Guthrie, C. (1991). Messenger RNA splicing in yeast: clues to why the spliceosome is a ribonucleoprotein. *Science* 253, 157-63.

Guthrie, C., and Fink, G. R. (1991). *Guide to yeast genetics and molecular biology*. San Diego: Academic Press.

Hamm, J., and Mattaj, I. W. (1989). An abundant U6 snRNP found in germ cells and embryos of *Xenopus laevis*. *EMBO J.* 8, 4179-4187.

Hanahan, D. (1983). Studies on transformation of *Escherichia coli* with plasmids. *J Mol Biol* 166, 557-80.

Hashimoto, C., and Steitz, J. A. (1984). U4 and U6 RNAs coexist in a single small nuclear ribonucleoprotein particle. *Nucleic Acids Res* 12, 3283-93.

Hausner, T. P., Giglio, L. M., and Weiner, A. M. (1990). Evidence for base-pairing between mammalian U2 and U6 small nuclear ribonucleoprotein particles. *Genes Dev* 4, 2146-56.

Hoffman, C. S., and Winston, F. (1987). A ten-minute DNA preparation from yeast efficiently releases autonomous plasmids for transformation of *Escherichia coli*. *Gene* 57, 267-272.

Hou, Y. M., Westhof, E., and Giege, R. (1993). An unusual RNA tertiary interaction has a role for the specific aminoacylation of a transfer RNA. *Proc Natl Acad Sci U S A* 90, 6776-80.

Ito, H., Fukuda, Y., Murata, K., and Kimura, A. (1983). Transformation of intact yeast cells treated with alkali cations. *J. Bacteriol.* 153, 163-168.

Jackson, I. J. (1991). A reappraisal of non-consensus mRNA splice site. *Nucleic Acids Research* 19, 3795-3798.

Jacquier, A., Rodriguez, J. R., and Rosbash, M. (1985). A quantitative analysis of the effects of 5' junction and TACTAAC box mutants and mutant combinations on yeast mRNA splicing. *Cell* 43, 423-30.

Jacquier, A., and Rosbash, M. (1986). Efficient trans-splicing of a yeast mitochondrial RNA group II intron implicates a strong 5' exon-intron interaction. *Science* 234, 1099-104.

Jacquier, A., and Michel, F. (1987). Multiple exon-binding sites in class II self-splicing introns. *Cell* 50, 17-29.

Jacquier, A., and Michel, F. (1990). Base-pairing interactions involving the 5' and 3'-terminal nucleotides of group II self-splicing introns. *J Mol Biol* 213, 437-47.

Jacquier, A., and Jacquesson-Breuleux, N. (1991). Splice site selection and role of the lariat in a group II intron. *J Mol Biol* 219, 415-28.

Jarrell, K. A., Dietrich, R. C., and Perlman, P. S. (1988). Group II intron domain 5 facilitates a trans-splicing reaction. *Mol Cell Biol* 8, 2361-6.

Jones, M. H., and Guthrie, C. (1990). Unexpected flexibility in an evolutionarily conserved protein-RNA interaction: genetic analysis of the Sm binding site. *EMBO J* 9, 2555-61.

Kandels-Lewis, S., and Séraphin, B. (1993). U6 snRNA is involved in 5' splice site selection. *Science* in press .

Kassavetis, G. A., Joazeiro, C. A., Pisano, M., Geiduschek, E. P., Colbert, T., Hahn, S., and Blanco, J. A. (1992). The role of the TATA-binding protein in the assembly and function of the multisubunit yeast RNA polymerase III transcription factor, TFIIB. *Cell* 71, 1055-64.

Keller, E. B., and Noon, W. A. (1984). Intron splicing: a conserved internal signal in introns of animal pre-mRNAs. *Proc Natl Acad Sci U S A* 81, 7417-20.

Keller, E. B., and Noon, W. A. (1985). Intron splicing: a conserved internal signal in introns of *Drosophila* pre-mRNAs. *Nucleic Acids Res* 13, 4971-81.

Kim, S. H., Smith, J., Claude, A., and Lin, R. J. (1992). The purified yeast pre-mRNA splicing factor PRP2 is an RNA-dependent NTPase. *EMBO J* 11, 2319-26.

Koch, J. L., Boulanger, S. C., Dib, H. S., Hebbar, S. K., and Perlman, P. S. (1992). Group II introns deleted for multiple substructures retain self-splicing activity. *Mol Cell Biol* 12, 1950-8.

Kohrer, K., and Domdey, H. (1991). Preparation of High Molecular Weight RNA. *Methods in Enzymology* 194, 398-405.

Konarska, M. M., Grabowski, P. J., Padgett, R. A., and Sharp, P. A. (1985). Characterization of the branch site in lariat RNAs produced by splicing of mRNA precursors. *Nature* 313, 552-7.

Konarska, M. M., and Sharp, P. A. (1987). Interactions between small nuclear ribonucleoprotein particles in formation of spliceosomes. *Cell* 49, 763-74.

Konforti, B. B., Koziolkiewicz, M. J., and Konarska, M. M. (1993). Disruption of base pairing between the 5' splice site and the 5' end of U1 snRNA is required for spliceosome assembly. *Cell* in press .

Krainer, and Maniatis, T. (1985). Multiple factors including the small nuclear ribonucleoproteins U1 and U2 are necessary for pre-mRNA splicing in vitro. *Cell* 42, 725-736.

Krämer, A., Keller, W., Appel, B., and Lührmann, R. (1984). The 5' terminus of the RNA moiety of U1 small nuclear ribonucleoprotein particles is required for the splicing of messenger RNA precursors. *Cell* 38, 299-307.

Krämer, A., and Utans, U. (1991). Three protein factors (SF1, SF3 and U2AF) function in pre-splicing complex formation in addition to snRNPs. *EMBO J* 10, 1503-9.

Kretzner, L., Krol, A., and Rosbash, M. (1990). *Saccharomyces cerevisiae* U1 small nuclear RNA secondary structure contains both universal and yeast-specific domains. *Proc Natl Acad Sci U S A* 87, 851-5.

Krol, A., Carbon, P., Ebel, J. P., and Appel, B. (1987). *Xenopus tropicalis* U6 snRNA genes transcribed by Pol III contain the upstream promoter elements used by Pol II dependent U snRNA genes. *Nucleic Acids Res* 15, 2463-78.

Kruger, K., Grabowski, P. J., Zaug, A. J., J., S., Gottschling, D. E., and Cech, T. R. (1982). Self-splicing RNA: autoexcision and autocyclization of the ribosomal RNA intervening sequence of Tetrahymena. *Cell* 31, 147-157.

Kunkel, G. R., Maser, R. L., Calvet, J. P., and Pederson, T. (1986). U6 small nuclear RNA is transcribed by RNA polymerase III. *Proc Natl Acad Sci U S A* 83, 8575-9.

Kunkel, T. A., Roberts, J. D., and Zakour, R. A. (1987). Rapid and efficient site-specific mutagenesis without phenotypic selection. *Methods Enzymol.* 154, 367-382.

Lamond, A. I., Konarska, M. M., Grabowski, P. J., and Sharp, P. A. (1988). Spliceosome assembly involves the binding and release of U4 small nuclear ribonucleoprotein. *Proc Natl Acad Sci U S A* 85, 411-5.

Lamond, A. I., Sproat, B., Ryder, U., and Hamm, J. (1989). Probing the structure and function of U2 snRNP with antisense oligonucleotides made of 2'-OMe RNA. *Cell* 58, 383-390.

Lee, C. G., and Hurwitz, J. (1993). Human RNA helicase A is homologous to the maleless protein of *Drosophila*. *J Biol Chem* 268, 16822-30.

Legrain, P., Séraphin, B., and Rosbash, M. (1988). Early commitment of yeast pre-mRNA to the spliceosome pathway. *Mol. Cell. Biol.* 8, 3755-3760.

Legrain, P., and Chouliska, A. (1990). The molecular characterization of PRP6 and PRP9 yeast genes reveals a new cysteine/histidine motif common to several splicing factors. *EMBO J* 9, 2775-81.

Legrain, P., Chapon, C., and Galisson, F. (1993). Interactions between PRP9 and SPP91 splicing factors identify a protein complex required in prespliceosome assembly. *Genes Dev* 7, 1390-9.

Lerner, M. R., Boyle, J. A., Mount, S. M., Wolin, S. L., and Steitz, J. A. (1980). Are snRNPs involved in splicing? *Nature* 283, 220-4.

Lesser, C. F., and Guthrie, C. (1993). Mutations in U6 snRNA that Alter Splice Site Specificity: Implications for the Active Site. *Science* in press .

Levitt, M. (1969). Detailed molecular model for transfer ribonucleic acid. *Nature* 224, 759-63.

Lin, R. J., Newman, A. J., Cheng, S. C., and Abelson, J. (1985). Yeast mRNA splicing in vitro. *J. Biol. Chem.* 260, 14780-14792.

Lopez, De, Leon, A., Librizzi, M., Puglia, K., and Willis, I. M. (1992). PCF4 encodes an RNA polymerase III transcription factor with homology to TFIIB. *Cell* 71, 211-20.

Lustig, A. J., Lin, R. J., and Abelson, J. (1986). The yeast RNA gene products are essential for mRNA splicing in vitro. *Cell* 47, 953-63.

Lührmann, R. (1988). snRNP proteins. In M. R. Birnstiel (Eds.), *Structure and function of major and minor small nuclear ribonucleoprotein particles* (pp. 71-99). Heidelberg, New York, London, Paris, Tokyo: Springer Verlag.

Madhani, H. D., Bordonné, R., and Guthrie, C. (1990). Multiple roles for U6 snRNA in the splicing pathway. *Genes Dev* 4, 2264-77.

Madhani, H. D., and Guthrie, C. (1992). A novel base-pairing interaction between U2 and U6 snRNAs suggests a mechanism for the catalytic activation of the spliceosome. *Cell* 71, 803-17.

Maniatis, T., Fritsch, E. F., and Sambrook, J. (1982). *Molecular cloning: A laboratory manual*. Cold Spring Harbor: Cold Spring Harbor Laboratory.

Maniatis, T., and Reed, R. (1987). The role of small ribonucleoprotein particles in pre-mRNA splicing. *Nature* 325, 673-678.

Mattaj, I. W., Dathan, N. A., Parry, H. D., Carbon, P., and Krol, A. (1988). Changing the RNA polymerase specificity of U snRNA gene promoters. *Cell* 55, 435-42.

McClary, J. A., Witney, F., and Geisselsoder, J. (1989). Efficient site-directed in vitro mutagenesis using phagemid vectors. *Biotechniques* 3, 282-289.

McPheeters, D. S., Fabrizio, P., and Abelson, J. (1989). In vitro reconstitution of functional yeast U2 snRNPs. *Genes Dev* 3, 2124-36.

McPheeters, D. S., and Abelson, J. (1992). Mutational analysis of the yeast U2 snRNA suggests a structural similarity to the catalytic core of group I introns. *Cell* 71, 819-31.

Michel, F., Hanna, M., Green, R., Bartel, D. P., and Szostak, J. W. (1989a). The guanosine binding site of the Tetrahymena ribozyme. *Nature* 342, 391-5.

Michel, F., Umesono, K., and Ozeki, H. (1989b). Comparative and functional anatomy of group II catalytic introns--a review. *Gene* 8222, 5-30.

Michel, F., Ellington, A. D., Couture, S., and Szostak, J. W. (1990). Phylogenetic and genetic evidence for base-triples in the catalytic domain of group I introns. *Nature* 347, 578-80.

Michel, F., and Westhof, E. (1990). Modelling of the three-dimensional architecture of group I catalytic introns based on comparative sequence analysis. *J Mol Biol* 216, 585-610.

Miraglia, L., Seiwert, S., Igel, A. H., and Ares, M. (1991). Limited functional equivalence of phylogenetic variation in small nuclear RNA: yeast U2 RNA with altered branchpoint complementarity inhibits splicing and produces a dominant lethal phenotype. *Proc. Natl. Acad. Sci.* 88, 7061-7065.

Moore, M. J., and Sharp, P. A. (1993). Evidence for two active sites in the spliceosome provided by stereochemistry of pre-mRNA splicing. *Nature* 365, 364-8.

Moore, M. J., Query, C. C., and Sharp, P. A. (1993). Splicing of Precursors to mRNA by the Spliceosome. In R. F. Gestland & J. F. Atkins (Eds.), *The RNA World* (pp. 303-358). Plainview, New York: Cold Spring Harbor Laboratory Press.

Mount, S. M., Pettersson, I., Hinterberger, M., Karmas, A., and Steitz, J. A. (1983). The U1 small nuclear RNA-protein complex selectively binds a 5' splice site in vitro. *Cell* 33, 509-18.

Myslinski, E., Segault, V., and Branlant, C. (1990). An intron in the genes for U3 small nucleolar RNAs of the yeast *Saccharomyces cerevisiae*. *Science* 247, 1213-1216.

Newman, A., and Norman, C. (1991). Mutations in yeast U5 snRNA alter the specificity of 5' splice-site cleavage. *Cell* 65, 115-23.

Newman, A. J., and Norman, C. (1992). U5 snRNA interacts with exon sequences at 5' and 3' splice sites. *Cell* 68, 743-54.

Noller, H. F., and Woese, C. R. (1981). Secondary structure of 16S ribosomal RNA. *Science* 212, 403-11.

Padgett, R. A., Konarska, M. M., Grabowski, P. J., Hardy, S. F., and Sharp, P. A. (1984). Lariat RNA's as intermediates and products in the splicing of messenger RNA precursors. *Science* 225, 898-903.

Parker, R., and Guthrie, C. (1985). A point mutation in the conserved hexanucleotide at a yeast 5' splice junction uncouples recognition, cleavage, and ligation. *Cell* 41, 107-18.

Parker, R., Siliciano, P. G., and Guthrie, C. (1987). Recognition of the TACTAAC box during mRNA splicing in yeast involves base pairing to the U2-like snRNA. *Cell* 49, 229-39.

Parker, R., and Siliciano, P. G. (1993). Evidence for an essential non-Watson-Crick interaction between the first and last nucleotides of a nuclear pre-mRNA intron. *Nature* 361, 660-2.

Patterson, B., and Guthrie, C. (1991). A U-rich tract enhances usage of an alternative 3' splice site in yeast. *Cell* 64, 181-7.

Peebles, C. L., Belcher, S. M., Zhang, M., Dietrich, R. C., and Perlman, P. S. (1993). Mutation of the conserved first nucleotide of a group II intron from yeast mitochondrial DNA reduces the rate but allows accurate splicing. *J Biol Chem* 268, 11929-38.

Penotti, F. E. (1991). Human pre-mRNA splicing signals. *J Theor Biol* 150, 385-420.

Peterson, E. T., Blank, J., Sprinzl, M., and Uhlenbeck, O. C. (1993). Selection for active *E. coli* tRNA(Phe) variants from a randomized library using two proteins. *EMBO J* 12, 2959-67.

Pikielny, C. W., Rymond, B. C., and Rosbash, M. (1986). Electrophoresis of ribonucleoproteins reveals an ordered assembly pathway of yeast splicing complexes. *Nature* 324, 341-345.

Puglisi, J. D., Wyatt, J. R., and Tinoco, I. J. (1990). Conformation of an RNA pseudoknot. *J Mol Biol* 214, 437-53.

Query, C. C., Moore, M. J., and Sharp, P. A. (1993). Branch Nucleophile Selection in Pre-mRNA Splicing: Evidence for the Bulged Duplex Model. *Cell* submitted, .

Reddy, R., Henning, D., Das, G., Harless, M., and Wright, D. (1987). The capped U6 small nuclear RNA is transcribed by RNA polymerase III. *J Biol Chem* 262, 75-81.

- Reed, R. (1989). The organization of 3' splice-site sequences in mammalian introns. *Genes Dev* 3, 2113-23.
- Reich, C. I., VanHoy, R. W., Porter, G. L., and Wise, J. A. (1992). Mutations at the 3' splice site can be suppressed by compensatory base changes in U1 snRNA in fission yeast. *Cell* 69, 1159-69.
- Rinke, J., Appel, B., Digweed, M., and Lührmann, R. (1985). Localization of a base-paired interaction between small nuclear RNAs U4 and U6 in intact U4/U6 ribonucleoprotein particles by psoralen cross-linking. *J Mol Biol* 185, 721-31.
- Rogers, J., and Wall, R. (1980). A mechanism for RNA splicing. *Proc Natl Acad Sci U S A* 77, 1877-9.
- Roiha, H., Shuster, E. O., Brow, D. A., and Guthrie, C. (1989). Small nuclear RNAs from budding yeasts: phylogenetic comparisons reveal extensive size variation. *Gene* 82, 137-144.
- Romero, D. P., and Blackburn, E. H. (1991). A conserved secondary structure for telomerase RNA. *Cell* 67, 343-53.
- Rose, M. D., Novick, P., Thomas, J. H., Botstein, D., and Fink, G. R. (1987). A *Saccharomyces cerevisiae* genomic plasmid bank based on a centromere-containing shuttle vector. *Gene* 60, 237-43.
- Rose, M. D., Winston, F., and Hieter, P. (1989). *Methods in yeast genetics*. .

Ruby, S. W., and Abelson, J. (1988). An early hierarchic role of U1 small nuclear ribonucleoprotein in spliceosome assembly. *Science* 242, 1028-35.

Ruby, S. W., Chang, T.-H., and Abelson, J. N. (1993). Four yeast spliceosomal proteins (PRP5, PRP9, PRP11, and PRP21) interact to promote U2 snRNP binding to pre-mRNA. *Genes Dev.* 7, 1909-1925.

Ruskin, B., Krainer, A. R., Maniatis, T., and Green, M. R. (1984). Excision of an intact intron as a novel lariat structure during pre-mRNA splicing in vitro. *Cell* 38, 317-31.

Ruskin, B., Zamore, P. D., and Green, M. R. (1988). A factor, U2AF, is required for U2 snRNP binding and splicing complex assembly. *Cell* 52, 207-19.

Rymond, B., and Rosbash, M. (1992). Yeast Pre-mRNA Splicing. In E. W. Jones, J. R. Pringle, & J. R. Broach (Eds.), *The Molecular and Cellular Biology of the Yeast Saccharomyces* (pp. 143-192). Plainview, New York: Cold Spring Harbor Laboratory Press.

Saenger, W. (1984). *Principles of nucleic acid structure*. New York: Springer-Verlag.

Sambrook, J., Fritsch, E. F., and Maniatis, T. (1989). *Molecular cloning: a laboratory manual*. Plainview, New York: Cold Spring Harbor Laboratory Press.

Sawa, H., and Shimura, Y. (1992). Association of U6 snRNA with the 5'-splice site region of pre-mRNA in the spliceosome. *Genes Dev* 6, 244-54.

Sawa, H., and Abelson, J. (1992). Evidence for a base-pairing interaction between U6 small nuclear RNA and 5' splice site during the splicing reaction in yeast. *Proc Natl Acad Sci U S A* 89, 11269-73.

Schena, M., Picard, D., and Yamamoto, K. R. (1991). Vectors for constitutive and inducible gene expression in yeast. *Methods Enzymol* 194, 389-98.

Schiestl, R. H., and Gietz, R. D. (1989). High efficiency transformation of intact yeast cells using single stranded nucleic acids as a carrier. *Curr Genet* 16, 339-46.

Schmelzer, C., and Muller, M. W. (1987). Self-splicing of group II introns in vitro: lariat formation and 3' splice site selection in mutant RNAs. *Cell* 51, 753-62.

Schmid, S. R., and Linder, P. (1992). D-E-A-D protein family of putative RNA helicases. *Mol Microbiol* 6, 283-91.

Schnieder, J. C., and Guarente, L. (1991). Vectors for Expression of Cloned Genes in Yeast: Regulation, Overproduction, and Underproduction. *Methods in Enzymology* 194, 373-388.

Schwer, B., and Guthrie, C. (1991). PRP16 is an RNA-dependent ATPase that interacts transiently with the spliceosome. *Nature* 349, 494-9.

Schwer, B., and Guthrie, C. (1992a). A conformational rearrangement in the spliceosome is dependent on PRP16 and ATP hydrolysis. *EMBO J* 11, 5033-9.

Schwer, B., and Guthrie, C. (1992b). A dominant negative mutation in a spliceosomal ATPase affects ATP hydrolysis but not binding to the spliceosome. *Mol Cell Biol* 12, 3540-7.

S raphin, B., Kretzner, L., and Rosbash, M. (1988). A U1 snRNA:pre-mRNA base pairing interaction is required early in yeast spliceosome assembly but does not uniquely define the 5' cleavage site. *EMBO J* 7, 2533-8.

S raphin, B., and Rosbash, M. (1989). Identification of functional U1 snRNA-pre-mRNA complexes committed to spliceosome assembly and splicing. *Cell* 59, 349-58.

S raphin, B., and Rosbash, M. (1990). Exon mutations uncouple 5' splice site selection from U1 snRNA pairing. *Cell* 63, 619-29.

S raphin, B., and Rosbash, M. (1991). The yeast branchpoint sequence is not required for the formation of a stable U1 snRNA-pre-mRNA complex and is recognized in the absence of U2 snRNA. *EMBO J* 10, 1209-16.

S raphin, B., and Kandels-Lewis, S. (1993). 3' splice site recognition in *S. cerevisiae* does not require base pairing with U1 snRNA. *Cell* 73, 803-12.

Shannon, K. W., and Guthrie, C. (1991). Suppressors of a U4 snRNA mutation define a novel U6 snRNP protein with RNA-binding motifs. *Genes Dev* 5, 773-85.

Sharp, P. A. (1985). On the origin of RNA splicing and introns. *Cell* 42, 397-400.

Sharp, P. A. (1987). Splicing messenger RNA precursors. *Science* 235, 766-771.

Sharp, P. A. (1991). Five easy pieces. *Science* 254, 663.

Shuster, E. O., and Guthrie, C. (1988). Two conserved domains of yeast U2 snRNA are separated by 945 nonessential nucleotides. *Cell* 55, 41-48.

Shuster, E. O., and Guthrie, C. (1990). Human U2 snRNA can function in pre-mRNA splicing in yeast. *Nature* 345, 270-273.

Siliciano, P. G., Brow, D. A., Roiha, H., and Guthrie, C. (1987). An essential snRNA from *S. cerevisiae* has properties predicted for U4, including interaction with a U6-like snRNA. *Cell* 50, 585-92.

Siliciano, P. G., and Guthrie, C. (1988). 5' splice site selection in yeast: genetic alterations in base-pairing with U1 reveal additional requirements. *Genes Dev* 2, 1258-67.

Sontheimer, E. J., and Steitz, J. A. (1993). Identification of U5 and U6 small nuclear RNA's as active site components of the spliceosome. *Science* in press .

Steitz, J. A., Black, D. L., Gerke, V., Parker, K. A., Krämer, A., Frendewey, D., and Keller, W. (1988). Functions of the abundant U-snRNPs. In M. L. Birnstiel (Eds.), *Structure and Function of Major and Minor Small Nuclear Ribonucleoprotein Particles* (pp. 115-154). Berlin: Springer-Verlag.

Stephens, R. M., and Schneider, T. D. (1992). Features of spliceosome evolution and function inferred from an analysis of the information at human splice sites. *J Mol Biol* 228, 1124-36.

Strauss, E. J., and Guthrie, C. (1991). A cold-sensitive mRNA splicing mutant is a member of the RNA helicase gene family. *Genes Dev* 5, 629-41.

Szostak, J. W., and Ellington, A. D. (1993). In Vitro Selection of Functional RNA Sequences. In R. F. Gestland & J. F. Atkins (Eds.), *The RNA World* (pp. 511-534). Plainview, New York: Cold Spring Harbor Laboratory Press.

Tani, T., and Ohshima, Y. (1989). The gene for the U6 small nuclear RNA in fission yeast has an intron. *Nature* 337, 87-90.

Tani, T., and Ohshima, Y. (1991). mRNA-type introns in U6 small nuclear RNA genes: implications for the catalysis in pre-mRNA splicing. *Genes Dev* 5, 1022-31.

Teem, J. L., and Rosbash, M. (1983). Expression of a β -galactosidase gene containing the ribosomal protein 51 intron is sensitive to the *ma2* mutation of yeast. *Proc. Natl. Acad. Sci. USA* 80, 4403-4407.

ten Dam, E., Pleij, K., and Draper, D. (1992). Structural and Functional Aspects of RNA Pseudoknots. *Biochemistry* 31, 11665-11676.

Tomizawa, J. (1993). Evolution of Functional Structures of RNA. In R. F. Gestland & J. F. Atkins (Eds.), *The RNA World* (pp. 419-445). Plainview, New York: Cold Spring Harbor Laboratory Press.

Turner, D. H., and Bevilacqua, P. C. (1993). Thermodynamic Considerations for Evolution by RNA. In R. F. Gestland & J. F. Atkins (Eds.), *The RNA World* (pp. 447-464). Plainview, New York: Cold Spring Harbor Laboratory Press.

van, der, Veen, R, Amberg, A. C., van, der, Horst, G, Bonen, L., Tabak, H. F., and Grivell, L. A. (1986). Excised group II introns in yeast mitochondria are lariats and can be formed by self-splicing in vitro. *Cell* 44, 225-34.

Vankan, P., McGuigan, C., and Mattaj, I. W. (1990). Domains of U4 and U6 snRNAs required for snRNP assembly and splicing complementation in *Xenopus* oocytes. *EMBO J* 9, 3397-404.

Vankan, P., McGuigan, C., and Mattaj, I. W. (1992). Roles of U4 and U6 snRNAs in the assembly of splicing complexes. *EMBO J* 11, 335-43.

Vijayraghavan, U., Parker, R., Tamm, J., Iimura, Y., Rossi, J., Abelson, J., and Guthrie, C. (1986). Mutations in conserved intron sequences affect multiple steps in the yeast splicing pathway, particularly assembly of the spliceosome. *EMBO J* 5, 1683-95.

Wassarman, D. A., and Steitz, J. A. (1992). Interactions of small nuclear RNA's with precursor messenger RNA during in vitro splicing. *Science* 257, 1918-25.

Weiner, A. M. (1993). mRNA splicing and autocatalytic introns: distant cousins or the products of chemical determinism? *Cell* 72, 161-4.

Wise, J. A., Tollervey, D., Maloney, D., Swerdlow, H., Dunn, E. J., and Guthrie, C. (1983). Yeast contains small nuclear RNAs encoded by single copy genes. *Cell* 35, 743-51.

Woese, C. R., Gutell, R., Gupta, R., and Noller, H. F. (1983). Detailed analysis of the higher-order structure of 16S-like ribosomal ribonucleic acids. *Microbiol Rev* 47, 621-69.

Wolff, T., and Bindereif, A. (1992). Reconstituted mammalian U4/U6 snRNP complements splicing: a mutational analysis. *EMBO J* 11, 345-59.

Wolff, T., and Bindereif, A. (1993). Conformational changes of U6 RNA during the spliceosome cycle: an intramolecular helix is essential both for initiating the U4-U6 interaction and for the first step of slicing. *Genes Dev* 7, 1377-89.

Wu, J., and Manley, J. L. (1989). Mammalian pre-mRNA branch site selection by U2 snRNP involves base pairing. *Genes Dev* 3, 1553-61.

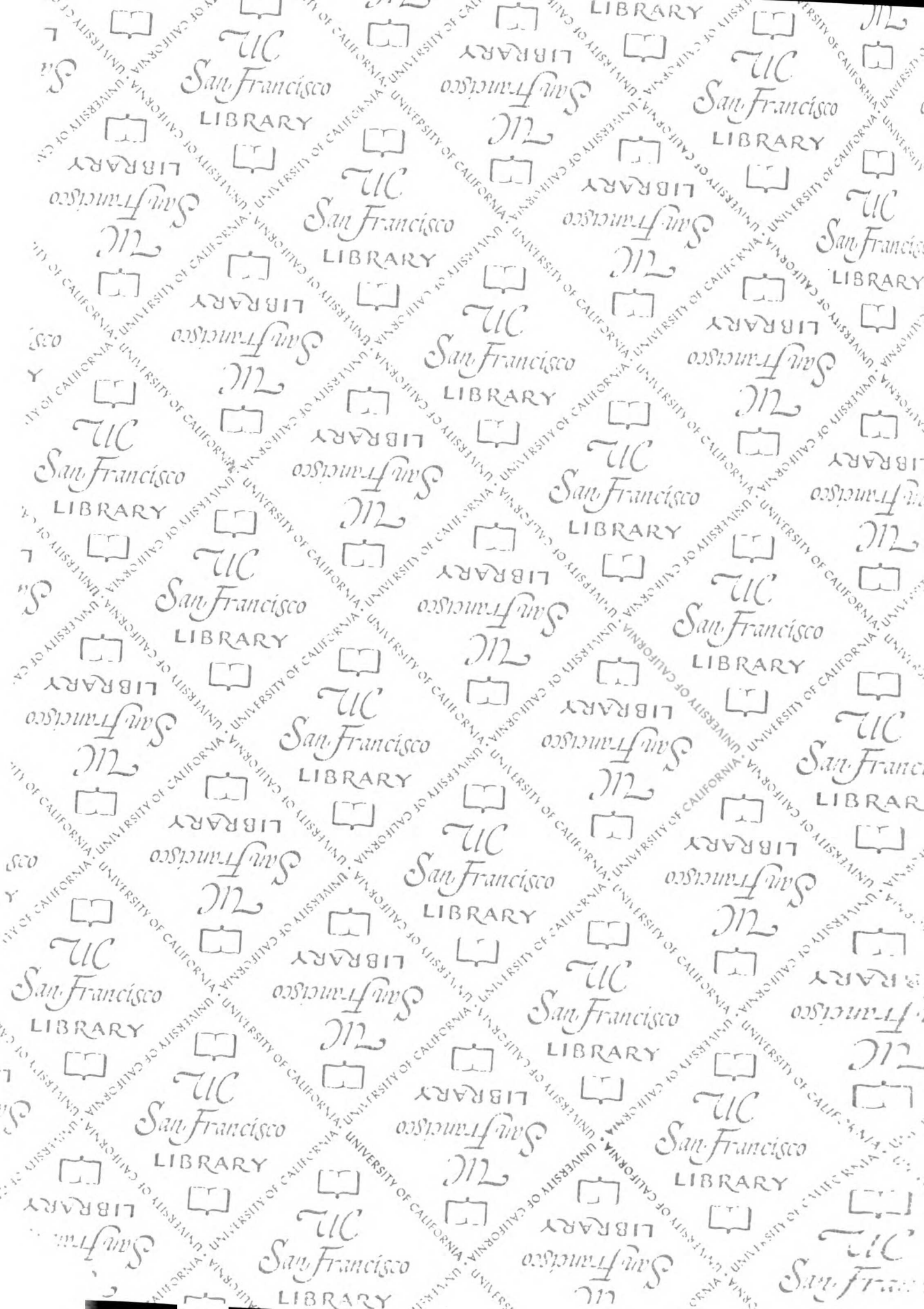
Wu, J. A., and Manley, J. L. (1991). Base pairing between U2 and U6 snRNAs is necessary for splicing of a mammalian pre-mRNA. *Nature* 352, 818-21.

Wyatt, J. R., Puglisi, J. D., and Tinoco, I. J. (1990). RNA pseudoknots. Stability and loop size requirements. *J Mol Biol* 214, 455-70.

Wyatt, J. R., Sontheimer, E. J., and Steitz, J. A. (1992). Site-specific cross-linking of mammalian U5 snRNP to the 5' splice site before the first step of pre-mRNA splicing. *Genes Dev.* 6, 2542-2553.

- Xu, Y., Petersen-Bjorn, S., and Friesen, J. D. (1990). The PRP4 (RNA4) protein of *Saccharomyces cerevisiae* is associated with the 5' portion of the U4 snRNA. *Mol. Cell. Biol.* 10, 1217-1225.
- Yarus, M., Illangsekare, M., and Christian, E. (1991a). Selection of small molecules by the *Tetrahymena* catalytic center. *Nucleic Acids Res* 19, 1297-304.
- Yarus, M., Illangsekare, M., and Christian, E. (1991b). An axial binding site in the *Tetrahymena* precursor RNA. *J Mol Biol* 222, 995-1012.
- Yean, S. L., and Lin, R. J. (1991). U4 small nuclear RNA dissociates from a yeast spliceosome and does not participate in the subsequent splicing reaction. *Mol Cell Biol* 11, 5571-7.
- Yu, Y., Maroney, P. A., and Nilsen, T. W. (1993). Functional reconstitution of U6 snRNA in nematode cis and trans-splicing: Branch formation between splicing substrates and U6. *Cell in press* .
- Zamore, P. D., and Green, M. R. (1989). Identification, purification, and biochemical characterization of U2 small nuclear ribonucleoprotein auxiliary factor. *Proc Natl Acad Sci U S A* 86, 9243-7.
- Zavanelli, M. I., and Ares, M. J. (1991). Efficient association of U2 snRNPs with pre-mRNA requires an essential U2 RNA structural element. *Genes Dev* 5, 2521-33.
- Zhuang, Y., and Weiner, A. M. (1986). A compensatory base change in U1 snRNA suppresses a 5' splice site mutation. *Cell* 46, 827-35.

Zhuang, Y.,and Weiner, A. M. (1989). A compensatory base change in human U2 snRNA can suppress a branch site mutation. *Genes Dev* 3, 1545-52.



For reference

Not to be taken from the room.

621203



3 1378 00621 2032

